



IGGC₁₂ *Georgetown*

12th Inter-Guiana Geological Conference
12-13 December 2022
Georgetown, Guyana



Contents

History of the Inter Guiana Geological Conferences	3
SAXI: The South American Exploration Initiative	4
IGGC 12 Organising Committee	5
Program.....	7
Posters.....	9
Stacey M. Amattaram - Stratigraphy and Geochemistry of the Paleoproterozoic manganese in the Guiana Shield, South America.	11
John Applewhite-Hercules - An assessment of trace element geochemistry of paleo-surface gravels, lateritic regolith and rock outcrops for the potential of Strategic Minerals (other minerals), Base Metals and Orogenic Gold Formation processes within Potaro Mining District # 2.....	15
John Applewhite-Hercules - 3 D modelling of paleo-surfaces using airborne electromagnetism (GeoTEM) and Digital Elevation Model(DEM) datasets, in Mali West Africa: adaptations for Small and Medium scale mine operations within the Guiana Shield.....	16
Marc Bardoux - OCSH, IH and IR Rhyacian gold deposits of the Guiana Shield.....	17
Carlos H. Bertoni - The Oko West gold deposit – a new discovery in the Guiana Shield.....	18
Frank F. Beunk - Transamazonian “Cusp Tectonics” in the Guiana Shield (Abstract only, no presentation)	32
B. Borba de Carvalho - Geochemistry and Sm-Nd isotopic data for unmetamorphosed dolerites in Matthews Ridge, Guyana, that are inferred to belong to the Avanavero LIP.....	36
B. Borba de Carvalho - Paleoproterozoic U-Pb ages and geochemistry of mafic and ultramafic rocks of Matthews Ridge, Guyana: A comparison with other Paleoproterozoic occurrences within the Guiana Shield ..	40
Kantharaja Chandrappa - Guyana’s Mineral Outlook: A Case for Traditional and Non-traditional Mineral Investment	45
Vincent Combes - Geometry and spatial distribution of shear zones and associated gold-bearing quartz veins, hosted by a TTG-like complex, at the Brothers Project, Eastern Suriname	47
Emond de Roever - Ultrahigh-temperature Metamorphism in the Bakhuis Granulite Belt (Suriname)	54
Lêda Maria Fraga - The Orocaima Igneous Belt and the 1.99-1.96 Ga SLIP in the Amazonian Craton.....	60
La Donna Fredericks - An Investigation into the Characteristics of Fault and Fault Zones of the Guyana Basin .	66
Kathleen Gersie - Tracing the influence of the Amazon River along the Suriname coastline from the Mid-Miocene to Holocene.....	70
Blandine Gourcerol - French Guiana: new insights into under-investigated region for geological assessment - A BRGM approach	72
Mauricio Ibañez-Mejia - A newly recognized 1.98 Ga large igneous province (LIP) in the Amazonian Craton and its relationship with the coeval Orocaima silicic LIP	76
Tramaine N. James - Preliminary investigation of the Toroparu Au-Ag-Cu Deposit, Guyana, South America.....	77
Mark Jessell - What do we know about the positioning of West Africa and the Guiana Shield during the Rhyacian Period?.....	79
Nicole Kioe-A-Sen - Gold mineralisation in the Paleoproterozoic greenstone belt of Suriname: Insights from the Overman deposit.....	81

Salomon Kroonenberg - The 1.98 Ga Goboy dolerite: a new dyke swarm in northern Suriname	82
Salomon Kroonenberg - Friedrich Voltz (1828–1855), discoverer of the Maronian greenstone belt in the Guiana Shield	86
Salomon Kroonenberg - Copper mineralisation in Paleoproterozoic cordierite-biotite-magnetite-apatite rocks at Weko Sula, SE Suriname: anatexis of a cupriferous argillaceous evaporite-to-red bed sequence	87
Salomon Kroonenberg - Regional mercury background values in soils and saprolites in the gold-producing greenstone belt of Suriname, Guiana Shield	88
Brice Lacroix - The role of polyphase folding in the distribution of Gold: Insights from the Guiana Shield.....	89
Jean Michel Lafon - U-Pb-Hf zircon geochronology of the northern border of the Archean Amapá Block, SE Guiana Shield: Further evidence of dominant Neoproterozoic magmatism.....	96
Serge Nadeau - Update on the Guyana-Brazil project and more recent zircon age results of alkaline intrusions in Southern Guyana: Makarapan Mountain and Muri Mountain Alkaline Complex.....	101
João M. Milhomem Neto - High-grade metamorphism in the central region of Amapá, Northern Brazil: age constraints from in situ U-Pb dating of monazite and zircon	105
Robert Loucks - Application of Trace-Element Indicators Cu and Au Metallogenic Fertility to Paleoproterozoic Granitoids and Zircons in Guyana (Abstract only, no presentation).....	110
Paul R.D. Mason - Age constraints on Early Proterozoic sedimentation during Transamazonian continental convergence in Suriname.....	111
Ramiro Matos - The Roboré microcontinent, SW Amazonian Craton: new insights on the Orosirian-Ectasian crustal evolution from U-Pb geochronology.....	113
Denbre McGarrell - Plutonic Rocks of the Karouni Basin: Characteristics and Significance to Mineralization ..	114
Renoesha Naipal - Hydrothermal desilicification, alkali leaching and oxidation in metapelites of the Rosebel gold district in the Paleoproterozoic Marowijne Greenstone Belt, Suriname.....	115
Renoesha Naipal - The Bemau Ultramafic Complex and the Borgia Hill Chromite Complex: Two contrasting ultramafic complexes in the Paleoproterozoic basement of Suriname.....	116
Kumar Persaud - Stratigraphy and Structure of the Makapa Project, Guyana	117
Alexis Plunder - Tectono-metamorphic framework of the Rosebel and Armina unit, French Guiana.....	123
Fydji Sastrohardjo - Nature of the relationship between the Marowijne greenstone belt and the Gran Rio granite of the Rhyacian Transamazonian orogenic belt, Suriname: Significance of the Sara's Lust migmatite.	128
Gabriel A. R. Soares - The Geological Setting and Hydrothermal Alteration at the Tucano Gold Deposit, Guiana Shield, Brazil	135
Michael Tedeschi - Preliminary Lithostratigraphy of the Rhyacian Greenstone Belts of Northern Guyana and Suriname	141
Nicolas Thébaud - Rhyacian crustal evolution of the Guyana Shield revealed through U-Pb and Lu-Hf analyses	146
Oclaya Verwey - Paleocene groundwater salinity mapping in coastal aquifers using geophysical well logs: A Suriname case study	152
Santoucha Woodly - Petrography of the metamorphic rocks in the Kabofe and Jaikreek area, Marowijne Greenstone Belt, Suriname	155

History of the Inter Guiana Geological Conferences

The idea of an Inter Guiana Geological Conference was first proposed by Hendricus (Henk) Schols in 1949, at that time head of the Geological and Mining Service of Suriname. He had graduated as a mining engineer from Delft University of Technology, and had passed the years of the Second World War in Suriname on secondment from a private organisation. After the war, he was asked by the governor of Suriname to set up the Geological and Mining Service.

He organised the first Inter Guiana Geological conference in Paramaribo from September 23 to October 3, 1950. It was attended from French Guiana by the famous Russian-born French geologist Boris Choubert, geologist of the Office Scientifique d'Outre-mer (now the IRD, l'Institut de Recherche pour le Développement), who already since the 1930s was a staunch supporter of Wegener's Continental Drift theory, against the mainstream consensus in those years. He had worked extensively in Gabon before, and wrote a number of important books and papers on the geology of French Guiana. British Guiana was represented by the Director of the British Guiana Geological Survey Smith Bracewell, also a prolific publisher on the geology of that country in the years before, and discoverer of a series of unusual chromium minerals in the Merume River of British Guiana, one of which was named after him (Bracewellite).

In the following years, the tradition of Inter Guiana Conferences was continued in the different Guianian capitals (see below). In the fourth one a Brazilian representative was present, and the fifth also one from Venezuela. Proceedings were published from the fourth conference onwards, always by local government institutes and all in different formats. Participants came from all Guianian countries including Colombia and also from beyond, including Bolivia, United States, Canada, UK, Switzerland, France, Gabon and Tanzania.

The 10th Conference in Belém, Brazil in 1975 was a hugely impressive event, in which the complete geological inventory of the Amazonian Craton was shown on the basis of radar images, the RADAMBRASIL programme. Also geomorphology, vegetation and soil maps were produced in the programme, and published in a great number of volumes with maps which even now are standard reference works.

Suriname committed itself during that conference to organise the 11th Interguiana conference in 1978. Somehow this did not materialise. The conference series was resuscitated after a long pause in 2019 thanks to the support of the AMIRA Global South American Exploration Initiative, and this current meeting represents the 12th in a long series of successful conferences dedicated to the region.

I thank Mrs Fiona Berrangé-Schols, daughter of Henk Schols, now in Phophonyane Falls, Swaziland, for information about her father.

Salomon Kroonenberg, Anton de Kom University of Suriname.

IGGC Conference Series and Proceedings

- 1st Sep 23-Oct 3, 1950, Paramaribo; GMD Jaarboek 1950 p. 74-77
- 2nd Mar 15-28, 1951, Cayenne; GMD Jaarboek 1951, p. 43-46
- 3rd Sep 21-27, 1953, Georgetown; GMD Jaarboek 1953, p. 20-23
- 4th Sep, 1957, Cayenne; Communications Quatrieme Conf Geol Guyanes, 1959, Paris, 139 pp.
- 5th Oct 28-Nov 6, 1959, Georgetown; Proc Fifth InterGuiana Geol. Conf,n 1961, Georgetown, 320 pp.

- 6th Oct 1-8, 1963, Belem; Anais da VI Conferencia Geologica das Guianas, 1966, Rio de Janeiro, 193 pp (scan)
- 7th Nov 21-25, 1966, Paramaribo; Proc 7th Guiana Geol. Conf, Verh Kon Ned geol Mijnb Gen., 27, 1969, 175 pp.+encl.
- 8th Aug 11-15, 1969, Georgetown; Proceedings of the Eighth Guiana Geological Conference, Georgetown, Guyana, 1970, 21 loose papers
- 9th May 7-14, 1972, Ciudad Guayana; Memoria de la 9a Conf Geol Inter-Guayanas. Min Minas Hidrocarb, Bol Geol (Caracas) Publ esp. 6, 692 pp
- 10th Nov 9-16, 1975, Belem; Anais da Decima Conferencia Geologica Interguianas, 1975, Belem, 820 pp
- 11th Feb 19-20, 2019, Paramaribo;
http://www.tectonique.net/saxi/wp-content/uploads/2019/03/IG11_proceedings.pdf
- 12th Dec 12-13, 2022, Georgetown; this volume

SAXI: The South American Exploration Initiative

The AMIRA Global Project P1061B South American Exploration Initiative aims to enhance the exploration potential of the Guiana Shield and neighbouring terranes in northeast South America through an integrated program of research and data gathering into its 'anatomy'. There is an equally strong commitment to training and training by research to produce the next generation of local industry-aware geoscientists.

Stage 2 of the SAXI project has brought together minerals exploration companies, geological surveys and Research organisations to develop the basis for a long-term renewal of our scientific understanding of the tectonics and metallogenesis of the region.

The current SAXI Partners are:

AMIRA Global, AngloGold Ashanti, Anton de Kom University of Suriname, Barrick, the BRGM, Centamin, the CPRM, Federal University of Minas Gerais at Belo Horizonte, Guyana Geology and Mines Commission, IRD, Laurentian University, Newmont, Reunion Gold, The University of Western Australia, Uni Lorraine, Universidad de Chile, Universidade Federal do Ceará, Universidad Federal do Pará, Université de Guyane, Utrecht University and the University of Toulouse.

IGGC 12 Organising Committee

Alexis Plunder, BRGM
Arnauld Heuret, Université de Guyane
Aurelien Eglinger, Université de Lorraine
Carlos Bertoni, Reunion Gold
Corinne Debat, University of Western Australia
Christopher Blackman, University of Guyana
Geoffrey Aergeerts, BRGM
Hayley McGillivray, AMIRA Global
Howard Bills, Centamin PLC
Jean-Michel Lafon, UFPA
LaDonna Fredericks, GGMC
Leda Fraga , CPRM
Marc Bardoux , Barrick
Mark Jessell, University of Western Australia
Michael Tedeschi, Laurentian University
Mol, Augusto Gonçalves, AngloGold Ashanti
Nicolas Thebaud, University of Western Australia
Nicole Kioe A Sen, ADEKUS
Olivier Vanderhaeghe, Université de Toulouse
Paul Morley, Newmont
Paul Mason, Utrecht University
Rosaline Silva, UFMG
Salomon Kroonenburg, TU Delft
Stano Ulrich, AngloGold Ashanti
Steffen Hagemann, University of Western Australia
Stephane Perrouty, Laurentian University
Theo Wong, ADEKUS

Program

Start	End	Monday 12th December	
8:30	9:00	Registration	AMIRA
9:00	10:00	Welcome & entertainment	Minister of Mines, Director, Jessell
10:00	10:30	Morning Tea & Posters	
10:30	11:10	Tectonics 1	Keynote: La Donna Fredricks- Guyana Mineral Outlook
11:10	11:30	Tectonics 2	Jean-Michel Lafon - U-Pb-Hf zircon geochronology of the northern border of the Archean Amapá Block, SE Guiana Shield: Further evidence of dominant Neoproterozoic magmatism
11:30	11:50	Tectonics 3	Leda Fraga - The Orocaima Igneous Belt and the 1.99-1.96 Ga SLIP in the Amazonian Craton
11:50	12:10	Tectonics 4	Nicolas Thébaud - Crustal evolution of the Guyana Shield: insights from coupled Lu-Hf and O isotopic analyses
12:10	13:40	Lunch & Posters	
13:40	14:00	Tectonics 5	Salomon Kroonenberg - The 1.98 Ga Goboy dolerite: a new dyke swarm in northern Suriname
14:00	14:20	Tectonics 6	Mark Jessell - What do we really know about the relationship between the Guiana Shield and the West African Craton?
14:20	14:40	Tectonics 7	Gerardo Ramiro Matos - The Roboré microcontinent, SW Amazonian Craton: new insights on the Orosirian-Ectasian crustal evolution from U-Pb geochronology
14:40	15:00	Tectonics 8	Alexis Plunder - Tectono-metamorphic framework of the Rosebel and Armina unit, French Guiana
15:00	15:40	Afternoon Tea & Posters	
15:40	16:00	Tectonics 9	Paul Mason - Age constraints on Early Proterozoic sedimentation during Transamazonian continental convergence in Suriname
16:00	16:20	Tectonics 10	Mike Tedeschi - Preliminary Lithostratigraphy of the Rhyacian Greenstone Belts of Northern Guyana and Suriname
16:20	17:00	Exploration 1	Keynote: Blandine Gourcerol - French Guyana: New insights into under-investigated region for geological assessment - A BRGM approach
17:30	19:00	Welcome Drinks	

Start	End	Tuesday 13th December	
8:40	9:00	Exploration 2	Serge Nadeau - Update on the Guyana-Brazil project and more recent zircon age results of alkaline intrusions in Southern Guyana: Makarapan Mountain and Muri Mountain Alkaline Complex
9:00	9:20	Exploration 3	John Applewhite-hercules - An assessment of trace element geochemistry of paleo-surface gravels, lateritic Regolith and Rock outcrops for potential Orogenic Gold Formation Processes in Guyana
9:20	9:40	Exploration 4	Salomon Kroonenberg - Friedrich Voltz (1828–1855), discoverer of the Maronian greenstone belt in the Guiana Shield
9:40	10:00	Exploration 5	Bruna Borba de Carvalho - Paleoproterozoic U-Pb ages and geochemistry of mafic and ultramafic rocks of Matthews Ridge, Guyana: A comparison with other Paleoproterozoic occurrences within the Guiana Shield
10:00	10:20	Exploration 6	Brice Lacroix- The role of polyphase folding in the distribution of Gold: Insights from the Guiana Shield
10:20	11:00	<i>Morning Tea & Posters</i>	
11:00	11:40	Mineralisation 1	Keynote: Marc Bardoux - OCSH, IH and IR Rhyacian gold deposits of the Guiana Shield
11:40	12:00	Mineralisation 2	Vincent Combes - Geometry and spatial distribution of shear zones and associated gold-bearing quartz veins, hosted by a TTG-like complex, at the Brothers Project, Eastern Suriname
12:00	13:30	<i>Lunch & Posters</i>	
13:30	13:50	Mineralisation 3	Tramaine James - Preliminary investigation of the Toroparu Au-Ag-Cu Deposit, Guyana, South America
13:50	14:10	Mineralisation 4	Nicole Kioe-A-Sen - Gold mineralisation in the Paleoproterozoic greenstone belt of Suriname: Insights from the Overman deposit
14:10	14:30	Mineralisation 5	Stacey Amattaram - Stratigraphy and Geochemistry of the Paleoproterozoic manganese in the Guiana Shield, South America
14:30	15:30	<i>Afternoon Tea & Posters</i>	
15:30	15:50	Mineralisation 6	Carlos Bertoni - The Oko West gold deposit – a new discovery in the Guiana Shield
15:50	16:10	Mineralisation 7	Gabriel Soares - Gabriel Soares - The Geological Setting and Hydrothermal Alteration of the Tucano Gold Deposit, Guiana Shield, Brazil
16:10	16:40	<i>Closing remarks</i>	

Posters

John	Applewhite-hercules	Three-dimensional modeling of Lateritic Paleo-surface(regolith mapping) using air borne electromagnetism surveys,in Mali West Africa
Frank	Beunk	Transamazonian “Cusp Tectonics” in the Guiana Shield (Abstract ONLY)
Bruna	Borba de Carvalho	Geochemistry and Sm-Nd isotopic data for unmetamorphosed units in Matthews Ridge, Guyana, that are inferred to belong to the Avanavero LIP.
Kathleen	Gersie	Tracing the influence of the Amazon River along the Suriname coastline from the Mid-Miocene to Holocene
Mauricio	Ibañez-Mejia	A newly recognized 1.98 Ga large igneous province (LIP) in the Amazonian Craton and its relationship with the coeval Orocaima silicic LIP
Salomon	Kroonenberg	Copper mineralisation in Paleoproterozoic cordierite-biotite-magnetite-apatite rocks at Weko Sula, SE Suriname: anatexis of a cupriferous argillaceous evaporite-to-red bed sequence
Salomon	Kroonenberg	Regional mercury background values in soils and saprolites in the gold-producing greenstone belt of Suriname, Guiana Shield
Denbre	McGarrell, K Higgins, G Neira	Intrusive Rocks of the Karouni Basin: Characteristics and Significance to Mineralization
Renoessa	Naipal	The Bemau Ultramafic Complex and the Borgia Hill Chromite Complex: Two contrasting ultramafic complexes in the Paleoproterozoic basement of Suriname
Renoessa	Naipal	Hydrothermal desilicification, alkali leaching and oxidation in metapelites of the Rosebel gold district in the Paleoproterozoic Marowijne Greenstone Belt, Suriname
Renoessa	Naipal	The Bemau Ultramafic Complex and the Borgia Hill Chromite Complex: Two contrasting ultramafic complexes in the Paleoproterozoic basement of Suriname
Milhomem	Neto	High-grade metamorphism in the central region of Amapá, Northern Brazil: age constraints from in situ U-Pb dating of monazite and zircon
Kumar	Persaud	Stratigraphy and Structure of the Makapa Project, Guyana
Fydji	Sastrohardjo	Nature of the relationship between the Marowijne greenstone belt and the Gran Rio granite of the Rhyacian Transamazonian orogenic belt, Suriname: Significance of the Sara’s Lust migmatite
Oclaya	Verwey	Paleocene groundwater salinity mapping in coastal aquifers using geophysical well logs: A Suriname case study
Santoucha	Woodly	Petrography of the metamorphic rocks in the Kabofe and Jaikreek area, Marowijne Greenstone Belt, Suriname

Stratigraphy and Geochemistry of the Paleoproterozoic manganese in the Guiana Shield, South America.

Stacey M. Amattaram
Utrecht University

Paul R.D. Mason
Utrecht University

Leo M. Kriegsman
Utrecht University &
Naturalis Leiden

Salomon Kroonenberg
Anton de Kom University of Suriname

s.m.amattaram@uu.nl

p.mason@uu.nl

leo.kriegsman@naturalis.nl

salomonkroonenberg@gmail.com

SUMMARY

Manganese-rich horizons of the Guiana Shield were formed during the Lomagundi Event, in response to changing redox conditions after the Great Oxidation Event. The Mn distribution in sedimentary rocks is linked to the resource potential of the Paleoproterozoic Greenstone Belt and gives insight into the depositional environment, atmospheric conditions, and the nature of early life during the Paleoproterozoic. Manganese-rich horizons might also represent an important stratigraphic marker horizon across the greenstone belt. The focus in this section is on Mn-rich metasediments from Apoema Sula, Maripa Hill and Pletrug in Suriname. Initial results show that the main Mn bearing minerals are spessartine, Ca-Mn-carbonate, Mg-Mn olivine, Mn-amphibole and pyrophanite.

Keywords: Manganese, Mn carbonates, gondites, Guiana Shield

The Paleoproterozoic Maronian Greenstone Belt (2.26-1.95 Ga) of the Guiana Shield was formed during the Lomagundi (LE) isotope excursion (Cabral et al., 2019; Maheshwari et al., 2010; Roy, 2006), a period of high-rate burial of organic material accompanied by the rise of oxygen concentrations in the atmosphere following the Great Oxidation Event (GOE; 2.50-2.32 Ga; Bekker & Holland, 2012). Mn deposition occurred toward the end of the LE as oxygen levels started to decrease again. The large positive excursion of $\delta^{13}\text{C}$ in carbonate sediments has been recorded in West-Africa (Goto et al., 2021; Kurzweil et al., 2016; Roy, 2006; Schier et al., 2020) and in Brazil (Cabral et al., 2019), but has not yet been found in the northern part of the Guiana Shield. The Mn deposits of the Guiana Shield are found across locations at Matthews Ridge (Guyana), Maripa Hill (Suriname), Pletrug (Suriname) and Apoema Sula (Suriname) (Holtrop, 1962, 1965) and have been interpreted as variably metamorphosed chemical sediments. These sedimentary intercalations occur within tholeiitic metabasalts and other metavolcanic host rocks that form the base of the greenstone belt.

In this study, an initial petrographic investigation is given of the Mn occurrences at Apoema Sula, Maripa Hill and Pletrug in Suriname. The rocks in these areas are metamorphosed to the greenschist to upper amphibolite facies (Kroonenberg et al., 2016), resulting in a mineralogy consisting of Mn-carbonates and gondites together with garnet-biotite-chlorite-amphibole quartzites, enriched in Mn. Because of the coincidence in time with the LE, these may be correlated to Mn-carbonates and gondites found in other cratons (Goto et al., 2021; Kurzweil et al., 2016; Roy, 2006; Schier et al., 2020).

Manganese-rich horizons are of key interest in the greenstone belt as they are likely to form an important stratigraphic marker, in response to favorable redox conditions for Mn deposition that occurred synchronously across depositional basin(s). In addition, they potentially provide constraints on: (I) the physical, chemical, volcano-sedimentary and paleoredox conditions of the basin(s), (II) the possible relation to the LE, and (III) its resource potential and economic implications.

METHODS AND PRELIMINARY RESULTS

Thin sections from existing drill cores of the Maripa Hill (Holtrop, 1962) and Pletrug (Bisschops, 1967) sites were obtained from the Geological and Mining Services of Suriname (GMD) and the Naturalis Biodiversity Center in Leiden (Netherlands). Preliminary fieldwork was carried out at Apoema Sula along the Marowijne River in Suriname.

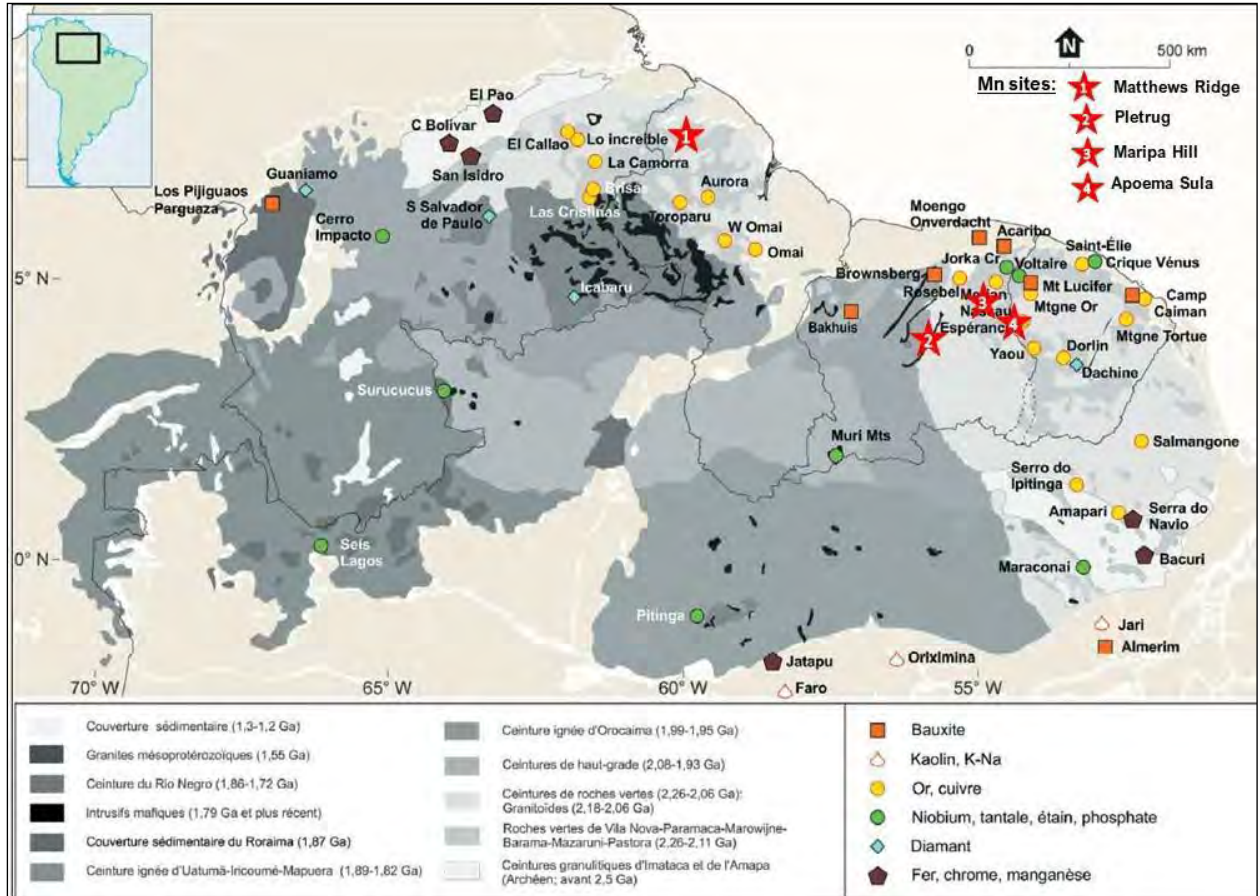


Figure 1: Manganese research areas of the Guiana Shield (reproduced after Jébrak et al. 2020.)

Apoema Sula (Fig.1): Apoema Sula lies within a synclinal fold. During recent fieldwork, rocks such as meta- gabbro and meta-sediments mostly phyllites, organic-rich schists, chloritoid-biotite-quartz schists (Fig.2a) and sericite-chlorite-biotite schists, slightly weathered carbonaceous-chlorite-quartz schists and conglomerates were mapped. Holtrop (1962) encountered spessartine rocks e.g., gondites and spessartine quartzites, which were not found during the recent fieldwork.

Maripa Hill (Fig.1): Maripa Hill is located east of the Brokopondo Lake in Afobaka. The deposit is composed of a folded sequence of alternating gondites, chlorite/biotite-sericite-quartz schist, chlorite/biotite- sericite quartzite, iron-rich quartzite, graphitic quartzite (Holtrop, 1962). Four drill core samples JH5605, JH5606, JH5608 and JH5894 were studied. The gondites are fine grained laminated rock composed of spessartine, biotite, chlorite, clino-suenoite ($\{Mn^{2+}\}Mg_5(Si_8O_{22})(OH)_2$), muscovite and quartz (Fig.2b,c). Tourmaline, calcite and albite locally occur as accessory minerals. Some gondites show distinct layering, crystal orientation and grain size distribution between layers. The organic-rich schists are composed of abundant sericite, graphite, quartz and chlorite. Chlorite commonly occurs as pseudomorph after garnet and sericite is formed at the expense of plagioclase.

Pletrug (Fig.1): Pletrug, located in the center at Suriname, forms a ~200 m high ridge east of the Emma Range. It is composed of metasediments such as spessartine-sericite quartzite, biotite-amphibole-quartz rock, pyroxene-quartzite with well-developed schistosity, amphibole rocks, leucocratic dikes of alkali-granite composition. Northwest of Pletrug ultramafic chromite schists are encountered (Bisschops, 1967). Four drill core samples LF1D, LH1H, LF1J and LB139C were studied. Mn carbonates are composed of ~45% Ca-Mn-carbonates, Mg-Mn olivine ($\{Mg\} 0.42-0.44$ $\{Mn^{2+}\} 1.41-1.74$ SiO_3) and spessartine. The chemistry of the carbonates minerals displays a mixture of Ca, Mg, Fe and Mn. Pyrophanite ($Mn^{2+}TiO_3$) occurs as an accessory mineral (Fig.2d,e). The Mg-Mn olivine crystals have spessartine, Ca-Mn-carbonate as well as pyrophanite inclusions. Most of the spessartine crystals show alteration and weathering both in the rim and in the core into Ca-Mn-carbonate, with few preserving their idiomorphic shape. Gondite is mainly composed of spessartine showing alteration and weathering in the core and the rim, Mn-actinolite, Mn-diospide, calcite (Fig.2f). Titanite occur as an accessory mineral. Barren carbonate rock is composed of calcite and forsterite (LF1H).

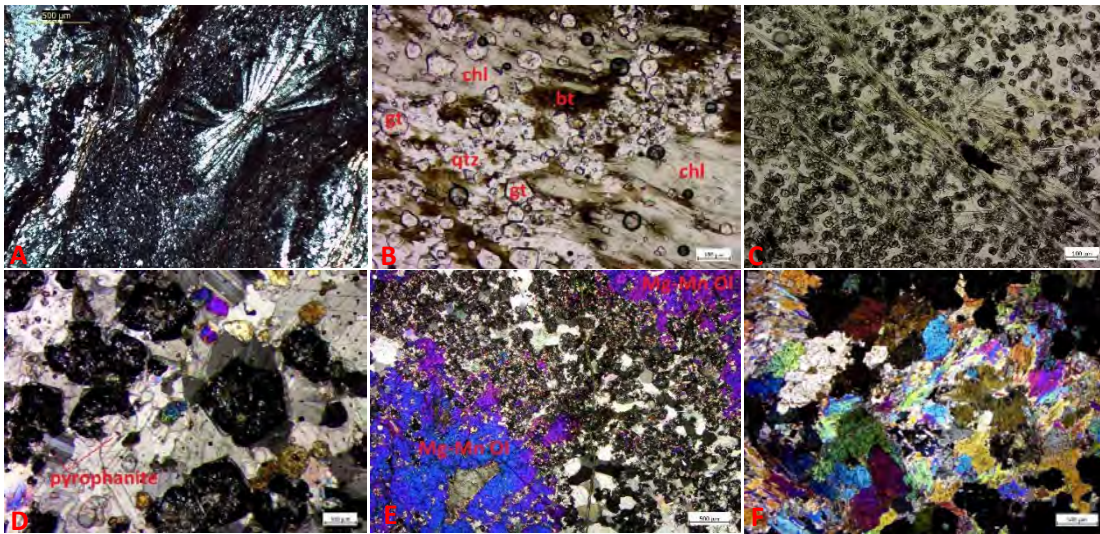


Figure 2: A) Organic-rich schists with radial chloritoid porphyroblasts (SA2123 Apoema Sula). B) Gondite: spessartine, biotite, chlorite and quartz (JH5608 Maripa Hill). C) Gondite: spessartine, clino-suenoite (amphibole) and quartz (JH5605 Maripa Hill). D) Mn carbonate: spessartine, Ca-Mn-carbonate and pyrophanite (LB139C Pletrug). E) Mn carbonate: spessartine, Mg-Mn olivine, Ca-Mn-carbonate and pyrophanite (LF1D Pletrug). F) Gondite: spessartine, Mn-actinolite, Mn-diospide and calcite (LF1J Pletrug).

The next step forward is the study of the chemical characteristics, REE behavior in the individual minerals of the Mn-carbonates and gondites, and to search for a possible seawater signature. Geochemistry and carbon isotope signals might reveal similarities or differences with deposits elsewhere in South America and West Africa. Fieldwork to Matthews Ridge is crucial because literature study shows that the metamorphic grade is lower than at Maripa Hill and Pletrug, possibly preserving primary signatures of the precursor of the Mn deposit.

ACKNOWLEDGEMENTS

Both SAXI and the University of Western Australia are thanked for sponsoring this PhD research.

REFERENCES

Bekker, A., & Holland, H. D. (2012). Oxygen overshoot and recovery during the early Paleoproterozoic. *Earth and Planetary*

Science Letters, 317–318, 295–304.

- Bisschops, J.H. (1967). Manganererts op de Pletbrug. Geologisch Mijnbouwkundige Dienst van Suriname. *Internal Report*, 40 p.
- Cabral, A. R., Zeh, A., Vianna, N. C., Ackerman, L., Pašava, J., Lehmann, B., & Chrastný, V. (2019). Molybdenum-isotope signals and cerium anomalies in Palaeoproterozoic manganese ore survive high-grade metamorphism. *Scientific Reports*, 9(1), 1–7.
- Goto, K. T., Sekine, Y., Ito, T., Suzuki, K., Anbar, A. D., Gordon, G. W., Harigane, Y., Maruoka, T., Shimoda, G., Kashiwabara, T., Takaya, Y., Nozaki, T., Hein, J. R., Tetteh, G. M., Nyame, F. K., & Kiyokawa, S. (2021). Progressive ocean oxygenation at ~2.2 Ga inferred from geochemistry and molybdenum isotopes of the Nsuta Mn deposit, Ghana. *Chemical Geology*, 567(February), 120116.
- Holtrop, J. F. (1962). De manganafzettingen van het Guyana Schild. Geologisch Mijnbouwkundige Dienst van Suriname. *Mededeling* 13, 514 p.
- Holtrop, J. F. (1965). The Manganese Deposits of the Guiana Shield. In *Economic Geology* (Vol. 60).
- Jébrak, M., Kroonenberg, S., Heuret, A. (2020). Les mines du Bouclier guyanais: esquisse historique et métallogénique. *Les ressources des guyanes*, 30-35.
- Kroonenberg, S. B., de Roever, E. W. F., Fraga, L. M., Reis, N. J., Faraco, T., Lafon, J. M., Cordani, U., & Wong, T. E. (2016). Paleoproterozoic evolution of the Guiana Shield in Suriname: A revised model. *Geologie En Mijnbouw/Netherlands Journal of Geosciences*, 95(4), 491–522.
- Kurzweil, F., Wille, M., Gantert, N., Beukes, N. J., & Schoenberg, R. (2016). Manganese oxide shuttling in pre-GOE oceans – evidence from molybdenum and iron isotopes. *Earth and Planetary Science Letters*, 452, 69–78.
- Maheshwari, A., Sial, A. N., Gaucher, C., Bossi, J., Bekker, A., Ferreira, V. P., & Romano, A. W. (2010). Global nature of the Paleoproterozoic Lomagundi carbon isotope excursion: A review of occurrences in Brazil, India, and Uruguay. *Precambrian Research*, 182(4), 274–299.
- Roy, S. (2006). Sedimentary manganese metallogenesis in response to the evolution of the Earth system. *Earth-Science Reviews*, 77(4), 273–305.
- Schier, K., Bau, M., Smith, A. J. B., Beukes, N. J., Coetzee, L. L., & Viehmann, S. (2020). Chemical evolution of seawater in the Transvaal Ocean between 2426 Ma (Ongeluk Large Igneous Province) and 2413 Ma ago (Kalahari Manganese Field). *Gondwana Research*, 88, 373–388

An assessment of trace element geochemistry of paleo-surface gravels, lateritic regolith and rock outcrops for the potential of Strategic Minerals (other minerals), Base Metals and Orogenic Gold Formation processes within Potaro Mining District # 2.

John Applewhite-Hercules,

Master Mineral Resources, University of Queensland, Brisbane Australia.

Senior Geologist, Guyana Geology and Mines Commission

Economic Geology and Applied Geophysics Lecture University of Guyana

Abstract

Paleo surface gravels found within Small and Medium Scale mining operations have keys that can unlock useful exploration insights for Orogenic Gold formation processes, strategic minerals (other minerals) and base metals occurrences, in Guyana. Trace element geochemistry analysis of paleo surface gravels were conducted within the Potaro Mining District #2, to assess the presence of geochemical proxies that are characteristic of these mineralization products. Good correlations were obtained for Orogenic Gold Mineralization with Arsenic (As), within the Salbora, Red Hole and Black Water locations within Mining District #2.

This research presents a novel exploration approach that utilizes easily accessible sampling mediums (paleo-surface gravels and pit basement sap rock, lateritic regolith and available rock outcrops) within well-established small and medium scale gold mining camps in Guyana. The geochemistry data derived from this and other similar projects within various mining camps/mining districts can give useful exploration insights into potential areas for follow up investigation where there are suspected geophysical and geochemical proxies of deep-seated orogenic gold mineralization processes and the occurrence of strategic minerals (other minerals) and base metals being present.

3 D modelling of paleo-surfaces using airborne electromagnetism (GeoTEM) and Digital Elevation Model(DEM) datasets, in Mali West Africa: adaptations for Small and Medium scale mine operations within the Guiana Shield

John Applewhite-Hercules,

Master Mineral Resources, University of Queensland, Brisbane Australia.

Senior Geologist, Guyana Geology and Mines Commission

Economic Geology and Applied Geophysics Lecture University of Guyana

Abstract

The combined analysis of airborne electromagnetic (AEM) and Digital Elevation Model (DEM) datasets has enabled the construction of a 3 D model of the sub surface's apparent conductivity, within the vicinity of the Syama Mines, Mali, West Africa. This combined analysis has been employed to estimate the thickness of the lateritic paleo-land surface ("glacis") and to identify areas for further exploratory investigations that exhibit anomalous conductivity values associated with high elevations and vice versa. This was accomplished by investigating the spatial relationships that exist between the Digital Elevation Model (DEM) and an ISO surface which represents a constant apparent conductivity value within the subsurface. A strong spatial correlation relationship is observed between the DEM and ISO surfaces of constant apparent conductivities. This spatial relationship allows the estimation of the thickness of the "glacis" of to 175m. This estimated thickness is comparable to thickness the ferricrete observed from drill cores logs of the nearby Mn ore deposit of Tambao in North Burkina Faso. Anomalous high conductivity areas associated with high digital elevation values were also identified within the subsurface 3D model, as possible paleo channels representing good targets for further investigation and research. In addition, comparison of the EM signatures of the VTEM and GEOTEM datasets over the same plot of ground was executed to observe if there are any significant differences in the EM signatures, obtained from the two systems.

OCSH, IH and IR Rhyacian gold deposits of the Guiana Shield

Marc Bardoux
Barrick Gold
mbardoux@barrick.com

Gold is the prime commodity of economic interest of the Rhyacian Cuyuni and Marowijne megabasins (respectively CMB in Guyana and MMB in Suriname and French Guiana) where three principal gold deposit types have been roughly defined to date and only briefly documented (4 PhD's; 3 MSc's in the last 20 years). Well-endowed vein hosted deposits of the MMB are somewhat exclusive to this basin for which a new classification terminology is proposed as OCSH (Orogenic Clastic Sediment Hosted) that emphasizes that auriferous sulphidic veins are nearly exclusively hosted in moderately strained coarse clastic sediments (conglomerate to sandstone) where veins are most related to very discrete (metric) high strain zones. Fluids in OCSH veins are likely predominantly of metamorphic origin. Tungsten anomalism is commonly related to altered rutile (not plutonic related). Arsenic anomalism is mainly related to black shales. Vein gold deposits of the CMB are generally hosted inside or on the immediate edges of felsic plutonic bodies of varied sizes (plugs to batholiths) where edge strain is amongst the highest encountered in the Rhyacian realm. A large variety of vein orientations and types occur in each of these IH deposits. Many IH veins are polymetallic and commonly yield telluride pathfinders confirming their SCLM sourcing. Strain regimes of most deposits vary from pure shear (coaxial, elongated) to simple shear (non-coaxial, no length change, rotational) states which produce different vein networks that need to be discerned to optimize targeting in 3D. Thus, a new terminology is also proposed for these orogenic gold deposit types as PSO (pure shear orogenic) and SSO (simple shear orogenic). Their determination relies principally on the final shape of strain markers and the finite orientation of mineral stretching lineations. There are clearly multiple gold events spread over nearly 80Ma across the Guiana Shield (starting with co-magmatic settings ca 2160Ma at Yaou, Las Christinas, Camp Caiman and ending with late tectonic phases ca 2080Ma at Karouni) supporting the concept that much Rhyacian gold started mobilizing in a magmatic (polymetallic) state and (additional?) gold ended up in mesothermal vein states (and confined sodic, potassic and calcic orogenic style alteration halos). Sparse geochronology suggests that tectonic regimes affecting the CMB deposits may have terminated 20Ma later than in the MMB. This may relate to tectonic partitioning between the two megabasins around a giant metamorphic/UHT/TTG landmass that separates the two basins and defined by the Bartica Gneiss Complex and the Bakhuis Horst (separated by the Mesozoic Takutu Grabben) that are two very prominent lithospheric highs that may have caused tectonic partitioning on their respective boundaries.

The Oko West gold deposit – a new discovery in the Guiana Shield

Carlos H. Bertoni
Interim CEO
Reunion Gold Corporation ,
cbertoni@reuniongold.com

Deuel Garner
Jorge Tachibana
Justin van der Toorn
Mauricio Felmer
Rayon Abrams
Reshud McLennan,
Zerihun Tsige

SUMMARY

Reunion Gold's Oko West project is a grassroots gold discovery at the Oko mining camp in northwest Guyana, located at the watershed of the Cuyuni and Mazaruni rivers. In 2021, following up on soil geochemical anomalies and trenching, an initial drill program discovered and confirmed the presence of gold mineralization in shear zones along the contact between a volcano-sedimentary sequence and a granitoid pluton. This trenching and drilling work tested the northern 2.5 km (the Kairuni zone) of a 6 km long soil geochemical gold anomaly, where most of the 40 thousand meters of follow-up drilling to date has taken place. The southern 3.5 km of that geochemical anomaly (called the Takutu zone) remains largely untested and represents one of several priority exploration targets on the project.

The Kairuni zone's ongoing drill program shows gold mineralization in saprolite and unweathered rocks and good continuity along its 2.5 km strike length. The deepest hole drilled intersected strong gold mineralization at a vertical depth of 575 meters, and the zone remains open along strike and depth. Reunion Gold continues drilling the Kairuni and Takutu zones and plans to release a maiden mineral resource in 2023.

Gold mineralization is typically orogenic type, hosted by Proterozoic clastic and volcanoclastic rocks strongly deformed by at least two tectonic events, which caused intense fracturing and shearing and created large and porous zones favourable for the emplacement of mineralizing fluids. Carbonate and sericite alteration accompanying pyrite in quartz veining and stockworks are typically associated with gold mineralization. The sedimentary sequence hosting gold mineralization in the Kairuni zone is flanked by hanging and footwall granitoids which appear to have had a significant role in the deformation history.

The Oko West gold deposit is an excellent example of the mineral endowment of the Guiana Shield, showing that there is still potential to discover large gold systems that are not necessarily indicated by artisanal mining. Fundamental geological thinking identifying features from orogenic gold deposits in other parts of the world, and using proper exploration tools will reward diligent explorers.

Key words: Guiana Shield, mineral exploration, Guyana, Oko West, orogenic gold.

INTRODUCTION

Reunion Gold's Oko West project is a grassroots gold discovery in northwest Guyana's historical "Oko" gold district, where alluvial and primary gold has been artisanally mined for decades. The project is about 100 km due west of Georgetown, at the watershed of the Cuyuni and Mazaruni rivers, and consists of one Prospecting License with an area of 44 square kilometres, accessible by laterite roads. Reunion Gold optioned the ground in 2018 from local entrepreneurs and controls 100% of the project.

EXPLORATION

The alluvial workings draining a ridge straddling the contact between a granitoid pluton and a greenstone sequence encouraged Reunion Gold to option the ground (Figure 1). The eastern flank of this ridge, and likely the source area for the alluvial gold, did not show any significant pits or workings, suggesting that the primary mineralization had not yet been

discovered. It was also noticeable that G2 Goldfields had identified significant primary gold mineralization at the Crusher Hill prospect, some 2 km north of the project boundary.

Reunion Gold flew the area with detailed airborne magnetometry and radiometric survey and launched a soil geochemistry program with samples collected at 50 m intervals over 200 m-spaced lines. The geophysical survey mapped the granitoid and greenstone contact, and soil geochemistry quickly identified a significant gold anomaly straddling the contact for approximately 6 km (Figure 1). To confirm the presence of gold mineralization in saprolite bedrock, trenches were dug along soil lines, and channel samples were collected systematically on trench walls. This trenching program focused on the northernmost 2.5 km section of the soil anomalies, which was named the Kairuni zone after the creek draining the target area. Several trenches revealed the presence of significant mineralized intervals in saprolite, like that of trench T21-44, which assayed 5.98 g Au/t over 69 m.

Late in 2020, Reunion Gold had limited exploration funds available, and the company tested the depth extension of mineralization with only 1,000 m of core drilling. The drilling results from this first campaign confirmed that gold mineralization extended into unweathered bedrock to a vertical depth of about 120 m, mainly in the sedimentary sequence – drill hole D-1 intersected 1.54 g/t over 20.1 m. Reunion Gold continued trenching, and only in June 2021 could raise sufficient funds to launch a comprehensive drilling program with two diamond drill rigs and one reverse circulation rig. In June 2022, Reunion Gold announced the deepest mineralized intersection in the Kairuni zone, where hole D-112 cut 3.68 g Au/t over 71.15 m at a vertical depth of 575 m (Figures 3 and 4). The drilling program continues to expand, and by November 2022, it had drilled more than 40,000 m of core and 25,000 m of reverse circulation (Figure 2).

GEOLOGY AND GOLD MINERALIZATION

The Oko West project area lies at the north-south striking contact between rocks of the Barama Group greenstone belt (2.12 Ga) to the west and a granitoid pluton to the east. The Barama Group sequence comprises mafic volcanic flows, volcanoclastics, and siliciclastic and carbonaceous sediments hosting significant gold mineralization.

The pluton flanking the Oko West deposit to the east and acting as its hanging wall does not appear to belong to the Bartica Gneiss complex (Figures 1, 2, 4 and 5). It is a later intrusion of unknown dimensions, being less foliated and lacking evidence of partial melting, hereby called the "Oko pluton." A sample from the "Bryan pit" area was dated by Tedeschi (2018) at 2107±6 Ma. The rock is mostly coarse-grained and little foliated, described petrographically by Thompson (2022) as a metamorphosed quartz-monzodiorite and granodiorite. At the deposit scale, its contact with the volcano-sedimentary sequence to the west is sharp and locally sheared. There is no evidence of pre- or syn-orogenic contact metamorphism. The locally fractured and sheared zones near its western contact can be mineralized but do not appear to build into significant masses.

The sequence hosting the bulk of the Oko West gold mineralization is composed essentially of sedimentary rocks: siliclastic, volcanoclastic, and carbonaceous, and is better understood in the so-called Kairuni zone, the 2.5 km northernmost extent of the soil anomaly (Figures 1 and 2). The sequence is 100-200 m wide and has an overall tabular shape, dipping steeply to the east and "sandwiched" between the Oko pluton to the east and a granitoid sill to the west (Figures 2, 4 and 5). The sedimentary units are intercalated and strongly deformed, their spatial position conditioned by their original deposition and polyphase folding.

- The siliclastic sediments correspond to interlayered sandstones and siltstones (Figures 4, 5 and 6). They present a pale green/beige colour and are usually highly sericitized and moderately chloritized, with quartz and probably fully sericitized and/or kaolinized feldspar. They show clear bedding, preserved even in zones of intense S_2 fabric development, and local evidence of crossbedding. The weathered product of these sedimentary rocks is generally yellow/orange. Sandstone-dominated rocks occasionally appear near the contact with volcanoclastics, in a transition zone between volcanic tuffs and siliclastic sediments.
- Mafic to intermediary volcanoclastics show evidence of bedding and crossbedding, suggesting a volcano-sedimentary origin, and present numerous imbricated quartz-carbonate veinlets transposed to the foliation (Figure 7). Volcanoclastic rocks are highly chloritized and usually have a dark green colour in unweathered rock and a purple colour in weathered rock. They can either be mainly composed of volcanic ashes or larger lapilli clasts. The volcanoclastics can also show some evidence of siliclastic elements, such as quartz and sericite, as a gradual transition zone between these tuffs and the siliclastic sediments can occur instead of a sharp contact. Increasing siliclastic elements can then be

observed towards the contact with siltstone or sandstone. Moreover, the frequent numerous transposed quartz-carbonate veinlets can give them a strong bedding-like characteristic.

- Carbonaceous sediments correspond to siliciclastic turbidite-like facies, alternating fine carbonaceous-bearing sandstone/siltstone, and fine graphite-rich (carbonaceous material) shale layers (graphitic schists) (Figure 8). Due to the weak nature of the carbonaceous material, this lithology also composes a preferential "decollement" layer accommodating most of the bedding-parallel slippage during folding. This bedding-parallel slippage is responsible for small intrusive bodies (intercalated sediments and granitoid) and the emplacement of mineralized dark grey quartz extension and shear veins.

The petrography study by Thompson (2022) shows that the metaclastites, matrix carbonate, plagioclase, chlorite, and white mica are recrystallized protolith minerals and/or metamorphism products and that the overall rock composition remains essentially unchanged.

The sedimentary sequence shows a strongly sheared contact with a footwall granitoid (Figures 4 and 5). This shear zone can be up to 20 m wide, showing even mylonitic textures, hosted mainly by the sediments. The footwall granitoid has a sill-like geometry up to 120 m wide, and its composition overlaps the classification boundaries between granodiorite and quartz monzonite. Bent plagioclase, polygonised quartz, and multiple chlorite-white mica-rutile-magnetite shear seams are evidence of deformation during lower greenschist regional metamorphism (Thompson, 2022).

The western contact of the granitoid sill is a mafic volcanic rock extending westwards to the center of the project area (Figures 1 and 2). Duricrust formed from the weathering of these rocks holds the topography on the ridge flanking the deposit and with a north-south orientation. A whole rock analysis by Tedeschi (2022, pers. comm.) reveals that it has a tholeiitic basalt composition.

Oko West outcrop and core observations by Lacroix (2022), Hainque & Lacroix, 2022), and the project geologists demonstrate that the area is marked by polyphase deformation, with a first N-S tight folding (from D_1 tectonic event) followed by a second E-W fold overprint (from D_2 tectonic event). Gold mineralization occurs predominantly within volcanoclastic, siliciclastic, and carbonaceous sediments, characterized by silica, carbonate, sericite, and sulphide alteration (Figures 9 and 10). The mineralized intervals are generally associated with boxwork or stockwork composed of quartz/quartz-carbonate shear veins (SV) and multiple generations of extension veins (EV). During fold tightening, the early-stage EV were transposed to the foliation by bedding-parallel slip. Later EVs are crosscutting $S_{1/0}$ and the first generations of EVs, marking a deformation continuum. One major D_1 event was probably responsible for the continuous development of the main quartz/quartz-carbonate EV-SV system (D_{1a} and D_{1b}). A late D_1 brittle deformation controlling the mineralization occurs as sulphide-bearing veins/veinlets crosscutting, and sometimes offsetting, previous generations of EV, SV, or veinlets. This deformation is probably related to a late stage of F_1 tightening, marked by a more brittle characteristic in a material hardened by metasomatism (from the intrusions and fluids), tight folding, and rocks being crushed against the two granitoids. The D_2 event is associated with the development of S_2 crenulation and may be related to the emplacement of the late EV_2 vein system, with a possible redistribution/concentration of gold along D_2 fold hinges. It results in a complex type-2 fold pattern, affecting both the stratigraphy and the main (D_1) bedding parallel mineralization system. In summary, the mineralized sediments record a complex history of vein formation and shearing that overlapped in time and space with lower greenschist regional metamorphism.

The understanding of Oko West's geology and mineralization is in its early days, but it is a classic example of an orogenic gold deposit in the Guiana Shield. It demonstrates the region's gold endowment and the opportunities for new discoveries, even in known mining camps, using adequate exploration methods and persistence.

ACKNOWLEDGEMENT

David Fennell, Reunion Gold's Executive Chairman, has been the visionary leader of gold exploration in the Guiana Shield. To his credit and the geology teams working with him, the discovery and development of most of the known gold deposits in the region: Omai, Rosebel, Paul Isnard (Montagne d'Or), Dorlin, Yaou, and now Oko West. David's persistence, knowledge, and faith in the Shield's endowment have bought remarkable and sustainable economic development to the region.

REFERENCES

Hainque, P-J. & Lacroix, B., 2022. Geological and structural investigation of the Oko West project. GexplOre report RP_022_2022.

Lacroix, B., 2019. Structural investigation of the Oko West project. GexplOre report RP_001_2022.

Lacroix, B., Hainque, P-J, Hauteville, A., Lahondes, D., L Goff, E., Fournier, D., Bertoni, C. Taravella, St. & Witasse, M., 2022. The role of polyphase folding in the distribution of gold: Insights from the Guiana Shield. SAXI, XII Interguiana Geological Conference.

Tedeschi, M., 2021. Oko prospect visit report. Internal Reunion Gold report.

Thompson, P.H., 2022. Protoliths, alteration and mineralization of metamorphosed clastic and granitoid samples from Oko West. Reunion Gold internal report.

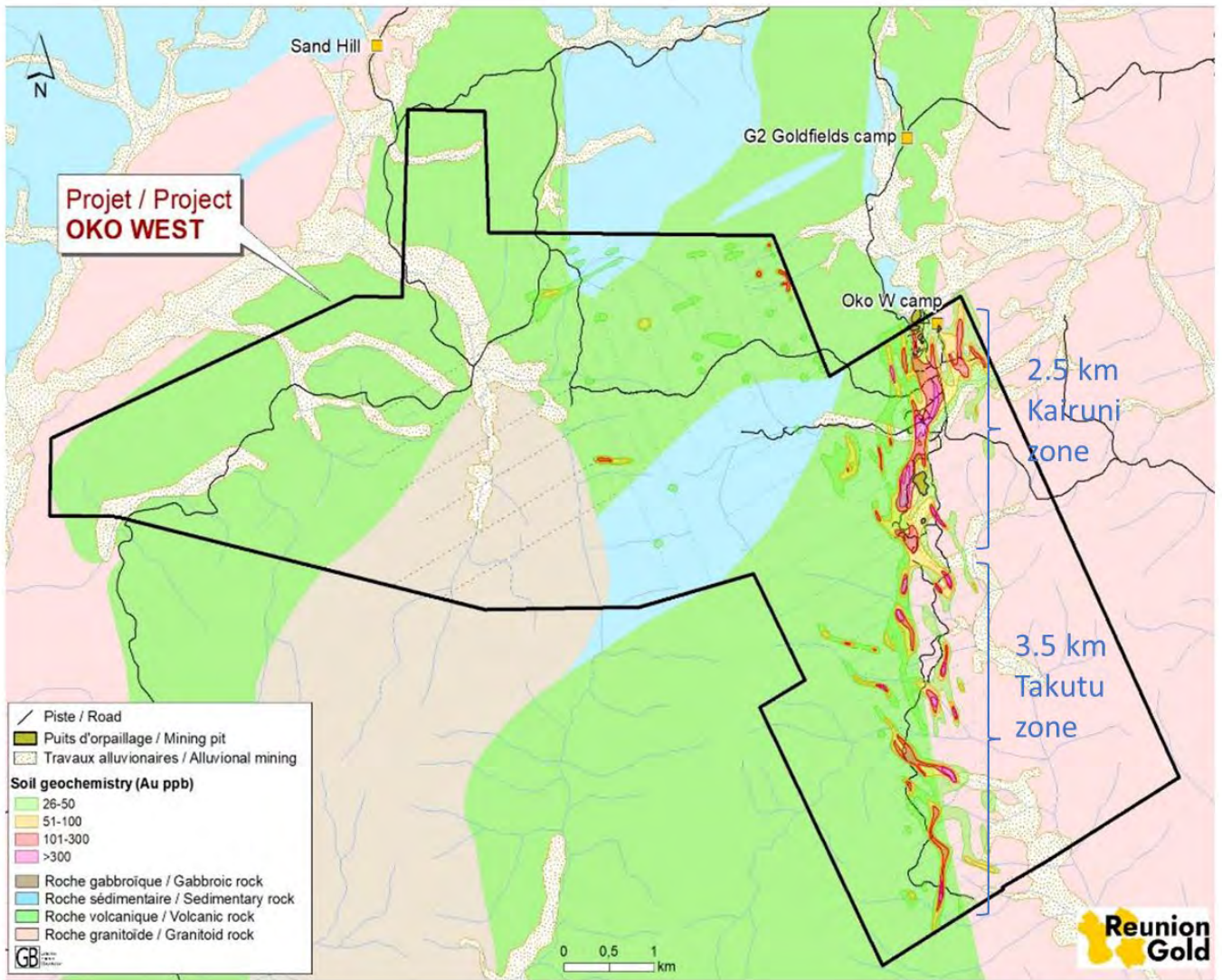


Figure 1. Simplified geological map of the Oko West area showing the soil geochemical anomalies along the contact of a granitoid pluton and a volcano-sedimentary sequence. The Kairuni and Takutu zones define exploration targets.

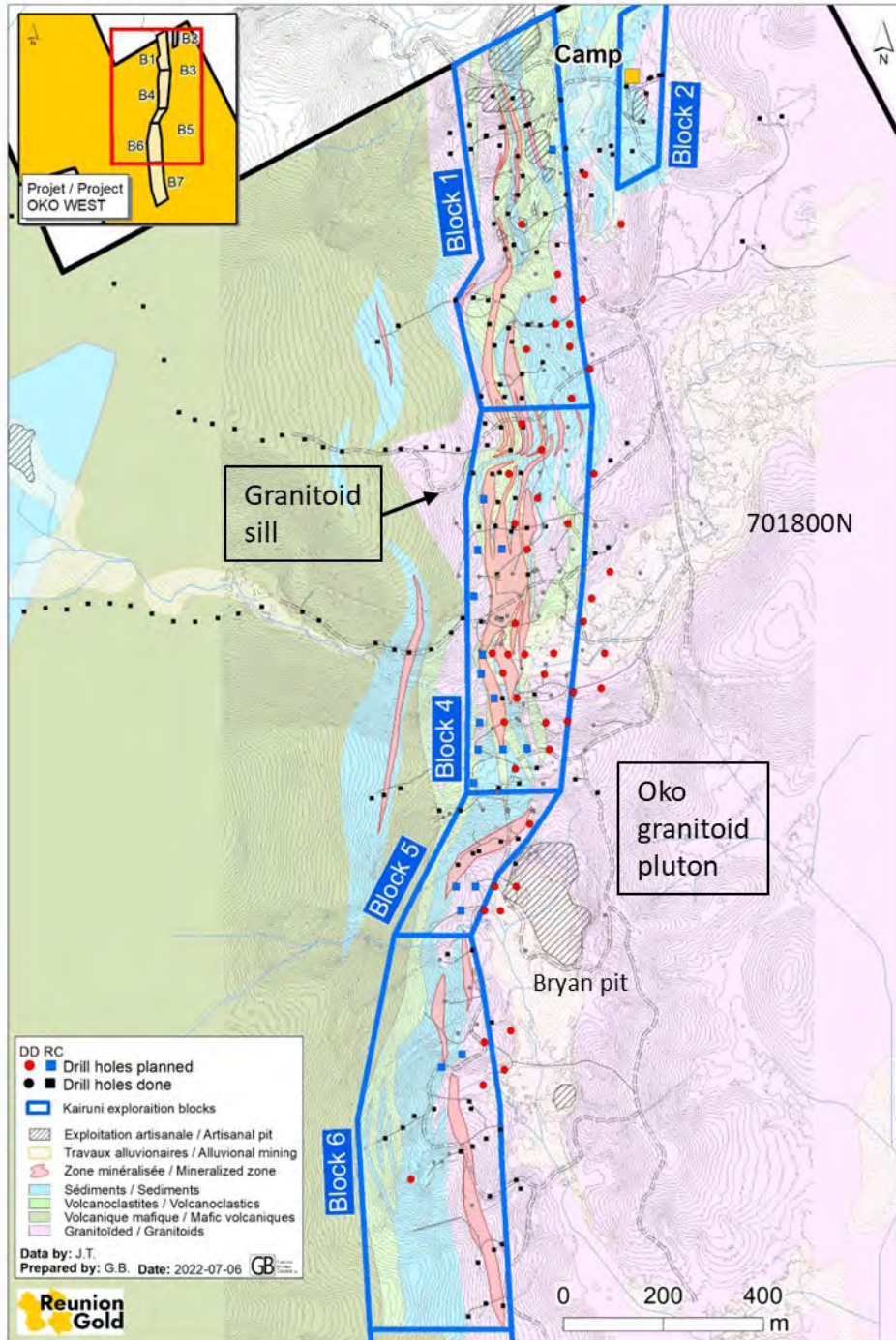


Figure 2. Oko West: Simplified geological map of the Kairuni zone showing existing and planned drill holes and projection of gold mineralized zones to the surface. The Kairuni zone was subdivided into exploration blocks (1 to 6) for planning purposes.

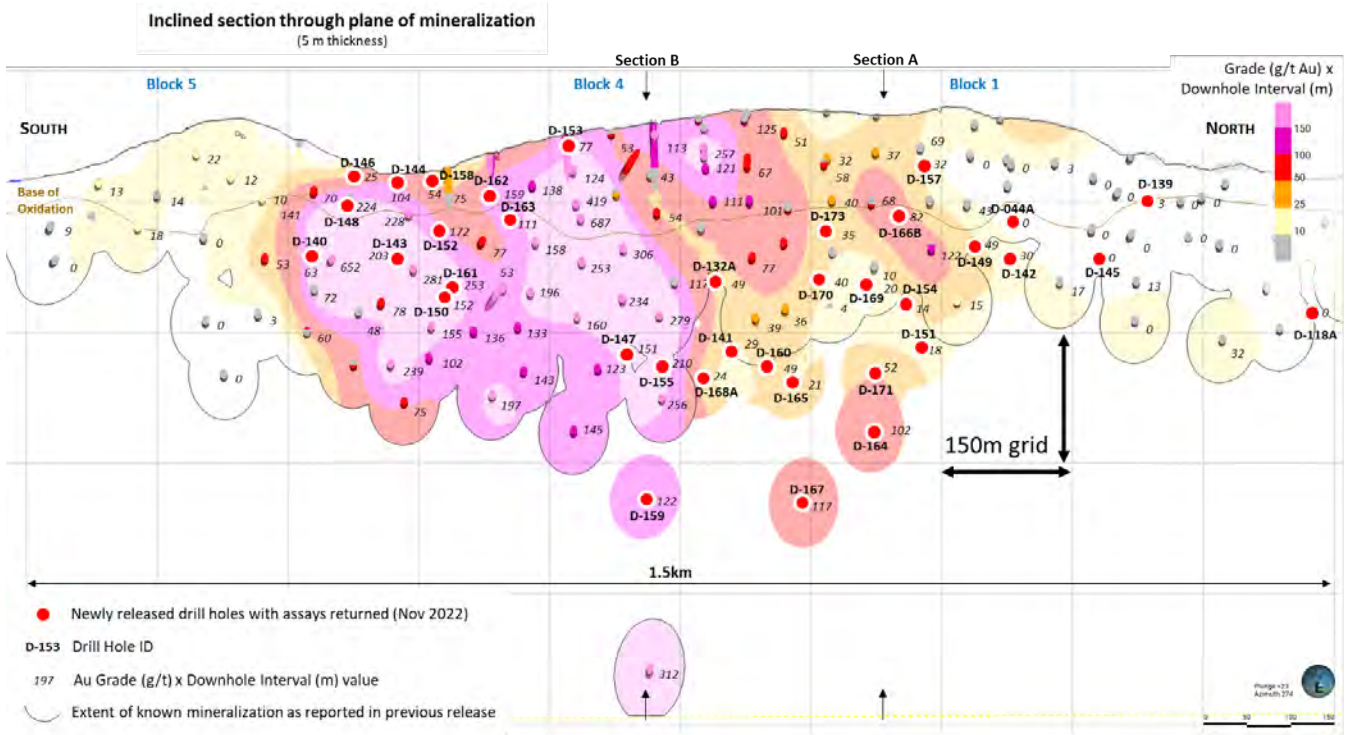


Figure 3. Oko West, Kairuni zone: Long section through plane of mineralization showing drillholes released in November 2022, grade x downhole interval values, and section locations on exploration blocks 1 and 4.

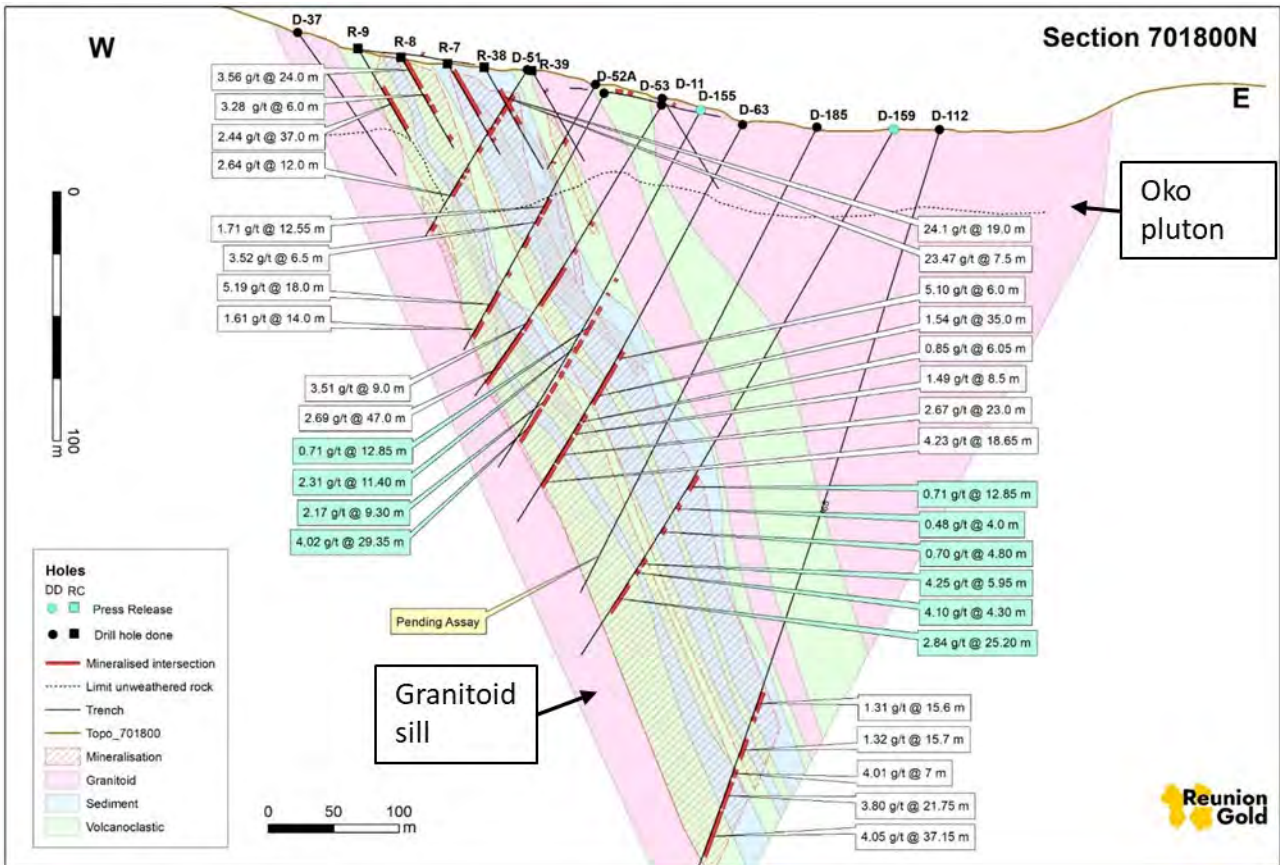


Figure 4. Oko West, Kairuni zone, block 4: Section B on figure 3, 701800N - Significant drill intervals overlain on geological interpretation. Green intersections were released in November 2022. Intervals shown in the section were calculated using a 0.3 g/t Au cutoff, 2 m minimum length, and 3 m maximum length for internal dilution.

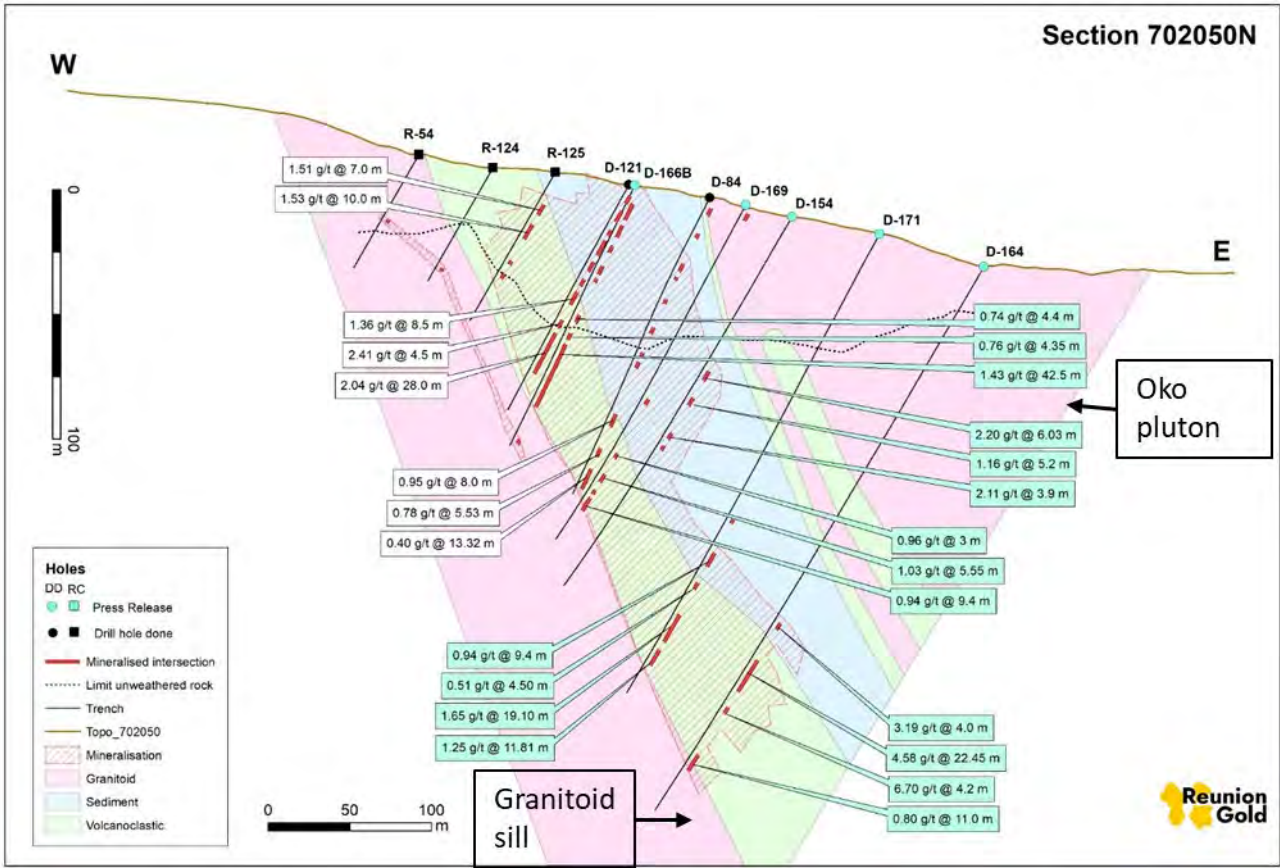


Figure 5. Oko West, Kairuni zone, block 1: Section A on figure 3, 702050N - Significant drill intervals overlain on geological interpretation. Green intersections were released in November 2022. Intervals shown in the section were calculated using a 0.3 g/t Au cutoff, 2 m minimum length, and 3 m maximum length for internal dilution.

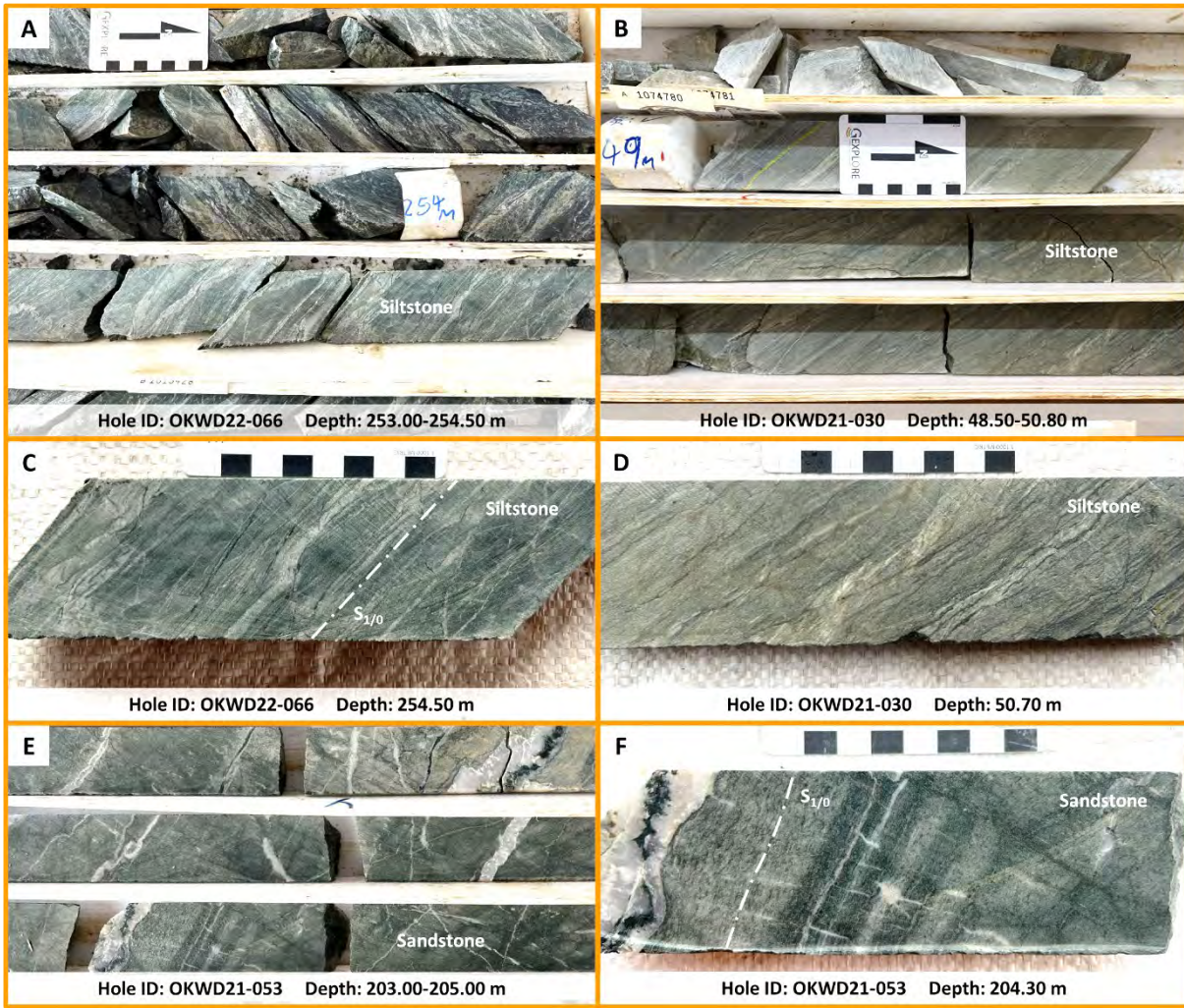


Figure 6. Oko West: Core samples of siltstone and sandstone.

A and B: Siltstone-dominated rock in holes OKWD22-066 and OKWD21-030. C and D: Detail pictures of bedded siltstones in holes OKWD22-066 and OKWD21-030. E: Sandstone-dominated rock in hole OKWD21-053, crosscut by several quartz veins. F: Detail picture of well-sorted sandstones in hole OKWD21-053.

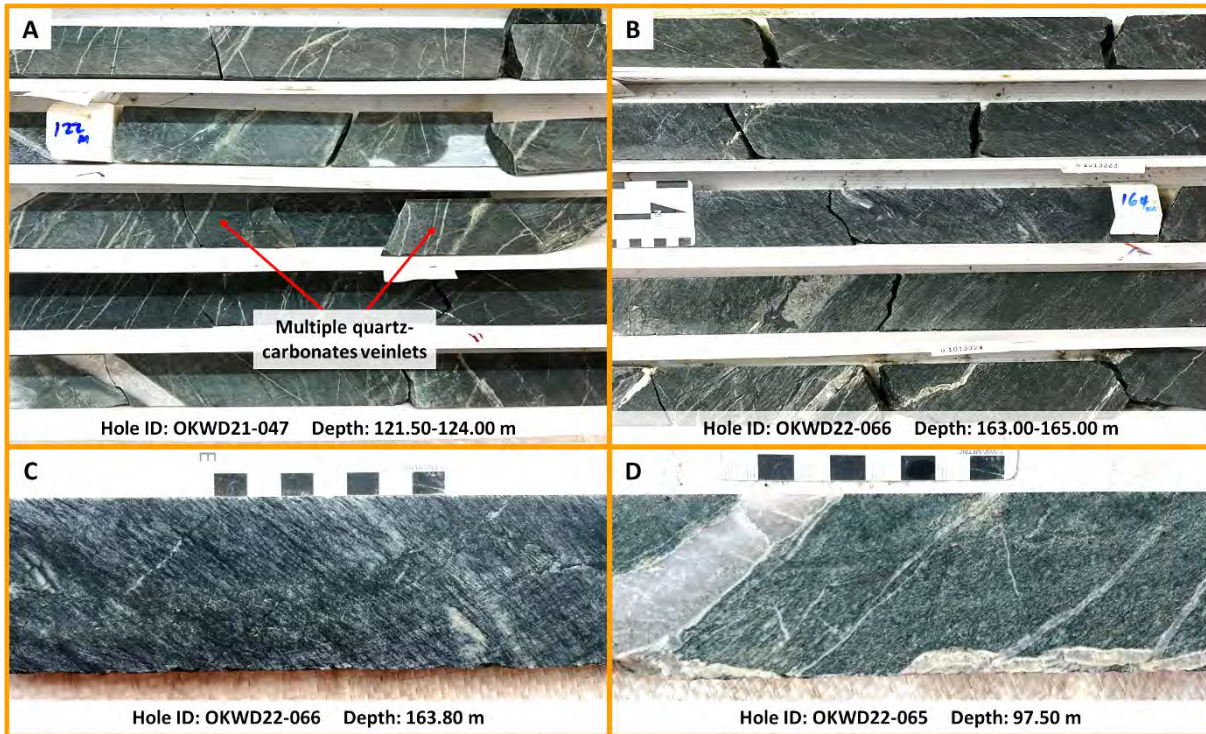


Figure 7. Core samples of volcanics.

A: Fine volcanics with imbricated quartz-carbonate veinlets transposed to the main foliation in hole OKWD21-047. B: Coarser and bedded volcanics showing evidence of bedding in hole OKWD22-066. C and D: Detail picture of bedded volcanics in holes OKWD22-066 and OKWD22-065.

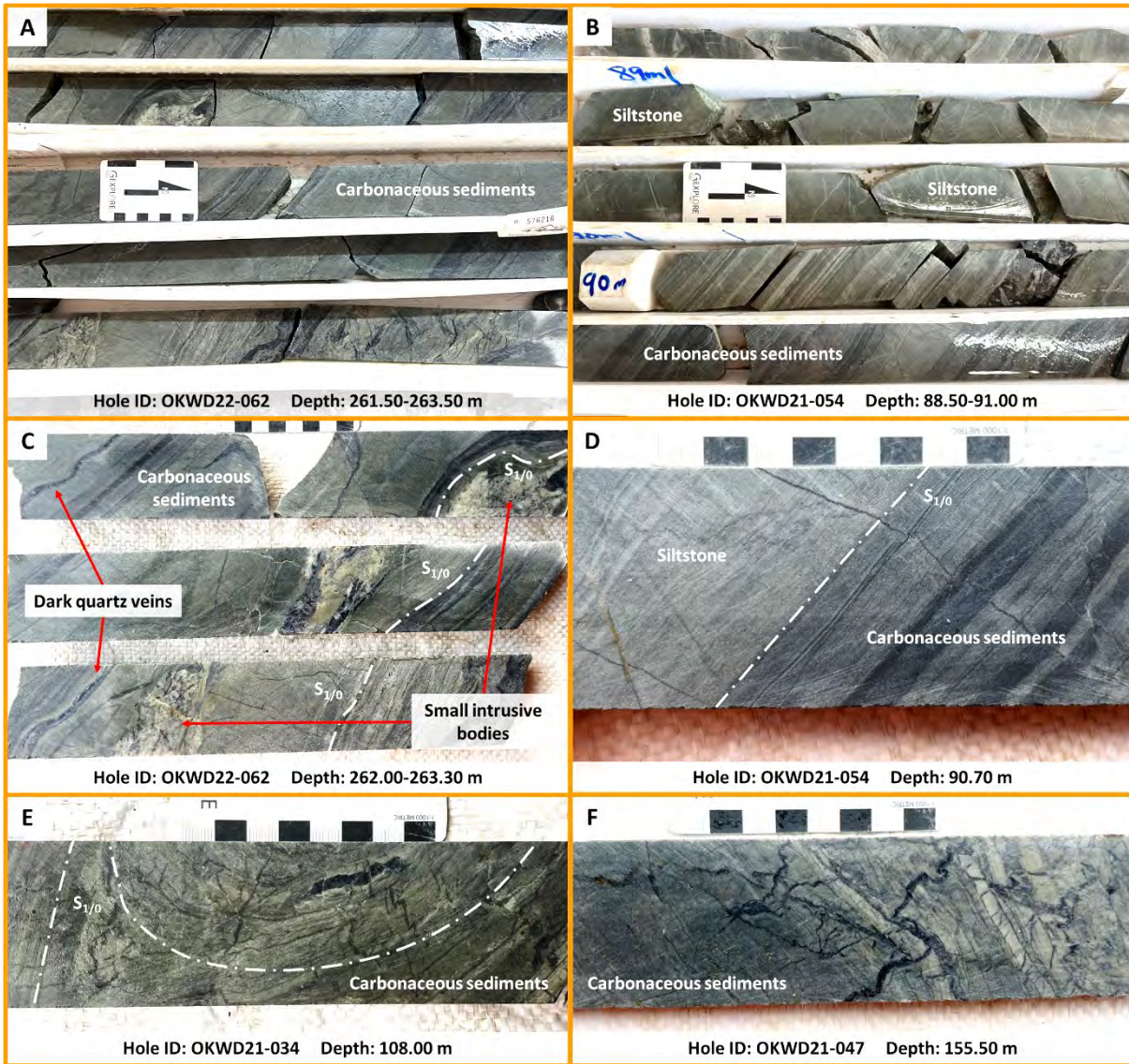


Figure 8. Oko West: Core samples of carbonaceous sediments.

A: Carbonaceous sediment in hole OKWD22-062, with clear bedding and several dark quartz veins. B: Bedded siltstone and carbonaceous sediment in hole OKWD21-054. C: Carbonaceous sediment in hole OKWD22-062, with several dark quartz veins, evidence of folding, and small intrusive bodies. D: Detail picture of contact between siltstone and carbonaceous sediment in hole OKWD21-054. E: Detail picture of folded carbonaceous sediment in hole OKWD21-034. F: Detail picture of carbonaceous sediment crosscut by multiple small dark quartz veins in hole OKWD021-047.

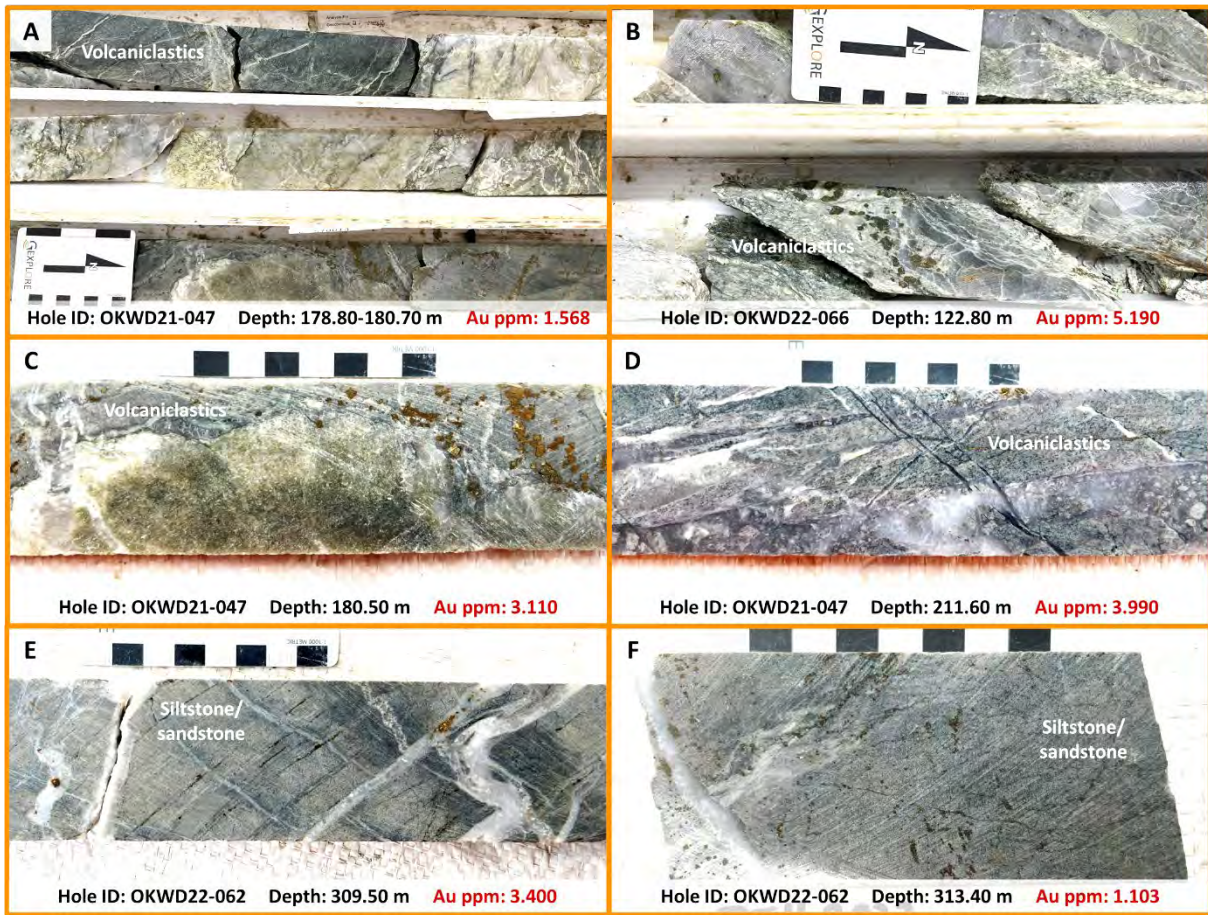


Figure 9. Oko West: Examples of mineralization in volcaniclastics and siltstones/sandstones.

A: Mineralized volcaniclastic interval in hole OKWD21-047, with strong silicification and carbonatization, associated with metasomatism. B: Mineralized volcaniclastic interval in hole OKWD22-066, with multiple large pyrites. C: Metasomatism from the hydrothermal fluid and multiple pyrites showing pressure shadows in hole OKWD21-047. D: Highly strained and fractured mineralized volcaniclastic interval with multiple sulphide-bearing quartz-carbonate veins in hole OKWD21-047. E and F: Mineralized siliciclastic interval with multiple sulphide-bearing quartz-carbonate veins and veinlets in hole OKWD21-062.

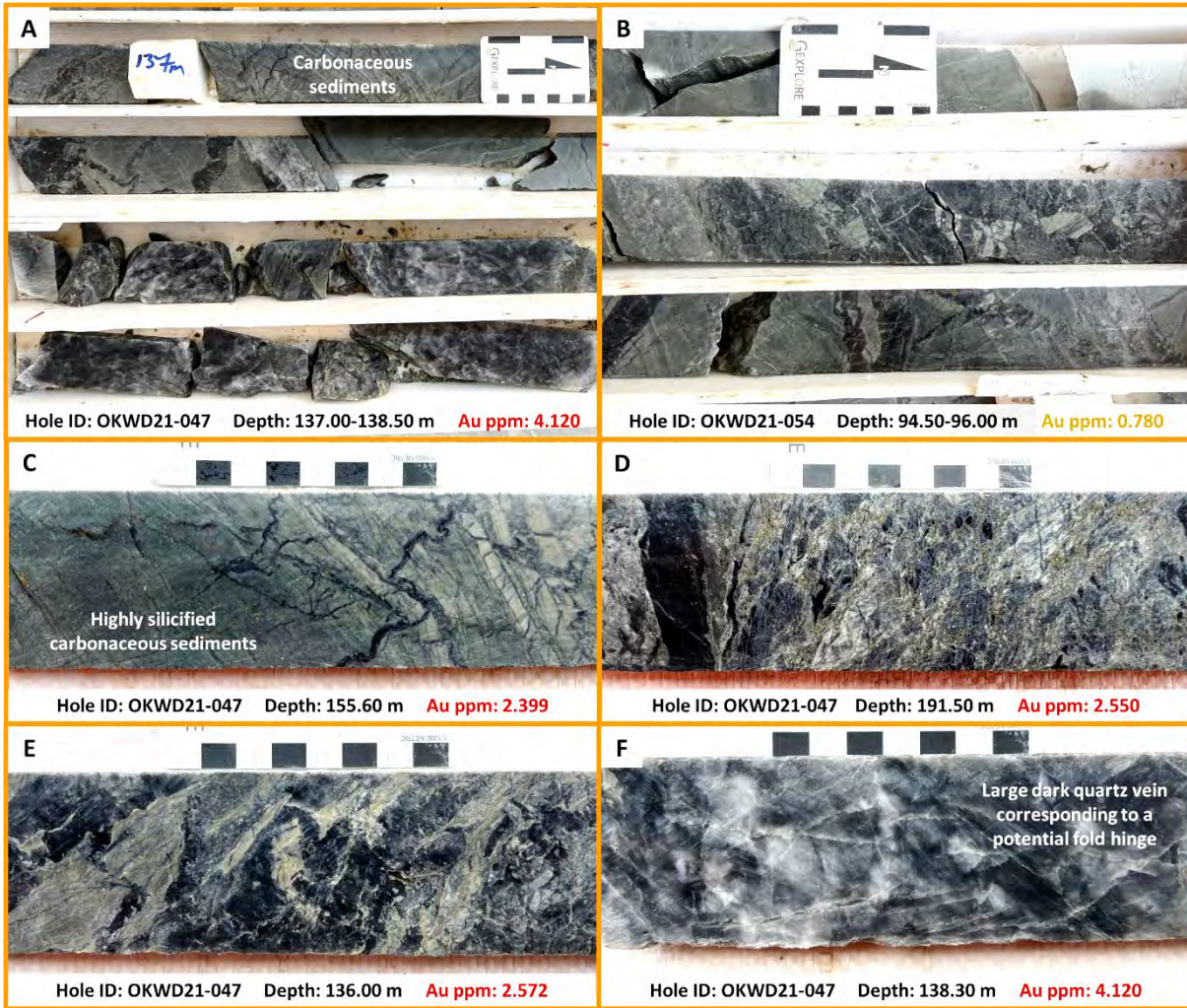


Figure 10. Oko West: Examples of mineralization in carbonaceous sediments.

A and B: Mineralized carbonaceous sediment intervals in holes OKWD21-047 and OKWD21-054, with strong silicification and carbonatization. C: Mineralized stockwork in hole OKWD21-047. D: Highly brecciated mineralized interval with strong silicification, carbonatization, and sulfidation in hole OKWD21-047. E: Folded sulphide-bearing dark quartz-carbonate veins in hole OKWD21-047. F: Large dark quartz-carbonate vein corresponding to a potential fold hinge in hole OKWD21-047.

Transamazonian “Cusp Tectonics” in the Guiana Shield (Abstract only, no presentation)

Frank F. Beunk

Emond W.F. de Roever

Vrije Universiteit, Dept. of Earth Sciences

De Boelelaan 1085, 1081 HV Amsterdam, the Netherlands

f.f.beunk@vu.nl

ederoever@ziggo.nl

Summary

Vertically plunging folds and lineations throughout the high-grade Cauarane-Coeroeni Belt in southern Guyana are ascribed to horizontal constriction imposed by a syntaxial bend (cusp) of a convergent plate boundary, centered on the Bakhuis Granulite Belt of W. Surinam.

Key words: Kanuku migmatites and granulites, Bakhuis granulite belt, orocline, orogenic syntax

The applicability of plate tectonic concepts to Precambrian Earth is still contentious. However, from the identification of 2.2-2.0 Ga blueschist facies metamorphism in Eburnean greenstones in the West African craton, temporally and tectonically equivalent to the Transamazonian orogen in the Guiana Shield, Ganne et al. (2019) concluded that modern-style plate tectonics existed in Palaeoproterozoic time (see also Cawood et al., 2018, and Brown et al., 2022). Then, identification of plate tectonic setting of Palaeoproterozoic magmatic suites by ‘chemo-tectonics’ based on present day settings is equally justified. In the Guiana Shield, Fraga et al. (2009) first identified subduction of the high-grade supracrustal Cauarane-Kanuku-Coeroeni belt (Fig. 1) to the north along the southern margin of the western granite-greenstone belt, starting around 2.04 Ga. Mahabier and De Roever (2018) showed that the Caicara-Dalbana felsic metavolcanics, part of the ca. 1700 km long and 1.99-1.95 Ga old volcano-plutonic Orocaima belt between the high-grade belt and the granite-greenstone belts (Fig. 1), have volcanic arc chemistry. McFarlane et al. (2019) concluded similarly for magmatic suites of the 2300-2070 Ma Sefwi greenstone belt of SW Ghana.

Cusped lithospheric plate boundaries, also known as ‘syntaxes’, occur in present day Earth where structural arcs are joined end to end (Hoffman, 2021). Beunk et al. (2021) identified a fossil syntax in the Guiana Shield, traceable by the map pattern of the 1.99-1.95 Ga old granites and felsic volcanics (Fig. 1), and posited that the syntax played a crucial role in the exhumation of the Orosirian lower crustal Bakhuis granulite belt in western Surinam amidst the upper crustal greenstone belts (Fig. 1). Here we explore tectonic consequences of this ‘Bakhuis syntax’ in the high-grade, 2.08-2.02 Ga Kanuku migmatites and granulites, which transect southern Guyana from west to east, and extend into northernmost Brazil (west) and Surinam (east), see Fig. 1. We summarize their compositional and structural characteristics from Berrangé (1977) and Fraga et al. (2009):

Migmatitic paragneisses form the bulk rock type, with subordinate calc-silicate rocks, dolomitic marbles, amphibolites, metacherts, quartzites, BIFs and metamorphosed mafic and ultramafic rocks. Foliation or gneissic layering is considered to be relic supracrustal stratification. Most of the foliation dips more than 75°. Lineations on the foliation plane are well developed, often better than foliation, and plunge steeply. Axial planar cleavage is absent (note: a common characteristic of migmatite terrains), with foliation-forming biotite flakes and sillimanite needles wrapping around fold hinges. Chaotic (polyclinal) and intrafolial F_1 folds, occasionally accompanied by F_2 chevron-type folds, considered to be synchronous to F_1 , have steeply plunging hinges, (sub)parallel to the lineations. Poles to foliation form gently dipping girdles orthogonal to fold axes and lineations.

The predominance of vertically plunging folds (‘vertical folds’) over large orogenic stretches is unusual. A common setting for their occurrence are oroclines, curved orogens that originate from tectonic bending of originally straight(er) belts, as for example in the Palaeoproterozoic oroclines in the Svecofennian orogen of Sweden (Beunk and Kuipers,

2012). There, apparently similar to the Kanuku mountains of Guyana, steeply dipping (volcano-)sedimentary stratification was rotated along vertical axes into vertical folds on the scales of the regional map down to thin sections for microscopy. A prerequisite for the development of vertical folds of sedimentary layering is their initial rotation from horizontal into the vertical; commonly a first phase of tight, upright 'horizontal folding' (rotation along horizontal axes) is responsible for the steepening. Although crossed girdles of foliation poles in Berrangé's map (1977) imply the presence of near-horizontal folds, these appear to postdate, not predate the vertical rotations. We expect that initial horizontal folding has steepened the sedimentary protoliths of the Kanuku migmatites and granulites.

The map pattern of the high-grade Cauarane-Kanuku-Coeroeni belt forms an broad arch, trending east-west in its western parts, and changing to southeast in its eastern branch in SW Surinam (Fig. 1). Whether such an open oroclinal bend would by itself be sufficient to generate belt-wide (oroclinal) vertical folds is uncertain, but we propose a dominant role for the Bakhuis syntax in the folding of the Kanuku migmatites and granulites. That role is a priori suggested by the map pattern: The axial plane of the bent Kanuku belt strikes right into the center of the syntax. Our proposed model is sketchily illustrated in Fig. 2. A plate subducting from the SW moves directly into the cusp and experiences lateral constriction and folding due to the cusp geometry (see also Hoffman, 2021).

Original (D_1) steepening of sedimentary stratification in the lower plate, by folding on horizontal axes parallel to the plate boundary prior to syntax-induced vertical folding (D_2), would be a logical consequence of the compressional nature of the plate boundary when the incoming plate carries buoyant continental crust. The geometry of Fig. 2 also suggests a transition of Z-type D_2 -folds to the left of the syntaxial axis, to M-type folds along its axis, to S-type folds on the opposite side.

References

- Berrangé, J.P., 1977. The geology of southern Guyana. South America. Institute of Geological sciences, Overseas Memoir 4, 112 pp.
- Beunk, Frank F., Gerrit Kuipers, 2012. The Bergslagen ore province, Sweden: Review and update of an accreted oroclinal, 1.9-1.8 Ga BP. *Precambrian Research* 216-219, 95-119; /10.1016/j.precamres.2012.05.007
- Beunk, Frank F., Emond W.F. de Roever, Keewook Yi, Fraukje M. Brouwer, 2021. Structural and tectonothermal evolution of the ultrahigh-temperature Bakhuis Granulite Belt, Guiana Shield, Surinam: Palaeoproterozoic to Recent. *Geoscience Frontiers*, 12 (2), 677-692; /10.1016/j.gsf.2020.05.021
- Brown M., T. Johnson, C.J. Spencer, 2022. Secular changes in metamorphism and metamorphic cooling rates track the evolving plate-tectonic regime on Earth. *Journal of the Geological Society, London*, 179; /10.1144/jgs2022-050.
- Cawood P.A., C.J. Hawkesworth, S.A. Pisarevsky, B. Dhuime, F.A. Capitanio, O. Nebel, 2018. Geological archive of the onset of plate tectonics. *Phil. Trans. R. Soc. A*, 376 (2132); /10.1098/rsta.2017.0405.
- Fraga, L.M., N.J. Reis, R. Dall'Agnol, 2009. The Cauarane-Coeroeni belt, the main tectonic feature of the central Guyana Shield, northern Amazonian Craton. SBG Núcleo Norte. Simposio de Geologia da Amazonia 11. Manaus, extended abstract, 3 pp.
- Fraga, L.M.B., M.T.L. Faraco, 2020. Geological and mineral resources map of sheet NA21 – TUMUCUMAQUE, 2nd Ed., Geological Survey of Brazil - CPRM, Rio de Janeiro.
- Ganne, J., V. De Andrade, R.F. Weinberg, O. Vidal, B. Dubacq, N. Kagambega, S. Naba, L. Baratoux, M. Jessell, J. Allibon, 2012. Modern-style plate subduction preserved in the Palaeoproterozoic West African craton. *Nature Geosci.* 5, 60-65; /10.1038/NGeo1321
- Hoffman, P.F., 2021. Cusp tectonics: an Ediacaran megakarst landscape and bidirectional mass slides in a Pan-African syntaxis (NW Namibia). *Geological Society, London, Special Publications* 503, 105-142; /10.1144/SP503-2019-253.
- Kroonenberg, S.B., E.W.F. de Roever, L.M. Fraga, N.J. Reis, T. Faraco, J.-M. Lafon, U. Cordani, T.E. Wong, 2016. Paleoproterozoic evolution of the Guiana Shield in Suriname: a revised model. *Neth. J. Geosciences* 95 (4), 491-522; /10.1017/njg.2016.10
- Mahabier, R., E.W.F. de Roever, 2018. The Caicara-Dalbana Belt, a belt of felsic and intermediate metavolcanics of 1.99 Ga in the Guiana Shield, and probably across. In: the Guaporé Shield. Abstract 4505, 49^o Congresso Brasileiro de Geologia, Rio de Janeiro.

McFarlane, H.B., N. Thébaud, L.A. Parra-Avila, R. Armit, C. Spencer, J. Ganne, L. Aillères, L. Baratoux, P.G. Betts, M.W. Jessell, 2019. Onset of the supercontinent cycle: Evidence for multiple oceanic arc accretion events in the Paleoproterozoic Sefwi Greenstone Belt of the West African Craton. *Precambrian Res.* 335, 105450; /10.1016/j.precamres.2019.105450.

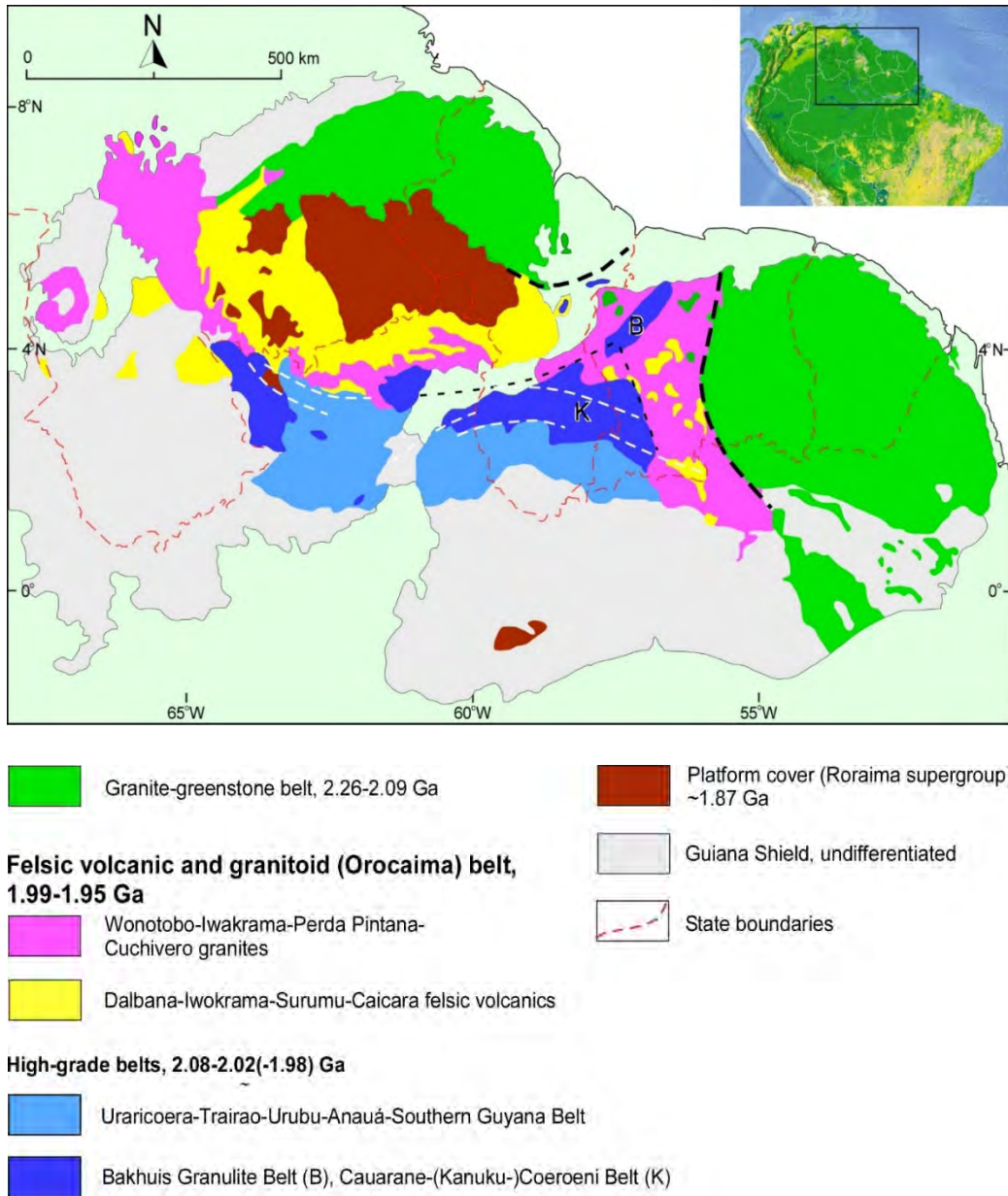


Fig. 1. Geological map of the Guiana Shield, simplified after Kroonenberg et al. (2016). Thick dashed black lines in between and along the southwestern boundary of the granite-greenstone belts trace, approximately, a NNE-trending orogenic 'Bakhuis' syntax', identified by Beunk et al. (2021). The actual plate boundary may have been located 100-200 km further to the southwest, schematically indicated by the thin black dashed line. White dashed lines: magnetic lineaments in the Cauarane-Coeroeni Belt (after Fraga and Faraco, 2020).

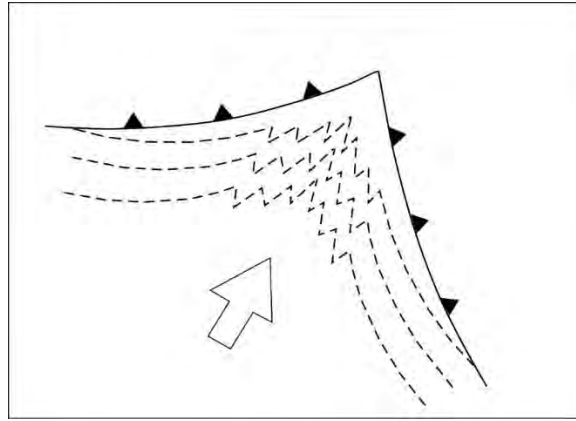


Fig. 2. Diagrammatic map of a cusped convergent plate boundary, oriented similarly to the Bakhuis syntax in Fig. 1. There, the upper plate, with shark teeth, contains granite-greenstone belts. The incoming lower plate carries previously steepened sedimentary stratification and is aimed directly into the syntax (open arrow). The syntaxial geometry induces lateral constriction of the lower plate, resulting in vertical folding (dashed lines).

Geochemistry and Sm-Nd isotopic data for unmetamorphosed dolerites in Matthews Ridge, Guyana, that are inferred to belong to the Avanavero LIP

B. Borba de Carvalho¹, B. Cousens¹, C. Hunter², K.R. Chamberlain⁴ and R.E. Ernst^{1,3}, ¹Department of Earth Sciences, Carleton University, Ottawa, Canada, ²First Quantum Minerals (FQM), Perth, Australia, ³Faculty of Geology and Geography, Tomsk State University, Tomsk, Russia, ⁴Department of Geology and Geophysics, University of Wyoming, USA

SUMMARY

The complete extent of the 1.79 Ga Avanavero magmatism is currently unclear. It has been found in places where it hadn't been previously mapped (e.g.: NW Guyana, the focus of this study) and has been linked with similar age units in the formerly adjacent West African craton. The Avanavero samples range from andesitic basalts to basalts and have a tholeiitic signature. In the literature, the Avanavero can be divided into high-Ti and low-Ti groups; however, all the samples from NW Guyana have low TiO₂. The chondrite-normalized diagram for the Rare Earth Elements (REE) displays a slight enrichment in the light-REE relative to the heavy-REE, and negative anomalies of Nb and Ti in the Primitive Mantle-normalized multielement diagram. The flat HREE patterns suggest that residual garnet was not left after melting, and that mantle melting was within the stability of spinel lherzolite, also seen in the TiO₂/Yb vs. Nb/Yb projection where the samples plot within the MORB+OPB+IAB array. The depletion of high field strength elements (HFSE), such as Nb and Zr, relative to the light-REE including La can be attributed to interaction with subduction-modified lithospheric mantle. This study presents new Sm-Nd isotopic data and expects to obtain and present new U-Pb ages to confirm whether these unmetamorphosed doleritic rocks of Matthews Ridge are part of the Avanavero LIP event.

Key words: Avanavero, Matthews Ridge, Guyana, Sm-Nd, U-Pb geochronology.

INTRODUCTION

Avanavero mafic dykes and sills are widespread in the Amazonian craton, South America. Although the complete extent of Avanavero magmatism is currently unclear, it has been found in places where it hadn't been previously mapped (e.g.: NW Guyana, the focus of this study). The 1.79 Ga Avanavero event is recognized to extend over 300,000 km² and to have a minimum volume of 30,000 km³ (Gibbs & Barron, 1993; Reis et al., 2013). It has also been proposed to be linked with similar age units in the formerly adjacent West African craton (Baratoux et al. 2019). A continental rifting origin was suggested by Choudhury and Milner (1971). Gibbs and Barron (1993) proposed that a weak juvenile Paleoproterozoic lithosphere undergoing partial melting generated the Avanavero magmatism. Because of its widespread distribution Ernst and Buchan (2001) inferred that it was a Large Igneous Province (LIP) caused by a plume rising from deep mantle.

RESEARCH APPROACH

We present new geochemical and isotopic data from unmetamorphosed diabase units from a previously unmapped area in NW Guyana which we correlate with the Avanavero LIP. These Avanavero samples from NW Guyana were analysed for geochemistry and radiogenic isotopes, integrated with Avanavero geochemistry elsewhere in Amazonia and these data are being used to characterize the source characteristics and differentiation history of the Avanavero LIP.

MATERIALS AND METHODS

A total of 53 mafic and ultramafic rocks were collected during one fieldtrip to NW Guyana (Fig. 1). The metamorphosed rocks were considered to belong to the Matthews Ridge events and are discussed in a separate abstract for this conference (Borba de Carvalho et al. 2022). The freshest samples are considered to belong to the Avanavero event since elsewhere in Amazonia this event does not show effects of metamorphism (Reis et al., 2013). Thus, 18 hand samples were grouped as possibly being part of the Avanavero group and are the focus of this abstract. The geochemical analyses of major, minor, trace and REE were determined by Inductively Coupled Plasma Mass Spectrometry (ICP-MS) by ALS Canada Ltd (www.alsglobal.com). The standard used to be measured along the target samples was BHVO-2 (from the Hawaiian Volcanic Observatory). For Nd whole-rock isotopic work, the samples were prepared and analyzed by a ThermoFinnigan Neptune

MC-ICP-MS at the Isotope Geochemistry and Geochronology Research Centre (IGRC), at Carleton University, Canada. For the isotopic analysis we used two different standards BHVO-2, and the Basalt Columbia River (BCR-2).

PETROGRAPHIC DESCRIPTIONS

A total of 53 mafic and ultramafic rocks were collected during one fieldtrip to NW Guyana (Fig. 1). The metamorphosed rocks were considered to belong to the Matthews Ridge events and are discussed in a separate abstract for this conference (Borba de Carvalho et al. 2022). The freshest samples are considered to belong to the Avanavero event since elsewhere in Amazonia this event does not show effects of metamorphism (Reis et al., 2013). Thus, 18 hand samples were grouped as possibly being part of the Avanavero group and are the focus of this abstract. The geochemical analyses of major, minor, trace and REE were determined by Inductively Coupled Plasma Atomic Emission Spectroscopy and Mass Spectrometry by ALS Canada Ltd (www.alsglobal.com). The standard measured along with the target samples was BHVO-2 (from the Hawaiian Volcanic Observatory). For Nd whole-rock isotopic work, the samples were prepared and analyzed by a ThermoFinnigan Neptune MC-ICP-MS at the Isotope Geochemistry and Geochronology Research Centre (IGRC), at Carleton University, Canada. For the isotopic analysis we used two different, BHVO-2 and the Columbia River Basalt (BCR-2).

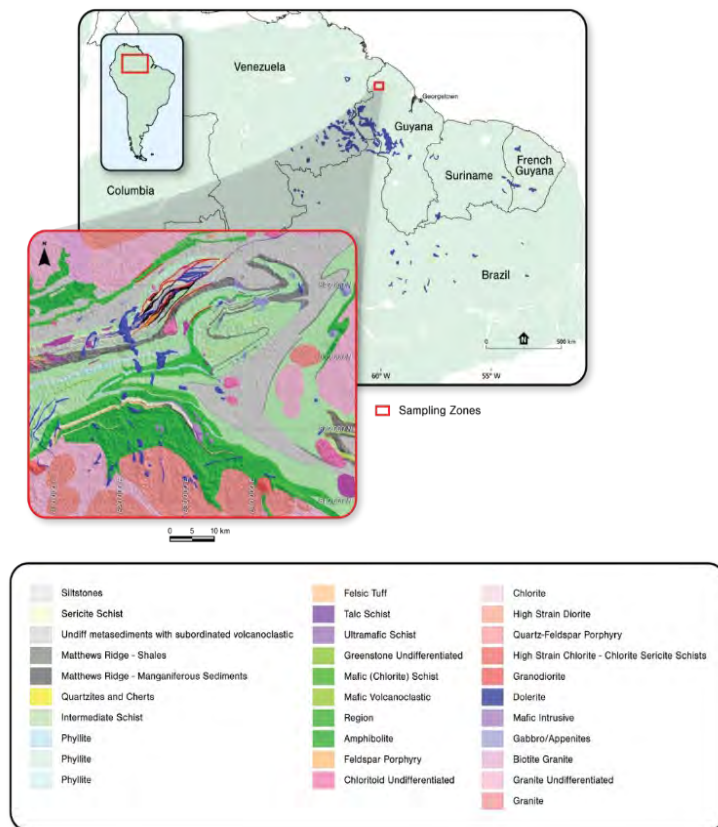


Fig. 1. Simplified geological map of the Guiana Shield, compiled after various sources. Modified from Kroonenberg et al., 2016. The detailed sampling zone map was provided by FQM (First Quantum Minerals exploration mining company).

WHOLE-ROCK GEOCHEMISTRY

The Avanavero rocks vary from tholeiitic andesitic basalts to basalt. In the overview of the Avanavero event by Reis et al. (2013), samples were divided into low-TiO₂ and high-TiO₂, which would represent the bulk of Avanavero samples and the

Quarenta Ilhas group, respectively. In the present study of Avanavero samples from NW Guyana, all samples belong to the low TiO₂ group. The chondrite-normalized diagram for the Rare Earth Elements (REE) and the Primitive Mantle-normalized multielement diagram show that all samples follow the same patterns as seen in Reis et. al. (2013), a slight enrichment in the light-REE relative to the heavy-REE, and negative anomalies of Nb and Ti. In Reis et. al. (2013), these negative anomalies of Nb and Ti, and an enrichment of mobile elements, such as Cs, Rb, Ba and K were interpreted to indicate a lithospheric mantle source that had been modified by a subduction process or by crustal contamination. A good positive correlation between Zr and Y, Nb, Th, Ce, Gd and Yb rules out significant mobilization, meaning that the geochemical data presented here reflects the primary mantle-derived composition. The depletion of high field strength elements (HFSE), such as Nb and Zr, relative to the light-REE including La can be attributed to subduction-related settings (Woodhead et al., 1993; Szilas et al., 2012). Assessing the nature of the source using the negative Nb anomaly, it is worth noting that there is a small group of samples that behave differently from the bulk of Avanavero samples. This small group comprises samples with Nb concentrations > 9 ppm (and are mostly from the Quarenta Ilhas group – High-Ti), while most Avanavero samples have Nb concentrations < 6 ppm.

According to Pearce et. al. (2021), the Th/Yb vs. Nb/Yb projection is sensitive to a magma that has interacted with a continental crust or with a lithospheric mantle that had been previously metasomatized, causing the compositions to move to the “Arc Array field” (=SZLM field of the Th/Nb vs TiO₂/Yb “LIP-printing diagram”). However, before plotting the data should be filtered (Pearce et. al. 2021). One filter removes more evolved (higher silica) samples in which crystallization of oxides not only increases silica but also reduces the TiO₂/Yb ratio. Another filter avoids samples that have been involved with alteration and metamorphism. **After filtering our data**, the Avanavero samples from this study and from Reis et. al. (2013) plot in the SZLM (subduction modified lithospheric mantle) field. As for the TiO₂/Yb ratios, a few samples from the Quarenta Ilhas region plot within the OIB+OPB (Ocean Island Basalts + Oceanic Plateau Basalts) array, which could indicate that they have different depth and degrees of mantle partial melting when compared to the main Avanavero group (Pearce et. al., 2021).

Sm-Nd ISOTOPIC GEOCHEMISTRY AND U-Pb GEOCHRONOLOGY

Analysis of Sm-Nd isotopes have been done in nine samples from NW Guyana. Five samples used in Reis et. al. (2013) was provided for the present study by the Geological Survey of Brazil (CPRM-Manaus) to be compared with the Matthews Ridge samples. The Sm-Nd results obtained so far for the Avanavero samples of NW Guyana shows no significant variation in the initial ¹⁴³Nd/¹⁴⁴Nd ratios and that their εNd values range from -0.5 to +0.5 with most samples being positive, which suggest that they did not suffer major interaction and/or contamination with crustal rocks. The data from the new samples from Brazil (in the main portion of the Avanavero) are under assessment.

The most precise age obtained using baddeleyite crystals from an Avanavero intrusion in northern Brazil is 1795.5 ± 1.6 Ma., MSWD = 0.2 (Reis et al., 2013). We have four samples from Matthews Ridge being dated using the U-Pb method on baddeleyite crystals at the SIMS laboratory of the University of California, Los Angeles, and we aim to present the new ages during the *SAXI-XII Interguiana Geological Conference 2022*.

CONCLUSION

One set of mafic rocks from NW Guyana are interpreted to belong to the Avanavero LIP on the basis of matching petrographic and whole-rock geochemistry with the other previously identified portions of this LIP elsewhere in Amazonia. With that being said, we conclude that:

- The Avanavero samples range from andesitic basalts to basalts and have a tholeiitic signature.
- In the literature, the Avanavero LIP samples can be divided into high-Ti and low-Ti groups; however, all the samples from the NW Guyana have low TiO₂.
- The chondrite-normalized diagram for the Rare Earth Elements (REE) displays a slight enrichment in the light-REE relative to the heavy-REE, and negative anomalies of Nb and Ti in the Primitive Mantle-normalized multielement diagram. The slightly flat HREE patterns suggest that residual garnet did not remain after partial melting of their mantle source, and that melting was within the stability of the spinel lherzolite, also seen by the TiO₂/Yb vs. Nb/Yb projection where the samples plot within the MORB+OPB+IAB array.

- The good positive correlation between Zr and Y, Nb, Th, Ce, Gd and Yb shows that there was not any significant mobilization by any post-magmatic alteration, meaning that the data presented here reflect the primary mantle melt composition. The depletion of high field strength elements (HFSE), such as Nb and Zr, relative to the light-REE including La can be attributed to interaction with, or derivation from, subduction modified lithospheric mantle.
- The Sm-Nd isotopic data shows a tight grouping of initial $^{143}\text{Nd}/^{144}\text{Nd}$ ratios for the Avanavero samples of NW Guyana.

ACKNOWLEDGEMENT

FQM has supported the May 2019 field work and provided access to samples and data as an In-Kind contribution to this PhD project of the LIPs Industry Consortium Program.

REFERENCES

- Baratoux, L., Söderlund, U., Ernst, R.E., de Roever, E., Jessell, M.W., Kamo, S., Naba, S., Perrouy, S., Metelka, V., Yatte, D., Grenholm, M., Diallo, D.P., Ndiaye, P.M., Dioh, E., Cournède, C., Benoit, M., Baratoux, D., Youbi, N., Rousse, S., Bendaoud, A. (2019) New U–Pb baddeleyite ages of mafic dyke swarms of the west African and Amazonian cratons: Implication for their configuration in supercontinents through time. In: Srivastava, R.K., Ernst, R.E., Peng, P. (eds.) *Dyke Swarms of the World – A Modern Perspective*. Springer, p. 263-314.
- Borba de Carvalho et al., 2022 Paleoproterozoic U-Pb ages and geochemistry of mafic and ultramafic rocks of Matthews Ridge, Guyana: A comparison with other Paleoproterozoic occurrences within the Guiana Shield. The SAXI-XII Interguiana Geological Conference 2022.
- Choudhuri, A., Milner, M.W. (1971). Basic magmatism in Guiana and continental drift. *Nature* 232, 154–155.
- Ernst, R.E., Buchan, K.L. (2001). Maximum size and distribution in time and space of mantle plumes: evidence from large igneous provinces. *Journal of Geodynamics* 34, 309–342.
- Gibbs A.K., Barron C.N. (1993). *The Geology of the Guiana Shield*. Oxford Monographs on Geology and Geophysics 22.
- Kroonenberg S.B, de Roever E.W.F., Fraga L.M., Reis N.J., Faraco M.T., Lafon J.M., Cordani U.G., Wong T.E. (2016). Paleoproterozoic evolution of the Guiana shield in Suriname: a revised model. *Netherlands Journal of Geoscience/Geologisch Mijnbouwkundige Dienst Suriname* 95: 491–522.
- Pearce, Julian & Ernst, Richard & Peate, David & Rogers, Chris. (2021). LIP printing: Use of immobile element proxies to characterize Large Igneous Provinces in the geologic record. *Lithos*. 392-393. 106068. 10.1016/j.lithos.2021.106068.
- Reis, N.J., Teixeira, W., Hamilton, M.A., Bispo-Santos, F., Almeida, M.E. & D’Agrella-Filho, M.S. (2013). Avanavero mafic magmatism, a late Paleoproterozoic LIP in the Guiana Shield, Amazonian Craton: U–Pb ID-TIMS baddeleyite, geochemical and paleomagnetic evidence. *Lithos* 174: 175–195.
- Szilas, K., Hoffmann, J.E., Schersten, A., Rosing, M.T., Windley, B.F., Kokfelt, T.F., Keulen, N., van Hinsberg, V.J., Naraa, T., Frei, R., Munker, C. (2012). Complex Calc-Alkaline Volcanism Recorded in Mesoarchaean Supracrustal Belts North of Frederikshab Isblink, Southern West Greenland: Implications for Subduction Zone Processes in the Early Earth. *Precambrian Research* 208 – 211. pp. 90–123.
- Woodhead, J.D., Eggins, S., Gamble, J.A. (1993). High field strength and transition element systematics in island arc and backarc basin basalts: evidence for multi-stage melt extraction and ultra-depleted mantle wedge. *Earth Planet. Sci. Lett.* 114, 491–504.

Paleoproterozoic U-Pb ages and geochemistry of mafic and ultramafic rocks of Matthews Ridge, Guyana: A comparison with other Paleoproterozoic occurrences within the Guiana Shield

B. Borba de Carvalho¹, B. Cousens¹, C. Hunter², K.R. Chamberlain⁴ and R.E. Ernst^{1,3}, ¹Department of Earth Sciences, Carleton University, Ottawa, Canada, ²First Quantum Minerals (FQM), Perth, Australia, ³Faculty of Geology and Geography, Tomsk State University, Tomsk, Russia, ⁴Department of Geology and Geophysics, University of Wyoming, USA

SUMMARY

New geochronology data from mafic to ultramafic igneous rocks of the Matthews Ridge area display ages of 2097±39 Ma. (MSWD=1.7); 2125±25 Ma. (MSWD=0.14); 2157±40 Ma. (MSWD=1.3) and 2238±81 Ma. (MSWD=0.13). Provisionally labelled as the Matthews Ridge events, these ages would suggest that a c. 2100 Ma, and possibly also c. 2200 Ma magmatic suite are present within the Guiana Shield. The geochemistry results indicate that the samples from Matthews Ridge represent more than one (ultra)mafic event, and that they can be divided into three different chemical groups. Through our analysis we aim to determine the geodynamic setting of each of these groups and assess which could represent parts of Large Igneous Province events and any potential link with the approximately coeval Trans Amazonian orogeny.

Key words: Matthews Ridge, Guyana, U-Pb geochronology

INTRODUCTION

The Guiana shield corresponds to five different countries, including Guyana, Suriname, French Guiana, Venezuela and small parts of Colombia and northern Brazil. The shield covers 900,000 km² and its boundaries are the Atlantic Ocean into the north, and the Amazon-Solimões basin in the south (Kroonenberg et al., 2016). Delor et al. (2003a) and Kroonenberg et al. (2016) summarize the Guiana Shield in two main Archean terrains, the Amapá block in the east and the Venezuelan Itamacá block in the west (Montgomery and Hurley, 1978; Lafon et al., 1998; Tassinari et al., 2001). A Paleoproterozoic (2.26-2.07Ga) greenstone-tonalite-trondhjemite-granodiorite (TTG) belt is present in the north portion of the shield, and it is commonly attributed to a convergent event between the Archean units of the Amazon Craton and the West African Craton, around 2.2 and 1.9 Ga (Cordani & Teixeira, 2007; Bispo Santos et al., 2014). New geochronology data of mafic and ultramafic rocks from the Matthews Ridge area show that they can be inserted in the geological regional context as part of the Rhyacian greenstone belt sequences that occur with different names within part of all the countries that comprise the Guiana Shield.

RESEARCH APPROACH

We are studying mafic and ultramafic rocks of Matthews Ridge, NW Guyana (Fig. 1), part of the Guiana Shield, to better characterize them, including determining the number of distinct events, their mantle sources, differentiation histories and to assess which belong to large igneous provinces (LIPs), and which can be linked to coeval units within the Guiana Shield, and also in the formerly adjacent West African craton.

MATERIALS AND METHODS

The material used for this project includes 83 hand samples, 71 thin sections, and 74 whole-rock geochemistry analyses (major and trace elements). These data have been used to classify and group potential distinct magmatic suites in NW Guyana. The geochemical analyses of major, minor, trace and REE were determined by Inductively Coupled Plasma techniques by ALS Canada Ltd (www.alsglobal.com).

MATTHEWS RIDGE PETROGRAPHIC DESCRIPTIONS

Petrographic characteristics of 71 thin sections including mineral paragenesis, alteration, metamorphism and deformation were used to identify possible different groups.

One magmatic group (consisting mostly of fresh unmetamorphosed dolerite), is linked to the 1790 Ma Avanavero LIP, and is the focus of a separate abstract in the *SAXI-XII Inter-Guiana Geological Conference 2022* (Borba de Carvalho et al. 2022). The remaining samples have been metamorphosed to a low-grade, greenschist facies where primary minerals were replaced by amphibole, chlorite, epidote, titanite, biotite, quartz, serpentine and talc. However, most samples still preserve an igneous texture. These samples were separated into three different groups by their distinct mineral paragenesis:

- Matthews Ridge Unit 1A: actinolite/tremolite + chlorite + plagioclase + other alteration mixtures ± opaque minerals.
- Matthews Ridge Unit 1B: serpentinized ultramafic samples
- Matthews Ridge Unit 2: actinolite/tremolite + plagioclase + epidote ± quartz ± opaque minerals.
- Matthews Ridge Unit 3: fine-grained samples showing basaltic texture with alteration of plagioclase and clinopyroxene.

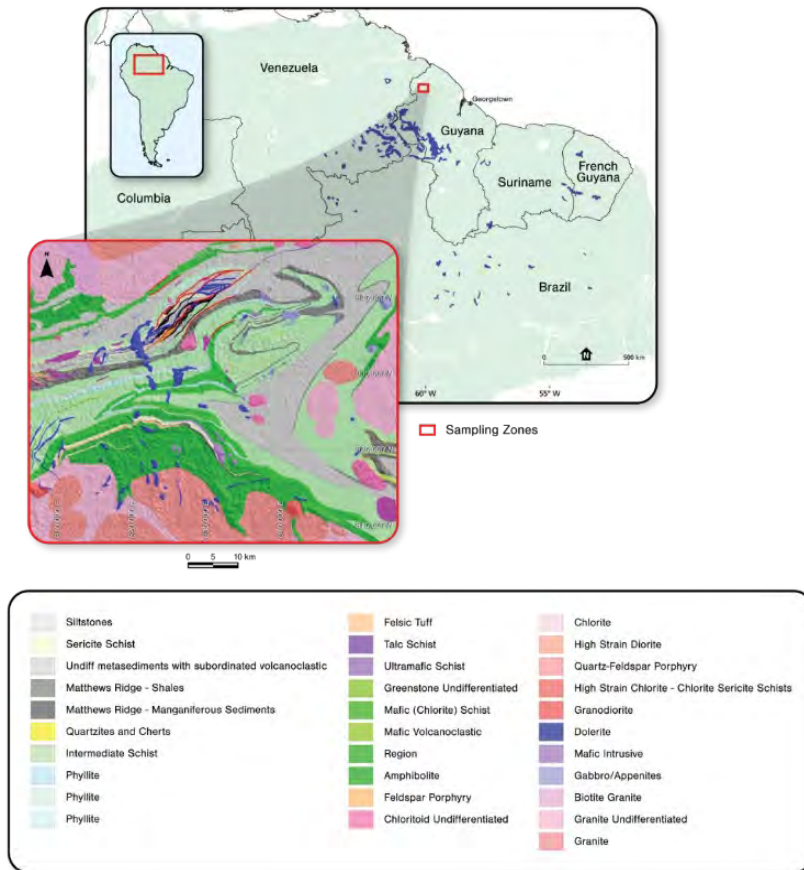


Fig.1. Simplified geological map of the Guiana Shield, compiled after various sources. Modified from Kroonenberg et. al., 2016. The detailed sampling zone map was provided by FQM.

MATTHEWS RIDGE WHOLE-ROCK GEOCHEMISTRY

The geochemical results show that the samples concentrate in the field of the basaltic composition and have a tholeiitic affinity when plotted on an AFM diagram. Their SiO₂ content ranges from 39 to 52 wt%, which support their interpretation as mafic and ultramafic rocks. Normalized REE diagrams divide the rocks into three main groups: Matthews Ridge Unit 1, 2 and 3. Matthews Ridge Unit 1 have a flat pattern, meaning that there is almost no difference in the relative concentration of light and heavy REE. However, the samples can be divided by their MgO content, Unit 1A (low-MgO) and Unit 1B (high-MgO), with the possibility of subgroups within them. Matthews Ridge Unit 2 patterns have a slightly negative slope showing a small excess of LREEs compared to the HREEs, while Matthews Ridge Unit 3 shows the opposite, a slightly positive sloped pattern that resembles a MORB-type pattern.

The Unit 1A presents a large variation of Fe₂O₃ and TiO₂, which reflects the abundance of Fe-Ti oxides in this group. In comparison with Unit 1A, Unit 1B presents generally low TiO₂, P₂O₅, Y, and Zr concentrations. The low incompatible element contents, such as Nb, Zr, and Y, suggest that Unit 1B rocks were cumulates. Within the Unit 1A group, there are samples with positive Sr and Eu anomalies, which suggest that some samples in Unit 1A may also have a cumulate origin.

The Primitive Mantle-normalized multi-element diagram shows that Matthews Ridge Unit 1 can be also subdivided by the size of their Ti anomalies, which range from positive to no anomalies (Unit 1A) and from slightly to highly negative Ti-anomalies (Unit 1B) meaning that it is possible to see how much crustal interaction affected the samples. Besides the range of Ti-anomalies, both groups show differences in the Nb, Ta and Th anomalies. Matthews Ridge Unit 2 presents negative anomalies of Nb, Ta, P and Ti; and positive anomalies of Th and Sr. Matthews Ridge Unit 3 do not present any significant anomalies.

U-PB GEOCHRONOLOGY

Mineral separation, and analysis of zircon and baddeleyite grains from 4 samples collected by FQM have been done at the SIMS laboratory at the University of California, Los Angeles. The obtained ages were 2097±39 Ma. (MSWD=1.7); 2125±25 Ma. (MSWD=0.14); 2157±40 Ma. (MSWD=1.3) and 2238±81 Ma. (MSWD=0.13). The ages show that these samples are not part of the Avanavero LIP, as the most precise age obtained using baddeleyite crystals from an Avanavero intrusion in northern Brazil, was dated at 1795.5 ± 1.6 Ma., MSWD = 0.2 (Reis et al., 2013).

These ages are provisionally labelled as the Matthews Ridge events, where these samples would indicate that a c. 2100 Ma, and possibly also c. 2200 Ma magmatic suite are present within the Guiana Shield. Similar ages have been reported in the literature from rocks of the greenstone-belt sequences that occur in other areas of the shield (see Table 1).

COMPARISON OF MATTHEWS RIDGE WITH OTHER OCCURRENCES WITHIN THE GUIANA SHIELD

The whole-rock geochemistry of mafic and ultramafic rocks of Matthews Ridge area were compared with other mafic and ultramafic rocks of Paleoproterozoic greenstone belt sequences within the Shield (Table 1). The data used are from the following places:

- Venezuela: Lo Increíble mining district – Pastora Supergroup;
- Guyana: 9 Mile Deposit – Barama-Mazaruni Supergroup;
- French Guiana: Central Guiana Complex (CGC) - Paramaca Group;
- Brazil: Vila Nova Group

Table 1. Ages of greenstone belts and intrusions in the Guiana Shield (Norcross, 2000)

Rock Type	Location	Age, Ma	Method	Reference
Metavolcanic	Pastora group Venezuela	2131 ± 10	U-Pb, zircon	Day et al., 1995
Metagraywacke	Barama-Mazaruni group Guyana	2250 ± 106 2244 ± 43	U-Pb, zircon	Gibbs and Olzewski, 1982
Metavolcanics	Marowijne group Suriname	1950 ± 150	Rb-Sr	Priem et al., 1982
Metavolcanics	Paramaca series French Guiana	2210 ± 90	Sm-Nd	Gruau et al., 1985
Bartica gneiss	Barama-Mazaruni group Guyana	2227 ± 39	U-Pb, zircon	Gibbs and Olzewski, 1982
Pegmatite, yaou granite	Paramaca series French Guiana	2123 ± 11 2127 ± 10	U-Pb, zircon	Lerouge et al., 1996
Omai intrusion and metavolcanics	Barama-Mazaruni group Guyana	2171 ± 140	Sm-Nd	Voicu et al., 1997
KM24 granit	Pastora group Venezuela	2087 ± 21	U-Pb, zircon	P. Klipfel, personal information - November 4, 1998
Granites	Paramaca series French Guiana	2030 ± 65 2083 ± 39 2032 ± 61	Rb-Sr, Pb-Pb, K-Ar	Teixeira et al., 1996 from Gibbs and Baron, 1993
Younger granite	Barama-Mazaruni group Guyana	2015 ± 80	K-Ar	Snelling and McConnell, 1969
Younger granite	Barama-Mazaruni group Guyana	1945 ± 100	K-Ar	Williams et. Al., 1967
Granitoids and acid volcanics	Marowijne group Suriname	1810 ± 40	Rb-Sr	Priem et al., 1971

The Matthews Ridge geochemical groups, mentioned in the previous section, were used to see if the other occurrences within the Guiana Shield had matching geochemistry. We note that samples from the 9 Mile Deposit in Guyana are very similar to the Vila Nova G1 group in Brazil, but not similar to any of Matthews Ridge groups; 9 Mile Deposit and the Vila Nova G1 show a much higher negative slope than observed in any other area. The slightly negative slope seen in Matthews Ridge Unit 2 is also observed within the volcanic samples of CGC in French Guiana, with three samples of Lo Increíble mining district in Venezuela and with the Vila Nova G2 group in Brazil. The samples with a flat pattern are the most abundant and is present in all the places when the samples have an ultramafic composition, which includes the Matthews Ridge Unit 1B, all the samples from the Vila Nova G3 and G4 groups, three samples from Lo Increíble in Venezuela and the ultramafic samples of CGC group in French Guiana. The flat pattern shown by the mafic samples from Matthews Ridge Unit 1A has not been seen in any other location yet. The same can be said for the Matthews Ridge Unit 3 that shows a MORB-like pattern type.

CONCLUSIONS

The Guiana Shield is one of the least explored areas in the world. Therefore, any new data will contribute to a better understanding of the Paleoproterozoic igneous history of the area. Up to this point, we can conclude that:

- NW Guyana samples represent more than one mafic and ultramafic event.
- Besides the Avanavero group, there are three more possible different chemical groups:
 - Matthews Ridge Unit 1

- Matthews Ridge Unit 2
- Matthews Ridge Unit 3
- Matthews Ridge Unit 1 can be divided into:
 - Low-MgO – Unit 1A
 - High-MgO – Unit 1B
- Cumulate rocks may be present in both Unit 1A and Unit 1B;
- U-Pb analysis indicate that a c. 2100 Ma magmatic suite is present;
- The different chemical groups found in Matthews Ridge can be observed in other countries within the Guiana Shield;
- The distinct geochemical pattern with high REE slope is present elsewhere in Guyana and Brazil but not seen in Matthews Ridge.

If we use trace elements to classify different chemical groups that belong to Paleoproterozoic mafic and ultramafic occurrences within the greenstone-belt in northern Guiana Shield, we could possibly have five different groups showing a range of negative to positive patterns, with some patterns occurring only locally.

Through our analysis we aim to determine the geodynamic setting of each of these five groups and assess which could represent parts of LIP events and any potential link with the approximately coeval Trans Amazonian orogeny.

ACKNOWLEDGMENTS

FQM has supported the May 2019 field work and provided access to samples and data as an In-Kind contribution to this PhD project of the LIPs Industry Consortium Program (www.supercontinent.org).

REFERENCES

- Bispo-Santos F., D'Agrella-Filho M.S., Trindade R.I.F., Janikian L., Reis N.J. 2014. Was there SAMBA in Columbia? Paleomagnetic evidence from 1790 Ma Avanavero mafic sills (Northern Amazonian craton). *Precambrian Research*, 244:139-155.
- Borba de Carvalho et al., 2022 Geochemistry and Sm-Nd isotopic data for unmetamorphosed dolerites in Matthews Ridge, Guyana, that are inferred to belong to the Avanavero LIP. The SAXI-XII Interguiana Geological Conference 2022.
- Cordani, U.G. & Teixeira, W. (2007). Proterozoic accretionary belts in the Amazonian Craton. In: Hatcher R.D. et al. (eds): 4-D framework of continental crust. *Geological Society of America Memoir* 200: 297–320.
- Delor, C., Lahondere, D., Egal, E., Lafon, J.M., Cocherie, A., Guerrot, C. & de Avelar, V., 2003a. Transamazonian crustal growth and reworking as revealed by the 1:500,000-scale geological map of French Guiana. *Géologie de la France* 2003 2-3-4: 5–57.
- Kroonenberg S.B, de Roever E.W.F., Fraga L.M., Reis N.J., Faraco M.T., Lafon J.M., Cordani U.G., Wong T.E. (2016). Paleoproterozoic evolution of the Guiana shield in Suriname: a revised model. *Netherlands Journal of Geoscience/ Geologisch Mijnbouwkundige Dienst Suriname* 95: 491–522.
- Lafon J.M., Rossi P., Delor C., Avelar V.G., Faraco M.T.L. (1998) - Novas testemunhas de relíquias arqueanas na crosta continental paleoproterozóica da Província Maroni-Itacaiúnas (Sudeste do Escudo das Guianas). In: Congresso Brasileiro de Geologia, 40, Belo Horizonte. Anais p. 64.
- Norcross C.E., Davis D.W., Spooner E.T.C., Rust A. (2000) - U-Pb and Pb-Pb age constraints on Paleoproterozoic magmatism, deformation and gold mineralization in the Omai area, Guyana Shield. *Precambrian Res.*, 102, 69-86.
- Montgomery, C. W. & P. M Hurley 1978 Total rock U-Pb and Rb-Sr systematics in the Imataca Series, Guayana Shield, Venezuela- *Earth Planet. Sci. Lett.* 39: 281-290.
- Tassinari C.C.G., Teixeira W., Nutman A.P., Szabó G.A., Mondin M., Sato K. (2001) - Archean crustal evolution of the Imataca Complex, Amazonian Craton: Sm-Nd, Rb-Sr & U-Pb (SHRIMP) evidence. In: Simpósio de Geologia da Amazônia, 7. Belém. (CD-ROM).

Guyana's Mineral Outlook: A Case for Traditional and Non-traditional Mineral Investment

Kantharaja D. Chandrappa, Ibrahim Abudu, La Donna Fredericks, Jason Downes and Asaf Mohamed
Geologists, Geological Services Division – The Guyana Geology and Mines Commission, Georgetown, Guyana.

The Guyana Geology and Mines Commission has conducted regional scale Geochemical and Geological Surveys throughout the country, since the late 1990s. Executed as a series of projects, these surveys have provided an extensive amount of high-quality datasets useful for mineral resource investigations, environmental assessments, and academic research. Over the past 23 years (1999 – present), the Geological Services has completed 70 Regional Geochemical and Geological survey projects that cover a total of 106,900 square kilometers (km²) of the area or the equivalent of the entire country of Iceland. Internally this equates to approx. 49.7 % of Guyana's total area.

Generally, stream-sediment samples are collected at a density of 1 sample per 4 – 6 km² and are analyzed for gold (Au) + 49 elements. All samples are analyzed at Activation Lab in Canada to preserve authenticity for international standards of sampling and analysis. The multi-element data obtained are stored in the Geographical Information System (GIS) platform which currently consists of more than 16,525 stream sediment samples and 2657 rock samples. This geospatial database integrates large datasets, retrieves and analyses spatial locations, and organizes layers of information into visualizations. The data generated continues to play an important role in finding mineralization target areas and redefining some of the known mineral fields.

These target areas delineate potential deposits of traditional mineral interests like gold, diamond and bauxite, as well as those non-traditional mineral commodities that are sometimes overlooked, like Rare Earth Elements (REEs) and metals such as chromium and nickel. There is no doubt that the mining sector is thriving, centred around the aforementioned traditional minerals, but there is still room for further growth. This is especially true for the materials that would bolster Guyana's ever-expanding infrastructure, as construction, and the demand for construction materials (sand and loam etc) is at an all-time high.

During the last three decades, there has been a marked increase in the application of REEs and their alloys in the manufacturing industry. With their unique properties and the lack of alternatives, they have proven invaluable the manufacture of electronics, green technologies such as renewable energy generation and storage, energy efficient lights and electric cars, as well as specific military and aerospace applications. REEs are needed to make rechargeable batteries, autocatalytic converters, super magnets, mobile phones, LED lighting, superconductors, glass additives, fluorescent materials, phosphate binding agents, solar panels, and Magnetic Resonance Imaging (MRI) agents. These elements have become known as the "**vitamins of modern industry**" and their current rate of utilisation is unprecedented.

Although REEs are not rare in terms of average crustal abundance, the concentrated deposits of REEs are limited in number. **Lanthanum**-based catalysts are used in petroleum refining, and cerium-based catalysts are used in automotive catalytic converters.

Neodymium-iron-boron magnets, which are the strongest known type of magnets, are used when space and weight are restricted. Nickel-metal hydride batteries use anodes made of lanthanum-based alloys.

Copper is a staple commodity that has been used in electrical wiring and motors for decades due to its ability to conduct heat and electricity.

Chromium & Nickel resists corrosion and are used to plate other metals as protection. Chromium is used in making alloys such as stainless steel and nickel in rechargeable nickel-cadmium batteries.

Uranium is valuable as nuclear fuel used to generate electricity, and with the shift to cleaner energy sources, uranium deposits are more valuable than ever.

Thorium sees use as an industrial catalyst and there is development underway in India and China for nuclear power plants with thorium reactors, which may yield even more power than fossil fuels and uranium.

The most important use of **lithium** is in rechargeable batteries for mobile phones, laptops, cameras, and electric vehicles. The metal is also made into alloys with aluminum and magnesium, improving their strength and making them lighter.

Scandium is mainly used for research purposes. It has great potential as its density is almost as low as aluminum and its melting point is much higher. It is used in the manufacture of fighter planes, high-end bicycle frames, and baseball bats.

One of the main uses of **tantalum** is in the production of electronic components, where tantalum is used to thinly coat other metals, achieving high capacitance in a small volume.

The geochemical data obtained from the lab based on the samples collected by the Geological Services Division are interpreted in conjunction with established historical information, to update and expand upon the knowledge for

Guyana's geology and geochemistry. The analysis has led to the creation of thematic maps that serve to highlight areas of interest (target areas) for the potential occurrences which create avenues for investment and development in the mining sector.

Keywords: Multi elements, GIS, Thematic, REEs, Green Technology, LED.

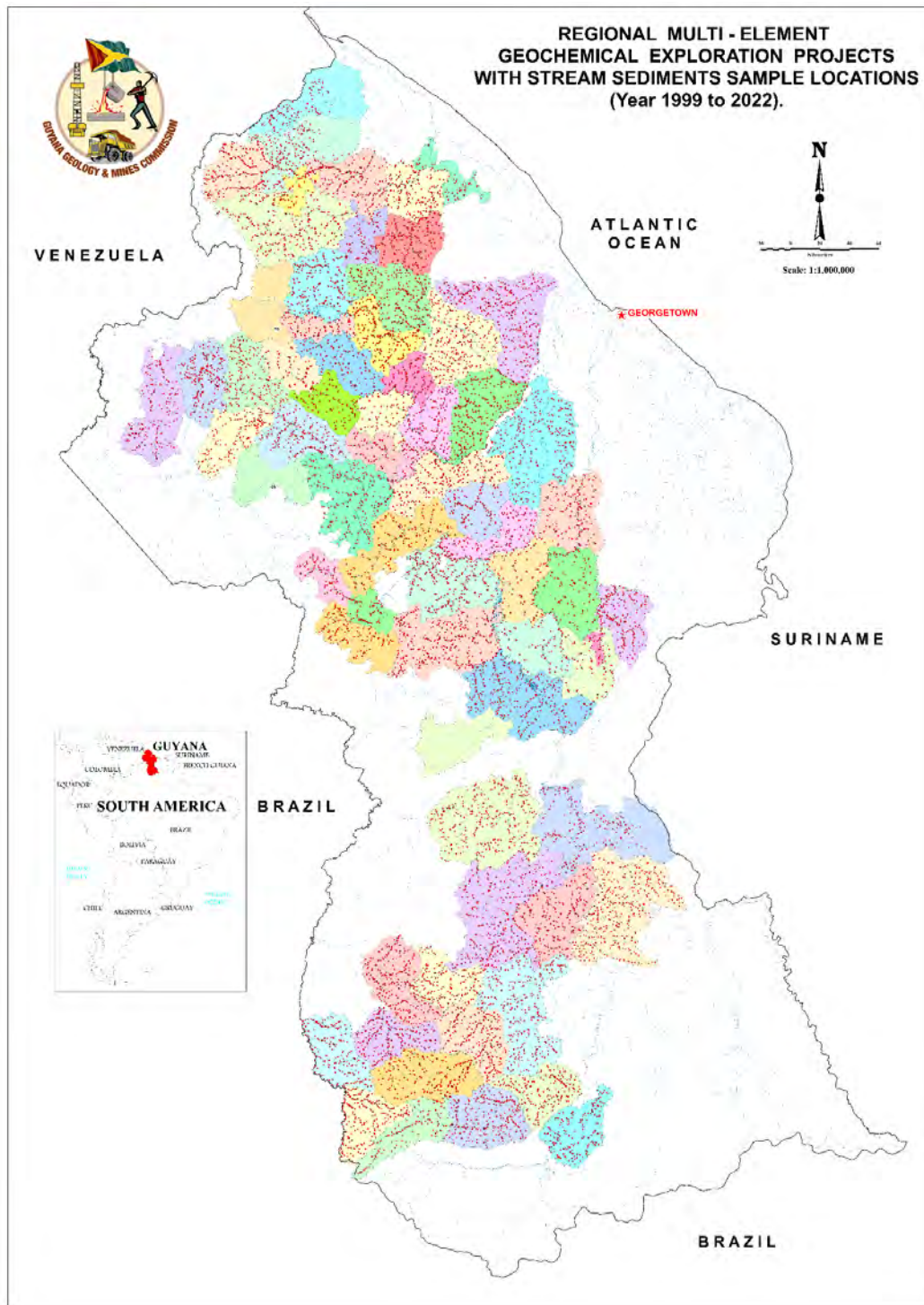


Figure-1. Completed Geochemical Exploration projects with stream sediment sample locations

Geometry and spatial distribution of shear zones and associated gold-bearing quartz veins, hosted by a TTG-like complex, at the Brothers Project, Eastern Suriname

Vincent Combes

Consulting Exploration Geologist, PhD

Cayenne, French Guiana

vincentcombes25@gmail.com

Rayiez Bhoelan

Senior Exploration Geologist, BSc, Maig

Paramaribo, Suriname

Dennis LaPoint

Appalachian Resources LLC

Chapel Hill, NC 27516

SUMMARY

The gold mineralization at the Brothers Project is hosted by ENE-striking shear corridors and associated quartz-carbonate vein sets developed within a large TTG-like complex. The proposed structural framework, based on investigations carried out at different scales, displays a polyphase history of deformation and related mineralization/alteration events with a first progressive ductile deformation phase, locally overprinted by a late-stage brittle event. The spatial distribution at the district-scale and ore shoot geometries at the target-scale are reflecting this complex deformation history with ENE structures overprinted by late NNW first order faults and associated ESE bends.

Keywords: quartz vein, shear zone, gold, Suriname, Guiana Shield

INTRODUCTION

The Brothers Project is located in the Eastern part of Suriname (Fig. 1) within Rhyacian volcano-sedimentary packages and TTG-like complexes, formed and deformed during the Trans-Amazonian Orogeny (Delor et al., 2003b and references therein). The Brothers concession encompasses two main domains with (1) a granitoid domain composed of a large, regional-scale TTG-like complex, and to its southeast (2) a volcano-sedimentary package (LaPoint, 2019). This study, focusing on the first domain within intrusive rocks, provides a unique opportunity to investigate the geometry and spatial distribution of shear zones and associated gold-bearing quartz veins. Field mapping is challenging there, with a deep weathering cover and complex regolith development. Since 2012, porknockers activities have expanded. These activities create outcrops and demonstrate the presence of gold but hide structures when pits flood.

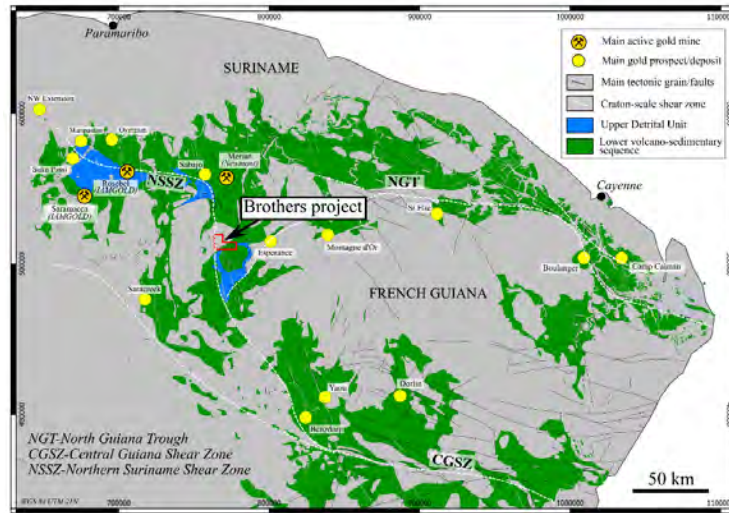


Figure 1. The Brothers Project within the Guiana Shield (modified from Kroonenberg et al. 2016 and Delor et al., 2003b).

METHODS

Structural controls on the gold mineralization are investigated at three different scales based on (1) detailed core logging of 20 diamond drillholes with oriented core (drilled by Rhyolite Resources Ltd), (2) structural mapping of 5 main targets located within the NW part of the Brothers concession and (3) structural interpretation using both airborne magnetic and airborne Lidar data. All structural measurements are reported in strike/dip (right-hand rule) and linear data as plunge/azimuth. Structural data were plotted on equal-area stereonet using the lower hemisphere convention.

RESULTS AND FIRST INTERPRETATIONS

Logging of 3000 m of drill core (example Fig. 2) shows multiple phases of veining, associated hydrothermal alterations and mineralization, hosted by intrusive rocks described as tonalite, diorite and porphyritic granodiorite.

From (m)	To (m)	Cb-alteration	Si-alteration	Tur-alteration	Pyrite generation	Pyrite content per interval (pts)	Vein type	Cumulative corrected thickness of vein per interval (cm)		Au grade (g/t)	Hostrock grain size	Strain Low → high	Mylonitization	Oriented data (strike/dip) Qz vein			Oriented data (strike/dip) Shear plane		
								0	100					Dip 0°	50°	90°	Dip 0°	50°	90°
43.0	44.0				Py ₂		ev				medium		Protomylonite	AN					
44.0	45.0				Py ₂		ev				medium		Protomylonite						
45.0	46.0				Py ₂		ev				medium		Protomylonite						
46.0	47.0				Py ₁		lcv, cv				fine		Protomylonite						
47.0	48.0				Py ₁		ffv, tva				fine		Mylonite						
48.0	49.0				Py ₁₋₂		ffv, ev				fine		Mylonite						
49.0	50.0				Py ₂		ffv, ev				fine		Mylonite						
50.0	51.0				Py ₁₋₂		ffv				fine		Mylonite						
51.0	52.0				Py ₁		ffv, tva, cv				fine		Mylonite						
52.0	53.0				Py ₁		ffv				fine		Mylonite						
53.0	54.0				Py ₁		ffv				fine		Mylonite						
54.0	55.0				Py ₁		ffv				fine		Protomylonite						
55.0	56.0				Py ₁		ffv				medium		Protomylonite						
56.0	57.0				Py ₁		ffv				medium		Protomylonite						

Figure 2. Example of logging with characterization of observed/measured parameters plotted against the gold content per interval to identify what controls the grades. (Abbreviations ev: extensional vein, ffv: fault-fill vein, tva: tension vein arrays, lcv: late Cb veinlets).

The interpreted progressive ductile deformation, locally overprinted by a late-stage brittle veining/fracturing, is shown in Figures 3 and 4. The bulk of gold mineralization is associated with syn-shearing quartz veins in high strain zones and late-stage extensional veins. Lower grade gold mineralization is associated with syn-shearing Py₁ in protomylonite and fault-fill veins in low strain zones.

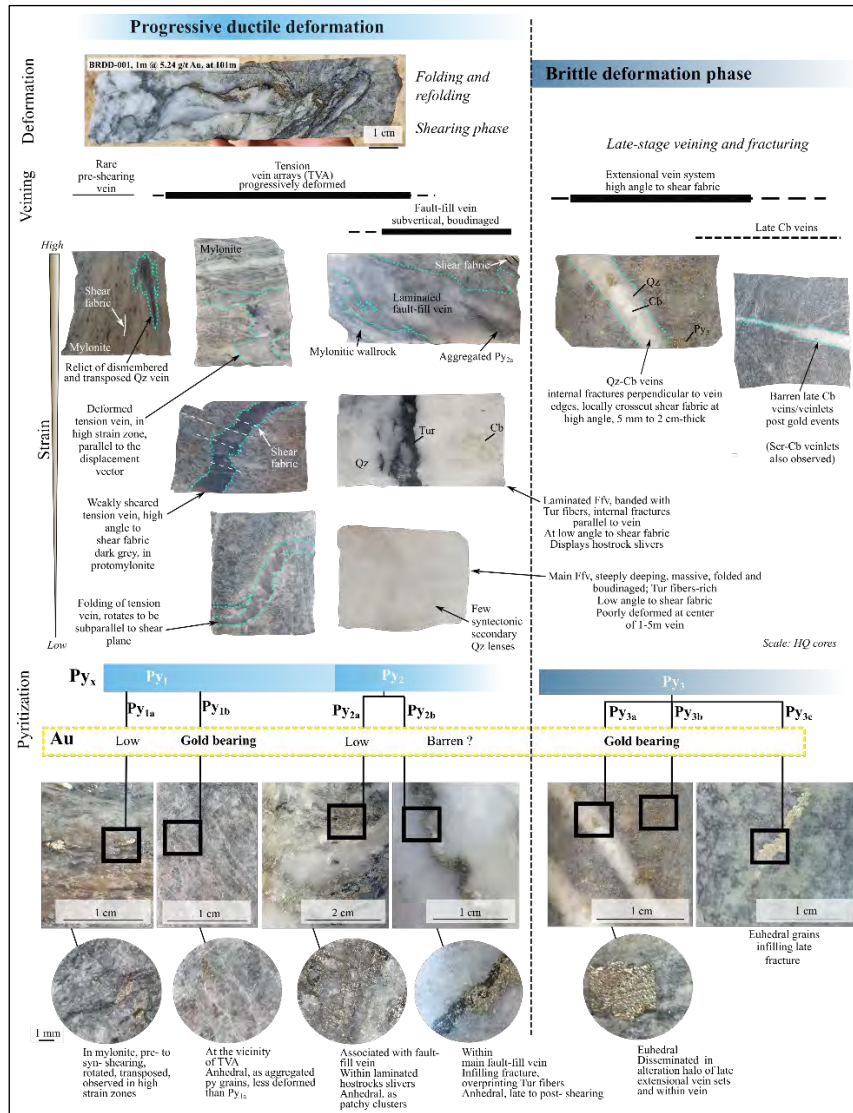


Figure 3. Summary of key observation regarding the deformation, veining and pyritization at the core-scale.

The main vein set is defined as tension vein arrays following the definition of Laing (2004) with planar quartz veins found in low strain zone that are rotated, folded, and transposed when observed in higher strain zone (ultimately being parallel to the displacement vector at the vicinity of metric fault-fill veins). These fault-fill veins (following the definition of Robert et al., 1994) display laminated textures with host rock slivers and tourmaline fibres. This progressive deformation is locally overprinted by late centimetric extensional quartz-carbonate veins developed at high angle to the shear fabric. The pyritization history is complex with at least 3 generations of pyrite (syn-shearing in mylonite, late shearing associated with the fault-fill veins and at selvages of extensional veins). Visible gold is spatially associated with the late brittle deformation phase (possibly from remobilization).

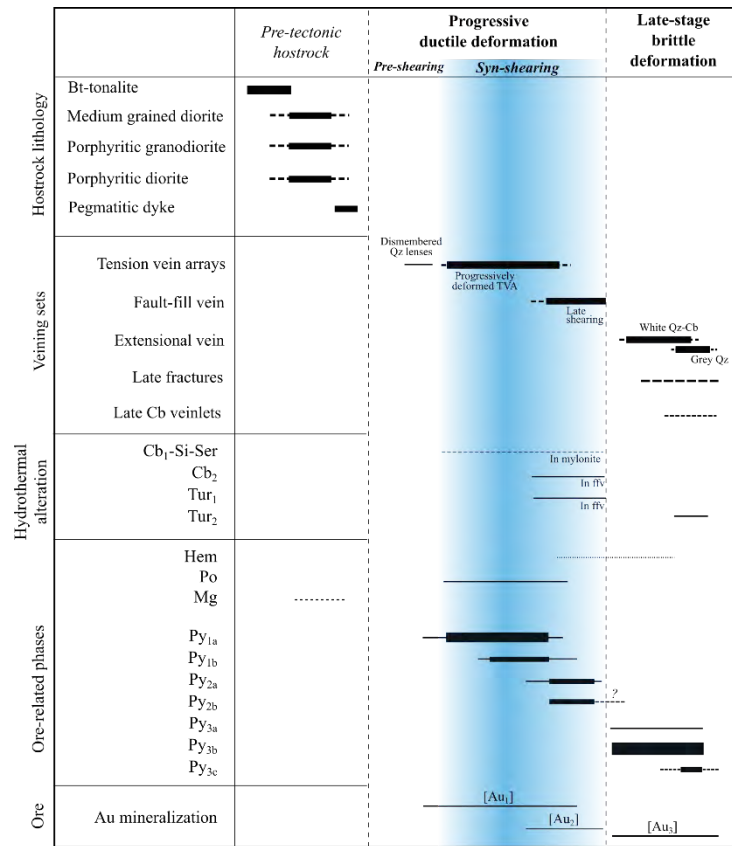


Figure 4. Paragenetic sequence established while logging. All intrusive rocks are predating deformation. When observed within the shear corridor, the pegmatitic dykes are folded and transposed. To improve this chart, a detailed study of the microstructural settings using thin sections would be needed.

Hydrothermal alteration related to shearing consists of proximal carbonate-silica-sericite assemblage. Minor carbonatization and silicification have also been identified at extensional vein’s margins. Two generations of tourmaline are visible, one being syn-shearing, with folded tourmaline fibres and only developed within the fault-fill veins, while the second generation is post-deformation and related to late quartz-carbonate veining.

At the target-scale (0.5 to 1 km²), porkknockers’ open pits were mapped. Examples of two mapped targets are given in Figure 5 where 10 to 50 m-wide NW-dipping shear zones were identified. Main host lithologies are tonalite, diorite and porphyritic granodiorite. The shear zones frequently reuse lithology contacts. The strain gradient varies greatly along strike of the mapped shear corridors creating protomylonite to mylonite in higher strain zones with a strong grain size reduction. Within these targets, the fault-fill veins are subparallel to the shear planes and change along strike and at depth from small, isolated quartz-tourmaline lenses to large (up to 5 m) veining structures while the shear corridor’s width remains relatively homogeneous. The shear zones are locally offset by late NNW-striking brittle structures (see district-scale) where late veining/fracturing seem more abundant near these structures. It is worth noticing that a deflection of the ENE shear zones has also been observed near these NNW fault zones with shear fabrics striking N160. The key parameters of the mineralized system at the Brothers Project are illustrated in Figure 6A. The ore shoot locations and plunges are controlled by (1) the subvertical jogs/dilational zones, (2) the strain gradient (vertical and along strike), (3) the density of tension veins arrays (and late-stage extensional veins when close to NNW structures) and (4) the euhedral post-shearing pyrite content. Ore plunges are interpreted as subvertical (possibly the fault-fill veins and tension vein intersections) where oblique to strike-slip regimes are observed (subhorizontal slickenlines measured on shear planes surfaces on drill cores). Although 4 mapped/drilled targets show similar geometries with a main fault-fill vein and subvertical tension veins (Fig. 6B), in one target (Jordal target), a stack of subhorizontal tension vein arrays with no fault-fill vein is mapped, witnessing a more oblique to dip-slip regime (Fig. 6C).

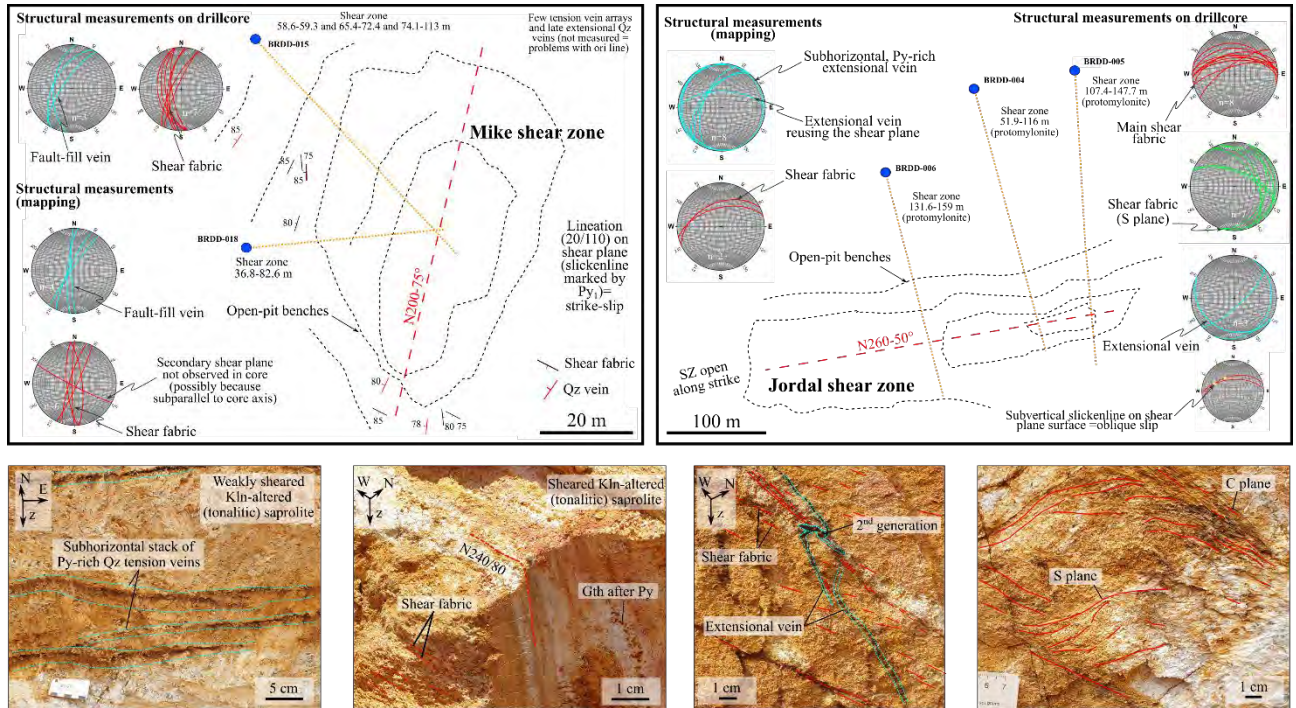


Figure 5. Example of two mapped targets (Mike and Jordal targets) with main orientations of shear fabric and spatially associated veining systems. The Mike structure is interpreted as being a strike-slip shear zone while the Jordal structure displays an oblique to dip-slip regime.

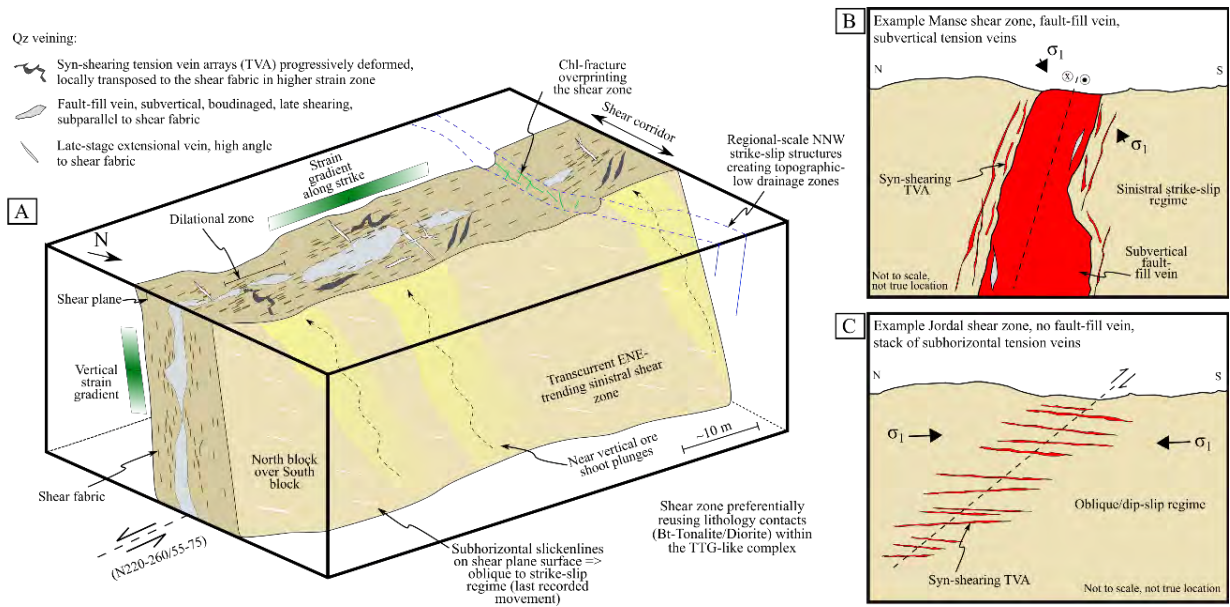


Figure 6. Illustration of the main settings observed at the target-scale (A) with subvertical ore shoots in a transcurrent ENE-striking sinistral shear zone (based on the Manse target). Regarding the veining system within the Brothers project two end members are observed: a main fault-fill vein and subvertical tension vein (B) in the case of a more strike-slip to oblique-slip regime and a stack of tension vein arrays due to an oblique- to dip-slip regime (C).

At the district-scale (~12 km²), the topography (Lidar) and airborne magnetic sets are used to draw the structural patterns (Fig. 7) in correlation with the mapped and drilled shear zones. A preliminary deformation history can be defined as follow:

- (1) a N-S to NW-SE compressional phase D_{1BR} creates the E-W to ENE structures (light black lineaments in Fig. 7, observed in the whole district marked by topographic lows features); this N-S to NW-SE shortening may be responsible for the sinistral strike-slip to oblique-slip shear zones (*in red in Fig. 7*) that are gold bearing (fault-fill veins and syn-shearing tension veins).
- (2) followed by a NNW-SSE tectonic event D_{2BR} producing large-scale brittle structures (*in black*) that can locally offset/modify the strike of the ENE shear zones (and be responsible for the late-stage brittle veining and fracturing phase observed at intersections- *in yellow*). This deformation phase could also be responsible for the ESE bends (in green) that correspond in the field to large drainage zones. The NNW structures are interpreted as left stepping strike-slip faults with a sinistral component if the ESE structures are releasing bends. These NNW-trending structures can be traced at the regional-scale toward the Rosebel district (see Fig. 1).

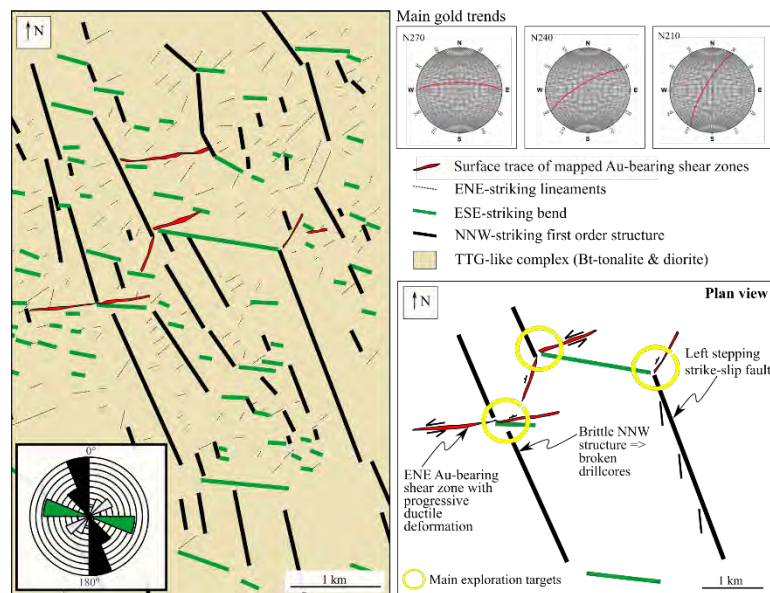


Figure 7. Interpreted structural patterns at the district-scale with *in red* the surface traces of main identified gold-bearing shear zones. At the bottom right, a simplified representation of the spatial distribution of three mapped structures and location of targets corresponding to the intersection of these features.

CONCLUSIONS

The gold mineralization is associated with ENE-striking shear corridors hosting gold-bearing quartz veins in a TTG-like complex. The proposed structural framework, based on investigations carried out at different scales, shows a polyphase history of deformation with a progressive ductile deformation phase, locally overprinted by a late-stage brittle event (higher gold grades from remobilization and/or new gold input). The spatial distribution at the district-scale reflects this complex deformation history with ENE structures overprinted by late NNW first order structures and associated ESE bends. Unlike the Yaou deposit in French Guiana (Combes et al., 2021a; 2022) where the TTG-like rocks hosting the main vein set (strong rheological control) are small intrusive bodies (plutons and dykes) within a volcano-sedimentary sequence, the mineralization at Brothers is developed within a large kilometric TTG-like complex with no volcanic or sedimentary units at the vicinity.

ACKNOWLEDGEMENT

This study is based on consulting work for Rhyolite Resources Ltd between August 2021 and June 2022.

REFERENCES

- Combes, V., Eglinger, A., Andre-Mayer, A.-S., Teitler, Y., Heuret, A., Gibert, P., Beziat, D., 2021a. In: Torvela, T., Chapman, R.J., Lambert-Smith, J. (Eds.), *Polyphase Gold Mineralization at the Yaou Deposit, French Guiana*, vol. 516. Geological Society, London, Special Publications. <https://doi.org/10.1144/SP516-2020-29>.
- Combes, V., Eglinger, A., André-Mayer, A. S., Teitler, Y., Jessell, M., Zeh, A., Reisberg, L., Heuret, A., Gibert, P., 2022. Integrated geological-geophysical investigation of gold-hosting Rhyacian intrusions (Yaou, French Guiana), from deposit-to district-scale. *Journal of South American Earth Sciences*, 114, [103708]. <https://doi.org/10.1016/j.jsames.2021.103708>
- Delor, C., de Roever, E.W.F., Lafon, J-M., Lahondère, D., Rossi, P., Cocherie, A., Guerrot, C., Potrel, A., 2003b, The Bakhuis ultra-high-temperature granulite belt (Suriname): II. Implications for the late Transamazonian crustal stretching in a revised Guiana Shield framework: *Geologie de la France* 2-3-4, 207-230.
- Kroonenberg, S.B., de Roever, E.W.F., Fraga, L., Reis, N., Faraco, T., Lafon, J.-M., Cordani, U., Wong, T., 2016. Paleoproterozoic evolution of the Guiana Shield in Suriname: a revised model. *Neth. J. Geosci.* 95, 491–522.
- Laing, W.P., 2004, Tension vein arrays in progressive strain: Complex but predictable architecture, and major hosts of ore deposits: *Journal of Structural Geology*, v. 26, p. 1303–1315, doi:10.1016/j.jsg.2003.11.006.
- LaPoint, D. J., 2019, Technical report, Brothers Project, Sipaliwini District, Eastern Suriname, South America, unpublished report.
- Robert, F., Poulsen, K.H., Dubé, B., 1994, Structural analysis of lode gold deposits in deformed terranes: Geological Survey of Canada, Open File Report 2850, 140 p.

Ultrahigh-temperature Metamorphism in the Bakhuis Granulite Belt (Suriname)

Emond de Roever

*Dept. of Earth Sciences
VU Amsterdam
De Boelelaan 1085
1081 HV Amsterdam
ederoever@ziqgo.nl*

Frank Beunk

*Dept. of Earth Sciences
VU Amsterdam
De Boelelaan 1085
1081 HV Amsterdam*

Keewook Yi

*KBSI (Korea Basic Science Institute)
YangCheong 804-1, Ochang
Cheongwon, Chungbuk 363-883, Korea
kyi@kbsi.re.kr*

Rinse-Jan Donker

*(previously)
Dept. of Earth Sciences
VU Amsterdam*

Wouter van de Steeg

*(previously)
Dept. of Earth Sciences
VU Amsterdam*

Bertram Uunk

*Dept. of Earth Sciences
VU Amsterdam*

G.R. Davies

*Dept. of Earth Sciences
VU Amsterdam*

F. M. Brouwer

*Dept. of Earth Sciences
VU Amsterdam*

SUMMARY

The UHT metamorphism (UHTM) in the BGB occurred at temperatures of up to 1020-1050°C and estimated pressures of ~ 11 kbar. Dykes of (meta)dolerite were formed during UHTM. They have insufficient volume to form the heat source for UHTM, but provide evidence for mafic magmatism and/or mantle upwelling during UHTM. Fluid inclusions (FI) in quartz in the leucosomes of metapelitic granulites contain CO₂ without H₂O. CO₂ in FI in samples from the core of the BGB has a δ¹³C value of -5 to -9 ‰, typical of CO₂-rich fluids released by mantle-derived magmas. During UHTM CO₂-rich cordierite was formed in most metapelitic granulites, with a CO₂ level of more than 2½ wt%. The high CO₂ level required for the cordierite formation was in large part derived externally, from a mantle source. Mantle upwelling took place in a zone of maximal weakness between two greenstone arms, as suggested by Delor et al (2003), or in a slab tear in the subducted West-African slab, as proposed by Klaver et al. (2015).

Key words: Bakhuis Granulite Belt, Ultrahigh-temperature metamorphism (UHTM), Mantle upwelling, Dolerites, CO₂, Fluid inclusions, Cordierite

INTRODUCTION

The Bakhuis Granulite Belt (BGB) represents a >100 km long zone of metasedimentary and metavolcanic rocks comparable to the rocks in the greenstone belt (see the Roever et al., 2019). After subduction, the belt underwent ultrahigh-temperature metamorphism (UHTM) deep in the Trans-Amazonian crust. The factors leading to its subduction and UHTM probably were related to the development of the greenstone belt.

P-T CONDITIONS OF UHT METAMORPHISM IN THE BGB

In the NE part of the BGB lies the Upper Fallawatra (UF) area, ~ 50 km² of pelitic granulites, which shows the widespread assemblage orthopyroxene + sillimanite + quartz, characteristic of UHT metamorphism. Extensive metapelitic occurrences elsewhere in the BGB show cordierite + sillimanite, locally with orthopyroxene. Feldspar thermometry by Nanne et al. (2020) showed temperatures of 900 – 1050°C for mesoperthite and antiperthite throughout the BGB, indicating that UHTM was not limited to the UF area but took place throughout most of the Belt and that the cordierite + sillimanite assemblage was also formed at UHT conditions. Raman microspectroscopy showed that the cordierite is rich in CO₂. This was confirmed by SIMS analysis, indicating 2.6 % CO₂ (Harley, pers. comm.). The high CO₂ level would have extended the stability of cordierite to higher temperatures and so explain the unique occurrence of cordierite as a primary UHT mineral, unknown from the 70+ UHT occurrences around the world.

Peak UHT temperatures were above 1020°C in a NE zone around the UF occurrence and 1020 – 1050°C in a large zone in the SW. For the pressure during UHTM there is only limited evidence, from the UF area. In the UF area only one sample

with orthopyroxene and possibly coeval garnet was found, but it is now considered more probable that the garnet is younger. The orthopyroxene in the UF area has a maximum Al_2O_3 level of 10 – 10½ wt%. Using the method of Tateishi (2004) this would give a pressure of 9½ - 10 kbar. A somewhat higher pressure is indicated by the CO_2 content of the cordierite, at ~ 1000°C a pressure of approx. 11 kbar would be required for its formation (Harley, pers. comm.).

The ultrahigh temperatures in the BGB, in part above 1000°C, would require a major heat source. Furthermore, the high CO_2 level of the cordierite would imply a major role of CO_2 during UHTM. Three hypotheses have been proposed for the heat source, all based on mantle upwelling and/or mafic underplating, by Delor et al (2003), Klaver et al. (2015), and Beunk et al. (2021).

METADOLERITE DYKES IN THE BGB

Mafic magmatism contemporaneous with the UHTM would form evidence for mantle upwelling. However, the large mafic to ultramafic intrusions in the SW of the BGB are clearly younger, at ~1984 Ma (Klaver et al., 2016), 50 – 100 Ma after UHTM. The only evidence for mantle upwelling might be formed by narrow metadolerite dykes which have been found in the NE, center and SW of the BGB. Zircon dating by Pb-Pb evaporation (de Roever et al., 2003) showed the same age for two metadolerite samples as for the UHTM.

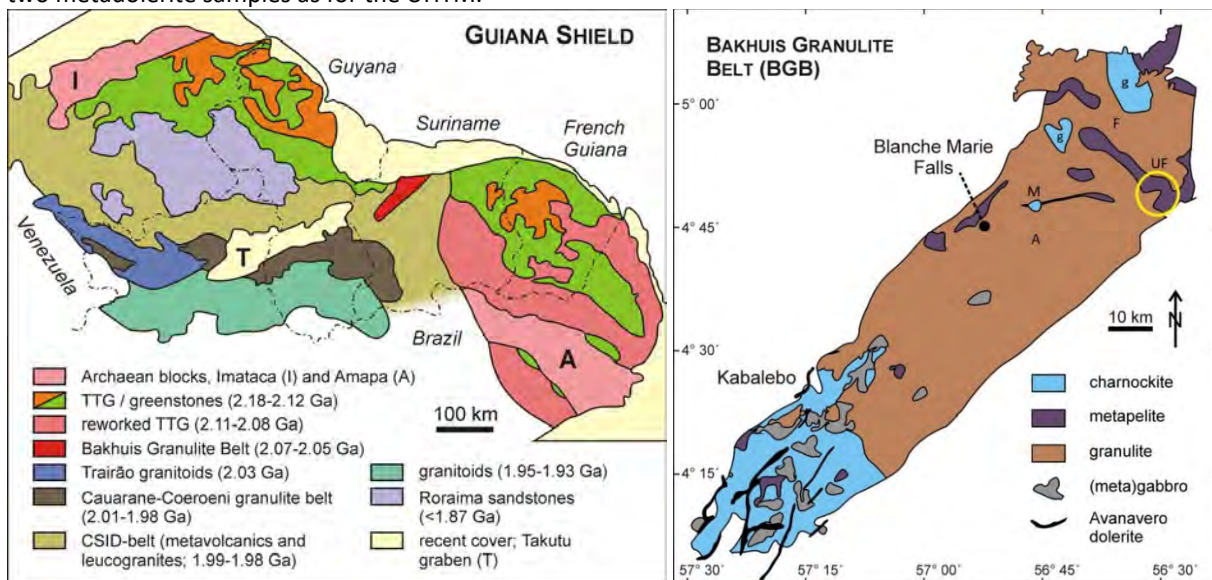


Figure 1. Left : simplified geology of the northern part of the Guiana Shield (Klaver et al., 2015); Right : geology of the BGB. M : Mozes creek; F : Fallawatra creek; A : anorthosite; UF Upper Fallawatra area (yellow circle); g biotite granite

However, microprobe investigation of zircons from a m wide dyke showed strong resorption of the zircon grains, they probably were taken up from surrounding rocks.

Near Blanche Marie Falls metadolerite boudins have been found along granulite layers which are interpreted as dykes stretched-out during UHTM folding (Fig. 2). A folded dyke was also found here. Near Mozes creek a large open fold in granulites was found with three narrow dykes parallel to the axial plane. The boudins and dykes, all fully metamorphosed, have a composition different from nearly all dolerite types from Surinam, mostly tholeiitic dolerites with $\text{MgO} < 8$ wt%. The metadolerites contain ~8 – 16 wt% MgO . This picritic composition shows their unique character. The high MgO level can best be explained by variable cumulative enrichment of olivine in the mafic magma, as indicated by the correlation of MgO with Ni resp. Cr (Fig. 2). More olivine would imply more Ni. Association of the olivine with a Cr spinel phase, as inclusion in the olivine, might explain the MgO -Cr correlation. The trace element geochemistry is consistent with a subduction zone origin, with in particular negative Nb and Ta anomalies and a positive Pb anomaly (Uunk, 2015). Both LILE and HFSE are enriched, but this is interpreted to be the result of contamination of the narrow dykes by the hosting granulites, e.g., in the form of xenocrystic accessory phases such as zircon.

In view of their narrow width and limited occurrence, the metadolerite dykes cannot be the heat source for the UHTM. However, they form clear evidence for mafic magmatism contemporaneous with UHTM, related to mantle upwelling and/or

mafic underplating.

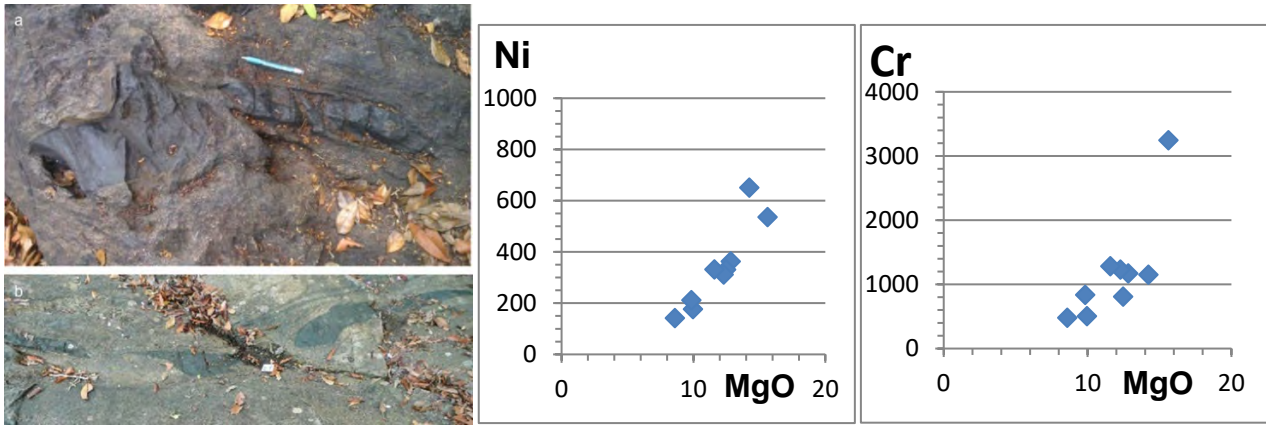


Figure 2. a. Deformed metadolerite boudin. b. Four metadolerite boudins along one level. **Right** : Ni-MgO and Cr-MgO diagrams

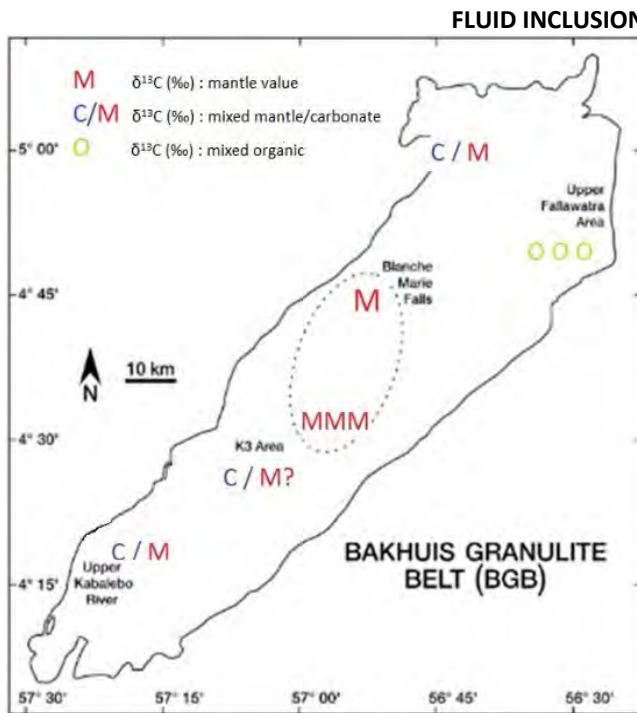


Figure 3. Distribution of $\delta^{13}C$ values in FI in the BGB

Quartz (and feldspar) in the leucosomes of pelitic granulites and in intermediary granulites frequently show trails of fluid inclusions (FI). The FI contain one component, with the high relief characteristic of CO_2 . MicroRaman analysis of such FI showed CO_2 without H_2O . The occurrence of FI with CO_2 in granulites is rather common. The CO_2 might originate from mantle-derived magmas but it might also be derived locally, from carbonate rocks. In the BGB Ca silicate granulites have been found with or without some carbonate, their composition suggests that they probably were relatively rich in CO_2 before metamorphism. The carbon isotope ratio $^{13}C/^{12}C$, commonly expressed as $\delta^{13}C$, indicates whether the CO_2 is derived from organic carbon ($-30 < \delta^{13}C < -20$ ‰), from carbonates (+4 to -2 ‰) or from the mantle (-4 - -9 ‰; Correale, 2015). Donker (2021) determined the $\delta^{13}C$ value for CO_2 from FI in 10 granulite samples and a BGB Ca silicate sample. Four samples from the core of the Bakhuis Belt show a mantle-like value, with $\delta^{13}C$ between -5 and -9 ‰, for CO_2 in the FI. The Ca silicate sample used as BGB reference for carbonates had a clear carbonate signature of +4 ‰ for its fluid inclusions. A granulite sample taken near the reference sample gave a value of 0 ‰, which may be interpreted as a carbonate value or possibly as a mixture of carbonate and

mantle CO_2 . A sample from the NW of the Bakhuis Belt had a $\delta^{13}C$ value of -2½ ‰, suggesting mixed carbonate and mantle CO_2 . Three samples from the Upper Fallawatra area in the NE show lower values, -10 to -16 ‰, suggesting an organic carbon source mixed with mantle or carbonate carbon.

One might explain the "mantle" signature for samples from the core of the BGB as a mixture of carbonate carbon ($\delta^{13}C + 4 - 0$ ‰) and organic carbon (-25 ‰). However, two samples from the core contained abundant FI and had a CO_2 content of ~30 and ~400 $\mu l/g$. If these high levels were formed from a mixture of carbonate and organic carbon, such high levels of organic carbon would have to be present in the samples with organic carbon from the NE, as well, but the UF samples have a CO_2 content of only 0.2 - 0.4 $\mu l/g$, far too low to explain the high CO_2 content of BGB core samples as a mixture of organic carbon and carbonate. In summary, four samples from the core of the BGB show a mantle-like carbon signature, whereas a sample from the NW shows a mixture of carbonate and mantle-like carbon. The mantle-like carbon signature suggests a direct relation between the UHTM and mantle magmatism and/or upwelling asthenosphere.

AGE OF UHT METAMORPHISM

De Roever et al. (2003) gave UHTM ages of 2072 – 2055 Ma, based on zircon Pb-Pb evaporation : 2072 Ma for a sillimanite gneiss from Blanche Marie Falls and around 2057 Ma for a pegmatite from Blanche Marie Falls and a garnet granulite from near the Fallawatra river. Later zircon analyses were carried out by LA-ICP-MS and SHRIMP. A sillimanite gneiss from the Kabalebo river (MKS 40) gave an LA-ICP-MS age of 2073 +/- 7 Ma (MSWD 1.5). SHRIMP Ile analysis at KBSI (Korean Basic Science Institute) on another set of zircon grains of this sample gave 2077 +/- 7 Ma (MSWD 1.2), with white rims 2030 +/- 8 Ma (MSWD 3.1, only six analyses). SHRIMP analysis of 32 spots on zircons of the sillimanite gneiss from Blanche Marie Falls gave 2074 +/- 7 Ma (MSWD 6.3). The very high MSWD suggests 2 or more populations. Unmixing resolved 3 populations, 2052 +/- 5 Ma (MSWD 0.83), 2078 +/- 5 Ma (MSWD 0.56) and 2091 +/- 5 Ma (MSWD 1.3) (van de Steeg, 2016) The oldest population had not been found before. SHRIMP analysis of zircons from a 1-2 m-wide quartz-feldspar vein at Blanche Marie Falls (Fig. 4) gave a nearly identical age, 2088.4 ± 4.4 Ma (MSWD 0.78). The zircons crystallized without monazite and, therefore, had higher Th/U ratios, varying from ca. 0.15 to 0.6 (van de Steeg, 2016). Monazite from the same vein had a younger age, 2057 Ma ± 16 Ma (SHRIMP). The 2088 Ma age is the oldest age found for the UHT metamorphism. In view of the crystallization of zircon without monazite and the resulting higher Th/U ratio of the zircons, it is assumed that this age represents a higher temperature stage within the UHTM, probably the peak of UHT metamorphism. The age coincides with the 2.11 – 2.08 Ga interval for the collision of the West-African and Amazonian plates (Delor et al., 2003). Younger zircon and monazite ages center around 2072 – 2078 Ma and around 2052 – 2058 Ma in samples from 3 locations in the BGB. It is not clear what the explanation is for these younger age concentrations with regard to the UHT metamorphism.

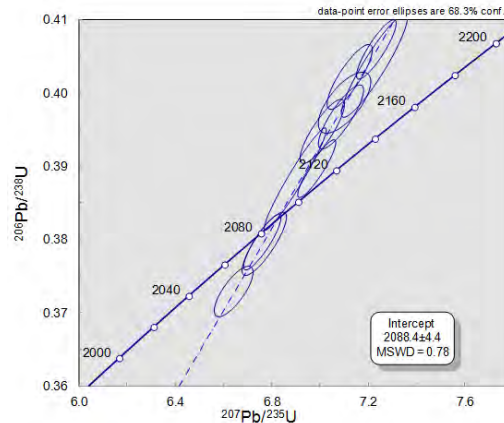


Figure 4. Left : Quartz-feldspar vein of 1-2 m wide at top, in contact with granulites at Blanche Marie Falls. Right : Concordia diagram

for 11 spots on 8 zircon grains (SHRIMP analysis) from the quartz-feldspar vein.

HEAT SOURCE OF UHT METAMORPHISM

Three different scenarios have been proposed to account for the heat source of the UHT metamorphism of the BGB. Delor et al (2003) proposed late Trans-Amazonian (2.07-2.05 Ga) mantle upwelling in a zone of maximum crustal stretching (where the BGB is situated) between two E-W TTG-greenstone continental-scale boudins. The continental-scale boudinage was enhanced by prolonged sinistral shearing of the greenstone crust. Klaver et al. (2015) modified this to “mantle upwelling in a slab tear in the subducted West African slab that formed as a result of crustal scale shearing and boudinage”. After the suturing of the TTG-greenstone belt with the Amapa Block and the West African shield in French Guiana and adjacent Brazil at 2.11-2.08 Ga (Delor et al., 2003), the collision continued. A change in subduction direction and resulting sinistral shearing possibly caused the opening of a slab window, causing mantle upwelling (Klaver et al., 2015). It has to be mentioned that the western and eastern greenstone arms are not identical. They have a large lithological similarity in their older formations, but only the eastern belt has an upper detrital unit, deposited in pull-apart basins. Furthermore, the eastern belt is bound to the south by the Archean Amapa Block and probably started cooling around 2.05 Ga. Such an Archean Block is lacking for the western arm, where orogeny and subduction probably continued (de Roever et al., 2015).

Beunk et al. (2021) envisaged a different mechanism for mantle upwelling, that is slab break-off along the length of the greenstone belt at the end of subduction, followed by mantle upwelling and/or mafic underplating. That might be possible for the 2.07 – 2.05 Ga age of UHTM given in De Roever et al (2003). However, the discovery of an earlier start of UHTM in the BGB, at ~ 2.09 Ga, would imply that the end of subduction and slab break-off should have occurred early, during the

collisional stage of 2.11 – 2.08 Ga, which is less likely. Moreover, Beunk et al. (2021) envisaged slab break-off along the length of the greenstone belt. This should have resulted in similar upwelling and UHTM along the length of the greenstone belt, but no other terrains with UHT assemblages have been found here (de Roever et al., 2003). It would also have resulted in a homogeneous distribution of UHTM assemblages in the BGB itself. Most BGB metapelitic granulites are characterized by the assemblage CO₂-rich cordierite + sillimanite, but in the Upper Fallawatra area in the NE, near the BGB border, cordierite is lacking and a normal UHTM assemblage of Al-rich orthopyroxene + sillimanite occurs. This distribution may suggest that in the S and NW parts of the BGB sufficient CO₂ became available for CO₂-rich cordierite formation. This was not the case for the UF area in the NE. Both assemblages represent UHT metamorphism, requiring a comparable heat source, but CO₂ advection differed in the BGB and was very low in the UF area in the NE, as also shown by the $\delta^{13}\text{C}$ values for CO₂ from fluid inclusions in granulites from that area.

According to Beunk et al (2021), the BGB was situated in an orogenic syntax during the 1.99 – 1.98 Ga felsic and mafic magmatism that led to the formation of charnockites in the SW of the BGB, during subduction from the south. The scenarios of Delor et al. (2003) and Klaver et al. (2015) are based on the concept that the BGB formed in a zone of maximum crustal stretching during the main Trans-Amazonian event. This would imply that the syntax proposed by Beunk et al. (2021) formed in a pre-existing zone of weakness.

ACKNOWLEDGMENTS

The Dr. Schürmann Foundation is thanked for financing expeditions and fieldwork in the BGB since 2005, and SHRIMP, LA-ICP-MS and EMP analyses. The Molengraaff Foundation and the Faculty of Science of VU Amsterdam financed travel and lodging costs of MSc students. The Geological and Mining Service (GMD) and its Director are thanked for support and use of its facilities.

SELECTED REFERENCES

- Beunk, F.F., de Roever, E.W.F., Yi, K., Brouwer, F.M., 2021. Structural and tectonothermal evolution of the ultrahigh-temperature Bakhuis Granulite Belt, Guiana Shield, Surinam : Paleoproterozoic to recent. *Geoscience Frontiers* 12, 677-692
- Correale, A., Paonita, A., Rizzo, A., Grasso, F., and Martelli, M., 2015. The carbon-isotope signature of ultramafic xenoliths from the Hyblean Plateau (southeast Sicily, Italy) : evidence of mantle heterogeneity. *Geochemistry, Geophysics, Geosystems* 16, 600-611
- Delor, C., de Roever, E., Lafon, J.-M., Lahondère, D., Rossi, P., Cocherie, A., Guerrot, C. and Potrel, A., 2003b. The Bakhuis ultrahigh-temperature granulite belt (Suriname): II. Implications for late Transamazonian crustal stretching in a revised Guiana Shield framework. *Géologie de la France*, 2003, 2–3–4 : 207–230
- de Roever, E., Beunk, F.F., Yi, K., de Groot, K., Klaver, M., Nanne, J.A.M., van de Steeg, W., Thijssen, A.C.D., Uunk, B., Vos, H., Davies, G.R., Brouwer, F.M., 2019. The Bakhuis Granulite Belt in W Suriname, its development and exhumation. *SAXI- XI Inter Guiana Geological Conference 2019*, Paramaribo, Suriname.
- de Roever, E., Lafon, J.M., Delor, C., Cocherie, A., Rossi, P., Guerrot, C., Potrel, A., 2003. The Bakhuis ultrahigh-temperature granulite belt (Suriname): I. petrological and geochronological evidence for a counterclockwise P–T path at 2.07–2.05 Ga. *Géologie de la France*, 2003, 2–3–4 : 175–206
- de Roever, E., Lafon, J.M., Delor, C., Cocherie, A., Guerrot, C., 2015. Orosirian magmatism and metamorphism in Suriname : new geochronological constraints. *Contribuicoes a Geologia da Amazonia (CGA)* vol 9, 359-372.
- Donker, R.S., 2021. On the origin of CO₂ inclusions in ultrahigh-temperature metamorphic rocks from the Bakhuis Granulite Belt, western Suriname. MSc thesis VU Amsterdam
- Klaver, M., de Roever, E., Nanne, J., Mason, P. and Davies, G., 2015. Charnockites and UHT metamorphism in the Bakhuis Granulite Belt, western Suriname: Evidence for two separate UHT events. *Precambrian Research* 262, 1–19
- Klaver, M., de Roever, E., Thijssen, A., Bleeker, W., Söderlund, U., Chamberlain, K., Ernst, R., Berndt, J., and Zeh, A., 2016. Mafic magmatism in the Bakhuis Granulite Belt (western Suriname): relationship with charnockite magmatism and UHT metamorphism : *GFF*, 138:1, 203-218
- Nanne, J.A.M., de Roever, E.W.F., de Groot, K., Davies, G.R., Brouwer, F.M., 2020. Regional UHT metamorphism with widespread, primary CO₂-rich cordierite in the Bakhuis Granulite Belt, Surinam : a feldspar thermometry study. *Precambrian Research* 350, 105894.

- van de Steeg, W., 2016. The geochemistry and geochronology of the north-eastern opx-bearing granitoids in relation to UHT metamorphism in the Bakhuis Granulite Belt, Suriname. MSc thesis VU Amsterdam
- Tateishi, K., Tsunogae, T., Santosh, M., Janardhan, A.S., 2004. First report of sapphirine-quartz assemblages from Southern India :l implications for ultrahigh-temperature metamorphism. *Gondwana Research* 7, 899-912.
- Uunk, B., 2015. Geochemistry of mafic magmatism in the Bakhuis Granulite Belt, western Surinam : implications for UHT metamorphism. MSc thesis, VU Amsterdam

The Orocaima Igneous Belt and the 1.99-1.96 Ga SLIP in the Amazonian Craton

Lêda Maria Fraga*

*Dept. of Geology
Geological Survey of Brazil
Av. Pasteur 404, Urca, Rio de
Janeiro, RJ, Brazil
leda.fraga@sqb.gov.br*

Nelson Joaquim Reis

*Dept. of Geology
Geological Survey of Brazil
Av. André Araújo 2010, Manaus,
AM, Brazil*

Evandro Klein

*Dept. of Mineral Resources
Geological Survey of Brazil
SBN, Quadra 02, Bloco H, Brasília-DF,
Brazil*

Ana Dreher

*(previously)
Dept. of Geology
Geological Survey of Brazil*

Jaime Scandola

*Dept. of Geology
Geological Survey of Brazil
SBN, Quadra 02, Bloco H, Brasília-DF, Brazil*

SUMMARY

The Orocaima Igneous Belt (OIB) is formed by high-K calc-alkaline volcanics and granitoids with subordinate shoshonitic, A-type and S-type rocks with ages in the 1.99 - 1.96 Ga range. The OIB borders to north the high-grade supracrustal Cauarane-Coeroeni Belt in the central part of the Guiana Shield. The 1.99 - 1.96 Ga magmatism also occupies large areas outside the OIB, in the central part of the Amazonian Craton, and has been recognized as a SLIP. In the northern part of the Guiana Shield, north of the OIB, uranium occurrences, IOCG mineral alteration assemblages and gold deposits hosted by Rhyacian rocks were dated at 1.99-1.96 Ga. Molybdenite-bearing granites occurs along the OIB and important gold deposits of the Tapajós Mineral Province, in the Brazil Central Shield are tentatively, associated with the Orocaima SLIP. Pre-collisional, syn-collisional and post-collisional settings or a post-orogenic evolution after the stabilization of this portion of the Amazonian Craton have been envisaged for the Orocaima SLIP. The distribution of OIB magmatism shows a close relationship with the areas of occurrence of 2.05-2.03 Ga magmatic arcs, that in the Guiana Shield were related to the Akawai Orogeny, suggesting a post-collisional setting for the Orocaima Igneous Belt and the homonymous SLIP. However, the geodynamic significance of this huge magmatism remains under debate.

Key words: Orocaima Igneous Belt, Orocaima SLIP, Eo-Orosirian evolution of the Amazonian Craton, Akawai Orogeny

INTRODUCTION

The Orocaima Igneous Belt (OIB) is formed by volcanic rocks and shallow crustal level granitoids with ages ranging from 1.99 Ga to 1.96 Ga (Fraga et al., 2017a), and extends from Venezuela to Suriname, north of the Cauarane-Coeroeni Belt (CCB) for more than 1400 km (Fig. 1). The ca. 2.02-2.00 Ga CCB is a sinuous high-grade supracrustal belt, bordered to the south by the 1.96-1.92 Ga granitoid-gneiss Rio Urubu Belt (RUB) (Fraga and Cordani, 2019). Crustal fragments of 2.05-2.03 Ga occur in the vicinities of the belts.

These huge continental-scale Eo-Orosirian belts, are the main tectonic features of the central part of the Guiana Shield, north Amazonian Craton, and mark the approximate limit between two main domains (Fig. 1). Preserved, mainly juvenile Rhyacian, 2.26-2.08 Ga old, TTG – greenstone belt terranes, Archean blocks with important Paleoproterozoic reworking, and a ca. 2.06 Ga old granulite belt occur to the north, northeast and east of the CCB and OIB. Contrasting with the north/northeast domain, to the south of the CCB and RUB, basement rocks are younger than ca.1.82 Ga in the southwestern part of the shield, and along its south-central sector, basement rocks have been intensely obliterated by the 1.89-1.87 Ga Uatumã Silicic Large Igneous Province (SLIP) (Klein et al., 2012; Reis et al., 2021) (Fig. 1).

Rock units correlated with the Eo-Orosirian terranes, so well represented in the central part of the Guiana Shield, also occurs elsewhere along the Amazonian Craton, and 1.99-1.96 Ga granitoid and volcanic rocks occupy vast areas in the southern Guiana Shield and the central part of the Brazil Central Shield. These rocks form an elongated NW-SE domain that almost enclose the Uatumã SLIP, and separate Archean terranes to east/northeast from terranes with basement rocks younger than ca.1.82 Ga, exposed to west/southwest (Fig. 1). The craton-scale distribution, volume, chemical composition, predominance of rocks with more than 65% SiO₂, and short time span of the Orocaima magmatism led Reis et al. (2021) to consider it as a SLIP.

The mineral resources potentially linked to the Orocaima SLIP were summarized by Reis et al. (2021). In the northern part of the Guiana Shield, uranium occurrence, associated with east–west shear zones, typical IOCG mineral alteration assemblages and gold deposits that are hosted by Rhyacian rocks of the TTG-granite greenstone belts furnished ages in the 1.99-1.96 Ga range (Reis et al., 2021 and references therein). In Venezuela, and in the northeastern portion of the Roraima State, Brazil, molybdenite-bearing granites were described along the OIB. Moreover, important magmatic-hydrothermal gold deposits of the Tapajós Mineral Province, in the Brazil Central Shield are tentatively, associated with the Orocaima SLIP. These deposits are hosted by 1.99–1.96 Ga old volcanic and plutonic rocks and correspond to Au and Au–Ag (Cu–Pb–Zn) polymetallic mineralization of low- to intermediate-sulfidation epithermal, intrusion-related and Au-rich porphyry deposits hosted in oxidized granites (Reis et al., 2021 and references therein).

We present an overview of the Orocaima Igneous Belt and the homonymous SLIP and highlight that in order to understand the geodynamic significance of this huge magmatism, it must be evaluated as a craton-scale event.

GEOLOGICAL SETTING

The granitoid and volcanic rocks of the OIB received different names along the Guiana Shield. In Venezuela, granitoids and volcanics are collectively encompassed in the Cuchivero Group and the volcanic rocks are included in the Caicara Formation (Sidder

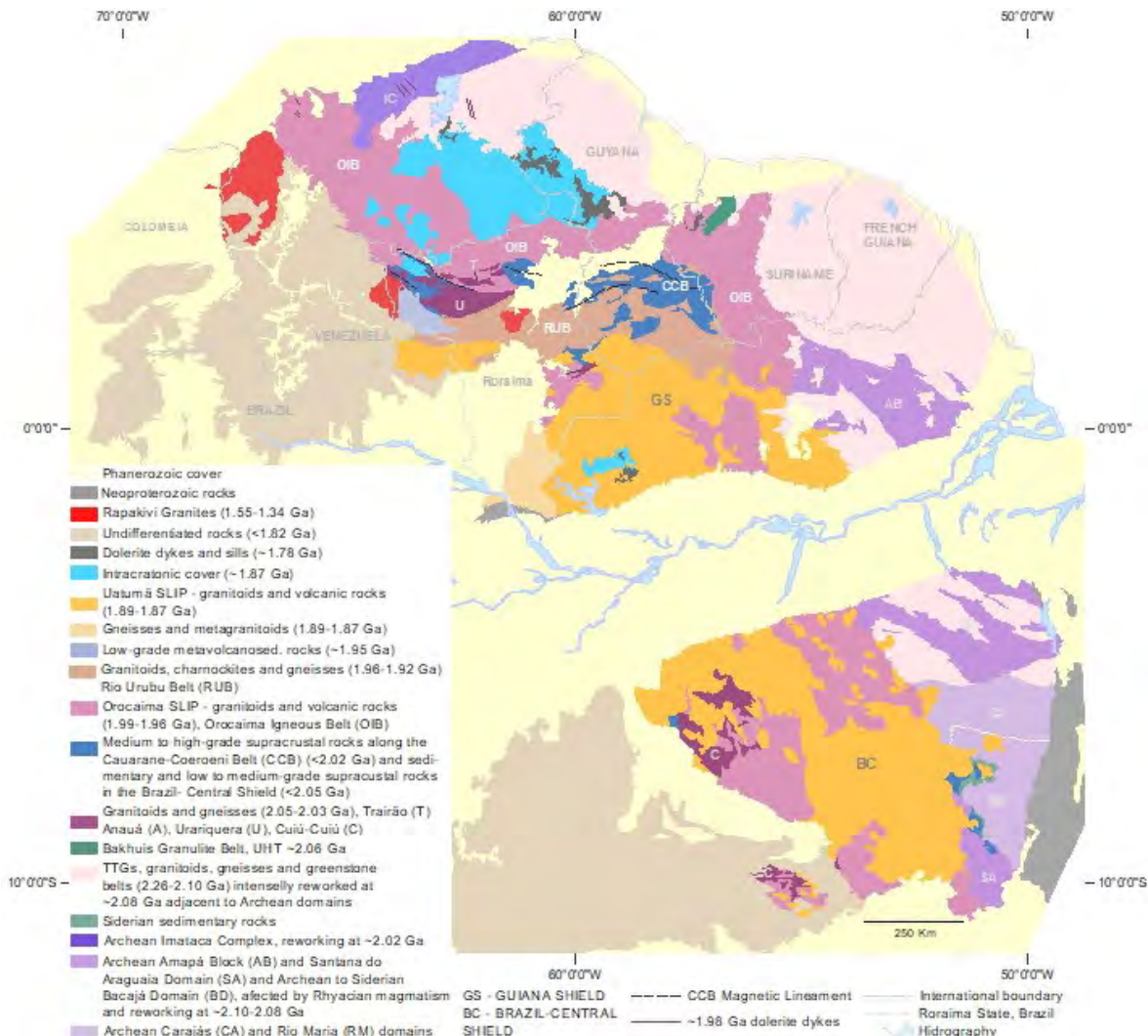


Figure 1 – Simplified geological map of the Amazonian Craton.

and Mendoza, 1995). In Brazil, the granitoids of the Pedra Pintada, Aricamã, Saracura, Tocobirém, Puruê, Mixiguana and Reislândia suites and the volcanic rocks of the Surumu Group and the Cachoeira de Ilha Formation occur. In Guyana, the

volcanic rocks (Iwokrama Formation) and associated granitic bodies are designated as the Burro-Burro Group (Berrangé, 1977), and the Makarapan Mountain Granite has been recently also recognized as part of the OIB (Fraga et al., 2017 a). In Suriname the volcanic rocks are named Dalbana Formation and the 1.99-1.96 Ga granitoids belong to the Wonotobo, Sipaliwini, Coppename and Werekitto units (Kroonenberg et al., 2016; Fraga et al. 2017 b). The granitoids of the OIB are usually isotropic only affected by the K'Mudku Episode along localized shear zones. However, rocks with compositional banding and magmatic foliation, were locally recognized in the vicinity of high-grade supracrustals of the Cauarane-Coeroeni Belt.

High-K calc-alkaline granitoids predominate along the OIB and A-type and shoshonitic rocks are subordinate as well as S-type granites. Most of the calc-alkaline varieties in Brazil pertain to the Pedra Pintada Suite, which is correlated with the Wonotobo Granite in Suriname and with most of the granitoids included in the Burru-Burro and Cuchivero groups. The Saracura and Aricamã suites, in Brazil, encompass reduced and oxidized A-type granites, and tin-specialized varieties were recognized (CPRM, 2010). The Sipaliwini Granite in Suriname is correlated to the Aricamã and Saracura granites and few A-type, peralkaline, riebeckite granite bodies also occurs in Brazil (Serra da Lontra Granite) and in Guyana (Makarapan Mountain Granite) (Fraga et al., 2017a, b). Granitoid rocks exhibiting a shoshonitic affinity were recognized along the OIB in the northern part of the Roraima State of Brazil, and belong to the Tocobirén Suite (CPRM, 2010), and few S-type granite bodies of the Coppename Muscovite Granite occur in Suriname (Kroonenberg et al., 2016).

With respect to the volcanic rocks of the OIB, pyroclastic varieties largely predominate over lavas and subvolcanic intrusives. Compositionally, rhyolitic types predominate over rhyodacitic and dacitic varieties, and andesites and basaltic andesites are subordinate (Sidder and Mendoza, 1995; CPRM, 2010, and references therein; Berrangé, 1977; Anandbahadoer-Mahabierr and De Roever 2019). Most of the volcanic rocks of the Surumu, Caicara and Dalbana units are geochemically akin to high-k calc-alkaline rocks (Sidder and Mendoza, 1995; CPRM, 2010; Anandbahadoer-Mahabierr and De Roever 2019). However, effusive rocks with geochemical affinity with A-type granites occur in northern Roraima State and are included in the Cachoeira da Ilha Formation (CPRM, 2010).

The available data confirm that the OIB was formed during a short period of time, in the 1.99-1.96 Ga range, by coeval magmatism of different typologies, including high-K calc-alkaline and reduced and oxidized A-type rocks as well as shoshonitic and S-type granitoids.

Along the northern part of the shield, outside the main exposition of the OIB, subordinate charnockitic and granitic bodies, as well as gabbroic and anorthositic bodies (Kroonenberg et al., 2016) and dolerite dykes (Yanez-Mejia et al., 2015) with ages in the 1.99-1.97 Ga were identified.

In the southern part of the Guiana Shield (Fig. 1), the Orocaima SLIP is formed by the high-K, calc-alkaline to shoshonitic granitoids of the Cachipacoré and Martins Pereira units and the volcanic rocks of similar geochemical affinity of the Igarapé Paboca Formation (Almeida et al. 2007; Leal et al., 2018). Subordinate bodies of the S-type Serra Dourada Granite (Almeida et al. 2007) also occur. Along the Brazil Central Shield the Orocaima plutono-volcanism is also represented by high-K calc-alkaline to shoshonitic volcanic and granitoid rocks. The volcanics are included in the Vila Riozinho, Novo Progresso and Jarina units and the granitoids pertain to the Creporizão, Vila Rica, Nhandu and Pé Quente suites (Guimarães and Klein, 2020; Alves et al., 2020; Vasquez et al, 2019, and references therein). Recently a migmatitic gneiss with ~1.98 Ga leucosome, was identified in a restricted area in the Brazil Central Shield and was interpreted as recording the crustal melt related to the generation of the Orosirian felsic magmatism

The vast expositions of the Orocaima Magmatism along the Amazonian Craton, are spatially associated with 2.05-2.03 Ga granitoids and gneisses represented in the Guiana Shield by the Trairão, Anauá units and possibly also by the Urariquera Complex and in the Brazil Central Shield by the Cuiú-Cuiú Complex, and to ~2.02-2.00 Ga supracrustal rocks (Fig. 1). The supracrustal rocks are better represented along the high-grade Cauarane-Coeroeni Belt, but also occurs in the Brazil Central Shield (Jacareacanga Group). The 2.05-2.03 Ga granitoids and gneisses exhibit a medium-K calc-alkaline affinity and juvenile isotopic signature, and have been interpreted as representing magmatic arcs or island arcs (Santos, 2003; Almeida et al. 2007; Guimarães and Klein, 2020; CPRM, 2010; Alves et al., 2020). The supracrustal rocks are envisaged as orogenic basins that were closed during the assembling of the Eo-Orosirian arcs at around 2.02-2.00 Ga. This collisional phase of the evolution of the Guiana Shield is related to the Akawai Orogeny, and marks the second collision of the Transamazonia Cycle, after the main Rhyacian one, that occurred around 2.08 Ga (Fraga and Cordani, 2019). The collisional phase of the Akawai Orogeny otherwise is mainly represented by the CCB and the Imatoca Complex. The PTt evolution path of the supracrustal

rocks of the CCB is not yet understood. However, for the Imataca Complex, a clockwise P-T path with metamorphic peak at 2.02 Ga, with an initial high T/P rate metamorphism, followed by tectonic loading, decompression, rapid uplift, and finally isobaric cooling was characterized by Tassinari et al., (2004). The tectonic controlled rapid exhumation of the complex had ceased before the rocks passed below 600°-550°C at around 1.96 Ga (Tassinari et al., 2004).

DISCUSSION AND CONCLUSIONS

Considering the geological context depicted for the central part of the Guiana Shield, Fraga et al. (2017 a) envisaged a post-collisional, intracontinental, setting for the OIB magmatism. Intense high-K calc-alkaline magmatism and subordinate peraluminous (S-type), alkaline and peralkaline granitoids are typical of the post-collisional stage in several orogens (Bonin, 2004), and are related to thermal instability in the mantle generated after the collision and slab break-off. This magmatism is concentrated along narrow zones aligned with important tectonic features, in a remarkably similar scenario to that of the OIB, that border the CCB to north (Fig. 1). The high-K calc-alkaline signature that predominate over the OIB reflects the partial melting of crustal material with subduction signature inherited from the pre-collisional stage, with possible contribution of mantle sources previously enriched by subduction components, during the evolution of the 2.05-2.03 Ga arcs. In a different point of view, many authors envisaged a syn-subduction setting for the OIB, reflecting the evolution of a continental magmatic arc (Santos, 2003; Anandbahadoer-Mahabierr and De Roever 2019). However, this proposition is difficult to conciliate with the coeval magmatism of different typologies, including peralkaline granite bodies, with almost identical ages and without any zoning along the belt (Fraga et al. 2017 a).

For the Orocaima magmatism outside the OIB a syn-subduction setting have also been proposed (Santos, 2003; Leal et al., 2018) and an evolution in a long-lived magmatic arc in the 2.05-1.95 Ga range, was suggested by some authors (Alves et al., 2020, and references therein). Alternatively, a syn-collisional setting related to the evolution of the Anauá arc (Almeida et al, 2007) was interpreted for southern part of the Guiana Shield, and a post-collisional setting, after the assembling of the Cuiú-Cuiú arc (Guimarães and Klein 2020), was envisaged for the 1.99-1.96 Ga magmatism along the Brazil Central Shield.

Finally, contrasting with previous models that recognized a link between the 1.99-1.96 Ga magmatism, and different phases of the Eo-Orosirian orogenic processes, related by Fraga and Cordani (2019) to the Akawai Orogeny, Reis et al. (2021) proposed the evolution of the Orocaima SLIP in an intraplate, post-orogenic setting after the stabilization of this portion of the Amazonian Craton. In a similar way, Ibanez-Menjia (2015) interpreted 1.98 Ga dyke swarms of the northern border of the shield as related to a plume, that would be responsible for the evolution of the Orocaima SLIP, in an intraplate (anorogenic) setting. The plume-head would be situated in the central part of the Roraima State of Brazil.

The tectonic setting of SLIPS continues under debate (Bryan and Ferrari, 2013). Some of them have been characterized as related to intraplate magmatism in a continental break-up context, while others were interpreted as related to the extensional collapse immediately after the main orogenic phase, or to a supra-subduction zone setting (Bastías-Mercado et al. 2020 and references therein).

As shown above, the tectonic setting of the Orocaima SLIP remains under debate. Considering the OIB, many A-type and calc-alkaline bodies were dated at 1.99 Ga (Fraga et al 2017 a) and are temporally very close the 2.02-2.00 Ga period envisaged for the collisional phase of the Akawai Orogeny, recorded along the Imataca Complex and the CCC. In the Imataca Complex the rapid exhumation had ceased at around 1.96 Ga (Tassinari et al., 2004; Swapp and Onstott, 1989). This scenario fits well with the proposition of an intracontinental, post-collisional evolution for the OIB. Otherwise important deformation and deep seated magmatism was concentrated in the central part of the shield in the 1.96-1.93 Ga along the RUB, suggesting that the final stabilization of this portion of the Amazonian Craton had not yet been achieved when the OIB was installed.

At the craton scale Fraga et al. (2017 c) also envisaged a post-collisional setting for the 1.99-1.96 Ga plutono-volcanism. These authors suggested that the formation of hydrated and fertile sources at the base of the crust during the Eo-Orosirian orogenic processes allowed large-scale crustal melting to form the 1.89-1.87 Ga Uaumã SLIP, attesting the importance of the Akawai Orogeny for the evolution of the Amazonian Craton.

As a final remark, the Orocaima SLIP represents a huge intracontinental magmatism that rests to be better understood, in order to elucidate its metallogenic potential, geodynamic significance, and also to enhanced the geological correlations with other segments of the Columbia Supercontinent like the West Africa Craton and the Baltic Shield.

ACKNOWLEDGMENTS

The Geological Survey of Brazil – SGB/CPRM is thanked for supporting this research.

SELECTED REFERENCES

- Almeida M.E., Macambira M.J.B., Elma, C.O., 2007. Geochemistry and zircon geochronology of the I-type, high-K calc-alkaline and S-type granitoid rocks from southeastern Roraima, Brazil: Orosirian collisional magmatism evidence (1.97–1.96 Ga) in central portion of Guyana Shield. *Precambrian Research*. **155**, 69–97.
- Alves, C.L., Rizzotto, G.J., Rios, F.S., de Barros, M.A., S., 2020. The Orosirian Cuiú-Cuiú magmatic arc in PEIXOTO de Azevedo domain, Southern of Amazonian craton. *J. South Am. Earth Sci.* <https://doi.org/10.1016/j.jsames.2020.102648>.
- Anandbadoer-Mahabier, R., De Roeveer, E.W.F., 2019. The Caicara-Dalbana Belt, a Belt of Felsic and Intermediate Metavolcanics of 1.99 Ga in the Guiana Shield, and Probably Across, in the Guapore Shield. In: 11th Inter Guiana Geological Conference: Tectonics and Metallogenesis of NE South America Paramaribo, Suriname. Geol. Mijnbouwkund. Dienst Suriname Meded. 29.
- Bastías-Mercado F, González J, Oliveros V., 2020. Volumetric and compositional estimation of the Choiyoi Magmatic Province and its comparison with other Silicic Large Igneous Provinces. *J. South Am. Earth Sci.* <https://doi.org/10.1016/j.jsames.2020.102749>.
- Berrangé, J.P., 1977. The geology of southern Guyana, South America. Overseas Memoir 4, Institute of Geological Sciences, London, p. 12.
- Bonin, B., 2004. Do coeval mafic and felsic magmas in post-collisional to within-plate regimes necessarily imply two contrasting, mantle and crustal, sources? A review. *Lithos* **78**, 1-24.
- Bryan, S.E. and Ferrari, L. 2013. Large igneous provinces and silicic large igneous provinces: progress in our understanding over the last 25 years. *Geological Society of America Bulletin*, 125, 1053–1078, <https://doi.org/10.1130/B30820.1>
- CPRM, Geological Survey of Brazil, 2010. Programa Geologia do Brasil. Programa Cartografia da Amazônia. Geologia e Recursos Minerais da Folha Vila de Tepequém, NA.20-X-A-III. Escala 1:100 000. Estado de Roraima. In: Fraga, L.M. and Dreher, A.M. (eds). Projeto Roraima Central, Manaus, <http://rigeo.cprm.gov.br/jspui/handle/doc/10920>
- Fraga, L.M.B, Cordani, U., 2019. Early Orosirian tectonic evolution of the Central Guiana Shield: insights from new U-Pb SHRIMP data. In: SAXI- XI Inter Guiana Geological Conference. Paramaribo, Suriname. Extended abstract, p. 59–62.
- Fraga, L.M.B, Cordani U.G., Reis N.J., Nadeau S., Maurer V.C., 2017 a. U-Pb SHRIMP and LA-ICP-MS new data for different A-Type granites of the Orocaina Igneous Belt, Central Guyana Shield, Northern Amazonian Craton. In: 15°. Simpósio de Geologia da Amazônia. Belém, Pará, Soc. Brasileira de Geol. – Núcleo Norte, Anais, p. 482-485.
- Fraga, L.M.B., Dreher A.M., Kroonenberg S., De Roeveer E., Faraco T., Wong T., Reis N., Lisboa Lago A., 2017 b. Geological and geodiversity mapping on the Brazil-Suriname border project. Explanatory note for the geological, mineral resources and geodiversity maps. Brasília, CPRM. 52pp.
- Fraga, L.M.B, Vasquez, M.L., Almeida, M.E., Dreher, A.M., Reis, N.J. 2017 c. A Influência da Orogenia Eo-Orosiriana na formação da SLIP Uatumã, parte central do Cráton Amazônico. In: 15°. Simpósio de Geologia da Amazônia. Belém, Pará, Soc. Brasileira de Geol. – Núcleo Norte, Anais, p. 405-409.
- Guimarães, S.B. and Klein, E.L. 2020. Geochemical and isotopic constraints on the host rocks of the magmatic-hydrothermal Coringa gold–silver (Cu–Pb–Zn) deposit of the Tapajos mineral province, Amazonian Craton, Brazil. *J. South Am. Earth Sci.*, 103, <https://doi.org/10.1016/j.jsames.2020.102726>
- Ibanez-Mejia, M. 2015. The c. 1.98 Ga Yanomami LIP: A new Large Igneous Province in the Amazon Craton. In: Reconstruction of Supercontinents Back too 2.7 Ga Using The Large Igneous Province (LIP) Record. With Implications For Mineral Deposit Targeting, Hydrocarbon Resource Exploration, and Earth System Evolution. 14p.
- Kroonenberg, S. B., Roeveer, E.W.F. de, Fraga, L.F., Reis, N.J., Faraco, T.M., Lafon, LM, Cordani, U., Wong, T.E. 2016. Paleoproterozoic Evolution of the Guyana Shield in Suriname: A revised model. *Netherland Journal of Geosience-Geologie en Mijnbouw*, **95**, 491–522.
- Klein E., Almeida M., Rosa-Costa L.T., 2012. The 1.89-1.87 Ga Uatumã Silicic Large Igneous Province, northern South America. *Large Igneous Provinces Commission* (<http://www.largeigneousprovinces.org>), November 2012 LIP of the Month.
- Leal, R.E., Lafon, J.M., Rosa-Costa, L.T. da and Dantas, E.L. 2018. Orosirian magmatic episodes in the Erepecuru-Trombetas Domain (southeastern Guyana shield): implications for the crustal evolution of the Amazonian Craton. *J. South Am. Earth Sci.*, **85**, 278–297.

- Reis, J. R., Teixeira, W., D'Agrella-Filho, M. S., Bettencour, J. S., Ernst, R. E and Goulart, L. E. A. 2021. Large igneous provinces of the Amazonian Craton and their metallogenic potential in Proterozoic times. Srivastava, R.K., Ernst, R. E., Buchan, K. L., and Kock, M., (eds.). Large Igneous Provinces and their Plumbing Systems. Geological Society, London, Special Publications, 518, 37 p. <https://doi.org/10.1144/SP518-2021-7>.
- Santos J. O. S. 2003. Geotectônica dos Escudos das Guianas e Brasil Central. In: Bizzi, L.A.; Schobbenhaus, C.; Vidotti, R.M Gonçalves, J.H. *Geologia, tectônica e Recursos Minerais do Brasil*. Brasília: CPRM. p. 198.
- Sidder, G.B., Mendoza V.S., 1995. Geology of the Venezuelan Guayana Shield and its relation to the Geology of the entire Guayana Shield. *U. S. Geol. Survey Bull.*, 2124 (B):1-33.
- Tassinari, C.G., Munhá, J.M.U., Teixeira, W., Palácios, T., Nutman, A.P., Sosa, C., Santos, A.P., Calado, B.O., 2004. The Imataca Complex, NW Amazonian craton, Venezuela: Crustal evolution and integration of geochronological and petrological cooling histories. *Episodes*, **27**, 3-12.
- Vasquez, M.L., Cordani, U.G., Sato, K., Barbosa, J.P.O., Faraco, M.T.L. and Maurer, V.C. 2019. U–Pb SHRIMP dating of basement rocks of the Iriri–Xingu domain, Central Amazonian province, Amazonian craton, Brazil, *Brazilian Journal of Geology*, 49. <https://doi.org/10.1590/2317-4889201920190067>.

An Investigation into the Characteristics of Fault and Fault Zones of the Guyana Basin

La Donna Fredericks^{1,2}

Dr. Helen Lewis¹

Dr. Andy Gardiner¹

¹Heriot Watt University, Campus the Avenue, Edinburgh EH14 4AS, United Kingdom

²GGMC, Upper Brickdam Georgetown

SUMMARY

The interpretation of 2D seismic data indicated that the Jurassic and Pliocene normal faults and listric normal faults acted as conduits from the Canje shale source rocks and is a possible explanation for the accumulation of hydro- carbon in the shelf and shelf edge carbonate build ups. It is possible that many sub-seismic faults and fractures occurred in the Guyana Basin similarly to the Maracaibo and Santos basins.

INTRODUCTION

The Guyana Basin is located in north-eastern South America along a passive margin. It covers an area of 120,000 km² (46,332 mi²) and encloses onshore and offshore Guyana, Suriname, Venezuela, and French Guiana (Figure 1). It currently has four producing fields namely the Liza Field (offshore Guyana) and the Calcutta, Tambaredjo and Tambaredjo North West Fields (onshore Suriname). The Guyana Basin is estimated to have reserves greater than 16 billion barrels equivalent and the gas reserves exceed 30 trillion cubic feet. The magnitude of discovery to date is constantly increasing with Exxon's continued exploration success. During extension events, deformation in the Guyana sedimentary basin was accommodated by SW-NE steeply dipping normal and listric normal faults. These faults were mainly observed in the volcanic basement rocks, and the important Cretaceous- Pliocene basin fills (clastics and carbonates). Faults provide a pathway for hydrocarbon to flow through, however they may act as barriers to flow. They may also act as structural traps. The characteristics of the faults and fault zone are thus critical, as they help us to understand the transmissivity of potential reservoirs.

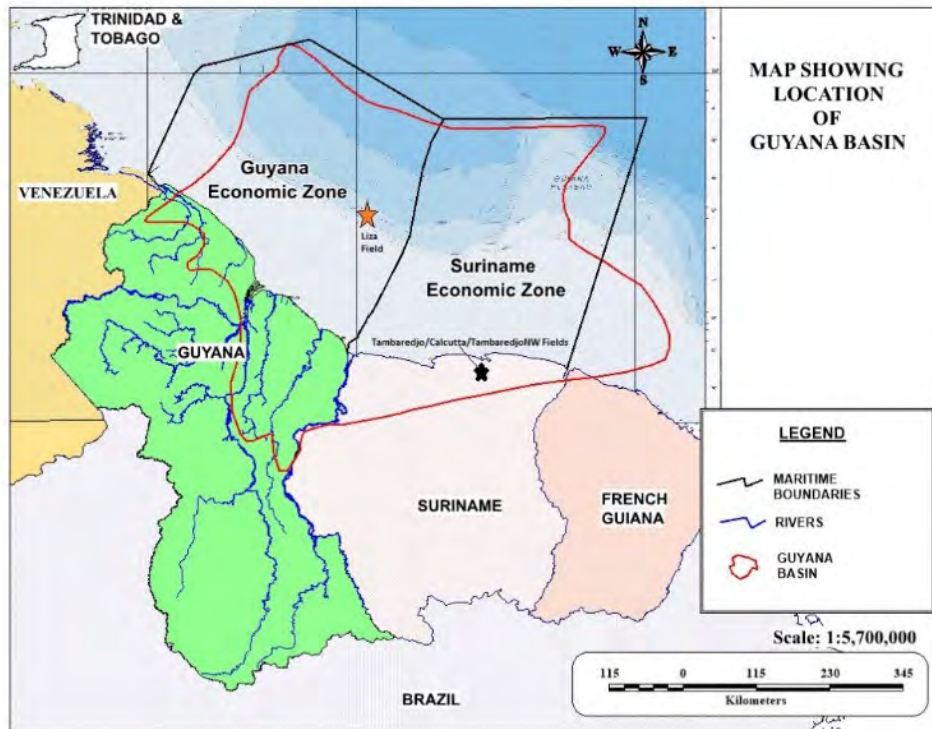


Figure 2: Location Map of Guyana Suriname Basin

Geological Setting of the Guyana Basin

The Guyana Basin is located offshore Guyana and Suriname and is bounded to the north by the Pomeroon Arch, south by the Demerara Plateau and southwest by the Proterozoic Amazon craton. The Guyana Basin was formed during the Mesozoic to Cenozoic from the South Atlantic Oceans formation and West Gondwana rifting (Bryant *et al.*, 2012). It was formed in three stages, Central Atlantic rifting phase (200-145 Ma), African rifting phase (145-113Ma) and passive margin phase (113Ma - present). In the first phase, rifting of the South and North American plates caused NW-SE extension and dextral shearing, which led to the formations of grabens in the Guyana Basin and in the onshore Takutu Basin (Gouyet *et al.*, 1994). Stratigraphy associated with this phase consists of thick mafic basaltic volcanics, followed by non-marine (fluvial, lacustrine) sediments. The lacustrine sediments in this syn-rift succession include type II kerogen black shales which is the main source rock for hydrocarbon generation also known as the Canje Formation Shale. The second phase, marine transgressions from the proto-Atlantic led to the deposition of extensive shelf carbonates and shallow marine clastics. The formation of the carbonate shelf system, including the Demerara Rise on the Guyana margin and the Guinea rise on the African Margin. In the South Atlantic, further separation of the South American and African plates was accommodated by clockwise rotation of Africa in relation to South America resulting in the separation of the Demerara and Guinea Rises. Normal faults trending northwest-southeast with en echelon folds were recorded in the Demerara Rise. Gradual subsidence along the passive margin was followed by an abrupt uplift (Gouyet *et al.* 1994., Yang & Escalona, 2011). Deposition of the organic rich shale source rock was re-established along the passive margin. Upwelling and oceanic anoxic events drove the organic enrichment and reduced water circulation in the basin (Meyers *et al.*, 2006). Additionally, subsidence along the now passive margin led to a deepening of the basin and the establishment of significant submarine fan systems especially offshore from long- established river systems forming the reservoir rock in Liza-1 field. Both clastic and carbonate successions in this drift phase have provided excellent hydrocarbon reservoirs in the Guyana Basin and on both sides of the South Atlantic Ocean. The stratigraphic seals were created by incision of channel systems filled with mud. Listric faults, foot wall blocks along paleo shelf edge, rollover anticlines and the Pomeroon Arch are the main structural traps of the Guyana Basin. Workman and Birnie (2007), suggested that the Guyana Basin architecture corresponds to a trap door setting that plunges from the Pomeroon Arch and adjacent to the Demerara Plateau.

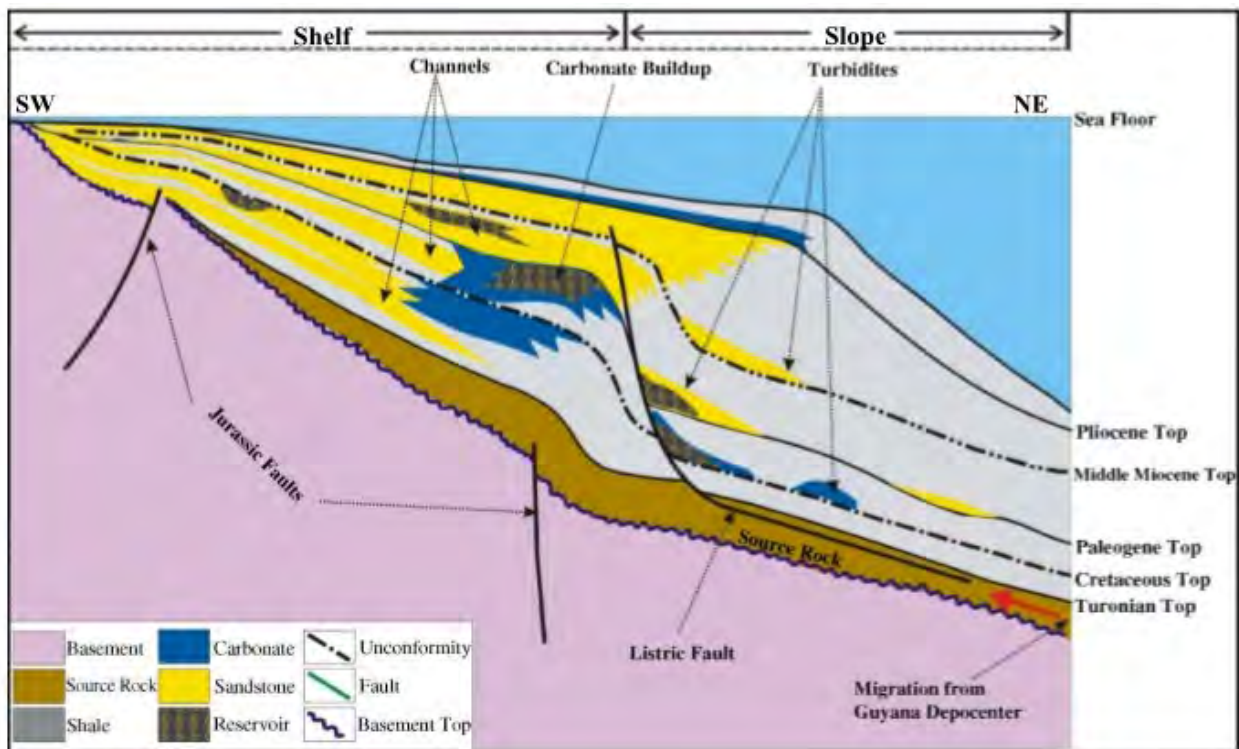


Figure 2: Cross Section of the Guyana Offshore Basin (from: Yang & Escalona, 2011)

RESEARCH APPROACH

In this study, the focus was to identify the fault types, geometry, throw and offset, spacing, frequency, the lithologies they crosscut, orientation, transmissibility and contents of the fault zone within the Guyana Basin from the review of pre-existing literature. There is some information about the macro faults available in Yang and Escalona (2011), however there is no published data for the fault characteristics. Therefore, better-known, but otherwise analogous basins were reviewed. Raw 2D seismic data acquired by CGX for the landward to shelf edge portion of the Guyana Basin presented in the Yang & Escalona, (2011) were reinterpreted to identify the faults in the different geological time and rock types.

RESULTS

In total twenty-three Jurassic normal faults were observed. These faults dip to the SW and NE with varying fault height, throw and separation. Jurassic and Pliocene normal faults height is smaller and range from 200 – 4,500 m while the listric fault height is between 1,000-14,500 m. The normal fault separation ranges from 1,600 – 20,000 m while the listric fault separation is smaller and ranges from 2,500 – 6,000 m. The Pliocene faults are much closer to each other with separation ranging from 1000-2000 m. The main curved listric fault has smaller synthetic faults running parallel and merging within the cretaceous sediments.

These curved faults were observed in sandstones with thickness ranging from 50- 400 m, limestones greater than 50 m thick and shales with thickness greater than 150 m. The throw of the Jurassic normal faults ranges from 140 – 1,800 m. The cumulative fault frequency for seismically resolvable macro faults for the smallest range of 0 – 500 m is 12 and the largest range greater than 1,500 m is 2. The Miocene and Pliocene faults follow similar trend. The Miocene faults throw ranges from 140- 980 m with a cumulative frequency of 5 faults between the range of 0 – 500 m and 1 in the 500- 1000 m range. The Pliocene fault throw range from 70 – 840 m with 3 faults less than 500 m and 1 greater than 500 m.

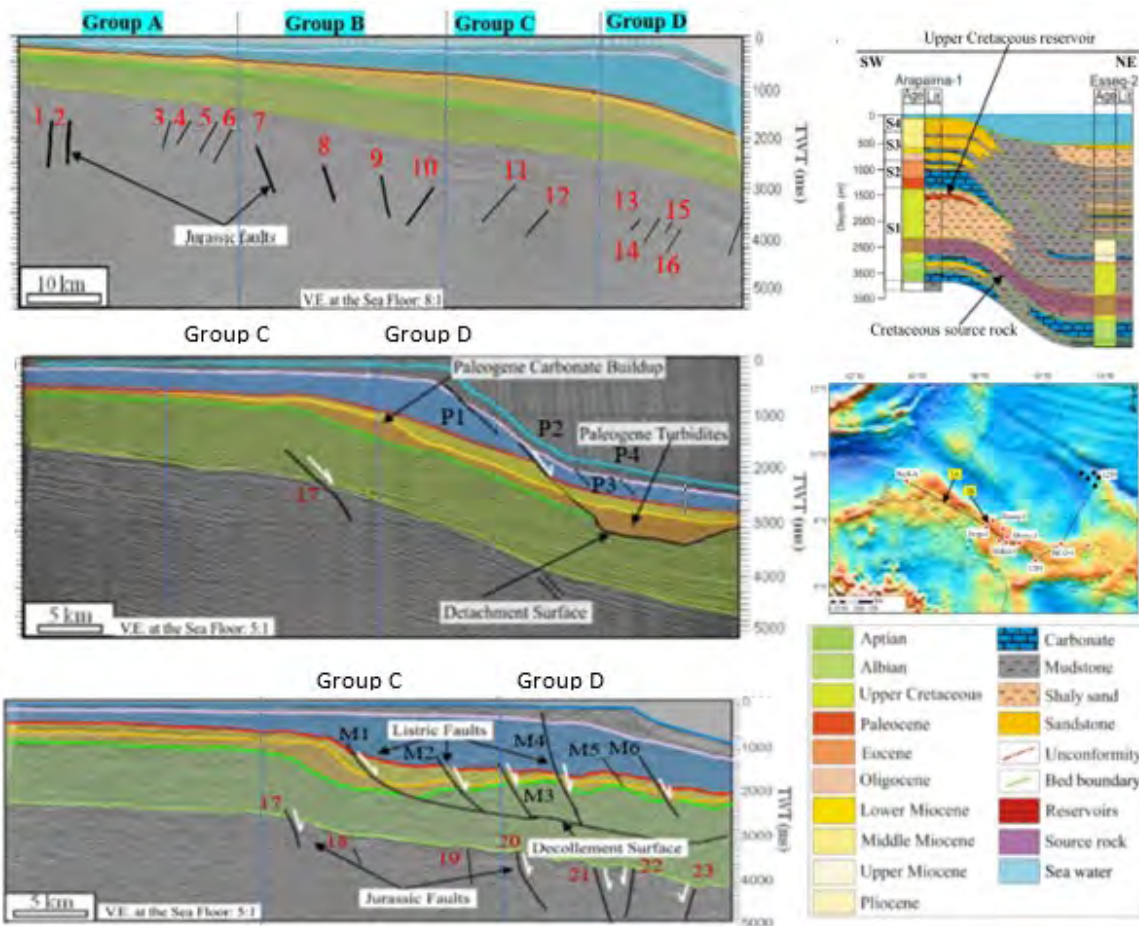


Figure 3: Faults reinterpreted from 2D seismic data (Yang and Escalona, 2011)

CONCLUSIONS

The findings of this research indicate the main units affected by faulting in the Guyana Basin are the Cretaceous sediments (sandstone, limestone, mudstone, and shale) and the volcanic basement. The basement was affected by twenty-three SW-NE steeply dipping normal faults identified in this study that have increasing fault throw with respect to the fault height. Twelve faults had throw ranging from 0 – 500 m from which the cumulative fault frequency decreased as the maximum throw increase following the power law relationship. The throw of the Miocene and Pliocene listric normal and normal faults identified in this study follows the same relationship as the Jurassic faults. As the maximum throw for each range increase the cumulative frequency of the fault throw decreases. It was observed that the faults were following the power law which assumes the strain is the same at all scale (King et al., 2007). The synthetic listric faults are believed to be acting as fluid conduits since it is a possible explanation for the accumulation of hydro- carbon in the shelf and shelf edge carbonate build-ups. The faults presumably transported hydrocarbons from the Canje Formation shale to the underlying and overlying carbonate and sandstone reservoirs, however there is a possibility that these faults will have sealing characteristics. In the Cretaceous Formations, sand on shale juxtaposition exist where the Stabroek Formation and New Amsterdam Formation sandstones are next to the Canje shale. In the Canje Formation the sealing capacity may be a function of the clay smear potential or shale gouge ratio since its solely composed of over 150 m to 400 m of anoxic black shale. There may also be sealing sand on sand contact in the Stabroek formation which has more than 50 m sandstone package and no record of shale or mudstone. The study of the fault characteristics will help us to better understand fault behaviour and thus their impact on the basin properties, transmissivity, compartmentalization and assist in getting maximum recoveries from the reservoirs.

REFERENCES

- Bryant I., Dailly P., Dribus J. R., et al. (2012). Basin to Basin: Plate Tectonics in Exploration. Schlumberger.
- Gouyet S., Mascle. A., and Unternehr P., (1994). The French Guyana margin and the Demerara Plateau: Geological history and petroleum plays. European Association of Petroleum Geoscientist.
- King C.P.G., and Sammis G.C. (2007). Mechanical origin of power law scaling in fault zone rock. American Geophysical Union.
- Meyers A. P., Astrid F., and Stefano B.M., (2006). Origins and accumulation of organic matter in expanded Albian-Santonian black shales sequences on the Demerara Rise, South American Margin: Organic Geochemistry.
- Naruk S.J., Dula., W.F., Busch J.P., et al. (2002). Common Characteristics of Proven Sealing and Leaking Faults. Shell Petroleum Development Company.
- Workman W., and Birnie D.J., (2007). The Guyana- Suriname Basin: An evolving exploration Opportunity, GEOSEIS Inc., Calgary, AB, Canada.
- Yang W., Escalona A., (2011). Techno stratigraphic Evolution of the Guyana Basin. The American Association of Petroleum Geologists.

Tracing the influence of the Amazon River along the Suriname coastline from the Mid-Miocene to Holocene

Author: Kathleen Gersie and Carina Hoorn

Contact: k.gersie@uva.nl/ Kathleen.gersie@uvs.edu/ kgersie@hotmail.com

Abstract

The Suriname coast is part of the extensive coastline along northeastern South America. This coastline stretches from the Amazon River, Brazil, to the Orinoco River in Venezuela. The continental shelf, located in front of the Guyanas, was a carbonate platform in the period prior to the late Miocene (11 million years ago). This platform received siliciclastic sediments from the crystalline basement in eastern Amazonia. Previous research revealed that since the late Miocene tectonic evolution of the Andes and global sea level changes a bulk of Andean-derived sediments were delivered by the Amazon River that resulted in the onset of the buildup of the Amazon fan, which in turn has affected the Guyana coastline (Figueiredo et al., 2009). Although, the exact age of the onset of the Amazon River is debated, this is an important matter to many scientists because of the global and regional influence of the Amazon River on continental and marine processes (Hoorn et al., 2017; Araujo et al., 2022). To determine the age of onset, and the influence of the Amazon River on the coastal landscape and vegetation of Suriname coast, we must study sediment changes and link these to pollen sources.

Method

In this project we will work with material that has been collected from exploration wells from the State Oil Company in the nearshore area of the Suriname coast near Paramaribo (Suriname). Specifically, we will (1) count and classify the different sporomorph types using reference literature; (2) select the most important sporomorphs for photography using light microscopy and scanning electron microscopy; (3) process the data and apply multivariate data analysis to establish ecological groups; (4) compare data with other Miocene records from the Amazon, and determine how past flora and prevailing climatic conditions can be linked. The results of your work should be published in collaboration with the project leaders and an international team of researchers.



Figure 1: (A) The coastline of Suriname between French Guiana and Guyana, South America; (B) Close up picture of the Suriname coast with mudflats and mangrove forests

Techniques:

- Palynological analysis
- Light Microscopy and Scanning Electron Microscopy
- Dinoflagellate analysis

Background reading

- Araujo, G.S., Rocha, L.A., Lastrucci, N.S., Luiz, O.J., Di Dario, F. and Floeter, S.R., 2022. The Amazon-Orinoco Barrier as a driver of reef-fish speciation in the Western Atlantic through time. *Journal of Biogeography*.
- Figueiredo, J., Hoorn, C., van der Ven, P., Soares, E. Late Miocene onset of the Amazon River and the Amazon deep-sea fan: Evidence from the Foz do Amazonas Basin (2009). *Geology* 2009; 37; 619-622; doi: 10.1130/G25567A. 1.
- Hoorn, C., Bogota-A, G.R., Romero-Baez, M., Lammertsma, E.I., Flantua, S.G.A., Dantas, E.L., do Carmo, D.A., Chemale Jr., F. (2017). The Amazon at sea: Onset and stages of the Amazon River from a marine record, with special reference to Neogene plant turnover in the drainage basin. *Global and planetary change* 153, 51-65; <http://dx.doi.org/10.1016/j.gloplacha.2017.02.005>.
- Hoorn, C., Wesselingh, F.P., Ter Steege, H., Bermudez, M.A., Mora, A., Sevink, J., Sanmartin, I, Sanchez-Meseguer, A., Anderson, C.L., Figueiredo, J.P., Jaramillo, C., Riff, D., Negri, F.R., Hooghiemstra, H., Lundberg, J., Stadler, T., Sarkinen, T., Antonelli, A. (2010). Amazonian through time: Andean uplift, climate change, landscape evolution, and biodiversity. *Science*, 330, 927; doi: 10.1126/science.1194585
- Salamanca Villegas, S., van Soelen, E.E., Teunissen van Manen, M.L., Flantua, S.G.A., Ventura Santos, R., Roddaz, M., Luiz Dantas, E., van Loon, E., Sinninghe Damste, J.S., Kim, J-H., Hoorn, C. (2016). Amazon forest dynamics under changing abiotic conditions in the early Miocene (Colombian Amazonia). *Journal of Biogeography*. doi:10.1111/jbi.12769
- Van de Hammen, T., Wijmstra, T. A. (1964). A palynological study on the Tertiary and Upper Cretaceous of British Guiana. *Leidse Geologische Mededelingen*, DL. 30 p.p. 183-241, Preissued 15-12-1964.

French Guiana: new insights into under-investigated region for geological assessment - A BRGM approach

Blandine Gourcerol*

Aertgeerts G.,

Rivera L.,

*French Geological Survey
BRGM*

*French Geological Survey
BRGM*

*French Geological Survey
BRGM*

45060 Orléans, France
b.gourcerol@brgm.fr

35700, Rennes, France
g.aertgeerts@brgm.fr

97300 Cayenne, French Guiana, France
l.rivera@brgm.fr

SUMMARY

French Guiana is a France' department historically prospect for gold mineralization. Several studies conducted by the BMG and the BRGM have helped to identify some mineral targets for mineral industry in the early XXe. However, with the economic growth, the energy and numerical transition, critical raw materials have been identified by the European commission and may represent future targets in the near future for European countries including the French Guiana as France's department. In this context innovative tools could be applied on historical datasets to assess and identify this related potential.

Key words: French Guiana, gold deposits, critical raw material, mineral exploration

INTRODUCTION

In a context of climate change and related international renewable energy policy, fast growth of emerging economies as well as rapid development of innovative technologies have led to drastic increase of demand for several commodities. Accordingly, supply reliability in Critical Raw Materials (CRM) and strategic metals (e.g. Cu, Li, graphite) is one of the major challenges facing Europe. Thus, identification of mineral resources represents a critical step in securing strategic sectors for European industries leading European territories and related countries to conduct mineral resources inventories and resources assessment in order to evaluate countries' competitiveness (European Commission, 2020a,b). In this context, French Guiana that has been historically prospected for gold mineralization may represent a great potential for CRM and strategic metals, which were not well studied in the past.

A STRONG GOLD HISTORY

French Guiana is an overseas France's department located on the northern Atlantic coast of South America. It forms part of the South American Guiana Shield extending from the Venezuela to the northernmost part of Brazil (Billa et al., 2013) and consists of Paleo- to Neoproterozoic granite-greenstone terranes. Economically, the French department represents the first French Au province with about 213 tons (identified) of gold extraction reported since 1855. Geologically, gold occurrences are closely related to the ca. 2.25 to 1.95 Ga Transamazonian orogenic system (eg Vanderhaeghe et al., 1988; Enjoly, 2008; Milési et al., 2003), which consists of a period of crustal growth/recycling with oceanic crust formation. This stage is illustrated by collision tectonics and erosion/sedimentation of sandstones and fluvial conglomerates named the Upper Detrital Unit (UDU), which crops out in the Northern Guiana Greenstone belt (NGGB) along the major fracture zone named the "North Guiana Trough".

Historically, presence of gold in the Guiana Shield has been documented since ancestral times but also fantasized by the first Spanish, Portuguese and English explorers between the XVIth and XVIIth centuries, related to numerous legends such as those of the *El Dorado*, the *Manoa city* and the *Lake Parimé*. Indeed, according to the latter, the heart of the Guiana Forest may contain "very rich and abundant deposits of gold and precious stones, as well as valleys covered with auriferous material", already suggesting that gold had been noticed both in outcrops and related to alluvial deposits. In 1854, first official discovery of gold represents the beginning of the Gold Rush.

Between 1975 and 1995, exploration and mapping programs led both by the governmental institutions (e.g. BMG, BRGM) and mining companies allowed the identification of a great variety of commodities such as gold, niobium, tantalum, lithium, copper, bauxite, kaolin, heavy minerals and diamond among others (Figure 1). Since, the identification and discovery mostly of gold occurrences, both related to primary and secondary processes, has continued in French Guiana (e.g., Guiraud et al., 2020; Combes et al., 2021a, b, 2022) and across the Guiana Shield (Daoust et al., 2011; Velásquez et al., 2011, 2014, 2018; Tedeschi et al., 2018a, b, 2020).

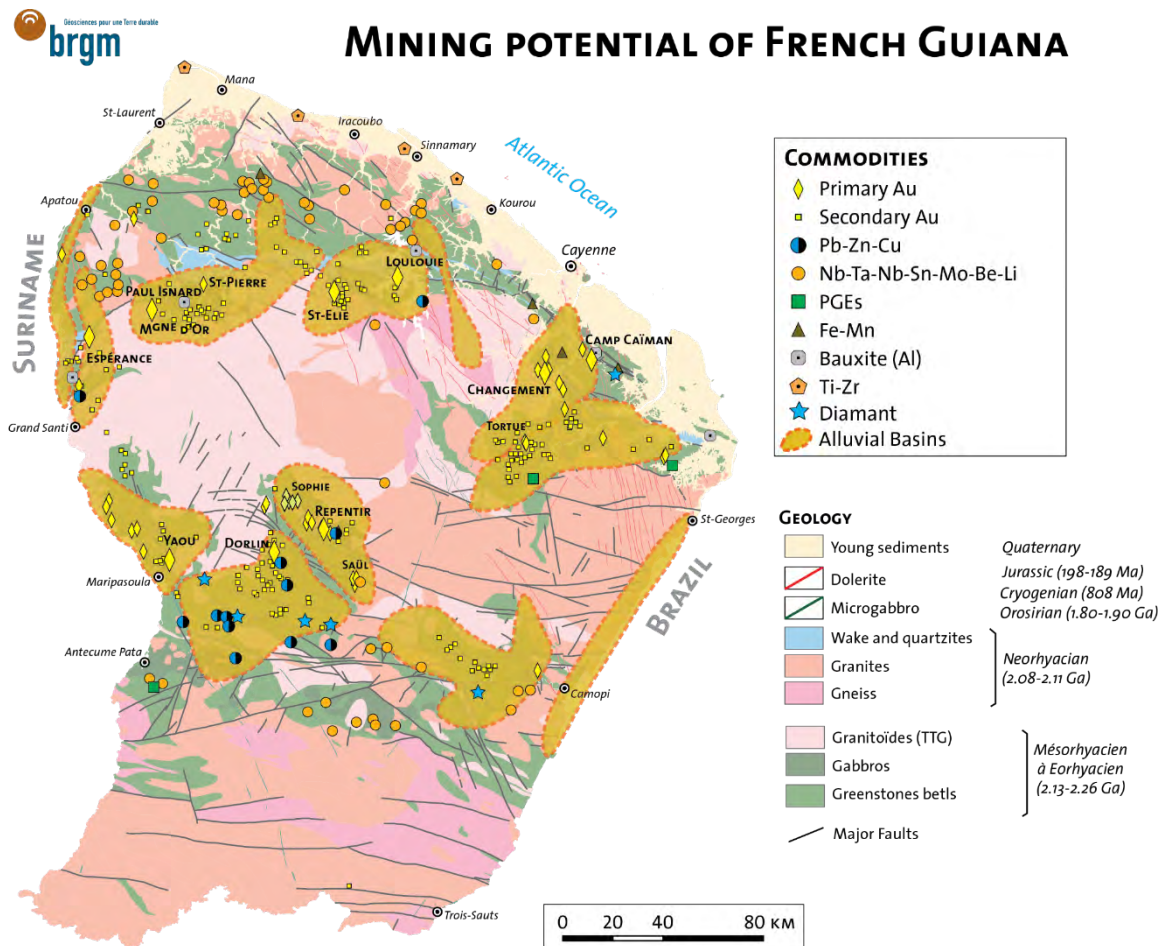


Figure 3 : Simplified map of the main alluvial basins location and their related identified mineralization in French Guiana (on a 1/500 000 geological base, after Delor et al, 2001, modified from Thomassin et al., 2017).

However, climate change and related international renewable energy policy may drive new mineral prospections especially on strategic and CRM in French Guiana (eg Billa et al., 2013).

IMPLICATIONS FOR MINERAL EXPLORATION

Elsewhere, geological Precambrian terrane boundaries that have been historically explored for their significant gold (Au) potential (e.g. Abitibi greenstone belt, Canada) represent currently strategic targets for other commodities (e.g. Li Case Lake project and Au-Cu Côte-Gold Deposit, Canada).

Indeed, the related geodynamic context is known to represent a favourable site for several magmatic and hydrothermal events along with various ore deposit types (Cox, 2005). Recent studies have demonstrated that various mineralization styles along regional fault systems show a regular spatial distribution of the ore deposits (eg Groves et al., 1998; Weinberg et al., 2004). Active and repetitive crustal deformation is necessary to generate and maintain permeability and to sustain large-scale fluid flow such as hydrothermal system (Cox, 2005). Consequently, the longevity and complexity of a regionally

considered “ore system” may represent a great opportunity to assess regional geodynamical context and related exploration for various metals including the CRM necessary for the energy and digital twin-transitions. Thus, geostatistical approaches including mineral prospectivity methods on CRM and strategic metal databases applied on the Historical Mineral Inventor may help to target new commodities and may drive regional policy.

ACKNOWLEDGMENTS

This abstract and related presentation reflects work conducted by the BMG and the BRGM in the last decades. Thus, authors would like to acknowledge all the participants of the historical and current works on and in French Guiana.

REFERENCES

- Billa M., Chevillard M., Tourlière B., Marteau P., Cassard D., Théveniaut H. (2013) – Guyane et gisements, hors or : état des connaissances et réexamen du potentiel minier. Rapport Final. BRGM/RP-62003-FR, 157p., 64fig., 16tab.
- Combes V., Eglinger A., André-Mayer A.-S., Teitler Y., Heuret A., Gibert P., Béziat D. (2021a). Polyphase gold mineralisation at the Yaou deposit, French Guiana. Geological Society, London, Special Publications 516.
- Combes V., Eglinger A., André-Mayer A.-S., Teitler Y., Jessell M., Zeh A., Reisberg L., Heuret A., Gibert P. (2022). Integrated geological-geophysical investigation of gold-hosting Rhyacian intrusions (Yaou, French Guiana), from deposit-to district-scale. *Journal of South American Earth Sciences* 114, 103708.
- Combes V., Teitler Y., Eglinger A., André-Mayer A.-S., Heuret A., Pochon A., Cathelineau M., Gibert P. (2021b). Diversity of supergene gold expressions and implications for gold targetting in an equatorial regolith (AMG’s Couriège Exploration Prospect, French Guiana). Geological Society, London, Special Publications 516.
- Cox (2005). Coupling between Deformation, Fluid Pressures, and Fluid Flow in Ore-Producing Hydrothermal Systems at Depth in the Crust; *Geology*
- Daoust C., Voicu G., Brisson H., Gauthier M. (2011) Geological setting of the Paleoproterozoic Rosebel gold district, Guiana Shield, Suriname. *Journal of South American Earth Sciences* 32, 222–245.
- Enjolvy (2008). PhD thesis, Université Montpellier II, sciences et Techniques du Lanquedoc, 305p.
- European Commission (2020a). Study on the EU’s List of Critical Raw Materials Final Report 2020; European Commission: Brussels, Belgium
- European Commission (2020b). Critical Raw Materials Resilience: Charting a Path Towards Greater Security and Sustainability 2020; European Commission: Brussels, Belgium.
- Guiraud J., Tremblay A., Jébrak M., Ross P.-S., Lefrançois R. (2020). Stratigraphic setting and timing of the Montagne d’Or deposit, a unique Rhyacian Au-rich VMS deposit of the Guiana Shield, French Guiana. *Precambrian Research* 337, 105551.
- Groves D.I., Goldfarb R.J., Gebre-Mariam M., Hagemann S.G., Robert, F. (1998). Orogenic gold deposits: A proposed classification in the context of their crustal distribution and relationship to other gold deposit types, *Ore Geology Reviews*, Vol. 13, Issues 1–5, 1998, 7-27,
- Milési J. P., Egal E., Ledru P., Vernhet Y., Thiéblemont D., Cocherie A., Tegye M., Martel-Jantin B., Lagny P. (1995) Northern French Guiana ore deposits in their geological setting. *Chronique de la Recherche Minière* 63, 5–58.
- Milési J.-P., Lerouge C., Delor C., Ledru P., Lahondère D., Lasserre J.-L., Marot A., Martel-Jantin B., Rossi P., Tedeschi M., Hagemann S.G., Davis J. (2018a). The Karouni Gold Deposit, Guyana, South America: Part I. Stratigraphic Setting and Structural Controls on Mineralization. *Economic Geology* 113, 1679–1704.
- Tedeschi M., Hagemann S. G., Roberts M. P. and Evans N. J. (2018b). The Karouni Gold Deposit, Guyana, South America: Part II. Hydrothermal Alteration and Mineralization. *Economic Geology* 113, 1705–1732.
- Tedeschi M. T., Hagemann S. G., Kemp A. I. S., Kirkland C. L. and Ireland T. R. (2020). Geochronological constrains on the timing of magmatism, deformation and mineralization at the Karouni orogenic gold deposit: Guyana, South America. *Precambrian Research* 337, 105329.
- Tegye M., Théveniaut H., Thiéblemont D., Vanderhaeghe O. (2003) Gold deposits (gold-bearing tourmalinites, gold-bearing conglomerates, and mesothermal lodes), markers of the geological evolution of French Guiana: geology, metallogeny, and stable-isotope constraints. , 34.
- Thomassin J.-F., Urien, P., Verneyre, L., Charles N., Galin R., Guillon, D., Boudrie, M., Cailleau A., Matheus P., Ostorero C., Tamagno D. (2017). Exploration et exploitation minière en Guyane; tome 8, 141p.
- Vanderhaeghe O., Ledru P., Thiéblemont D., Egal E., Cocherie A., Tegye M., Milési J.-P. (1998). Contrasting mechanism of crustal growth Geodynamic evolution of the Paleoproterozoic granite-greenstone belts of French Guiana. *Precambrian Research*, vol. 29.

- Velásquez G., Salvi S., Siebenaller L., Béziat D., Carrizo D. (2018). Control of Shear-Zone-Induced Pressure Fluctuations on Gold Endowment: The Giant El Callao District, Guiana Shield, Venezuela. *Minerals* 8, 430.
- Velásquez G., Béziat D., Salvi S., Siebenaller L., Borisova A.Y., Pokrovski G.S., De Parseval P. (2014). Formation and Deformation of Pyrite and Implications for Gold Mineralization in the El Callao District, Venezuela. *Economic Geology* 109, 457–486.
- Velásquez G., Béziat D., Salvi S., Tosiani T., Debat P. (2011). First occurrence of Paleoproterozoic oceanic plateau in the Guiana Shield: The gold-bearing El Callao Formation, Venezuela. *Precambrian Research* 186, 181–192.
- Weinberg R.F., Hodkiewicz P.F., Groves D.I. (2004). What controls gold distribution in Archean terranes?; *Geology* 2004; 32 (7): 545–548

A newly recognized 1.98 Ga large igneous province (LIP) in the Amazonian Craton and its relationship with the coeval Orocaima silicic LIP

Mauricio Ibañez-Mejía*

*Dept. of Geosciences
University of Arizona
Tucson, AZ, USA
ibanezm@arizona.edu*

Richard Ernst

*Dept. of Earth Sciences
Carleton University
Ottawa, Ontario, Canada
richard.ernst@ErnstGeosciences.com*

Ulf Söderlund

*Dept. of Geology
Lund University
Lund, Sweden
ulf.soderlund@geol.lu.se*

Franco Urbani

*Escuela de Geociencias
University Central de Venezuela
Caracas, Venezuela
urbanifranco@yahoo.com
salomonkroonenberg@gmail.com*

Paul Antonio

*Géosciences
Université de Montpellier
Montpellier, France
paulantonio0931@gmail.com*

Salomon Kroonenberg

*Dept. of Geology
Anton de Kom University
Paramaribo, Suriname*

Martin Pepper

*Dept. of Geosciences
University of Arizona
Tucson, AZ, USA
mpepper@arizona.edu*

The Orocaima silicic large igneous province (SLIP) of the Amazonian Craton constitutes one of the largest SLIPs recognized on Earth and possibly the most voluminous Paleoproterozoic magmatic event in Amazonia. Nevertheless, the triggering mechanisms behind this episode of large-volume felsic magmatism and its relationships with regional tectonic and/or mantle processes remain debated. Here, we present new high-precision geochronologic as well as geochemical results from multiple mafic dike swarms in the Guyana Shield of the Amazonian Craton, namely the Guaniamo, Aro, Manteco-Supamo, and Goboy swarms, and show that these are geochemically unrelated but temporally and geographically associated with the Orocaima SLIP. The radial arrangement of these swarms, their clear tholeiitic geochemical affinity, and their emplacement in regions far from known arc-related magmatic centers in the Amazonian Craton at 1.98 Ga, suggest a plume-related origin for these mafic magmas. Discovery of this previously unrecognized LIP and its close association with the Orocaima suggests that heat transfer from an impacting plume triggered large-scale melting of the Amazonian lithosphere resulting in SLIP development, thus arguing against accretionary models for the origin of this voluminous silicic magmatic belt. Re-interpretation of paleomagnetic poles of the Aro swarm using our new geochronologic results, in addition to inter-cratonic correlations with other coeval LIPs globally, enables a better paleogeographic reconstruction of Amazonia in the Paleoproterozoic and a more accurate understanding of the role of this major craton in the global Precambrian supercontinent cycle.

Preliminary investigation of the Toroparu Au-Ag-Cu Deposit, Guyana, South America

Tramaine N. James¹, Stéphane Perroudy¹, Daniel J. Kontak¹, Michael Tedeschi¹, Philip Lypaczewski^{1,2} and Robert A. Creaser³

¹Harquail School of Earth Sciences, Laurentian University, 935 Ramsey Lake Road, Sudbury, ON, P3E 2C6, Canada.

²College of the North Atlantic, 1 Prince Philip Dr, St. John's, NL A1C 5P7, Canada.

³Department of Earth and Atmospheric Science, University of Alberta, Edmonton, Alberta, T6G 2E3, Canada.

The Paleoproterozoic Toroparu Au-Ag-Cu system is located within the Mazaruni greenstone belt of the Guiana Shield, Guyana, South America (Fig. 1). The Toroparu project consists of four main deposits – three at Toroparu called the Main, North West, and South East and one at Sona Hill – with a preliminary mineral resource estimate of 8.4 Moz Au, 6 Moz Ag, and 396 Mlb Cu (Nordmin Engineering Ltd., 2022).

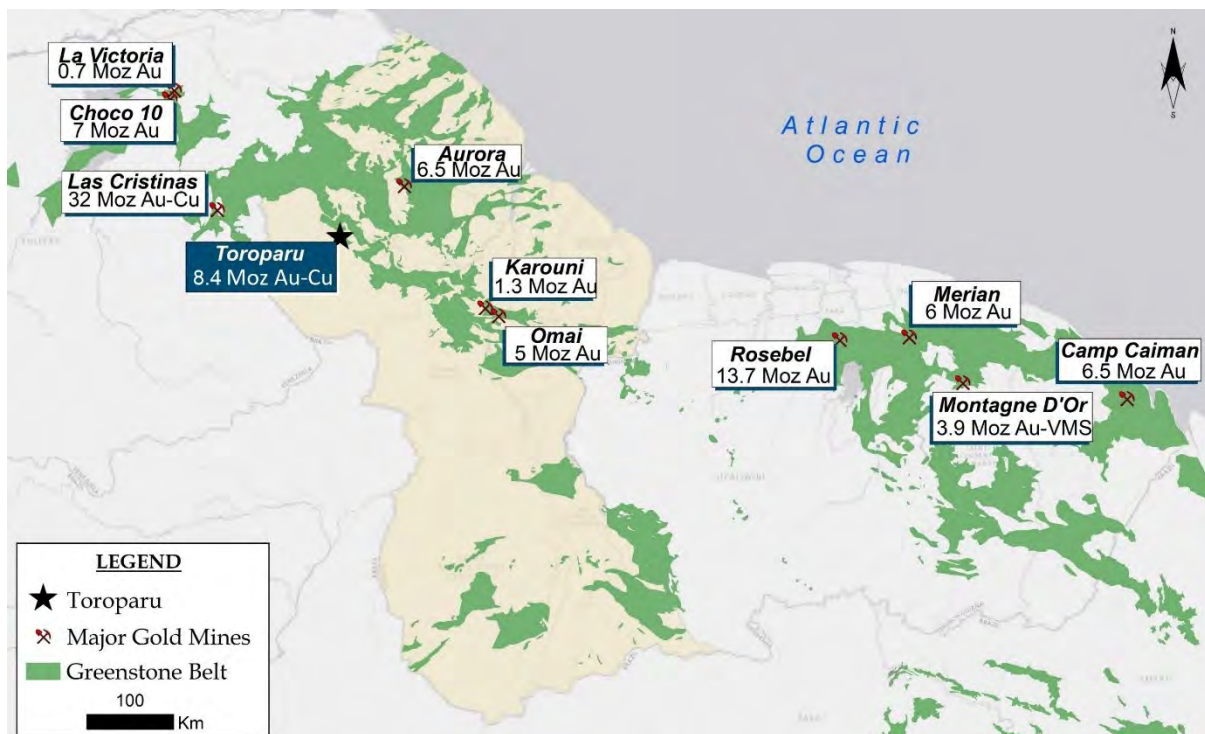


Figure 4: Map of major Au deposits within the Guiana Shield

The Toroparu project lies on a regional NW-trending, sub-vertical high-strained zone with a protracted deformation history. The Au-Ag-Cu system occurs within a Rhyacian-age assemblage of mafic to intermediate volcanic, volcanoclastic and intrusive rocks that have been metamorphosed to greenschist facies. Most of the Au-Ag-Cu mineralization is hosted within the polymictic to monomictic volcanoclastic rocks and a fine- to medium-grained porphyritic granodiorite intrusion with a U-Pb zircon age of ~2160 Ma. Petrography and hyperspectral imaging in long-, mid- and short-wave infrared show that these rocks have undergone an early chlorite and K-feldspar alteration with a later overprinting assemblage consisting of quartz, albite, sericite, biotite and calcite.

Two stages of Au mineralization are identified in the Toroparu project. The first has an assemblage of gold, chalcopyrite, bornite, pyrite, covellite, molybdenite, and magnetite (Figure 2a) hosted within NW-trending extensional quartz carbonate ± chlorite (QCBCHL) veins, veinlets and fractures associated with an early dextral strike-slip movement; these veins are present mainly in Toroparu Main. The molybdenite yielded a Re-Os age of ~2160 Ma that overlaps with emplacement of the mineralized granodiorite. The second ore stage contains pyrite ± gold (Fig. 2b) within SW-trending

and subhorizontal quartz carbonate (QZCB) veins associated with late sinistral transpressive movement; dominant at Sona Hill but also present in Toroparu as well.

Preliminary fluid inclusion petrographic studies indicate two different fluid types in the QZCBCHL and QZCB veins. The former contains two- and three-phase aqueous inclusions ($L_{H_2O}-V_{H_2O} \pm \text{Halite}$) whereas the latter has aqueous-carbonic inclusions (<10-15 vol % H_2O ; CO_2 phase homogenizes to L) characterized by decrepitate textures which suggest cycling of pressure as is typical of orogenic type veins.

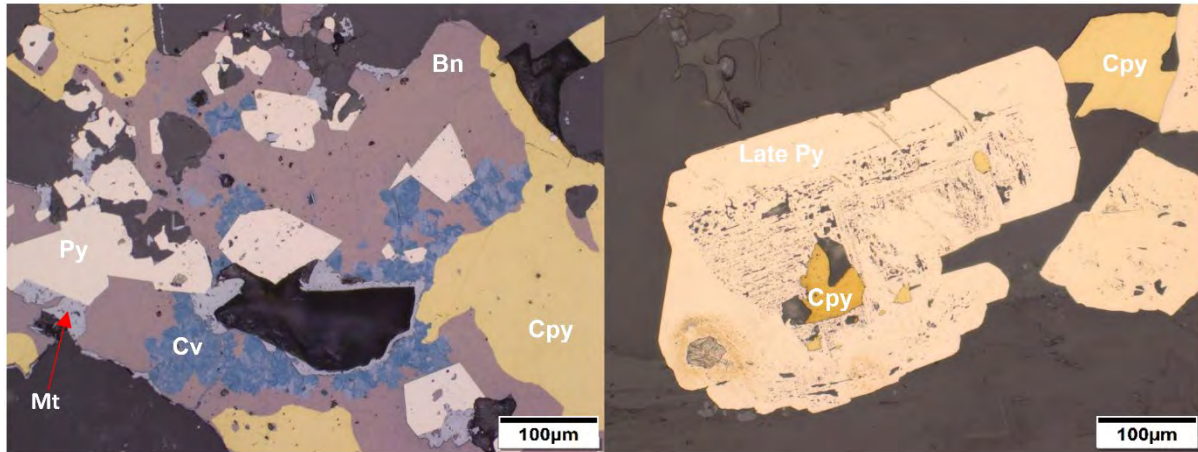


Figure 5: Photomicrographs in reflective light of mineralization assemblages at Toroparu. a) Early Au-Cu mineralization – Chalcopyrite (Cpy), Bornite (Bn), Pyrite (Py), Covellite (Cv), Magnetite (Mt). b) Overgrowth of Late Py surrounding early pitted Py with inclusions of Cpy in core

The Toroparu project has two stages of mineralization. Whereas most of the base metals and Ag are syn-magmatic at ~ 2160, the Au is both syn-magmatic but also late orogenic, possibly as young as ~ 2080 Ma as noted elsewhere in the Guiana Shield (Tedeschi et al., 2018). The Las Cristinas Au-Cu deposit (32 Moz) in Venezuela and the Million Mountain Au-Cu prospect in Guyana are hosted in a similar volcanoclastic setting which therefore emphasizes the potential for new discoveries of the Toroparu-type Au-Cu system elsewhere in the Guiana Shield.

What do we know about the positioning of West Africa and the Guiana Shield during the Rhyacian Period?

Mark Jessell*

School of Earth Sciences, CET,

UWA, 35 Stirling Highway

Crawley WA6009

mark.jessell@uwa.edu.au

SUMMARY

It has long been known that the West African Craton and the Guiana Shield were neighbours prior to the opening of the Southern Atlantic Ocean, however if anything the certainty about their positioning during the Rhyacian Period has if anything weakened as we collect new data. The combined data from the WAXI 3 and SAXI 1 research programs provide a unique opportunity to compare the geological, geochemical, and geophysical record of these two regions. At this stage we are not able to resolve this question, however we can at least lay out the evidence for and against a close geographic relationship at this period of intense crustal formation in both regions.

Key words: Plate reconstructions, West African Craton, Guiana Shield, Amazonian Craton. Rhyacian Period

INTRODUCTION

The prior inferred juxtaposition of South America and Africa was one of the earliest consequences of mobilist theories of tectonics, and as new data became available, increasingly precise placements of these continents, and of the West African Craton and the Guiana Shield have been proposed, most recently by Merdith et al., 2021 (Fig. 1).

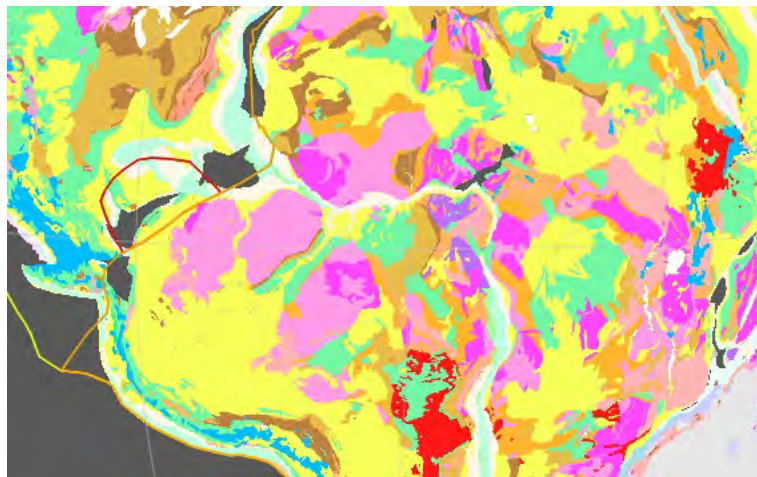


Fig. 1. 50M scale CGMW World geology placed in a 180Ma plate configuration

As we go back in time to the Rhyacian Period, although early authors preferred a “Pangaeen” configuration at 2000Ma (Ledru et al., 1994; Vanderhaeghe et al., 1998; Delor et al., 2003; Klein, 2005; Frimmel, 2014), more recent authors (Merdith et al., 2017; Perhsson et al., 2016; Rapalini et al., 2015, Traoré et al. 2022) have questioned the evidence for this configuration. This presentation will discuss the geological, geochronological, geochemical, magmatic, metallogenic,

lithospheric and structural evidence for the correlation or non-correlation of the Guiana Shield and the West African Craton during the Paleoproterozoic.

References

- Delor, C., Lahondère, D., Egal, E., Lafon, J.M., Cocherie, A., Guerrot, C. & de Avelar, V., 2003. Transamazonian crustal growth and reworking as revealed by the 1:500,000-scale geological map of French Guiana. *Géologie de la France* 2003 2-3-4: 5–57.
- Frimmel, H., 2014, Giant Mesoarchean crustal gold-enrichment episode: Possible causes and consequences for exploration: Society of Economic Geologists Special Publication 18, p. 209–234
- Klein, E.L., Moura, C.A.V., and Pinheiro, B.L.S., 2005, Paleoproterozoic crustal evolution of the São Luís craton, Brazil: Evidence from zircon geochronology and Sm-Nd isotopes: *Gondwana Research*, v. 8, p. 177–186.
- Ledru, P., Johan, V., Milési, J.P., Tegye, M. 1994. Markers of the last stages of the Palaeoproterozoic collision: evidence for a 2 Ga continent involving circum-South Atlantic provinces. *Precambrian Research*, 69, 169-191.
- Merdith, A. S., Collins, A. S., Williams, S. E., Pisarevsky, S., Foden, J. D., Archibald, D. B., et al. (2017). A full-plate global reconstruction of the Neoproterozoic. *Gondwana Res.* 50, 84–134.
- Merdith, A.S., Williams, S.E., Collins, A.S., Tetley, M.G., Mulder, J.A., Blades, M.L., Young, A., Armistead, S.E., Cannon, J., Zahirovic, S., Müller, R.D. 2021. Extending full-plate tectonic models into deep time: Linking the Neoproterozoic and the Phanerozoic, *Earth-Science Reviews*, Volume 214, 2021, 103477
- Pehrsson, S.J., Eglington, B.M., Evans, D.A.D., Huston, D. & Reddy, S.M. 2016. Metallogeny and its link to orogenic style during the Nuna supercontinent cycle in: Li, Z. X., Evans, D.A.D. & Murphy, J. B. (eds) 2016. *Supercontinent Cycles Through Earth History*. Geological Society, London, Special Publications, 424, 83–94
- Rapalini, A.E., Bettucci, L.S., Badgen, E., Vásquez, C.A. 2015. Paleomagnetic study on mid-Paleoproterozoic rocks from the Rio de laPlata craton: Implications for Atlantica
- Traoré, K., Chardon, D., Naba, S., Wane, O., Bouarée, L. 2022. Paleoproterozoic collision tectonics in West Africa: Insights into the geodynamics of continental growth. *Precambrian Research* Volume 376, 15 July 2022
- Vanderhaeghe, O., Ledru, P., Thiéblemont, D., Egal, E., Cocherie, A., Tegye, M. & Milési, J.P., 1998. Contrasting mechanism of crustal growth Geodynamic evolution of the Paleoproterozoic granite–greenstone belts of French Guiana. *Precambrian Research* 92: 165–193.

Gold mineralisation in the Paleoproterozoic greenstone belt of Suriname: Insights from the Overman deposit

Nicole Kioe-A-Sen^{1,2}, Manfred van Bergen², Gilian Alimoenadi³

¹*Department of Geosciences, Anton de Kom University of Suriname;* ²*Department of Earth Sciences, Utrecht University, the Netherlands;* ³*Iamgold, Paramaribo, Suriname*

Mineralization of primary gold in the Guiana craton is largely confined to Paleoproterozoic greenstone belts that surround voluminous domains of granitoids. With few exceptions, the major deposits belong to the orogenic clan but there is a significant diversity in host lithology, mode of emplacement and timing relative to major tectono-metamorphic events of the Transamazonian orogeny. Within this spectrum, the Overman deposit, situated near the Rosebel gold mining district in the Marowijne greenstone belt of Suriname, is exceptional, since gold accumulated in a conspicuous chert interval within a sequence of fine-grained phyllitic rocks metamorphosed under greenschist-facies conditions. Largely stratiform relationships and micro-textural evidence indicate that the chert originated from wholesale replacement of bedded detrital sediments by silica. The host metasediments are part of the Armina Formation, which is marked by the predominance of graded greywackes interpreted as turbidites. From the fine-grained nature of the metasediments and an association with graphitic intervals, the Overman sequence likely represents the distal deep-water facies of the basin.

Enrichment of visible and invisible gold is typically associated with arsenic and is largely restricted to sulphide-rich domains in the chert interval. The sulphide assemblages, consisting of pyrite, arsenopyrite and pyrrhotite in variable combinations and proportions, occupy pore spaces and micro-fractures in rock that is entirely composed of microcrystalline quartz. Micro-analytical data show that much of the gold was originally incorporated in arsenopyrite and As-rich pyrite. Arsenopyrite compositions point to an emplacement temperature of ca. 325-375°C, which is lower by >100°C than peak metamorphic temperatures recorded by the crystallinity of carbonaceous matter.

Ore formation was probably a relatively short-lived episode in the waning stages of the Main Transamazonian event. We infer that permeability for mineralizing fluid was promoted by dynamic re-crystallization of the micro-quartz, induced by deformation of the rigid silica body during folding and shearing of the entire package of phyllite-dominated metasediment. Liberation and mobilisation of native gold, resulting in short-distance displacement and accumulation, was presumably driven by thermal and deformational forces acting after the primary ore-bearing assemblage had crystallized.

Along with the major gold producing Rosebel and Merian deposits, the Overman anomaly is part of a sediment-hosted gold zone running parallel to the WNW-ESE trending North Suriname Shear Zone, an inferred mark of oblique collision of West African and Amazonian continental blocks that terminated subduction-related convergence. We propose that crustal-scale processes in a post-collisional geodynamic setting were instrumental for the emplacement of gold in metasediments of the greenstone belt in NE Suriname.

References

Daoust, C. (2016), Caractérisation stratigraphique, structurale et géochimique du District minéralisé de Rosebel (Suriname) dans le Cadre de l'évolution géodynamique du Bouclier Guyanais, PhD thesis, Université du Québec à Montréal (Montréal): 330 pp.

Kioe-A-Sen, N. van Bergen, M.J., Wong, Th. and Kroonenberg, S.B. (2016), Gold deposits of Suriname: geological context, production and economic significance. *Netherlands Journal of Geosciences-Geologie en Mijnbouw*, 95-4, 429-445

The 1.98 Ga Goboy dolerite: a new dyke swarm in northern Suriname

Salomon Kroonenberg^{1,2}, Shardhanand Ramlal³, Xiomara Tjin-Asjoe¹, Paul Mason⁴, Sandra Kamo⁵, Steve Denyszyn⁵, Richard Ernst⁶, Mauricio Ibáñez-Mejía⁷

¹ Anton de Kom University of Suriname; ² Delft University of Technology, the Netherlands; ³ IAMGOLD Rosebel Gold Mines, Suriname; ⁴ Utrecht University, the Netherlands; ⁵ Earth Science Department, University of Toronto, Canada; ⁶ Department of Earth Sciences, Carleton University, Ottawa, Canada; ⁷ University of Arizona.

Dolerite dyke swarms in the Precambrian cratons of the world are important markers enabling the localisation of Large Igneous Provinces and former mantle plumes, and play a role in the reconstruction of former supercontinents (Ernst, 2014). In the Guiana Shield, the northern half of the Amazonian Craton, three major dolerite dyke suites have been discovered: the Avanavero dykes with ages around 1.79 Ga, the Käyser Suite around 1.53 Ga and the 0.2 Ga CAMP suite of intrusions (De Roever et al., 2002, Deckart, 2005, Reis et al., 2013, 2022; Baratoux et al., 2019). All these intrude the Paleoproterozoic basement of the Guiana Shield formed during the Trans-Amazonian Orogeny (2.26-1.95 Ga; Delor et al., 2003; Kroonenberg et al., 2016).

Here we report the discovery of a still older dyke swarm of 1.98 Ga in northern Suriname. We discuss the exploration history, field, petrographical and geochemical data, and possible implications for gold mineralisation, while the details of the geochronology and the wider implications for the Guiana Shield tectonic history are given in an accompanying paper by Ibáñez-Mejía et al (2022, this volume).

During an aeromagnetic survey in 2010 by IAMGOLD Rosebel Gold Mines of their concession in Suriname (Ramlal et al., 2019), a conspicuous set of N50-65°E trending dykes was recorded. Because of confidentiality issues the aeromagnetic data cannot be shown here, but in Fig. 1 the traces of the dykes are drawn onto the Geological Map of Suriname (GMD, 2018). No outcrops are known within the concession area and apparently no field data have been collected by them. However, already in 1975 the exploration geologist Hans Schönberger discovered a rectilinear lateritic outcrop of 230 m long and 12 m in width and with an orientation of N64-69°E, which followed the course of the straight NE-running Goboy creek, a tributary of the Mindrineti River (Schönberger, 1975a,b). Schönberger thought it to be a so-called *gossan*, or iron hat, the expression of an ore vein at depth, and drilled several holes in the lateritic overburden to probe its chemistry. No anomalous value of the base metals Cu, Zn, Pb and Ni were found, and he did therefore not drill into the bedrock itself. Since then, it became clear that the so-called gossan coincides with one of the NE-SW dolerite dykes, and that the laterite is a weathering product of that dolerite. Although Schönberger did not find the dolerite itself, we propose to call this dolerite Goboy dolerite, because this is where its first traces were found.

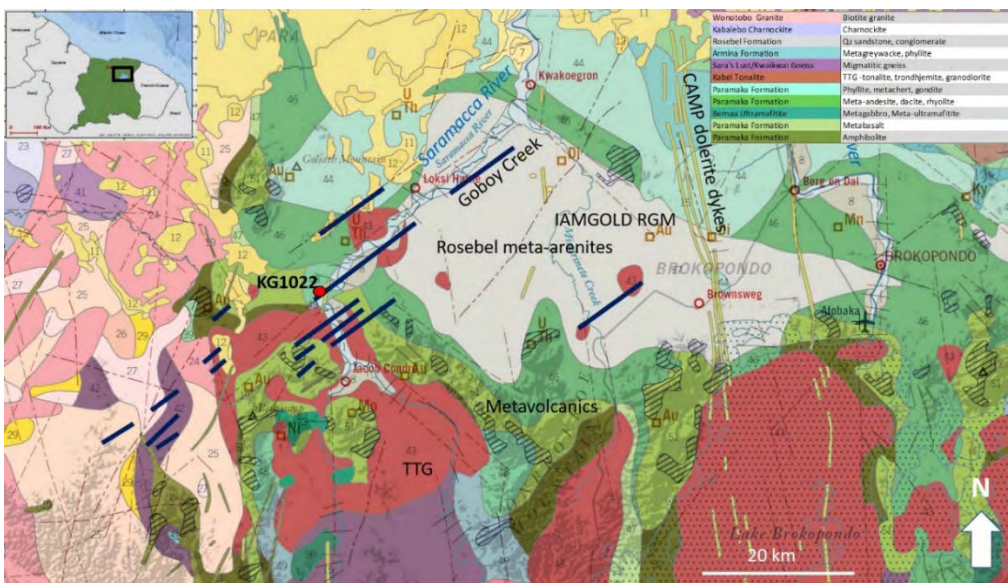


Fig. 1 Dark blue lines indicate traces of Goboy dolerite dykes, redrawn from IAMGOLD Rosebel Gold Mines and Harvest Gold Inc aeromagnetic images on part of Geological Map of Suriname (GMD, 2018). KG 1022 is sampling site for geochronology.

In aeromagnetic images of the Goliath-Tibiti gold prospect further SW the dyke swarm reappears (Lapoint, 2016), leading to a total length of the swarm of at least 60 km. One of the dykes is exposed in a stretch of the Saramacca River parallel to it. The outcrops were already known (D’Audretsch, 1955, Arjomandi et al., 1973) but did not receive special attention until the IAMGOLD aeromagnetics showed their importance. They were sampled for petrography and geochemistry in 2017 (Tjin-Asjoe, 2019), and by the first author in 2021 for geochronology (sample KG1022).



Fig. 2. Geochronology sampling site KG 2022 near camp California, Saramacca River.

The Goboy dolerites are almost fresh medium-grained subophitic dolerites with pigeonite as the only pyroxene, labradorite plagioclase and skeletal opaques. Minor hornblende and biotite fringe some clinopyroxene crystals. Geochemically they are low-Ti tholeiitic basaltic andesites and plot as within-plate tholeiites in the 2Nb-Zr/4-Y tectonic discrimination diagram of Meschede (1986).

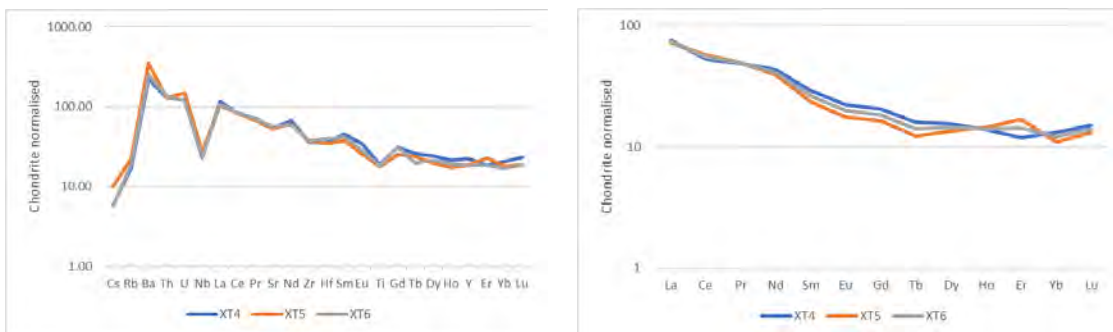


Fig 3a, b. Spidergram and REE diagrams for three Goboy dolerite samples from the Saramacca River.

The dykes intrude into the Maronian greenstone belt of the Guiana Shield, which stretches over 1500 km from eastern Venezuela through the three Guianas into Amapá, Brazil. This basement represents the pre-drift counterpart of the Birimian greenstone belt in West-Africa. In Suriname the greenstone belt is composed of mafic volcanics, volcanoclastic and chemical sediments of the Paramaka Formation, from which a single rhyolite has been dated at 2.16 Ga (Daoust, 2016). It is intruded by TTG bodies ranging in age between 2.18 and 2.12 Ga and undated ultramafic bodies. It is overlain by the turbiditic Armina

Formation and the epicontinental conglomerate and sandstones of the Rosebel Formation (Kroonenberg et al., 2016). Detrital zircon ages range between Archean and 2.06 Ga (Daoust, 2016). S-type granites with ages down to 2.06 Ga intrude the Armina Formation. These formations are strongly folded and metamorphosed to the greenschist to amphibolite facies. Gold mineralisation is mainly developed in quartz veins which traverse all previously mentioned formations (Kioe A Sen et al., 2016). The precise age of the veins and the mineralisation is unknown, but Daoust et al. (2011, Fig 16) suggest it to be between 2000 and 1950 Ma.

Most previous work about the origin of gold mineralisation in the greenstone belt suggests a link with long shear zones that traverse the northern part of the Guiana Shield (e.g., Voicu et al., 2001). However, the close correspondence between the supposed age of the gold mineralisation and the Goboy dyke suite may indicate that extensional forces and mafic magmatism also played a role in the ascent of gold-bearing fluids.

References

- Arjomandi, J., Krook, L., Bosma, W. & de Roever, E.W.F., 1973. Geological reconnaissance of the Tibiti-Coppename area, northern Suriname. *Mededelingen Geologisch Mijnbouwkundige Dienst Suriname* 22: 43–57.
- Baratoux, L. U. Söderlund, R. E. Ernst, E. de Roever, M. W. Jessell, S. Kamo, S. Naba, S. Perrouty, V. Metelka, D. Yatte, M. Grenholm, D. P. Diallo, P. M. Ndiaye, E. Dioh, C. Cournède, M. Benoit, D. Baratoux, N. Youbi, S. Rousse and A. Bendaoud 2019. New U–Pb Baddeleyite Ages of Mafic Dyke Swarms of the West African and Amazonian Cratons: Implication for Their Configuration in Supercontinents Through Time in: R. K. Srivastava et al. (eds.), *Dyke Swarms of the World: A Modern Perspective*, Springer Geology, <https://doi.org/10.1007/978-981-13-1666-1>
- Daoust, C., 2016. Caractérisation stratigraphique, structurale et géochimique du district minéralisé de Rosebel (Suriname) dans le cadre de l'évolution géodynamique du bouclier guyanais. Thèse Université de Québec à Montréal.
- Daoust, C., Voicu, G., Brisson, H. & Gauthier, M., 2011. Geological setting of the Paleoproterozoic Rosebel gold district, Guiana Shield, Suriname. *Journal of South American Earth Sciences* 32: 222–245.
- Deckart, K., Bertrand, H. & Liégeois, J.-P., 2005. Geochemistry and Sr, Nd, Pb isotopic composition of the Central Atlantic Magmatic Province (CAMP) in Guyana and Guinea. *Lithos* 82: 289–314.
- Delor, C., Lahondère, D., Egal, E., Lafon, J.M., Cocherie, A., Guerrot, C. & de Avelar, V., 2003. Transamazonian crustal growth and reworking as revealed by the 1:500,000-scale geological map of French Guiana. *Géologie de la France* 2003 2-3-4: 5–57.
- De Roever, E.W.F., Kroonenberg, S.B., Delor, C. & Phillips, D., 2003. The Käyser dolerite, a Mesoproterozoic alkaline dyke suite from Suriname. *Géologie de la France* 2003, 2-3-4: 161–174.
- Ernst, R.E., 2014. *Large Igneous Provinces*. Cambridge University Press, 653 p.
- GMD (Geological and Mining Service, Suriname), 2018, Geological Map of Suriname.
- Kioe-A-Sen, N.M.E., M. Van Bergen, Th. E. Wong, S.B. Kroonenberg, 2016 Gold deposits of Suriname: geological context, production and economic significance. *Netherlands Journal of Geosciences – Geologie en Mijnbouw*, 95, 429-445
- Kroonenberg, S.B., De Roever, E.W.F., Fraga, L.M., Reis, N.J., Faraco, M.T., Cordani, U.G., Lafon, J.-M & Wong, Th. E., 2016. Paleoproterozoic evolution of the Guiana Shield in Suriname – a revised model. *Netherlands Journal of Geosciences- Geologie en Mijnbouw* 95:491-522
- Lapoint, D. J., 2016. Goliat (Tibiti) Project, Sipaliwini District, Eastern Suriname, South America. Technical report prepared for Harvest Gold Corp.
- Meschede, M., 1986. A method of discriminating between different types of mid-ocean ridge basalts and continental tholeiites with the Nb-Zr-Y diagram. *Chemical Geology*, 56, 207–218.
- Ramlal, S., S.B. Kroonenberg, P.R.D. Mason, L.M. Kriegsman, P. O'Sullivan, 2019. Multiphase TTG intrusions in the Paleoproterozoic greenstone belt of Suriname and their role in gold mineralization in the Rosebel gold district. *Proceedings 11th Inter Guiana Geological Conference, Paramaribo. Mededeling Geologisch Mijnbouwkundige Dienst Suriname*, 29, 159-162

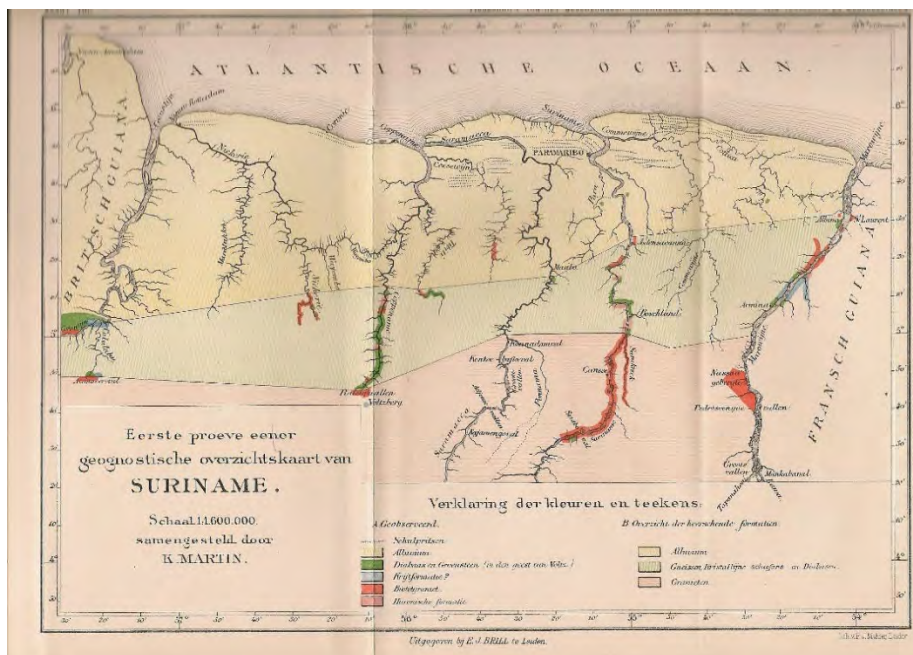
- Reis, N.J., Teixeira, W., Hamilton, M.A., Bispo-Santos, F., Almeida, M.E., and D'Agrella-Filho, M.S., 2013, Avanavero mafic magmatism, a late Paleoproterozoic LIP in the Guiana Shield, Amazonian Craton: U–Pb ID-TIMS baddeleyite, geochemical and paleomagnetic evidence: *Lithos*, v. 174, p. 175–195, doi: 10.1016/j.lithos.2012.10.014.
- Reis, N.J., Teixeira, W., D'Agrella-Filho, M.S., Bettencourt, J.S., Ernst, R.E., Goulart, L.E. (2022). Large Igneous Provinces of the Amazonian Craton and their metallogenic potential in Proterozoic times. In: Srivastava, R. K., Ernst, R. E., Buchan, K. L. and De Kock, M. (eds) *Large Igneous Provinces and their Plumbing Systems*. Geological Society, London, Special Publications, 518, p. 493-529, <https://doi.org/10.1144/SP518-2021-7>
- Schönberger, H. 1975a. Speciaal rapport Goboy kreek ijzeren hoed met Cu en Zn anomalie. Internal report Geological Mining Service, Suriname, 4 p.
- Schönberger, J.M.H., 1975b Diamond exploration between the Suriname and Saramacca River, (NE Suriname). *Mededeling Geologisch Mijnbouwkundige Dienst Suriname* 25, 228-238.
- Tjin-Asjoe, X., 2019 A new suite of dolerite dykes in the basement of Suriname. MSc thesis Anton de Kom Universiteit Suriname.
- Voicu, G., M. Bardoux, R. Stevenson 2001. Lithostratigraphy, geochronology and gold metallogeny in the northern Guiana Shield, South America: a review. *Ore Geology Reviews* 18, 211–236.

Friedrich Voltz (1828–1855), discoverer of the Maronian greenstone belt in the Guiana Shield

Salomon Kroonenberg

Anton de Kom Universiteit van Suriname, Leysweg 86, Paramaribo, Suriname. salomonkroonenberg@gmail.com

The German geologist Friedrich Voltz was employed in 1853 by the Dutch government as a member of a commission to assess opportunities for German settlers in Suriname. He surveyed the geology of all major rivers in the Precambrian basement in dugout canoes rowed by local indigenous and Maroon people, and collected over 900 rock samples from cataracts and other outcrops. He described his findings in letters to the Dutch geologist Winand Staring, who published parts of them in Dutch journals in 1854 and 1855. Before Voltz could return to Europe and write a full report, he died in Paramaribo of yellow fever, a week before his 28th birthday. Thirty years later, the Leiden professor of geology Karl Martin, on his return from his own expedition to Suriname, also published part of Voltz's letters (Martin, 1888a) and drew the first geological map of Suriname, largely based on Voltz's observations and samples, and a few of his own (Martin, 1888b).



The greenstone belt ('in the sense of Voltz') on the first geological map of Suriname (Martin, 1888b)

In his letters, Voltz recognized a W-E belt of greenstones stretching from British Guiana, previously surveyed by Robert Schomburgk, across Suriname into French Guiana, which was drawn by Martin on his map. This is the first mention of the gold-rich Maronian greenstone belt that extends over 1500 km in the Guiana Shield from eastern Venezuela through the Guianas and the Amapá state in Brazil, and continues across the Atlantic into the Birimian of West Africa. Voltz's letters, including comments on their context, were first published in full by the author (Kroonenberg, 2020). The letters themselves and the samples are stored at Naturalis National Biodiversity Centre in Leiden (Netherlands).

Kroonenberg, Salomon (2020). *De man van de berg. Friedrich Voltz (1828-1855), jonggestorven natuuronderzoeker in Suriname*. Walburgers Zutphen, 319 p.

Martin, K. (1888a). *Geologische Studien über Niederländisch West-Indien*. E.J. Brill, Leiden, 238 p.

Martin, K. (1888b). Aanteekeningen bij eene geognostische overzichtskaart van Suriname. *Tijdschrift Koninklijk Nederlands Aardrijkskundig Genootschap* 5, p. 444-453.

Copper mineralisation in Paleoproterozoic cordierite-biotite-magnetite-apatite rocks at Weko Sula, SE Suriname: anatexis of a cupriferous argillaceous evaporite-to-red bed sequence

Salomon Kroonenberg^{1,2}, Manfred van Bergen³, Leo Kriegsman^{3,4}, Paul Mason³, Nicolas Thébaud⁵

¹ Anton de Kom University of Suriname, Department of Geosciences; salomonkroonenberg@gmail.com, ² Delft University of Technology, the Netherlands, ³ Utrecht University, the Netherlands, ⁴ Naturalis National Biodiversity Centre, Leiden, the Netherlands, ⁵ University of Western Australia.

Precambrian copper deposits in South America are best known from the world-class Carajás mineral province on the south-eastern margin of the Amazon Craton where Archean rocks host numerous Iron Oxide Copper Gold (IOCG)-type varieties. Here, we document the presence of unusual cupriferous metasedimentary rocks in a vast domain of Paleoproterozoic granitoids in central-southern Suriname adjacent to the Maronian greenstone belt of the Guiana Shield. The Cu anomaly, originally discovered during exploration campaigns near the Weko Sula rapids in the Upper Tapanahony River in the late 1960s, covers a surface area of c. 1.5 km². Copper contents reach 0.5 wt.% in fresh rock and 4.5 wt.% in the overburden, which extends down to some 45 m depth. The fresh intervals are coarse grained, relatively undeformed plutonic-looking rocks, surrounded by a non-mineralised foliated clinopyroxene-hornblende granodiorite. Contact relations are obscured due to deep weathering and poor accessibility in the rainforest-clad territory.

The cupriferous rocks are characterized by a remarkable abundance of cordierite. About half the volume of a drill-core sample studied in detail consists of up to 1.5 cm-sized tabular crystals. Biotite and plagioclase are major constituents as well. Relict andalusite reflects a protracted metamorphic history, while tourmaline and traces of dumortierite and barite, co-existing with minor quartz and albite in leucosomes, signal an early enrichment in boron and other volatile elements. Abundant magnetite, apatite and biotite occupy the interstitial spaces between the cordierites, inferred to represent a former interconnected network of partial melt. Copper minerals, mainly bornite, chalcocite and covellite, as well as accessory tellurides are late-stage products, spatially associated with these interstitial phases. Muscovite is common as late metamorphic and secondary alteration phase.

The strongly peraluminous bulk composition (ASI=3.3), combined with relatively high FeO_{tot}+MgO (16.1 wt.%), K₂O+Na₂O (3.8 wt.%), and low SiO₂ (45 wt.%) contents is consistent with a restite that experienced segregation of a felsic melt, assuming a common metapelitic rock as precursor. A high P₂O₅ content (2.1 wt.%) is in line with a striking abundance of stubby F-apatite crystals. SHRIMP U-Pb zircon dating yielded an age of 2064±4 Ma, with Th/U ratios around 0.1 suggesting a metamorphic parentage.

From the mineral assemblage, textural relationships and bulk composition the rock resembles a cordierite-rich diatexite, which we interpret as a cupriferous argillaceous, evaporite-to-red bed sequence that underwent progressive metamorphism and partial melting during a high-temperature event at relatively low pressure. The heat source may have been either an as yet unidentified intrusive magma body, considerably younger than the c. 2.09 Ga pyroxene granites that dominate the area, or a more regional heating event. This latter option is conceivable since the zircon age falls in a 60-Ma period of UHT metamorphism in the Bakhuis granulite belt, some 200 km northwest of the study location.

The apatite-magnetite assemblage in the interstitial melt zones of the Weko Sula rock resembles that of classic iron oxide-apatite (IOA) deposits worldwide, the origin of which is a topic of ongoing debate. The copper sulfides and tellurides also suggest an affinity with the IOCG family of ore deposits. Our findings provide evidence for the existence of Fe-Ca-P melt under crustal conditions and suggest that typical IOA mineral phases can accumulate through partial melting of a metasedimentary rock, originally enriched in this element group and associated volatiles in a supracrustal deposition environment, possibly a shallow evaporitic water body.

Regional mercury background values in soils and saprolites in the gold-producing greenstone belt of Suriname, Guiana Shield

S.B.Kroonenberg*, Th. E. Wong, G. Bijnaar, R. Finkie, K. Goenopawiro, S. Asneel, M.M. Lin-Tsung, R. Nanan, K. V. Ramdas, P.V. Sitaram

All authors: Anton de Kom Universiteit van Suriname, Leysweg 86, Paramaribo, Suriname.

Background values of mercury have been established in 62 natural unpolluted soil and saprolite profiles on 16 different rock types in the greenstone belt of Suriname. The analytical data on Hg and other major and trace elements in three pilot projects show that Hg is residually concentrated in topsoils and indurated horizons by the laterization process up to levels of 200 µg/kg (Kroonenberg et al., 2022). This is up to 100 times the original concentration in the underlying hard rock. In the deeper pallid zone horizons of the profiles, Hg has often been leached almost completely together with iron by reducing groundwater action.



Pilot profiles AFO 1 and AFO 2, with Hg values in µg/kg.

Maximum and average Hg values of 196 samples from the 16 different rock types fall apart into two groups. Felsic rocks with predominance of quartz and feldspar have maximum Hg values around 100 µg/kg and averages around 50 µg/kg, mafic ones with less silica and higher Fe, Mg and Ca have maximum values around 250-300 µg/kg and averages around 150 µg/kg. In general the natural soil and saprolite Hg values fall in the same order of magnitude as many mine tailings and stream sediments, and therefore cannot be used to separate polluted from unpolluted materials.

Kroonenberg, S., T. Wong, G. Bijnaar, R. Finkie, K. Goenopawiro, S. Asneel, M. Lin-Tsung, R. Nanan, K. Ramdas, P. Sitaram, 2022. Mercury background values in soils and saprolites in the gold-rich greenstone belt of Suriname, Guiana Shield: the role of parent rock and residual enrichment. *Science of the Total Environment* 848 (2022) 157631.

*Corresponding author: salomonkroonenberg@gmail.com

The role of polyphase folding in the distribution of Gold: Insights from the Guiana Shield

Brice Lacroix*

Kansas State University
GexplOre
blacroix@ksu.edu

Pierre-Jean Hainque

University of Franche Comté
GexplOre
Nancy, France

Alix Hauteville

GeoRessources
Université de Lorraine
Nancy, France

Dennis Lahondès

GexplOre
Nancy, France

Etienne Le Goff

GexplOre
Nancy, France

Dominique Fournier

GexplOre
Nancy, France

Carlos Bertoni

Reunion Gold Corporation
Longueuil, Canada

Stéphane Taravella

GAIA SAS
Cayenne, France

Karim Robo

Auplata Mining Group
Cayenne, France

Maxence de Witasse

Auplata Mining Group
Cayenne, France

SUMMARY

We present results from detailed structural analyses coupled with geophysical interpretation from four gold exploration projects hosted in the Rhyacian greenstone belts from the Guiana shield. Our results suggest that, at deposit scale, the deformation evolution is complex, involving at least two folding events (D_1 and D_2), followed by several brittle deformation. The systematic presence of fold superposition offers new prospective for exploration in the Guiana Shield. The Au-grade and location of historical mining activities both seem spatially correlated with the geometry of the interference pattern, suggesting an important structural control of the mineralization grade. These findings suggest that the characterization of the exact fold interference pattern is fundamental for the targeting of favourable enriched zones at deposit scale. We suggest that this approach should be routinely applied by mineral exploration companies developing projects in the Guiana shield and elsewhere.

Key words: Structural analyses, polyphase deformation, interference patten, ore shoot, geophysics, mineral exploration.

INTRODUCTION

Greenstone belts are area of great interest as they host numerous mineral deposits including volcanic massive sulphide (VMS), Ni-Cu platinum-group element (PGE) sulphide deposit, and more particularly orogenic gold deposits, which compose an important source for global gold production (Groves et al., 1998; Poulsen et al., 2000; Goldfarb et al., 2001). Orogenic gold systems formed in deformed terranes at different geological times (from Paleoproterozoic to early Cenozoic; Neumayr et al., 1998; Craw and Koons 1989) and at various crustal levels (from low-grade greenschist to high-grade granulite metamorphic conditions) (e.g. Poulsen et al., 2000; Goldfarb et al., 2005; Dubb e and Gosselin 2007). Several decades of active research have almost univocally demonstrated that orogenic gold deposits form aqueous-carbonic fluid released during metamorphism through devolatilization reactions in the middle to lower crust (e.g., Cox et al., 1991; Philipps and Powell, 2010; Goldfarb and Grove 2015). The transfer pathways of mineralizing fluids as well as the trapping mechanisms of gold mineralization are strongly controlled by crustal structures (increasing porosity and permeability) (e.g., Voissey et al., 2020), and the deformation evolution during late orogenic stages (e.g. Combes et al., 2022). While pre-existing structures predating gold input may be of important control for the early stage of ore deposition (e.g., Chauvet et al., 2019), later deformation phases postdating gold input are significant for remobilization/reconcentration processes (also referred as gold endowment) (e.g., Tomkins and Mavrogenes 2002). As reported by numerous studies, orogenic gold mineralization is not generally associated with a single tectonic event, but rather benefits from polyphase deformation (e.g., Au grade endowment) (Th ebaud et al., 2018). This has been especially well documented in orogenic gold deposits from Alaska (Juneau terranes; Goldfarb et al., 2008) where grade endowment is linked to post-subduction transpressive deformation, (e.g. during strike slip reactivation of reverse crustal structures) (Goldfarb et al., 1993; Goldfarb and Groves, 2015). Therefore, determining an accurate deformation evolution at deposit scale is crucial to identify new and/or extensions of known deposits. To achieve these goals, it is fundamental to investigate with great detail the deformation evolutions at deposit scale and the associated veins (Perret et al., 2020; Combes et al., 2022).

In this presentation, we present new structural and geophysical dataset on four deposits located in the Rhyacian greenstone belts from the Guiana shield: Oko West in Guyana, and Boulanger, Dieu Merci and Crique Sophie deposits in French Guiana (Fig. 1). We particularly emphasize the important role of polyphase deformation in the gold remobilization processes.

RESEARCH APPROACH

Due to the deeply weathered profile, which is typical from humid and tropical region, surface geological information in the Guiana shield is sparse and rely on drill cores. In order to increase knowledge of the geology and the deformation style at property scale, the fabrics documented at micro- and macro-scales are integrated to the regional Airborne and Ground geophysical data. Structural analyses have been carried out during field visits in the different sites (Oko West in Guyana, and Boulanger, Dieu Merci and Crique Sophie deposits in French Guiana) (Fig. 1). Field outcrops and drill cores have been carefully examined in order to document the deformation style, and the associated mineralizing event. Specific attention has been given to alteration and vein systems. Structural measurements have been performed on selected outcrops, trenches and along oriented cores. Structural analyses have been performed in order to accurately document the geometry of fold interference patterns (Fig. 2). Because the field exposure of the outcrop is limited due to the important weathering profile, we used a novel approach based on the stereographic distribution of foliation that are compared to basic numerical 3D models. This dataset is used to characterize the exact fold interference pattern based on the fold classification from Ramsay and Hubert (1987). All the studied areas are also affected by several brittle deformation events. However, because they are not associated to mineralization, these events are not discussed here. The structural models proposed for each location are then used to better constrain the deposit-scale geometry based on airborne and ground geophysical data (magnetic, radiometric and Induced polarization) (Fig. 3). For the four studied sites presented here, all of them show the presence of complex polyphase folding which can be used to determine the presence of favourable mineralized zones.

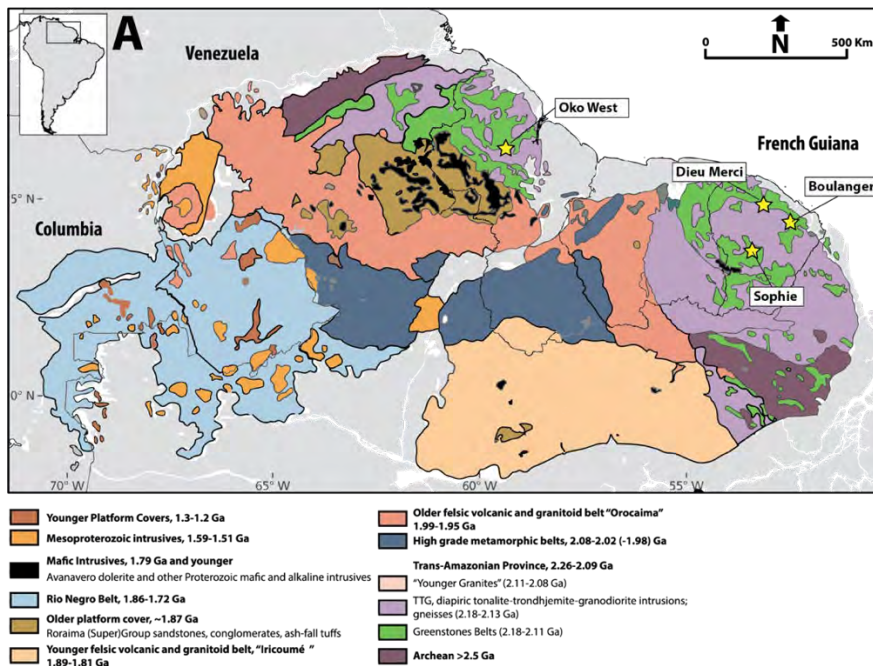


Figure 6: Geology of the Guiana shield (modified from Kroonenberg et al., 2016 and Tedeschi et al., 2020). Yellow stars: location of studied Au-deposits.

EVIDENCE OF POLYPHASE DEFORMATION IN THE GREENSTONE BELTS

In all studied areas, the deformation recorded in the greenstone belts is complex and consists to the superposition of at least two main tectonics events: D_1 and D_2 (the late brittle deformation events are not considered here). The stereographic projection of D_1 -related structures such as foliation (see example for Fig. 5), bedding and/or fold axes (Fig. 3A) are not parallel suggesting they have been affected by at least one other stage of deformation/folding. In order to fully understand the geometry of the interference pattern generated by the two successive deformation events (D_1 and D_2), we

used a quantitative approach based on stereographic distribution of the pole of $S_{1/0}$ and folds. A tentative of fold interpretation for each studied deposit is proposed in Figure 2. Except for Boulanger deposit, which shows a type-1 interference pattern, all the studied deposits are characterized by type-2 fold interference patterns (Figure 2). Note that the directions of the D_1 compressive stress are different from site to site.

Both airborne and ground- geophysical dataset provided by partner companies have been interpreted (Fig. 3). Interestingly, they also highlight interference pattern in agreement with the structural analyses. Figure 3 shows two examples of fold interference patterns from Boulanger and Dieu Merci prospects. The airborne magnetic data from Boulanger very well highlights the presence of type-1 interference patterns formed by the superposition of two successive compressive events, D_1 and D_2 , oriented NNE-SSW and WNW-ESE, respectively. Figure 3 B and C presents ground magnetic data from Dieu Merci prospect. Once again, these data clearly highlight the presence of a type-2 interference pattern formed by the superposition of NS (D_1) and EW (D_2) compressive events. Similar findings are made for the other studied areas.













	TECTONIC EVENTS		Fold superposition pattern
	D_1	D_2	
OKO WEST	 WNW-ESE tectonic stress Regional N020 folding Top-to-the west kinematic Development of S_1 Bedding-parallel veins (SV ₁) + Extension veins (EV ₁) N020 mineralization system	 NE-SW tectonic stress EW fold overprint EW Foliation S_2 Remobilization of Au along D2 hinges	Type-2 interference pattern 
DIEU MERCI	 N-S tectonic stress Regional EW folding Development of S_1	 E-W tectonic stress NS fold overprint NS foliation S_2	Type-2 interference pattern 
BOULANGER	 NNE-SSW tectonic stress Regional Folding (P_1) Emplacement of EV-SV Structures oriented N110 S_1 oriented N110	 WNW-ESE tectonic stress Dextral movement	Type-1 interference pattern 
CRIQUE SOPHIE	 WSW-ENE tectonic stress Regional N350 folding Top-to-the east kinematic Development of S_1	 NNW-SSE tectonic stress	Type-2 interference pattern 

Figure 7. Synthesis of the main folding events (late brittle deformation events are not considered in this study) and the resulting fold interference patterns for each studied deposit.

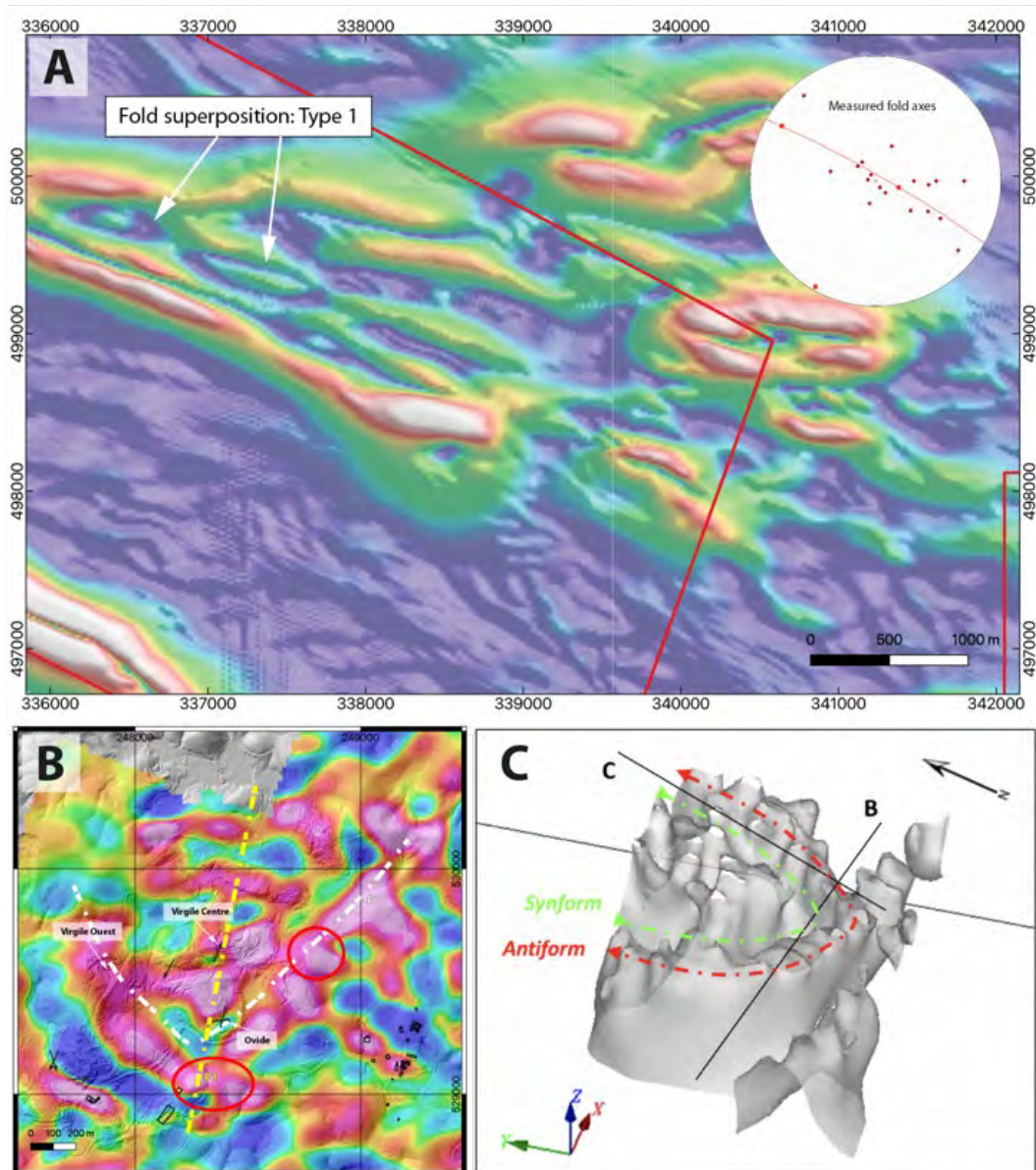


Figure 8: Example of structural interpretation of geophysical survey. A. Magnetic airborne (ASIG) showing the presence of type-1 fold interference pattern. B and C. Example of type-2 interference pattern developed at Dieu Merci deposit interpreted based on ground magnetic survey (GexplOre 2022). Note the historical activities (open pits) are located at the zone of D₂ influence. C. 3D model inversion of ground geophysical data.

DESCRIPTION OF THE AU-MINERALIZATION

In all studied deposits, the main mineralization is typical of orogenic gold deposits worldwide (e.g. Robert and Brown 1986). In Boulanger, Crique Sophie and Dieu Merci deposits, the Au mineralization consists of massive shear veins (steep veins) and stacked narrow extension veins (Fig. 4), both filled with quartz \pm tourmaline \pm pyrite \pm carbonate, and associated alteration of the direct host rock. Shear veins are generally massive and often present banded texture, with banding defined by trails of disseminated sulfides and/or host rocks. Extension veins and veinlets correspond to shallowly dipping sheeted veins which generally present blocky to elongate textures where quartz-carbonate-tourmaline -minerals are aligned perpendicular to vein boundaries. Extension veins vary from veinlets to a few tens of centimeters. Our observations also suggest the presence of “en-echelon” vein system aligned along discrete and shallow shear surfaces (likely the conjugate shear surface to massive shear veins). The mineralization system generally forms close to the contact between granodiorite and volcanoclastic series.

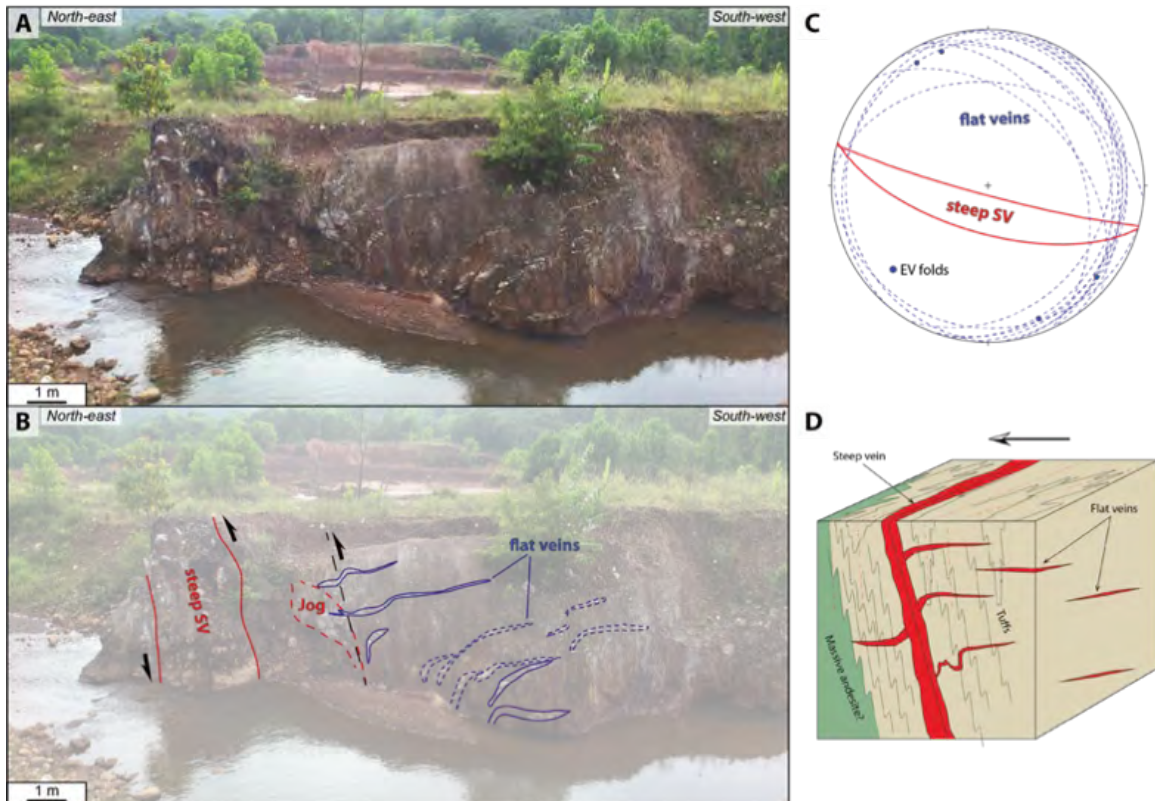


Figure 9: A-B. Example of quartz-tourmaline ore body from Boulanger prospect. C. Stereographic projection of flat veins and shear veins. D. Block diagram model of the mineralization

At Oko West, the mineralization is slightly different and consists to a set of veinlets parallel to sub-parallel to the bedding and stacked narrow extension veins filled with quartz, \pm carbonate, and \pm pyrite. Such structures are known to develop during flexural slip folding related to fold growth and generate by void opening between low cohesion stratigraphic interface at fold hinge. “En-echelon” veins are well developed along the fold limbs. Vein terminations crosscut the S_0 with a high angle whereas internal parts are transposed to it. Such geometry indicates that vein formation was associated with bedding-parallel slip during fold growth and tightening by flexural slip in low to intermediate incompetent beds. During later fold growth and tightening, bedding-parallel veins were transposed to stratigraphy by bedding-parallel slip.

In all studied deposits, the volumetrically significant mineralization is associated with the first deformation stage (D_1), exclusively related to shortening event and contemporaneous folding (D_1 event). Interestingly, the compressive stress orientation varies from site to site (Figure 2).

AU ENRICHMENT DURING D_2

For Boulanger, both structural analysis and geophysical interpretation suggest that this area is affected by type-1 fold interference pattern (Figure 2 and 3A). Interestingly, drill holes intersecting F_2 axial planes show the presence of pyrrhotite (not visible outside zone influenced by D_2) and visible gold (Fig. 5). In order to evaluate the potential contribution of D_2 deformation in the gold-mineralization, we projected the poles of $S_{1/0}$ foliation measured along DDHs from the 2018-2020 campaigns on stereodiagrams (Fig. 5). Each of the measured foliations was linked to the gold value from the same depth interval. Figure 5 represents 3 different stereodiagrams for <0.05 , $0.5-2$, and > 2 ppm gold values. For <0.05 ppm Au-value, the distribution of poles is in agreement with regional D_1 fold orientation ($\sim N130$). In contrast, the higher Au-values show strong influence of D_2 folding event, highlighting the important role of D_2 folding in gold reconcentration.

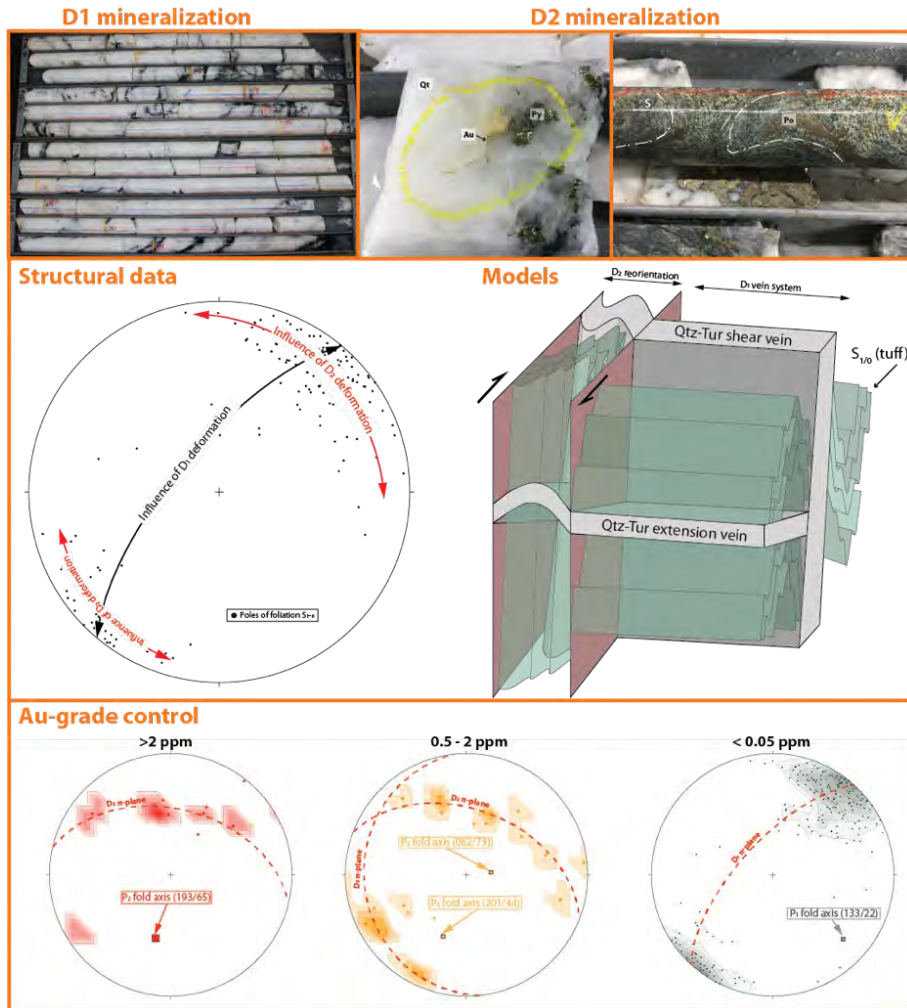


Figure 10: key summary of the Boulanger deposit including structural dataset, mineralization observation and stereographic distribution of Au-grade along drill cores.

IMPLICATIONS FOR MINERAL EXPLORATION

The systematic presence of fold superposition developed with greenstone belts in the locations studied here offers new prospective for exploration in the Guiana Shield. As suggested by the case study of Boulanger deposit, the Au-grade significantly increases during D_2 fold superposition, with the development of an ore shoot along D_2 axial planes. Although, no Au-grade available, similar observations have been made within Dieu Merci deposits, in which both geophysical and structural data support the presence of type-2 fold (Figure 3B and C). The historical mining operation (open pits) are located along D_2 fold hinges (Figure 3B). Therefore, in the greenstone belts from the Guiana shield, the intersection of D_1 and D_2 mineralized structures may represent favourable zones to investigate. In this context, refining the polyphase fold geometry (e.g. interference pattern) is fundamental. Accordingly, the recognition of the exact fold geometry appears critical for exploration targeting.

CONCLUSIONS

We report new results from four currently explored gold deposits (Oko west, Boulanger, Dieu Merci and Crique Sophie) hosted within the Rhyacian greenstone belts from the Guiana shield. Each of these deposits is affected by a complex deformation history marked by the development of fold superposition and, most likely, polyphase mineralization. Quantitative structural analysis approach, based on measured of foliations ($S_{1/0}$, S_2), bedding (S_0) and fold axes on outcrops, trenches or along cores, and geophysical data interpretation, are used to characterize the exact fold superposition patterns (also referred as fold interference patterns). Interestingly, for Boulanger and Dieu Merci deposits, the Au-grade and location of historical mining activities are both spatially correlated with the geometry of the interference pattern, suggesting an important structural control of the mineralization grade. These findings suggest that the characterization of the exact fold interference pattern is fundamental for the targeting of favourable enriched zones at deposit scale. We suggest that this approach should be routinely applied by mineral exploration companies developing projects in the Guiana shield and elsewhere.

ACKNOWLEDGMENTS

This work was supported by Reunion Gold Corporation, AuPlata Mining Group, GAIA SAS and GexplOre.

REFERENCES

- Chauvet, A., 2019. Structural control of ore deposits: The role of pre-existing structures on the formation of mineralised vein systems. *Minerals*, 9(1), 56.
- Combes, V., Eglinger, A., André-Mayer, A. S., Teitler, Y., Heuret, A., Gibert, P., & Béziat, D., 2022. Polyphase gold mineralization at the Yaou deposit, French Guiana. *Geological Society, London, Special Publications*, 516(1), SP516-2020.
- Cox, S. F., Wall, V. J., Etheridge, M. A., & Potter, T. F., 1991. Deformational and metamorphic processes in the formation of mesothermal vein-hosted gold deposits—examples from the Lachlan Fold Belt in central Victoria, Australia. *Ore geology reviews*, 6(5), 391-423.
- Craw, D., & Koons, P. O., 1989. Tectonically induced hydrothermal activity and gold mineralization adjacent to major fault zones.
- Dubé, B., Gosselin, P. A. T. R. I. C. E., Mercier-Langevin, P., Hannington, M., & Galley, A., 2007. Gold-rich volcanogenic massive sulphide deposits. *Geological Association of Canada, Mineral Deposits Division*, 75-94.
- Goldfarb, R. J., Groves, D. I., & Gardoll, S., 2001. Orogenic gold and geologic time: a global synthesis. *Ore geology reviews*, 18(1-2), 1-75.
- Goldfarb, R. J., & Groves, D. I., 2015. Orogenic gold: Common or evolving fluid and metal sources through time. *Lithos*, 233, 2-26.
- Goldfarb, R. J., Snee, L. W., & Pickthorn, W. J., 1993. Orogenesis, high-T thermal events, and gold vein formation within metamorphic rocks of the Alaskan Cordillera. *Mineralogical Magazine*, 57(388), 375-394.
- Groves, D. I., Goldfarb, R. J., Gebre-Mariam, M., Hagemann, S. G., & Robert, F., 1998. Orogenic gold deposits: a proposed classification in the context of their crustal distribution and relationship to other gold deposit types. *Ore geology reviews*, 13(1-5), 7-27.
- Kroonenberg, S. B., De Roever, E. W. F., Fraga, L. M., Reis, N. J., Faraco, T., Lafon, J. M., & Wong, T. E., 2016. Paleoproterozoic evolution of the Guiana Shield in Suriname: A revised model. *Netherlands Journal of Geosciences*, 95(4), 491-522.
- Neumayr, P., Ridley, J. R., McNaughton, N. J., Kinny, P. D., Barley, M. E., & Groves, D. I., 1998. Timing of gold mineralization in the Mt York district, Pilgangoora greenstone belt, and implications for the tectonic and metamorphic evolution of an area linking the western and eastern Pilbara Craton. *Precambrian Research*, 88(1-4), 249-265.
- Perret, J., Eglinger, A., André-Mayer, A. S., Aillères, L., Feneyrol, J., Hartshorne, C., & Bosc, R., 2020. Subvertical, linear and progressive deformation related to gold mineralization at the Galat Sufar South deposit, Nubian Shield, NE Sudan. *Journal of Structural Geology*, 135, 104032.
- Phillips, G. N., & Powell, R., 2010. Formation of gold deposits: a metamorphic devolatilization model. *Journal of Metamorphic geology*, 28(6), 689-718.
- Poulsen, K. H., 2000. Geological classification of Canadian gold deposits. *Bulletin of the Geological Survey of Canada*, 540, 1-106.
- Ramsay, J. G., Huber, M. I., & Lisle, R. J., 1987. *The techniques of modern structural geology: Folds and fractures* (Vol. 2). Academic press.
- Robert, F., & Brown, A. C., 1986. Archean gold-bearing quartz veins at the Sigma Mine, Abitibi greenstone belt, Quebec; Part I, Geologic relations and formation of the vein system. *Economic Geology*, 81(3), 578-592.
- Tedeschi, M. T., Hagemann, S. G., Kemp, A. I. S., Kirkland, C. L., & Ireland, T. R., 2020. Geochronological constrains on the timing of magmatism, deformation and mineralization at the Karouni orogenic gold deposit: Guyana, South America. *Precambrian Research*, 337, 105329.
- Tomkins, A. G., & Mavrogenes, J. A., 2002. Mobilization of gold as a polymetallic melt during pelite anatexis at the Challenger deposit, South Australia: a metamorphosed Archean gold deposit. *Economic Geology*, 97(6), 1249-1271.
- Voisey, C. R., Willis, D., Tomkins, A. G., Wilson, C. J., Micklethwaite, S., Salvemini, F., ... & Rickard, W. D., 2020. Aseismic refinement of orogenic gold systems. *Economic Geology*, 115(1), 33-50.

U-Pb-Hf zircon geochronology of the northern border of the Archean Amapá Block, SE Guiana Shield: Further evidence of dominant Neoproterozoic magmatism

Jean Michel Lafon

*Instituto de Geociências
Universidade Federal do Pará, Brazil
lafonjm@ufpa.br*

João M. Milhomem Neto

*Instituto de Geociências
Universidade Federal do Pará, Brazil
milhomem@ufpa.br*

Renato Cantão Gonçalves

*Instituto de Geociências,
Universidade Federal do Pará, Brazil
renatocg.mineracao@gmail.com*

João Alberto E. Pinto

*Instituto de Geociências
Universidade Federal do Pará, Brazil
joaoalbertoep@gmail.com*

Luisa Dias Barros

*Instituto de Geociências
Universidade Federal do Pará, Brazil
luisa.barros@ig.ufpa.br*

SUMMARY

We present new combined U-Pb and Lu-Hf geochronological results on zircon of Archean orthogneisses and granitoids from the northern border of the Amapá Block, in the Brazilian part of SE Guiana Shield. Apart from one Mesoproterozoic sample from the Tumucumaque Complex with an age of 2845 Ma, all the samples yielded Neoproterozoic ages between 2696 Ma and 2618 Ma. These results when compiled with previous U-Pb and Pb-Pb dating point to a Neoproterozoic protracted magmatic episode of at least 110 Ma (~2.70 Ga to ~2.59 Ga) as the main event that built up the northern part of the Amapá Block. The presence of Mesoproterozoic and early Neoproterozoic inherited zircon in most of the samples indicated that this protracted Neoproterozoic magmatic episode reworked older basement units. The subchondritic $\epsilon_{\text{Hf}}(t)$ values and Hf-TDM model ages between 3.7 and 3.2 Ga reinforce the existence of a Paleoproterozoic episode of crustal growth for this part of the Amapá Block.

INTRODUCTION

The Guiana Shield represents the northern segment of the Amazonian Craton separated from the Brazil Central Shield, in the south, by the Solimões-Amazonas sedimentary basins. The occurrence of Archean terranes is restricted to the eastern part of the Amazonian Craton, represented by the Carajás Province in the Brazil Central Shield and by the Amapá Block and Imataca Complex in the Guiana Shield. The Carajás Province is the unique preserved Archean crust segment in the Amazonian Craton while in the Guiana Shield, the Amapá Block in the southeast and the Imataca Complex in the northwest were intensely reworked, respectively, during the Rhyacian and Early Orosirian by the Transamazonian orogenic cycle (2.26-1.95 Ga) (Rosa-Costa et al., 2006, Fraga and Cordani, 2019). The SE of the Guiana Shield (north of Brazil, French Guiana and Suriname) consists of a widespread Paleoproterozoic orogenic belt that includes granulitic-gneissic-migmatitic complexes, greenstone belts and granitic plutons (Kroonenberg et al., 2016 and reference therein). The Transamazonian magmatic and tectono-metamorphic events are related to crustal accretion in a subduction setting, followed by tectonic accretion and crustal reworking during the collision between the Amazonian and West African cratons (Vanderhaeghe et al., 1998; Delor et al., 2003). In a global context, the SE Guiana Shield correlates to the Birimian terranes and Archean shields that form the West African Craton, which was affected by the Paleoproterozoic Eburnean Orogeny (Grenholm et al., 2019 and references therein).

The Amapá Block (north of Brazil) is a wide Archean landmass surrounded to the north and south by the Rhyacian Lourenço and Carecuru domains, respectively. Its basement is composed of Meso-Neoproterozoic granulitic-gneissic-migmatitic complexes (Rosa-Costa et al., 2006; 2017; Lafon and Rosa-Costa, 2020). Whole-rock Nd model ages indicated that the main period of crust generation in Amapá Block was during the Meso-Paleoproterozoic (Rosa-Costa et al., 2006, 2014; Milhomem Neto and Lafon, 2019). Zircon Lu-Hf geochronology indicated an older period of crustal accretion, with some Eoarchean Hf model ages (Borghetti et al., 2018; Milhomem Neto & Lafon, 2019). Most of the units of this Archean basement were delimited, mainly, by aerogeophysical mapping and localized dated outcrops. Therefore, the extension of these tectono-stratigraphic units remains controversial, especially in the northern part of the domain, where geochronological data are still limited. Here we provide a set of combined U-Pb-Lu-Hf isotope data on zircon from Archean units in the northeastern portion of the Amapá Block, at the border with the Rhyacian Lourenço domain. At the light of these new data, it was possible to investigate the extension of the Mesoproterozoic and Neoproterozoic magmatism in this portion of the Block. In addition, we intend to identify the crustal growth and reworking episodes that occurred during the Archean in this domain of the SE Guiana Shield.

GEOLOGICAL CONTEXT

The Amapá Block is a large crustal segment with a WNW-ESE direction, around 250 km wide and, at least, 400 km long. It consists essentially of a granulitic-gneissic-migmatitic association with amphibolite to granulite facies metamorphism (Rosa-Costa et al., 2017 and references therein). The Transamazonian Orogeny is responsible for those metamorphic events, deformation, deposition of greenstone belt sequences and the emplacement of granitic bodies during the Rhyacian. Two main magmatic episodes have been dated by zircon Pb-Pb and U-Pb dating at 2.85-2.79 Ga and 2.69-.260 Ga and an older magmatic episode (~ 3.19 Ga) has been locally evidenced at the northern border of the Amapá Block (Avelar et al., 2003; Rosa-Costa et al., 2006, 2014; Borghetti et al., 2018; Milhomem Neto & Lafon, 2019). Some evidence of isolated Paleoproterozoic magmatic rocks has also been identified (Spier et al., 2022 and reference therein). The Nd isotopic signature of the basement rocks of the Amapá Block points to Paleo-Mesoarchean episodes of crustal growth whereas the Neoproterozoic is dominated by crustal reworking (Milhomem Neto & Lafon, 2019). Zircon Lu-Hf data point to the predominance of crustal reworking processes of Eo-Paleoproterozoic sources during the formation of the basement of the Amapá Block. However, some Hf model ages with slightly positive $\epsilon_{\text{Hf}}(t)$ values suggest a Neoproterozoic juvenile source for some magmatic rocks from the southern part of the block (Borghetti et al., 2018; Milhomem Neto & Lafon, 2019).

In the northern portion of the Amapá Block, the main Archean tectono-stratigraphic units include Mesoarchean and Neoproterozoic orthogneisses (Porfírio Gneiss, 3.19 Ga, Tumucumaque Complex, 2.81-2.85 Ga, Guianense Complex, 2.61-2.69 Ga), Neoproterozoic granulite gneisses (Jari-Guaribas Complex, ~2.79 Ga) and granitic orthogneisses (Baixo Mapari Complex, ~2.65 Ga), Neoproterozoic granitoids (2.59 Ga Pedra do Meio Metagranitoid, 2.61 Ga Mungubas, 2.63 Ga Riozinho and 2.79 Ga Anaupicuru, granites). The Paleoproterozoic units are Rhyacian metavolcano-sedimentary sequences (Vila Nova Group) and granitoids (Flexal Intrusive Suite, Porto Grande and Carrapatinho granites), and a late Rhyacian granulitic complex (Tartarugal Grande Complex) with both Archean and Rhyacian protoliths. In the studied region, the Archean lithological units are the Tumucumaque and Guianense complexes, the Porfírio gneiss and the Riozinho, Mungubas and Pedro do Meio granitoids (Rosa-Costa et al., 2017, Milhomem Neto and Lafon 2019 and references therein).

SAMPLING AND ANALYTICAL PROCEDURES

Seven samples of orthogneisses and granitoids were selected for U-Pb and Lu-Hf zircon dating, except for sample RPJ-1908A, for which only U-Pb analyses have been performed: Two samples from the central-northern part of the Amapá Block (granodioritic orthogneiss of the Guianense Complex – JAP-02 and Mungubas Leucomonzogranite – JAP-01), and 5 samples from the northern border of the Amapá Block with the Lourenço Domain, collected along a cross section on the Tartarugal Grande river (A granodioritic orthogneiss from the Tumucumaque Complex - RPJ-1906, two granodioritic orthogneisses - RPJ-1909 and JAP-1806, one monzogranitic orthogneiss RPJ-1908A and one amphibole-biotite metagranodiorite RPJ-1910A, from the Guianense Complex).

Zircon U-Pb and Lu-Hf analyses were performed on a high-resolution multi-collector Neptune Thermo Finnigan ICP-MS coupled with a Nd:YAG LSX-213 G2 CETAC laser probe, according to the procedure described in Milhomem Neto and Lafon (2019) at the Isotope Geology Laboratory of the UFPA (Belém-Brazil). For sample RPJ-1908A the U-Pb analyses were performed on a quadrupole Thermo iCAPQ ICP-MS coupled to the same Laser probe. The U-Pb and Lu-Hf raw data reduction were processed using in-house Excel spreadsheets and the U-Pb ages were calculated using the Isoplot/Ex program (Ludwig, 2003). The error on the ages is calculated at a 2σ level. The crustal model ages (Hf-TDM) and ϵ_{Hf} were calculated using the present-day $^{176}\text{Lu}/^{177}\text{Hf}$ and $^{176}\text{Hf}/^{177}\text{Hf}$ ratios of 0.0336 and 0.282785 for the chondritic uniform reservoir (CHUR) (Bouvier et al., 2008) and $^{176}\text{Lu}/^{177}\text{Hf}$ and $^{176}\text{Hf}/^{177}\text{Hf}$ of 0.0388 and 0.28325 for the depleted mantle (DM) (Andersen et al., 2009). A $^{176}\text{Lu}/^{177}\text{Hf}$ ratio of 0.015 was assumed as a continental crust average value (Griffin et al., 2004).

RESULTS

The U-Pb data of the leucomonzogranite (JAP-01A) show a complex distribution of the concordant points, with one Neoproterozoic date and three groups of Neoproterozoic ages. Two groups of Neoproterozoic concordant crystals of four grains each yielded $^{207}\text{Pb}/^{206}\text{Pb}$ mean ages of 2696 ± 21 (MSWD = 0.32) and 2651 ± 21 Ma (MSWD = 0.04). In addition, two Neoproterozoic zircons yielded a $^{207}\text{Pb}/^{206}\text{Pb}$ mean age of 2742 ± 24 Ma (MSWD = 0.56) and a zircon core provided a Neoproterozoic $^{207}\text{Pb}/^{206}\text{Pb}$ date of 2844 ± 17 Ma. For the Neoproterozoic zircons with an age of 2.70 Ga, the ϵ_{Hf} values ranged from -7.5 to -1.5 and the Hf-TDM model ages for these Neoproterozoic zircons ranged between 3.6 to 3.2 Ga.

As for the previous sample, the Neoproterozoic concordant crystals from the sample JAP-02A of granodioritic orthogneiss provided two different $^{207}\text{Pb}/^{206}\text{Pb}$ mean ages of 2696 ± 17 Ma ($n = 5$, MSWD = 0.57) and 2651 ± 18 Ma ($n = 6$, MSWD = 0.42). One inherited crystal yielded a Mesoarchean $^{207}\text{Pb}/^{206}\text{Pb}$ date of 2995 ± 36 Ma. The ϵ_{Hf} values for the 2.70 Ga old zircons ranged between -5.7 and -4.4 and the Hf-TDM model ages varied between 3.5 and 3.4 Ga. Seven zircon crystals from the sample RPJ-1906 of granodioritic orthogneiss yielded an upper intercept age of 2845 ± 15 Ma (MSWD = 1.6). In addition, one concordant crystal yielded a Neoproterozoic $^{207}\text{Pb}/^{206}\text{Pb}$ date of 2634 ± 20 Ma. For the concordant zircon grains with an age of 2.85 Ga, the ϵ_{Hf} values ranged between -7.3 and -0.4 with Hf-TDM ages between 3.7 and 3.3 Ga.

Ten concordant crystals from the amphibole-biotite metagranodiorite (RPJ-1910A) yielded a $^{207}\text{Pb}/^{206}\text{Pb}$ mean age of 2654 ± 12 Ma (MSWD = 1.04). Two concordant zircons yielded a younger $^{207}\text{Pb}/^{206}\text{Pb}$ mean age of 2594 ± 35 Ma (MSWD = 0.03). In addition, two others concordant crystals provided $^{207}\text{Pb}/^{206}\text{Pb}$ dates of 2500 ± 23 Ma and 2251 ± 33 Ma, respectively. The ϵ_{Hf} values for the 2.65 Ga old crystals ranged between -7.1 and -1.5, with Hf-TDM model ages between 3.5 and 3.2 Ga.

Five zircon crystals from another sample of granodioritic orthogneiss (RPJ-1909) yielded an upper intercept age of 2632 ± 28 Ma (MSWD = 0.93) and another concordant zircon provided an older $^{207}\text{Pb}/^{206}\text{Pb}$ date of 2767 ± 28 Ma. For the 2.63 Ga old concordant zircon grains, the ϵ_{Hf} values ranged between -5.2 and -4.5 with Hf-TDM ages around 3.4 Ga.

For the sample JAP-1806 of granodioritic orthogneiss five crystals yielded a $^{207}\text{Pb}/^{206}\text{Pb}$ mean age of 2618 ± 22 Ma (MSWD = 0.71). Three other concordant crystals provided an older $^{207}\text{Pb}/^{206}\text{Pb}$ mean age of 2714 ± 31 Ma (MSWD = 0.16). In addition, two crystals yielded a Neoproterozoic $^{207}\text{Pb}/^{206}\text{Pb}$ age of 2522 ± 40 Ma (MSWD = 0.73) and another one a $^{207}\text{Pb}/^{206}\text{Pb}$ date of 2887 ± 27 Ma. For the concordant zircon grains with an age of 2.62 Ga, the ϵ_{Hf} values ranged between -10.6 and -7.5 with Hf-TDM between 3.5 and 3.7 Ga. Nine concordant zircon crystals from sample RPJ-1908A of a monzogranitic orthogneiss yielded a $^{207}\text{Pb}/^{206}\text{Pb}$ mean age of 2684 ± 12 Ma (MSWD = 0.78). U-Pb and Lu-Hf results are summarized in table 1.

Table 1. U-Pb and Lu-Hf results for the orthogneiss and granitoid samples from the northern part of the Amapá Block. The ϵ_{Hf} values for the inherited zircon and those that suffered ancient Pb loss are not reported.

Sample ID	Lithology/ Unit	Crystallization ages	Inherited ages	Rejuvenated ages (Ancient Pb loss)	ϵ_{Hf}^3	Hf-TDM age
RPJ-1906	Granodioritic orthogneiss Tumucumaque Complex	2845 ± 15 Ma ¹	-	2634 ± 20 Ma	-7.3 to -0.4	3.3-3.7 Ga
JAP-02	Granodioritic orthogneiss Guianense Complex	2696 ± 17 Ma	3.0 Ga and 2.74 Ga	2651 ± 18 Ma	-5.7 to -4.4	3.4-3.5 Ga
JAP-01A	Leucomonzogranite Mungubas Granitoid	2696 ± 21 Ma	2.84 Ga	2651 ± 21 Ma	-7.5 to -1.5	3.2-3.6 Ga
RPJ-1908A	Monzogranitic orthogneiss Guianense Complex	2684 ± 12 Ma ²	-	-	-	-
RPJ-1910A	Anf-Biot metagranodiorite Guianense Complex	2654 ± 12 Ma	-	2594 ± 35 Ma	-7.1 to -1.5	3.2-3.5 Ga
RPJ-1909	Granodioritic orthogneiss Guianense Complex	2632 ± 28 Ma ¹	2.77 Ga	-	-5.2 to -4.5	~3.4 Ga
JAP-1806	Granodioritic orthogneiss Guianense Complex	2618 ± 22 Ma	2.89 Ga and 2.72 Ga	2552 ± 40 Ma	-10.6 to -7.5	3.5-3.7 Ga

1 - Upper intercept age; 2 - LA-Q-ICP-MS; 3 - ϵ_{Hf} at the crystallization time

IMPLICATIONS FOR REGIONAL LITHOSTRATIGRAPHY AND ARCHEAN EVOLUTION OF THE AMAPÁ BLOCK

The new set of U-Pb geochronological data indicate that, apart from one Mesoarchean sample of the Tumucumaque Complex with an age of 2845 Ma, all the samples have Neoproterozoic ages between 2696 Ma and 2618 Ma indicating that the Neoproterozoic Guianense Complex and associated Neoproterozoic granitoids are the

dominant lithologies in the northern part of the Amapá Block. These new results led to a reappraisal of the lithostratigraphic sequence of the northern border of the Amapá Block with the Lourenço Domain. In this sector, the dominant unit is the Neoproterozoic Guianense Complex while the Mesoproterozoic Porfírio Gneiss and the Tumucumaque Complex occur only as xenoliths. The Neoproterozoic Pedra do Meio Granitoid, previously considered as the main unit in this sector is now limited to a small charnockitic intrusion within the Guianense Complex. Together with the previous geochronological data (Rosa- Costa et al., 2014; Milhomem Neto and Lafon, 2019), the results of the present study point to a Neoproterozoic protracted magmatic episode of about 110 Ma, or more (~2.70 Ga to ~2.59 Ga) as the main event that built up the northern part of the Amapá Block. The complex distribution of dates observed in the zircon population of most samples are attributed to ancient Pb loss probably due to high temperature gradient that has been maintained during the protracted magmatic episode. The frequent metamict chaotic internal features observed in the zircon population of the dated samples may have favoured this ancient lead loss. The same behaviour has been previously reported by Milhomem Neto and Lafon (2019) for another Neoproterozoic sample of the same area. The presence of inherited zircon in most of the Neoproterozoic samples, with Mesoproterozoic (3.0, 2.89, 2.84 Ga) and early Neoproterozoic (2.77, 2.74, 2.72 Ga) ages indicated that this protracted Neoproterozoic magmatic episode reworked older basement units. The $\epsilon_{\text{Hf}(t)}$ values are subchondritic for all the samples ($-10.6 < \epsilon_{\text{Hf}(t)} < -0.4$) and Hf- T_{DM} ages between 3.7 and 3.2 Ga are further evidence for a Paleoproterozoic episode of crustal growth for this part of the Amapá Block.

ACKNOWLEDGMENTS

This work was supported through the South American Exploration Initiative Stage 2 (SAXI-2) and the CNPq-Universal project n°423625/2018-7. We acknowledge AMIRA Global and sponsors for their support of the SAXI project (AMIRA P1061B). We also acknowledge the Geological Survey of Brazil (CPRM-Belém) for sharing field information from their mapping projects in Amapá.

REFERENCES

- Andersen, T., Andersson, U.B., Graham, S., Åberg, G., Simonsen, S.L., 2009. Granitic magmatism by melting of juvenile continental crust: new constraints on the source of Paleoproterozoic granitoids in Fennoscandia from Hf isotopes in zircon. *Journal of the Geological Society* 166: 233–248.
- Avelar, V.G., Lafon, J.M., Delor, C., Guerrot, C., Lahondère, D., 2003. Archean crustal remnants in the easternmost part of the Guiana Shield: Pb–Pb and Sm–Nd geochronological evidence for Mesoproterozoic versus Neoproterozoic signatures. *Géologie de la France* 2–3–4, 83–100.
- Borghetti, C., Philipp, R.P., Mandetta, P., Hoffmann, I.B., 2018. Geochronology of the Archean Tumucumaque Complex, Amapá Terrane, Amazonian Craton, Brazil. *Journal of South American Earth Sci.* 88: 294–311.
- Bouvier, A., Vervoort, J.D., Patchett, P.J., 2008. The Lu–Hf and Sm–Nd isotopic composition of CHUR: constraints from unequilibrated chondrites and implication for the bulk composition of terrestrial planets. *Earth and Planet. Science Letters* 273: 48–57.
- Cordani U.G., Texeira W., D’Agrella-Filho M.S., Trindade R.I. 2009. The position of the Amazonian Craton in supercontinents. *Gondwana Res.*, 15: 396–407.
- Delor C., Lahondere D., Egal E., Lafon J.M., Cocherie A., Guerrot C., Rossi P., Truffert C., Theveniaut H., Phillips D., Avelar V.G. 2003a. Transamazonian crustal growth and reworking as revealed by the 1:500.000 – scale geological map of French Guiana (2nd edition). *Géologie de la France – Special Guiana Shield*. BRGM – SGF Editor. 2-3-4: 5-58.
- Fraga, L.M., Cordani, U., 2019. Early Orosirian tectonic evolution of the Central Guiana Shield: insights from new U-Pb SHRIMP data. In: SAXI – XI Inter Guiana Geological Conference. Paramaribo, Suriname. Extended abstract, p.59-62.
- Grenholm, M., Jessell, M., Thébaud, N., 2019. A geodynamic model for the Paleoproterozoic (ca. 2.27–1.96 Ga) Birimian Orogen of the southern West African Craton – Insights into an evolving accretionary-collisional orogenic system. *Earth Sci. Rev.* 192, 138–193.

- Griffin, W.L., Belousova, E.A., Shee, S.R., Pearson, N.J., O'Reilly, S.Y., 2004. Archean crustal evolution in the northern Yilgarn Craton: U–Pb and Hf-isotope evidence from detrital zircons: *Precambrian Research* 131(3-4): 231-282.
- Kroonenberg, S.B., de Roever, E.W.F., Fraga, L.M., Reis, N.J., Faraco, T., Lafon, J.M., Cordani, U., Wong, T.E., 2016. Paleoproterozoic evolution of the Guiana Shield in Suriname: A revised model. *Netherlands Journal of Geosciences - Geologie en Mijnbouw* 95-4, 491-522.
- Lafon, J.M.; Costa, L.T.R. 2020. Compartimentação tectônica na porção sudeste do Escudo das Guianas: as províncias Maroni- Itacaiúnas e Amazônia Central. In: A. Bartorelli; W. Teixeira; B.B. de Brito Neves. (Org.). *Geocronologia e evolução tectônica do continente Sul-Americano: a contribuição de Umberto Giuseppe Cordani*. 1ed. São Paulo: Solaris Edições Culturais, p. 79-91.
- Ludwig, K.R. 2003. User's Manual for Isoplot/Ex version 3.00 – A Geochronology Toolkit for Microsoft Excel. Berkeley Geochronological Center, Special Publication 4, 70 p.
- Milhomem Neto, J.M., Lafon, J.M. 2019. Zircon U-Pb and Lu-Hf isotope constraints on Archean crustal evolution in Southeastern Guyana Shield. *Geoscience Frontiers*, 10:1477-1506.
- Rosa-Costa, L.T., Lafon, J.M.; Delor, C. 2006. Zircon geochronology and Sm–Nd isotopic study: Further constraints for the Archean and Paleoproterozoic geodynamical evolution of the southeastern Guiana Shield, north of Amazonian Craton, Brazil. *Gondwana Res.* 10: 277-300.
- Rosa-Costa, L.T., Chaves, C.L., Klein, E.L. 2014. Geologia e recursos minerais da Folha Rio Araguari - NA-22-Y-B, Estado do Amapá, Escala 1:250.000, in: CPRM, S.G.d.B.-. (Ed.), Belém, 159p.
- Rosa-Costa, L.T., Chaves, C.L., Silva, C.M.G., Campos, L.D., Abrantes, B.K.C., Tavares, F.M., Lago, A.L. 2017. Área de relevante interesse mineral: Reserva Nacional do Cobre e Associados – RENCA. (Informe de Recursos Minerais. Série Províncias Minerais do Brasil, nº 12). 182p.
- Spier, C.A.; Ferreira Filho, C.F.; Daczko, N. 2022. Zircon U-Pb isotopic and geochemical study of metanorites from the chromite- mineralised Bacuri Mafic-Ultramafic Complex: Insights of a Paleoproterozoic crust in the Amapá Block, Guyana Shield, Brazil. *Gondwana Res.*, 105: 262-289.
- Vanderhaeghe, O., Ledru, P., Thiéblemont, D., Egal, E., Cocherie, A., Tegye, M., Milési, J., 1998. Contrasting mechanism of crustal growth Geodynamic evolution of the Paleoproterozoic granite-greenstone belts of French Guiana. *Precambrian Res.* 92: 165-193.

Update on the Guyana-Brazil project and more recent zircon age results of alkaline intrusions in Southern Guyana: Makarapan Mountain and Muri Mountain Alkaline Complex

Serge Nadeau*, La Donna Fredericks and Jimmy Reece
Geo-Services Division, Guyana Geology and Mines Commission
Upper Brickdam, Georgetown, Guyana
goldenserge@hotmail.com

SUMMARY

Update on the report of the Brazil-Guyana border geological and geodiversity project is presented in the first section. A summary of the main outcomes up to today will be presented from the 447 zircon analyses performed by Laser ICP-MS. In the second section more recent zircon age results were obtained by Laser ICP-MS for two alkaline intrusions located in Southern Guyana. An age of 1,987 \pm 19 Ma was measured in a sample from the Makarapan Mountain Alkaline Intrusion which implies that it is part of the Iwokrama Formation of the Burru Burru Group formed during the Orocaima Igneous Belt magmatic event extending from Brazil to Guyana and to Suriname. The age of the Muri Mountain Alkaline Complex is estimated to range between 1086 \pm 43 and 1,110 \pm 26Ma and is significantly older than an age of 1026 \pm 28 Ma obtained in a syenite sample of the Mutum Mountain of Brazil considered to be co-magmatic.

Key words: Brazil-Guyana project, Southern Guyana, Makarapan Mountain, Muri Mountain, zircon, U-Pb, Laser-ICP-MS

INTRODUCTION

1. The Brazil-Guyana border geological and geodiversity mapping project

The Brazil-Guyana border geological and geodiversity mapping project was proposed following an agreement for Scientific and Technical Cooperation between the Governments of Brazil and Guyana (signed on September 14th, 2009). The geological work was performed by the CPRM (Companhia de Pesquisa de Recursos Minerais) of Brazil and the GGMC (Guyana Geology and Mines Commission) of Guyana. Geological mapping was performed along a buffer zone of 20km on both side of the border between parts of northern Brazil and southwestern Guyana. (Fig.1). The aim of the project was to correlate the geological units on both side of the border and produce a unified geological map.

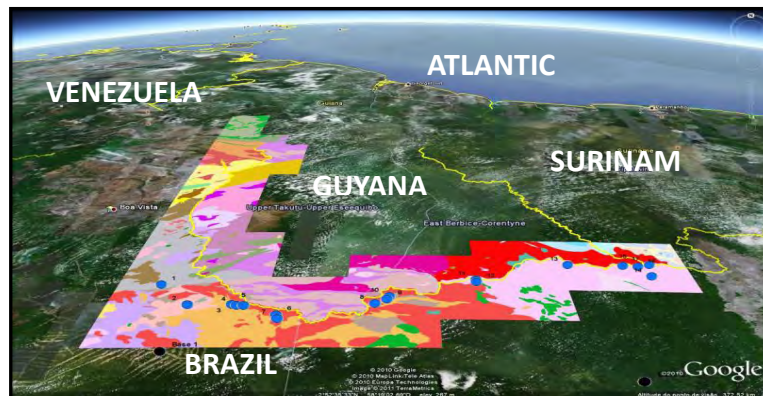


Fig. 1 Guyana and Brazil geology in the buffer zone of 20km on both side of the border.

The work included geological mapping in the field, rocks petrography, chemical analyses, and age dating of rocks (10 in each country). Field mapping was done in 2011 and more than 75 rock samples were collected during fieldwork despite difficult weather conditions in Guyana. Between 20 and 25 zircon crystals were separated in each of the eighteen rocks dated using the U-Pb isotopic system with their isotopic ratios measured by LA-ICP-MS at the State Key Laboratory of Mineral Deposit Research, Nanjing University, Nanjing China.

The Portuguese version of the report is expected to be completed by the end of 2022, translation of the report in English and final publication of the two versions to be completed in the Spring of 2023.

BRAZIL-GUYANA GEOLOGY AND GEODIVERSITY BORDER MAPPING PROJECT RESULTS

The main outcomes of the Brazil-Guyana geology and geodiversity border mapping project are:

- A) Finding of Archean (2,852-3,778 Ma) and Hadean ages (4,100-4,219 Ma) in zircon xenocrysts contained in younger volcanic and granitic rocks of the Iwokrama Formation (Fig.2a-b).
- B) Ages of volcanic and subvolcanic granites of the Iwokrama Formation range from at 1,980-1,991 Ma (Fig. 2a and Nadeau et al. 2013;) overlapping with the zircon ages of $1,977 \pm 8$ Ma and $1,984 \pm 7$ Ma measured by ion probe in two rocks of the Surumu Group in Brazil, considered to be correlative with the Iwokrama Formation (Reis et al. 2000). Other zircon xenocrysts ages in the Iwokrama Formation cluster at ca. 2,196 – 2,202 Ma, ca. 2,395 – 2,489 Ma.
- C) Rock samples from the Southern Guyana Granite Complex yielded ages ranging between 1,925 and 1,984 Ma (Fig. 2a)
- D) Metamorphic ages between 1,956 and 1,979 Ma were obtained in rocks of the Kanuku Complex (Fig. 2a). Detrital zircons with older age values clustered at ca. 2,200 – 2,269 Ma, ca. 2,450 – 2,520 Ma and ca. 2,635 – 2,721 Ma.

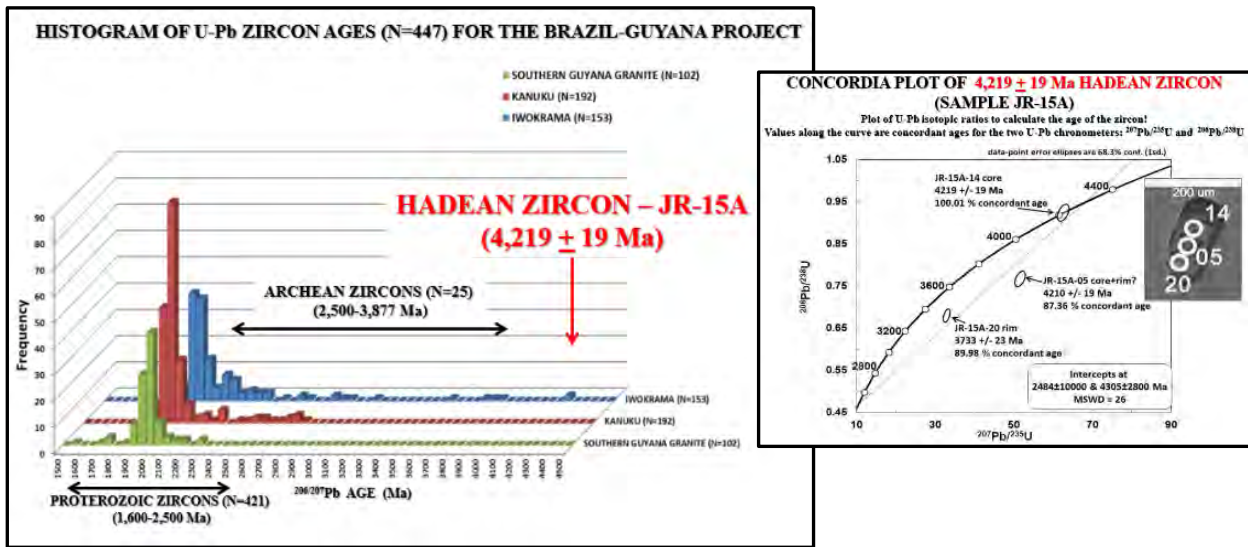


Fig. 2a-b: 2a. Histograms of 447 zircon ages from the Southern Guyana Granite, Kanuku Complex and Iwokrama Formation. 2b. Zircon crystal from sample JR-15 yielding a Hadean age of 4,219 Ma.

- E) The geology of Guyana and Brazil were correlated by samples taken in the middle of the border along the Takutu River.
- F) A unified geological map of Northeastern Brazil, and southern parts of Guyana, Surinam and French Guyana was published by the CPRM at the 1:1,000,000 scale in the Geological and Mineral Resources Map of South America Project: Sheet NA.21: Tumucumaque, (Fraga et al. 2020).
- G) Integration of this new geological map of Brazil and Guyana within the Tectonic Map of South America Second edition, at a scale of 1:5,000,000 (Cordani et al. 2016).

2. Alkaline intrusions in Southern Guyana

Two alkaline intrusions, Makarapan Mountain and Muri Mountain Alkaline Complex were mapped by geologists of the former Geological Survey of British Guiana (Berrangé 1977, Gibbs and Barron 1993 and ref. therein). The zircon of one rock from Makarapan Mt and from two rocks from the Muri Mt Alkaline Complex were extracted by crushing, gravity separation and Frantz Magnetic separator. More than 12 to 15 zircon crystals in each rock were dated using the U-Pb isotopic system with their isotopic ratios measured by LA-ICP-MS at the Centro de Pesquisas Geocronológicas of the University of São Paulo.

2a. Makarapan Mountain Alkaline Intrusion

Rock sample MRK-6 was collected during the field work of La Donna Fredericks investigating the Makarapan Mountain alkaline intrusion as part of her B.Eng. Geology thesis at the University of Guyana in 2015. MRK-6 was collected towards the central part of the intrusion.

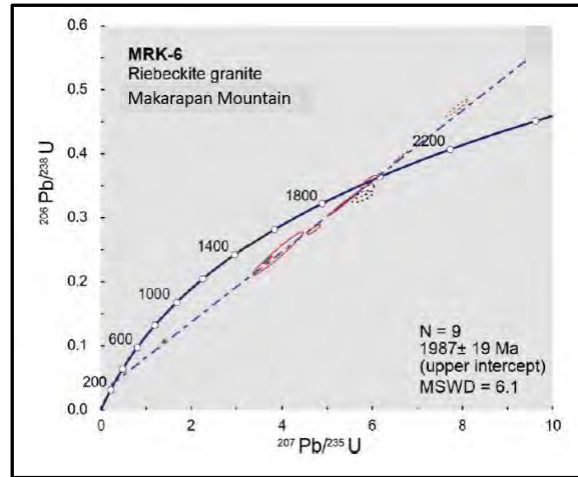


Fig. 3 Zircon age derived from the 206Pb/207Pb isotopic ratio in rock MRK-6. 95% confidence level

A zircon age of 1,987 +/- 19 Ma derived from the 206Pb/207Pb isotopic ratio was obtained (Fig.3 and Fraga et al. 2022). This zircon age is similar to the age range of 1,980 to 1,991 Ma measured in the adjacent volcanic and granitic intrusions present in the Iwokrama Formation implying it was emplaced during the same magmatic event (Fig. 2a and Nadeau et al., 2013). The Iwokrama magmatic rocks are associated to the large Orocaima Igneous Belt extending over 1400 km across Brazil, Guyana, and Suriname (Fraga et al, 2022). The age of MRK-6 is much younger than ages previously measured by the K-Ar isotopic method yielding an age of 2,595 +/- 125 Ma (Snelling and McConnell, 1969) later revised to a younger age of 2392 +/- 47 Ma by Berrangé (1977). These older ages were interpreted by the later author to represent rocks of the Kanuku Complex uplifted in a horst structure or a granitic intrusion derived from melting of meta-sediments or peralkaline tuff-lavas by anatexis at the granulite facies conditions.

2b. Muri Mountains Alkaline Complex

The Muri Mountains Alkaline Complex is composed of several intrusions and is part of the Muri-Mutum Mountains present in southern Guyana and northern Brazil (Fig. 4). The mountains are composed of a group of alkaline intrusions forming circular mountains rising up to 375m above the flat topography of the surrounding granitic rocks. The alkaline intrusions are called Muri Mountains in Guyana and Mutum Mountain in Brazil and they are considered co-magmatic (Gibbs and Barron, 1993). A possible phosphate-rich carbonatitic intrusion is inferred under a thick of laterite at Twareitau Mountain in the NE corner of the Muri Mountain Alkaline Complex (Fig. 4).

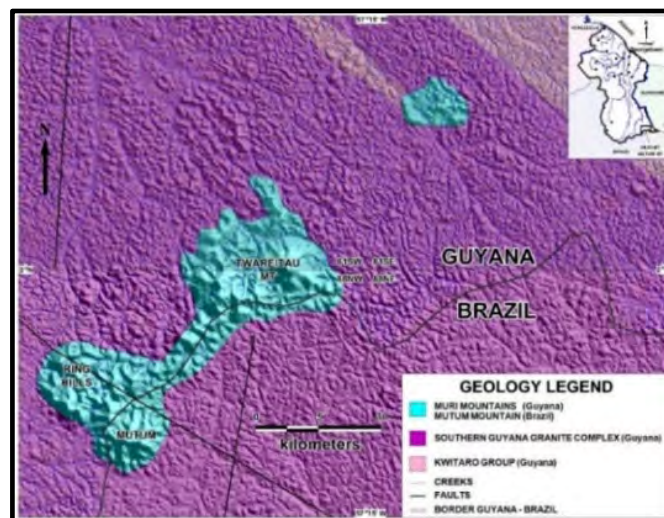


Fig.4 Geology map of the Muri-Mutum Mountains alkaline intrusions overlying the STRM image.

The zircon ages are derived from the $^{206}\text{Pb}/^{238}\text{U}$ isotopic ratio and corrected for ^{204}Pb common lead. At the 95% confidence level the age for the nepheline syenite MM-19B is 1086 ± 43 Ma (Fig. 5a) and nepheline syenite MM-20B is $1,110 \pm 26$ Ma (Fig. 5b).

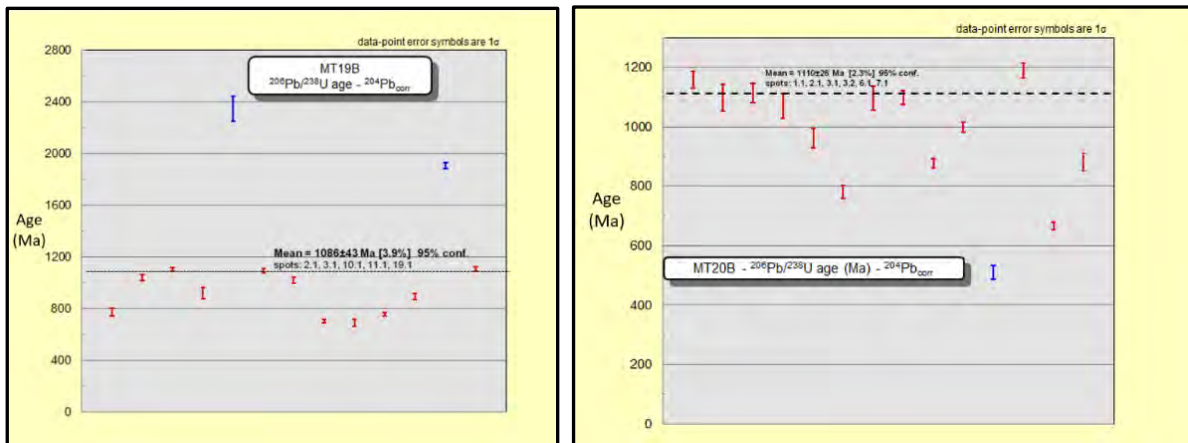


Fig. 5a-b Zircon age derived from the $^{206}\text{Pb}/^{238}\text{U}$ isotopic ratio. Fig. 6a Sample MM-19B and Fig. 6b Sample MM-20B. 95% confidence level

The zircon ages of 1086 ± 43 Ma and of $1,110 \pm 26$ Ma in the nepheline syenite samples are implying an older age of emplacement for the alkaline intrusions of the Muri-Mutum Mountains than the previous K-Ar age estimate of $1,026 \pm 28$ Ma measured in a K-feldspar from a syenite sample of the Mutum intrusion in Brazil, which was considered a minimum age by Oliveira et al. (1975).

CONCLUSIONS

Significant improvements on the geology, timing of formation and metamorphism of the main lithostratigraphic units of southern Guyana have been obtained during the Brazil-Guyana Geology and Geodiversity Border Project and during subsequent collaboration with geologists from the CPRM of Brazil and with Professor Cordani from the University of Sao Paulo, Brazil. Additional age dating work is recommended to better constrain the geological history of rock units in other parts of southern Guyana.

ACKNOWLEDGMENTS

Dr. Wei Chen is thanked for the 447 zircon analyses performed by LA-ICP-MS at the State Key Laboratory of Mineral Deposit Research, Nanjing, China. Professor Umberto G. Cordani and Koji Kawashita are acknowledged for the age dating work done by laser ICP-MS at the Centro de Pesquisas Geocronológicas of the University of São Paulo.

REFERENCES

- Berrangé J.P. (1977) The Geology of Southern Guyana, South America, London, Institute of Geological Science. Memoir 4, p. 112
- Fraga L.M., Cordani U., Dreher A.M., Reis N.J., Nadeau S., Kroonenberg S., De Roever E., and Maurer V.C. (2022 in prep.) U-Pb geochronology of the Cauarane-Coeroeni Belt, Orocaima Igneous Belt and Rio Urubu Belt: Implications for the Eo-Orosirian geodynamic evolution of the Guiana Shield, Northern Amazonian Craton.
- Gibbs, A.K. & Barron C.N. 1993. The Geology of the Guiana Shield. Oxford Monograph on Geology and Geophysics No.23. ISBN 0-19-507350-9.
- Nadeau S., W. Chen, J. Reece, D. Lachhman, R. Ault, T. Faraco, L. Fraga, N. Reis and Betiollo L. (2013) Guyana: The Lost Hadean Crust of South America? Brazilian Journal of Geology 43(4): 601-606.
- Oliveira, A. da S., Fernandes, C.A.A., Issler, R.S., Abreu, A.S., Montalvão, R.M.G. de, and Teixeira, W. (1975) Geologia. In Brasil, Departamento de Producao Mineral, Projecto RADAMBRASIL, Folha NA.21, Tumucumaque e parte da Folha NB.21, Levantamento de Recursos Naturais, v. 9, pp. 17-114.
- Snelling N.J. and McConnell. R.B. (1969) The geochronology of Guyana. Geol. Surv. Guyana Records 6, Paper IX, 23 pp.
- Reis N.J., Faria M.S.G. de Fraga L.M., Haddad R.C. 2000. Orosirian calc-alkaline volcanism and the Orocaima event in the northern Amazonian Craton, eastern Roraima State, Brazil. Revista Brasileira de Geociências, 30(3):380-383.

High-grade metamorphism in the central region of Amapá, Northern Brazil: age constraints from in situ U-Pb dating of monazite and zircon

João M. Milhomem Neto*

Geoscience Institute – UFPA

66075-110 – Belém, Brazil

milhomem@ufpa.br

Jean Michel Lafon

Geoscience Institute – UFPA

66075-110 – Belém, Brazil

lafonjm@ufpa.br

Dominique de P. Amaral Ferreira

Geoscience Institute – UFPA

66075-110 – Belém, Brazil

dominiqueafd.16@gmail.com

Sarah Silva Miranda

Geoscience Institute - UFPA

66075-110 – Belém, Brazil

sarah.miranda@ig.ufpa.br

Elton Luiz Dantas

Geoscience Institute – UnB

70910-900 – Brasília, Brazil

elton@unb.br

SUMMARY

We present new LA-ICP-MS U-Pb results on monazite and zircon of two leucogneisses, a neosome derived from a migmatitic leucogneiss and an amphibolite from a late Rhyacian high-grade metamorphic complex (Tartarugal Grande Complex - TGC), in the central region of Amapá, north of Brazil. The monazites yielded ages of 2056 ± 5 Ma (neosome) and 2058 ± 19 Ma (garnet-biotite leucogneiss). Together with previous radiometric dating, these new results provide a robust dataset that indicates a period around 2.06-2.04 Ga for the granulite metamorphism, anatexis and intrusion of charnockitic plutons. In addition, an episode of mafic magmatism in the TGC is dated at 2069 ± 11 Ma.

Key words: High-grade metamorphism, Southeastern Guiana Shield, U-Pb geochronology, Monazite, zircon, Rhyacian

INTRODUCTION

The Tartarugal Grande Complex (TGC; Rosa-Costa et al., 2014, Gorayeb et al., 2021 and references therein) is located at the transition between the Rhyacian Lourenço domain and the Archean Amapá block, in the central eastern region of the state of Amapá, Brazil, southeastern Guiana Shield (Rosa-Costa et al., 2006, 2014). The Amapá Block, to the south, is a large Archean continental landmass roughly oriented in a WNW-ESE direction. It consists mainly of a high-grade metamorphic granulitic-migmatitic-gneiss complex of Meso- to Neoproterozoic age (2.85-2.60 Ga), which has been strongly reworked during the Transamazonian orogeny, responsible for its deformation, metamorphism and granitic magmatism. The Lourenço Domain, to the north, is constituted predominantly by a Rhyacian lithological association of granitoid-greenstones, with dominant granitoids and orthogneisses and restricted metavolcanosedimentary sequences metamorphosed in the greenschist to amphibolite facies, locally granulite (Rosa-Costa et al., 2006, Milhomem Neto and Lafon, 2019). This granitoid-greenstone association formed in a long-lived continental magmatic arc setting (~2.26-2.12 Ga), which evolved to a collisional setting with the amalgamation of the Amapá Block and the Lourenço Domain at 2.11–2.08 Ga (Rosa-Costa et al., 2014; Milhomem Neto & Lafon, 2020; Vianna et al., 2020).

The TGC rocks outcrop in the beds of the Tartarugal Grande and Falsino Rivers, on the margins of the BR-156 highway (Macapá-Oyapock) and nearby roads. The TGC encompasses an association of high-grade metamorphic rocks that has been described and studied for more than five decades since Scarpelli (1969). It is composed by dominant felsic granulites and aluminous leucogneisses, besides of rare mafic granulites and amphibolites that occur as tabular bodies or lenses of metrical dimensions intruded in the felsic granulite and leucogneiss protoliths, before metamorphism. It also includes some charnockite and granite bodies with preserved magmatic structures. Both granulites and gneisses were affected by thrust and transcurrent shear zones along a NW-SE trend. Quartz-feldspathic neosomes, with or

without orthopyroxene and garnet-rich neosomes occur in the felsic granulites and the leucogneisses, respectively, as a product of anatexis. Gorayeb et al. (2021) carried out a detailed petrological study on these rocks and established the metamorphic paragenesis and P-T conditions. The peak of granulite metamorphism was estimated at a temperature of 800 ± 20 °C and pressure of 6-7 Kbar. Retro-metamorphism and cooling during exhumation to higher crustal levels was also evidenced. Lafon et al. (2000) obtained (SHRIMP) zircon U-Pb ages of 2623 ± 13 Ma and 2602 ± 12 Ma for a garnet-bearing felsic granulite and a charnockitic granulite, respectively. Avelar (2002) obtained a zircon Pb-evaporation age of 2053 ± 1 Ma for a contemporaneous charnockite. Zircon Pb-evaporation ages (2100 ± 4 Ma, 2092 ± 7 Ma and 2078 ± 4 Ma) and LA-ICP-MS zircon U-Pb (2671 ± 15 Ma to 2597 ± 55 Ma) ages were obtained for the protoliths of enderbitic to charnockitic granulites by Rosa-Costa et al. (2014). In addition, Gorayeb et al. (2021) obtained LA-ICP-MS zircon U-Pb age of 2082 ± 5 Ma for the igneous protolith of a charnoenderbitic granulite. This geochronological data set indicates that the TGC includes rocks formed during the Rhyacian and the Neoarchean and metamorphosed during a late Transamazonian granulitic episode. In this work we present a new set of LA-ICP-MS U-Pb ages for monazites from two leucogneisses and zircons from an amphibolite from the TGC to better constrain the timing of the high-grade metamorphism in this part of the of the southeast Guiana Shield.

SAMPLING AND ANALYTICAL METHODS

To carry out this work, samples from previous studies (Paiva, 2016; acronym HP) and from the collection of the Research Group in Isotope Geology at UFPA (Acronym DAM) were used. Thus, four samples including leucogneisses and one amphibolite from the eastern portion of the TGC were selected (See Paiva, 2016 and Gorayeb et al., 2021 for sample location). Separation and concentration procedures for monazite and zircon included crushing/grinding, followed by granulometric, magnetic and gravimetric separation. The best grains, preferably euhedral, non-magnetic, transparent, without visible metamict features, fractures, porosity and/or inclusions, were hand-picked under a binocular microscope. Backscattered electron (BSE) images were obtained in scanning electron microscope (SEM) to assess internal structures and to select the sites in the crystals for in situ isotopic analyses. All these procedures were performed using at the laboratory facilities of the UFPA Geoscience Institute. LA-MC-ICP-MS monazite U-Pb analyses were carried out using a high resolution multi-collector Neptune Thermo Finnigan mass spectrometer coupled with a Nd:YAG LSX-213 G2 CETAC laser microprobe at the UFPA Isotope Geology laboratory (Pará-Iso). The analytical conditions, instrumental corrections, raw data reduction and age calculation are described in Ferreira (2022). LA-MC-ICP-MS zircon U-Pb dating of the amphibolite sample was carried at the Geochronological Laboratory of the Brasília University, using similar equipment to those of the Pará-Iso and following the procedures described in Buhn et al. (2009).

RESULTS

The samples of this study were petrographically classified as a garnet-biotite leucogneiss of monzogranitic composition (Sample HP-04), a garnet-biotite leucogneiss of syenogranitic composition (Sample HP-17), a neosome derived from a migmatitic leucogneiss (HP-09C) associated with felsic granulites and one biotite-clinopyroxene amphibolite which occurs as centimeter lenses in felsic granulites (DAM-05B sample). Metamorphic conditions are similar to those described by Gorayeb et al. (2021). All ages were calculated based on concordant analytical points (< 2% of discordance), with the exception of the age calculated for the sample HP-17 whose analyzes were discordant and a U-Pb upper intercept age was determined. Among the analyzed points, those that presented significant common Pb contribution were not included in the age calculations. As monazites commonly do not have significant contribution of common Pb, this criterion was used as a filter only for zircon analyses. U-Pb ages obtained on monazite and zircon grains are listed in Table 1.

Table 1- Summary of the LA-ICP-MS U-Pb ages obtained in this work for the samples of the Tartarugal Grande Complex

Litology	Sample	U-Pb assigned age (Ma)	Statistical parameters	Mineral
Neosome of migmatitic leucogneiss	HP-09C	$2056 \pm 5^*$	2σ ; n = 30; MSWD = 0.31	Monazite

Garnet-biotite leucogneiss	HP-17	2058 ± 19**	2σ; n = 51; MSWD = 0.64	Monazite
Garnet-biotite leucogneiss	HP-04	2096 ± 16 to 2056 ± 16***	2σ; n = 27	Monazite
Biotite-clinopyroxene amphibolite	DAM-05B	2069 ± 11*	2σ; n = 6; MSWD = 0.47	Zircon

*U-Pb Concordia Age, **Upper intercept age, ***²⁰⁷Pb/²⁰⁶Pb range dates.

TIMING CONSTRAINTS ON THE HIGH-GRADE METAMORPHISM OF THE TARTARUGAL GRANDE COMPLEX

Most of the previous isotopic studies on the metamorphic rocks of the TGC aimed to investigate the crystallization age of their magmatic protoliths. Furthermore, the available geochronological dataset is for felsic granulite and associated leucogneisses, but radiometric dating of the mafic lithologies is still lacking in the TGC. So far there have been few attempts to date the metamorphism recorded in the TGC: (i) Oliveira et al. (2008) determined Sm-Nd whole rock-garnet isochronous ages between 2037 ± 8 Ma and 1982 ± 3 Ma for felsic granulites and garnet leucogneisses; (ii) Enjolvy (2008) performed U-Pb LA-ICP-MS dating of a population of monazite from a garnet leucogneiss (from the same outcrop of sample HP-17), which provided a ²⁰⁷Pb/²⁰⁶Pb mean age of 2043 ± 8 Ma; and (iii) Gorayeb et al. (2021) that obtained a LA-ICP-MS U-Pb age of 2045 ± 14 Ma for three metamorphic zircons from an enderbite granulite.

The U-Pb dating of the monazites from sample HP09C yielded an age of 2056 ± 5 Ma for the formation of the neosome during anatexis. The monazites of the garnet-biotite leucogneiss (Sample HP-17) yielded a similar age of 2058 ± 19 Ma. These ages agree with the metamorphic ages determined in monazite and zircon by Enjolvy (2008) and Gorayeb et al. (2021) and with the age of emplacement of a charnockite body (Avelar, 2002). These results provide a robust dataset that indicates a metamorphic peak at 2.06-2.04 Ga.

The concordant ²⁰⁷Pb/²⁰⁶Pb dates of the monazites from the garnet-biotite leucogneiss (Sample HP-04) range from 2096 ± 16 Ma to 2056 ± 16 Ma. This complex distribution along the Concordia curve can be interpreted as the gradual resetting of the U-Pb system of the magmatic monazite grains formed in the leucogneiss protolith, during the metamorphic event. This hypothesis is consistent with the fact that the region was probably warmed from ~2.10 Ga to 2.08 Ga by the numerous granitic pluton intrusions surrounding the TGC (Bom Jesus and Porto Grande granites; Vianna et al., 2020, Batista, 2021) or within the TGC as Rhyacian protoliths of high-grade metamorphic rocks (Rosa-Costa et al. 2014, Gorayeb et al. 2021). Alternatively, the ~2.10-2.06 Ga timespan observed for the monazites from the HP-04 sample may represent the progressive growth of metamorphic monazites during a long-lived metamorphic process (30-40 Ma).

The 2069 ± 11 Ma zircon U-Pb age of the amphibolite (DAM-05B) is interpreted as the crystallization age of its mafic protolith. A crystallization age of 2.07 Ga is consistent with the interpretation by Rosa-Costa et al. (2014) and Gorayeb et al., (2021) in which the mafic rocks occur as small bodies of diabase tholeiitic dykes that have intruded the felsic granulite and paragneiss protoliths, for which the youngest crystallization age is 2.08 Ga. However, it cannot be ruled out that this age of 2.07 Ga may represent a metamorphic age by resetting the U-Pb system during the metamorphic peak.

The new U-Pb results on monazite and zircon and the previous geochronological data on rocks from the TGC and neighboring magmatic units indicate an evolution at the end of the Rhyacian and beginning of the Orosirian in the central region of Amapá marked by an intense magmatic episode between ~2.10 and 2.08 Ga. This magmatic episode triggered regional warming and was followed by a high temperature, intermediate pressure metamorphic event that affected both Archean ortho and paraderived rocks and Rhyacian granitoids. This episode, with a metamorphism peak around 2.06-2.04 Ga, produced granulitic rocks, local migmatization and the intrusion of charnockitic plutons. Metamorphic cooling occurred between ~2.04 and ~1.98 Ga until reaching a temperature below 300°C around 1.97 Ga (⁴⁰Ar-³⁹Ar biotite metamorphic cooling age; Enjolvy, 2008).

The ages between 2.06 and 2.04 Ga of the high-grade metamorphism in central Amapá confirm that the TGC is coeval with the ultra-high temperature (UHT) metamorphism of the Bakhuis granulitic belt in Suriname (2.09-2.03 Ga; De Roever et al., 2003, 2019, Klaver et al., 2015, 2016). Delor et al. (2003) proposed that late orogenic crustal stretching and prolonged sinistral shear during an oblique continental collision account for the structural framework of the granite-greenstone terranes of the Guiana Shield, limited by granulitic belts (Imataca Complex in NW Guiana Shield, Bakhuis granulitic belt and the TGC). The authors suggest that the UHT conditions and the P-T-t path of granulite metamorphism in the Bakhuis Belt were caused by mantle upwelling in a zone of maximum crustal thinning associated with vertical tectonics. De Roever et al. (2003) and Klaver et al. (2015) also suggested that crustal thinning and mantle perturbation provided the heat needed to achieve these metamorphic conditions. However, Klaver et al. (2015) proposed that asthenospheric upwelling would be related to subduction, with a change in direction and opening of a slab window. An alternative scenario involves slab break-off and rifting to explain mantle upwelling as a heat source (Kroonenberg et al. 2016). Recently Beunk et al. (2021) associated the UHT metamorphism with slab break-off and asthenospheric heat advection with exhumation of the subducting African plate.

The fact that the high-grade TGC metamorphism is coeval with the Bakhuis Belt UHT metamorphism does not imply that were generated by the same metamorphic processes. The TGC did not present a UHT paragenesis, however, the occurrence of amphibolites and mafic granulites in the TGC points to a contribution of the mantle as a source for heat flow. The collision of a Rhyacian long-lived continental magmatic arc and aggregation to the Archean block at around 2.11 Ga was proposed by Vianna et al. al. (2020). Slab break-off with asthenospheric advection would explain the high-grade metamorphic conditions of the TGC. However, a time interval of ~50 Ma between the end of subduction around ~2.11 Ga and the slab break-off appears to be too long. Thus, even if a slab break-off context cannot be ruled out, the proposal by Delor et al. (2003) seems more consistent to explain the formation of the TGC.

ACKNOWLEDGMENTS

This work was supported through the P1061B AMIRA PROJECT “South American Exploration Initiative Stage 2 (SAXI 2)-module 7A” and by the Conselho Nacional de Desenvolvimento Científico e Tecnológico (CNPq)/UNIVERSAL PROJECT (Grant No. 423625/2018-7). This contribution is part of the Master’s thesis of the third author (D.P.A.F.).

REFERENCES

- Avelar, V.G., 2002. Geocronologia Pb-Pb em zircão e Sm-Nd em rocha total da porção centro-norte do Estado do Amapá-Brasil: Implicações para a evolução geodinâmica do setor oriental do Escudo das Guianas (Ph.D. Dissertation). Federal University of Pará-Brazil, 213 p (in Portuguese).
- Batista, P.H.M. 2021. Geocronologia U-Pb e geoquímica isotópica Hf- Nd do granito Porto Grande, Centro-leste do Amapá (Final course work). Federal University of Pará-Brazil, 102 p (in Portuguese).
- Beunk, F.F., Roeveer, E.W.F., Yi K., Fraukje, M.B. 2021. Structural and tectonothermal evolution of the ultrahigh-temperature Bakhuis granulite belt, Guiana Shield, Surinam: Palaeoproterozoic to recente. *Geoscience Frontiers* 12:677-692.
- Bühn, B., Pimentel, M.M., Matteini, M., Dantas, E.L. 2009. High spatial resolution analysis of Pb and U isotopes for geochronology by laser ablation multi-collector inductively coupled plasma spectrometry (LA-MC-ICP-MS). *An. Acad. Bras. Cienc.* 81: 99–114.
- De Roeveer, E.W.F., Lafon, J.M., Delor, C., Cocherie, A., Rossi, P., Guerrot, C., Potrel, A. 2003. The Bakhuis ultrahigh-temperature granulite belt (Suriname): I- Petrological and geochronological evidence for a counterclockwise P-T path at 2.07 and 2.05 Ga. *Géologie de la France* 2:175–206.
- De Roeveer, E.W.F., Beunk, F.F., Yi K., Groot, K., Klaver, M., Nanne, J.A.M., Steeg, W., Thijssen, A.C.D., Uunk, B., Vos, H., Davies, G.R., Brouwer, F.M. 2019. The Bakhuis granulite belt in W Suriname, its development and exhumation. In: 11th

- Guiana geol conference: the tectonics and resource potential of NE south America, Paramaribo. Geol. Mijnbouwk. Dienst Suriname Meded. 29:53–58
- Delor, C., Lahondère, D., Egal, E., Lafon, J.M., Cocherie, A., Guerrot, C., Rossi, P., Truffert, C., Theveniaut, H., Phillips, D., Avelar, V.G. 2003. Transamazonian Crustal Growth and Reworking as Revealed by the 1:500.000 - Scale Geological Map of French Guiana, second ed., 2-3-4. Géologie de la France - Special Guiana Shield. BRGM-SGF Editor, pp. 5-58.
- Enjolvy, R. 2008. Processus d'accrétion crustale et régimes thermiques dans le bouclier des Guyanes: signatures géochimiques et thermochronologiques au transamazonien (2250-1950 Ma) (Ph.D. Dissertation). University of Montpellier II-France, 305 p.
- Ferreira, D.P.A. 2022. Implantação da metodologia U-Pb em monazita por LA-ICP- MS no Laboratório de Geologia Isotópica da UFPA (Pará-Iso): aplicação em rochas de alto grau metamórfico da região central do Amapá, Sudeste do Escudo das Guianas (Master's Thesis). Federal University of Pará-Brazil, 121 p (in Portuguese).
- Gorayeb, P.S.S., Paiva, H.P.S., Lafon, J.M., Rosa-Costa, L.T., Dantas, E.L. 2021. Petrology and crustal evolution of the Tartarugal Grande Granulitic Complex - Northeastern Amazonian Craton. *Journal of South American Earth Sciences* 112: 103549.
- Klaver, M., Roever, E.W.F., Nanne, J.A.M., Mason, P.R.D., Davies, G.R. 2015. Charnockites and UHT metamorphism in the Bakhuis Granulite Belt, western Suriname: evidence for two separate UHT events. *Precambrian Research* 262:1–19.
- Klaver, M., Roever, E.W.F., Thijssen, A.C.D., Bleeker, W., Soderlund, U., Chamberlain, K., Ernst, R., Berndt, J., Zeh, A. 2016. Mafic magmatism in the Bakhuis Granulite Belt (western Suriname): relationship with charnockite magmatism and UHT metamorphism. *GFF* 138:203-218.
- Kroonenberg, S.B., De Roever, E.W.F., Fraga, L.M., Reis, N.J., Faraco, T., Lafon, J.-M., Cordani, U., Wong, T.E. 2016. Paleoproterozoic evolution of the Guiana Shield in Suriname: a revised model. *Netherlands Journal of Geosciences* 95:491-522.
- Lafon, J.M., Avelar, V.G., Rossi, P., Delor, C., Guerrot, C., Pidgeon, R.T. 2000. Geochronological evidence for reworked neoproterozoic crust during Transamazonian orogeny (2.1 Ga) in southeastern Guiana shield. In: *International Geological Congress*, vol. 31. CD-ROM, Rio de Janeiro.
- Milhomem Neto, J.M., Lafon, J.M. 2019. Zircon U-Pb and Lu-Hf isotope constraints on Archean crustal evolution in Southeastern Guyana Shield. *Geoscience Frontiers* 10: 1477–1506.
- Milhomem Neto, J.M., Lafon, J.M. 2020. Crustal growth and reworking of Archean crust within the Rhyacian domains of the southeastern Guiana Shield, Brazil: Evidence from zircon U–Pb–Hf and whole-rock Sm–Nd geochronology. *Journal of South American Earth Sciences* 103: 102740.
- Oliveira, E.C., Lafon, J.M., Gioia, S.M.C.L., Pimentel, M.M. 2008. Datação Sm-Nd em rocha total e granada do metamorfismo granulítico da região de Tartarugal Grande, Amapá Central. *Revista Brasileira de Geociências* 38: 116-129 (in Portuguese).
- Paiva, H.S. 2016. Caracterização petrográfica, geoquímica e geocronológica U-Pb das rochas de alto grau metamórfico do Complexo Tartarugal Grande, Sudeste do Escudo das Guianas, Amapá (Master's Thesis). Federal University of Pará-Brazil, 89p (in Portuguese).
- Rosa-Costa, L.T., Lafon, J.M., Delor, C. 2006. Zircon geochronology and Sm-Nd isotopic study: further constraints for the geodynamical evolution during Archean and Paleoproterozoic in the Southeast of Guiana Shield, north of Brazil. *Gondwana Research* 10: 277-300.
- Rosa-Costa, L.T., Chaves, C.L., Klein, E.L. 2014. Geologia e recursos minerais da Folha Rio Araguari e NA.22-Y-B, Estado do Amapá, Escala 1:250.000. CPRM, Belém, 159p (in Portuguese).
- Rubatto, D., Williams, I.S., Buick, I.S. 2001. Zircon and monazite response to prograde metamorphism in the Reynolds Range, central Australia. *Contributions to Mineralogy and Petrology* 140(4): 458–468.
- Scarpelli, W., 1969. Preliminary geological mapping of the Falsino River, Amapá. Brazil. *Verh. Ned. Geol. Mijnbouwkundig.* 27: 125–130.
- Vianna, S.Q., Lafon, J.M., Milhomem Neto, J.M., Silva, D.P.B., Barros, C.E.M. 2020. U-Pb geochronology, Nd-Hf isotopes, and geochemistry of rhyacian granitoids from the Paleoproterozoic Lourenço domain (Brazil), southeastern Guiana shield. *Journal of South American Earth Sciences* 104: 102937.

Application of Trace-Element Indicators Cu and Au Metallogenic Fertility to Paleoproterozoic Granitoids and Zircons in Guyana (Abstract only, no presentation)

Robert Loucks
School of Earth Sciences
Centre for Exploration Targeting, CET
UWA, 35 Stirling Highway
Crawley, Perth, WA 6009, Australia
Robert.Loucks@uwa.edu.au

Nicolas Thébaud
School of Earth Sciences
Centre for Exploration Targeting, CET
UWA, 35 Stirling Highway
Crawley, Perth, WA 6009, Australia
Nicolas.Thebaud@uwa.edu.au

SUMMARY

If Paleoproterozoic granitoid rocks and andesite-dacite-rhyolite volcanic rocks in the Guyana Shield were produced as differentiation products of juvenile mafic magmas from the mantle wedge above subduction zones, we anticipate that the whole-rock trace-element indicators of magmatic copper fertility (Sr/Y , $(Eu/Eu^*)/Yb$, V/Sc and trace-element indicators of magmatic gold fertility (Ba/Zr , Nb/Y , Th/Yb) that are successful discriminants of ore-productive intrusions in Phanerozoic subduction-related igneous suites should perform as well on early Proterozoic igneous suites. We describe the derivation and demonstrate the success of these whole-rock ratios and zircon trace-element ratios— $Ce/v(UxTi)$, $(Ce/Nd)/Y$, and $(Eu/Eu^*)/Yb$ —in discriminating Phanerozoic copper-ore-forming and gold-ore-forming magmas at convergent plate margins. We describe the results of these tests on Paleoproterozoic igneous suites in Guyana and offer preliminary interpretations of tectono-magmatic processes that produced these suites and indications of their potential for discovery of magmatic-hydrothermal ore deposits of copper and/or gold, with reference to penecontemporaneous ore-productive igneous suites in the conjugate West African Craton.

Age constraints on Early Proterozoic sedimentation during Transamazonian continental convergence in Suriname

Paul R.D. Mason

*Department Earth
Sciences
Utrecht University*

p.mason@uu.nl

**Manfred J. van
Bergen**

*Department Earth
Sciences
Utrecht University*

m.j.vanbergen@uu.nl

Leo M. Kriegsman

*Department Earth
Sciences
Utrecht University &
Naturalis Leiden*

*leo.kriegsman@natur
alis.nl*

**Salomon
Kroonenberg**

*Anton de Kom
University of
Suriname*

*salomonkroonenbe
rg@gmail.com*

SUMMARY

Detrital sedimentation marks the waning stages of Transamazonian mountain building in the Marowijne Greenstone Belt, but it remains unclear how the main stratigraphic divisions of the Armina and Rosebel Formations in Suriname are related to one another. Regional stratigraphic correlations remain challenging. Here we reassess the minimum and maximum ages of sedimentation in the Armina and Rosebel formations through newly obtained U-Pb zircon ages determined by laser ablation ICP-MS for selected greenstone belt sediments and associated granitoids. Our data indicate overlapping ages between the two formations, within current external measurement uncertainties, and a largely common source region for detrital zircons. Maximum deposition ages are ca. 2.09 to 2.07 Ga for both the Armina and Rosebel formations with a minimum deposition of ca. 2.07-2.05 Ga. This challenges a chronostratigraphic separation in Suriname and underscores the relevance of improving tectonostratigraphy across the region.

Key words: Lithostratigraphy, Basin Formation, U-Pb geochronology, Guiana Shield

The Paleoproterozoic Armina and Rosebel Formations, exposed in the north-eastern part of the Marowijne greenstone belt in Suriname and their equivalents in neighbouring French Guiana, are prominent sequences of detrital sediments marking the waning stages of Transamazonian mountain building in this sector of the Guiana Shield (Bosma et al., 1983; Bosma et al., 1984; Milési et al., 1995; Naipal & Kroonenberg, 2016; Kroonenberg et al., 2016). The Armina Fm is largely composed of low-grade metamorphic greywackes and pelitic sediments in alternating sequences interpreted as turbidite deposits in a deep marine environment. The Rosebel Fm consists of meta-arenites and meta-conglomerates with typical signatures of a fluvial terrestrial to shallow marine environment. Both formations unconformably overlie predominantly volcanic rocks of the Paramaka Formation. Although the Rosebel Fm is generally considered to be younger than the Armina Fm, their mutual stratigraphic relationship is poorly constrained. Daoust (2016) proposed that both were deposited in a single basin, and attributed their lithological differences to a lateral facies transition. Age constraints on basin formation and filling are highly relevant not only for the geodynamic reconstruction but also for our understanding of local ore forming processes, since Armina and Rosebel metasediments host important primary gold deposits. Nonetheless, available geochronological data are limited. Both formations must at least be younger than ca. 2.16-2.14 Ga, according to age dates for the Paramaka Fm in French Guiana (Delor et al., 2003).

We document new results from LA-ICP-MS dating of detrital zircons from metasediments and igneous zircons of granitoids in an attempt to bracket the deposition interval in Suriname more precisely. Samples were taken from some 15 locations in a W-E trending strip roughly between the Saramacca River and the Marowijne River along the border with French Guiana. We then compared our results against the available literature data for Suriname and French Guiana (Vanderhaeghe et al., 1998; Daoust, 2016; Kroonenberg et al., 2016). The ages of detrital zircons largely coincide with

those of the Paramaka volcanics and TTG intrusions, and include Archean populations similar to those discovered earlier. When combining the youngest ages with existing data (Daoust, 2016) we infer maximum deposition ages of ca. 2.09 and 2.07 Ga for the Armina and Rosebel Fm, respectively. Preliminary intrusion ages estimated for six granitoid bodies in this region range between 2.17 and ca. 2.05 Ga, indicating that some of the granitoids were present before the onset of sedimentation and may have acted as a source of detrital zircons. The youngest granites were probably emplaced around 2.07-2.05 Ga, which can be taken as minimum deposition age of the Armina sediments provided that the surrounding envelopes (Taffra Fm) are their contact-metamorphic equivalents.

Our findings suggest that deposition ages of the Armina and Rosebel sediments largely overlap within analytical error, lending support to arguments against a stringent chronostratigraphic separation in Suriname. The roughly similar timing inferred for the deposition of the Upper Detrital Unit (equivalent to the Rosebel Fm) in French Guiana (e.g., Delor et al., 2003) confirms that basin formation and filling was as a regional-scale feature along the entire northern boundary of the north-eastern Guiana Shield, presumably in response to (oblique) collision of the West African and South American continental blocks. The intrusion ages of granitoids in this part of the Marowijne Greenstone Belt point to protracted magmatic activity accompanying basin evolution and subsequent tectonometamorphism of the sediment sequences around the North Suriname Shear Zone.

ACKNOWLEDGEMENTS

Fieldwork activities were supported by the Dr Schürmann Foundation. Samples were provided by the Geological Survey of Suriname and Naturalis Biodiversity Center, Leiden, The Netherlands. This research has benefitted from discussions with researchers from the South American Exploration Initiative (SAXI).

REFERENCES

- Bosma, W., Kroonenberg, S.B., Maas, K. & De Roeve, E.W.F. (1983). Igneous and metamorphic complexes of the Guiana shield in Suriname. *Geologie en Mijnbouw*, 62, 241–254.
- Bosma, W., Kroonenberg, S.B., van Lissa, R., Maas, K. & De Roeve, E.W.F. (1984). Explanation to the Geological map of Suriname 1:500,000. *Mededelingen Geologisch Mijnbouwkundige Dienst van Suriname*, 27, 31–82.
- Daoust, C. (2016). Caractérisation stratigraphique, structurale et géochimique du district minéralisé de Rosebel (Suriname) dans le cadre de l'évolution géodynamique du Bouclier Guyanais. Thèse Université du Québec à Montréal, Canada, 330 pp.
- Delor, C., Egal, E., Lafon, J.M., Cocherie, A., Guerrot, C., Rossi, P., Truffert, C., Théveniaut, H., Phillips, D. & Avelar, V.G. (2003). Transamazonian crustal growth and reworking as revealed by the 1:500,000-Scale geological map of French Guiana (2nd edition), *Géologie de la France 2-3-4*, 5-57.
- Kroonenberg, S.B., de Roeve, E.W.F., Fraga, L.M., Reis, N.J., Faraco, T., Lafon, J.M., Cordani, U. & Wong, T.H. (2016). Paleoproterozoic evolution of the Guiana Shield in Suriname: A revised model. *Netherlands Journal of Geoscience*, 95, 491-522.
- Milési, J-P., Egal, E., Ledru, P., Vernhet, Y., & Thiéblemont, D., Cocherie, A., Tegye, M., Martel-Jantin, B. & Lagny, Ph. (1995). Les minéralisations du Nord de la Guyane française dans leur cadre géologique. *Chron. Rech., Min.*, n° 518, 5-58.
- Naipal, R., & Kroonenberg, S. (2016). Provenance signals in metaturbidites of the Paleoproterozoic greenstone belt of the Guiana Shield in Suriname. *Netherlands Journal of Geosciences*, 95(4), 467-489
- Vanderhaeghe, O., Ledru, P., Thiéblemont, D., Egal, E., Cocherie, A., Tegye, M., & Milési, J. P. (1998). Contrasting mechanism of crustal growth: geodynamic evolution of the Paleoproterozoic granite–greenstone belts of French Guiana. *Precambrian Research*, 92(2), 165-193.

The Roboré microcontinent, SW Amazonian Craton: new insights on the Orosirian-Ectasian crustal evolution from U-Pb geochronology.

Ramiro Matos

*Instituto de Investigaciones Geológicas y del Medio Ambiente, Universidad Mayor de San Andrés
Calle 27, Cota Cota, La Paz, Bolivia rmatoss@yahoo.com*

New U-Pb zircon ages and Nd and Hf zircon constraints for rocks of the Roboré microcontinent, the Eastern Precambrian Shield of Bolivia, in the SW of the Amazonian Craton. This microcontinent is subdivided into the San Diablo and Paraguá terranes. Zircon U-Pb datings determine that the continental crust underwent a long-lived tectonic-magmatic history, during three successive events: 1941-1849 Ma, 1690-1610 Ma, and 1430-1340 Ma. The Roboré microcontinent experienced crustal shortening, magmatism, and overprints due to the Sunsás/Grenville (1100-1000 Ma) orogeny that marks the Amazonia-eastern Laurentia collage. The oldest San Diablo terrane comprises amphibolite facies gneissic rocks (1941 ± 40 Ma), which were intruded by plutonic bodies of 1874 and 1849 Ma. The country rocks yield Sm-Nd T_{DM} ages and ϵ_{Ndt} values from 1.96 to 2.29 Ga, and +1.76 to -2.73 respectively, suggestive of derivation from short-lived protoliths. The Correraca intrusion is as young as 1874-1862 Ma with zircon Hf model ages of 2.68 Ga and 2.29 Ga with ϵ_{Hft} values varying from -4.63 to +2.76. The isotopic signatures for the San Diablo crust are consistent with magma genesis in a juvenile-like accretionary arc, have a calc-alkaline character, and show a subduction-related tectonic. The Paraguá terrane contains a granulitic crust dated to 1820 Ma. The available Sm-Nd T_{DM} model ages spread from ca. 1.7 to ca. 2.2 Ga and ϵ_{Ndt} values range from +3.0 to -2.9, with Paleoproterozoic protoliths. The basement rocks are crosscut by the Yarituses Suite (1683-1610 Ma) located to the west, which includes the following granites: La Cruz, Refugio, San Pablo, San Miguel, and Rosario. These granites exhibit Sm-Nd T_{DM} model ages of 1.8 to 2.5 Ga and ϵ_{Ndt} of +4.06 to -3.8. These units characterize the Suruquiso accretionary orogeny characterized here that coalesced the San Diablo and Paraguá terranes. Eventually, the Paraguá crust is crosscut by the San Ignacio granitoids, known as the Pensamiento Granitoid Complex (1440-1270 Ma). These rocks show Sm-Nd T_{DM} model ages between 1.6 and 2.4 Ga, and predominantly crustal-like isotopic signatures of +5.2 to -4.0 akin to a convergent arc setting. The granitoids are products of the Alto Guaporé orogeny in the Brazilian counterpart, distinguished by an accretionary phase (ca. 1440 Ma) and a collisional one (ca. 1330 Ma). The San Ramón and Coronación granodiorites (1429-1423 Ma) are pre- to syn-kinematic to the collisional phase, whereas the La Junta (ca. 1380 ± 17 Ma) and San Martín (1409 ± 17 Ma) granites are syn-to late kinematic. The Diamantina granite (1357 ± 19 Ma) is coeval with the collisional phase, while the San Andrés granite (1289-1275 Ma) is a post-kinematic pluton. The Pensamiento Granitoid Complex documents the Roboré microcontinent collision against the active margin of the proto-Azoniamia at the Ectasian. The Microcontinent ends with the Sunsás/Grenville collision leading to the tectonic stability of the Amazonian Craton.

Plutonic Rocks of the Karouni Basin: Characteristics and Significance to Mineralization

Denbre McGarrell, Keshana Higgins, and Giovanna Neira

The Karouni basin is a 3600 km² volcano-sedimentary basin comprised of up to 50% intrusive rocks of probable favorable mineralization age (e.g 2097Ma Karouni Granite; Tedeschi et al. 2020). In general, plutonic rocks in greenstone terranes are derived from the melting of the greenstone rocks themselves and are commonly denominated TTG's (Glikson and Sheraton, 1972; Jahn et al., 1981; Martin, 1987; Martin, 1994). Such plutons provide rheologic contrast that favors the development of high strain within the adjacent volcanosedimentary rocks, contributing to orogenic gold mineralization. This work intends to analyze and compare multiple characteristics of the plutons within the basin and ultimately contrast them with the intrusive rocks identified at the 800 Koz Karouni mine (Tedeschi M., et al.2018a, 2018b, 2020) to better refine the magmatic history of the basin, and guide the search of certain intrusive rocks to discover Au in the project area.

Previous work indicated that major deformation corridors in the Karouni basin registered E-W sinistral kinematics (Voicu et al., 1999) and a later NW-SE dextral-strike slip movement along the MKSZ structural corridors (Tedeschi et al 2018a). Felsic igneous intrusions of granodiorite and quartz monzonite composition are elongated in a generally NW-SE direction. Smaller (2088Ma) rhyolite porphyry dikes strike E-W to N-S. Andesite porphyry dikes oriented NW-SE prevail in the main Karouni corridor (Tedeschi M., et al.2018a, 2020). The southwestern margin of the Karouni basin is bounded by the MKSZ, which is inferred to have dextral strike-slip by extrapolation from kinematics resolved at Karouni (Tedeschi et al 2018a).

This study suggests that the southern Karouni basin contains igneous intrusive rocks that may have been emplaced along the structural corridors, at lithostructural contacts, major structural breaks/jogs and shear zones within the basin. The morphologies of these rigid bodies vary significantly, ranging from large sheets to oblong stocks or dikes that may either host mineralization, crosscut mineralized structures, or postdate mineralization. Plutonic rocks mapped in the basin are presented below in chronological order from older (deformed) to younger (underformed); however, exact age dates are pending at the time of writing.

Pre-syn tectonic intrusive bodies vary widely in terms of size, composition, and morphology. The largest of these is the Kuribrong intrusive body (KIB), a 24km by 6km syn- to pre deformation intermediate composition intrusive 6 km south of the Karouni granite. The KIB is an elongated NW-oriented pluton that is weakly to moderately strained and is comprised of 35-40% ferromagnesian minerals (Bt>Hbl), 10% quartz, and 45-50% cream-colored feldspars +/-1% disseminated pyrite after magnetite. It is locally cut by quartz (+/-epidote, carbonate, tourmaline) veinlets. Rare tourmalinization is observed in the groundmass. In addition to the KIB several newly mapped, small-volume weathered diorite bodies, which are generally oblong in shape and <2-3 km in width, penetrate the basin stratigraphy near the interpreted MKSZ. Most of the diorites are more finely crystalline bodies that are moderately to highly strained with stretched mineral grains in a strongly to moderately chloritized groundmass.

Post-tectonic granitoid bodies are coarsely crystalline (0.2 to 1.5cm crystals), have a phaneritic texture, and consist of ~15-20% anhedral quartz grains, 30-35% ferromagnesian (Bt, Hbl, Mt) and 40-45% feldspar, with localized basalt xenoliths (cm-scale, <1%). In the Makapa area, the largest and most significant post-tectonic intrusion is the multiphase Apanachi granite (1955Ma, Tedeschi M., et al., 2020). A second coarse intrusive body, which exhibits no strain, has been mapped 3 km W-SW of the Apanachi granite.

There are several differences in the nature of plutonic activity between the southern Karouni basin and the northern Karouni basin, where the Karouni deposit (800Koz) is located. The small-volume, elongate, foliated intermediate composition intrusives described above, which appear to be located primarily adjacent to the interpreted MKSZ and which may be intruded along its length, are visually similar to those described as intruding along the Smarts-Hicks, Goldstar, and Dominica shear zones to the north (Tedeschi et al, 2018a). Similarly, the Kuribrong Intrusive Body, located 6 km to the south of the Karouni mine, is visually similar to the Karouni granite in texture, size, morphology, and composition and exhibits similar hornfelses halos and deformation textures along its southern margin. However, the high MgO basalts and high TiO₂ dolerites described by Tedeschi (2018) as hosting the bulk of laminated V2a veins and sheeted V2b veins at Smarts have not been identified in the southern Karouni basin to date. Porphyritic felsic dikes and plutons, which host the highest grade and most coherent orebodies at Hicks, have also not been identified.

Hydrothermal desilicification, alkali leaching and oxidation in metapelites of the Rosebel gold district in the Paleoproterozoic Marowijne Greenstone Belt, Suriname

Renoesha Naipal¹, Salomon Kroonenberg^{1,2}, Leo Kriegsman^{3,4}, Manfred van Bergen³, Paul Mason³

¹ Department of Geosciences, Anton de Kom University of Suriname; ² Delft University of Technology, the Netherlands, ³ Utrecht University ⁴. Naturalis Biodiversity Center, Leiden.

The fluvial Rosebel Formation is the uppermost, epicontinental unit in the Marowijne Greenstone belt of Suriname (2.26-2.06 Ga). It consists of a polygenetic basal conglomerate, followed by a thick sequence dominated by cross-bedded arenites, with a characteristic lag deposit of heavy minerals at the base of the troughs, mainly made up of magnetite. The rocks have been metamorphosed to greenschist facies. Gold in the Rosebel gold district is mainly associated with quartz and quartz-carbonate veins, which cut across deformed sequences of the unit. The ubiquitous presence of sulfides in the gold-bearing veins suggests that most mineralizing fluids had a relatively reduced signature. Here, we document a contrasting case of oxidative hydrothermal alteration in the Rosebel area, which was accompanied by strong desilicification and alkali leaching.

Seven diamond drill holes were obtained by the Geological and Mining Service of Suriname in 1957 to follow up on an earlier report of copper mineralization in the Rosebel area. While no copper was found, one of the diamond drill cores sampled an unusual, very fine-grained series of orange chloritic rocks with epidote-piemontite-hematite veins, and without any quartz or feldspar. The total length drilled through this unit was only 7 meters, corresponding to about 3 m of stratigraphic thickness in view of the steep dip of the layers. Six core segments were studied in detail in this study. The uppermost part was found to consist of a very finely-laminated, dark green chlorite rock containing lighter laminae with fine-grained, zoned epidote and piemontite and small hematite flakes. Some laminae are rich in c. 50 μm -long zircon crystals, rutile and leucoxene. Lower in the stratigraphy, the lamination becomes slightly coarser, and the amount of epidote gradually increases at the expense of chlorite. The sequence is traversed by folded veins of coarse zoned epidote passing to piemontite, and specular hematite. One sample consists of orange-coloured very finely-laminated ferrichlorite.

Major elements (XRF) show very low Si contents, high Al and Mg and a virtual absence of alkali metals. The samples show increasing Si, Al, Ca, Mn and decreasing Ti, Fe, Mg with depth, probably reflecting the increase of epidote and piemontite at the expense of chlorite, hematite, and rutile. Trace element concentrations (LA-ICPMS) show a conspicuous decrease in Ti, Cr, Nb, Ta and Zr from top to bottom. Chondrite-normalised REE profiles shows a steep negative slope for the LREE, a pronounced negative Eu anomaly and an almost flat HREE profile. Textural evidence and semi-quantitative SEM analyses point to the presence of multiple generations of chlorite with variable Fe/(Mg+Fe) ratios within individual samples. XRD results on the orange variety are consistent with ferrian clinocllore. Zircon ages (LA-ICPMS), ranging between 2.03 ± 0.02 and 3.16 ± 0.02 Ga in different clusters, are typical for the detrital population previously identified in the Rosebel Formation.

The absence of felsic minerals, together with the low SiO_2 and high MgO, Cr and Ni contents suggest that the rocks represent fine-grained mafic volcanoclastics, but the total absence of alkali metals, elevated Al_2O_3 , signatures of immobile trace elements and the detrital nature of the zircons do not support such an origin. Relative to Post Archean Average Shale or typical mudstones from the Rosebel Formation, the rocks are considerably depleted in Si, K, Na and P, and enriched in Fe, Mn, Mg and Ca. Considering all the observations combined, the most plausible explanation is that these rocks represent relatively common Rosebel shales, but strongly altered by hydrothermal fluids. This would have led to strong desilicification and leaching of alkalis. Hematite, ferrichlorite and epidote are minerals incorporating Fe^{3+} , and piemontite contains Mn^{3+} , indicating an oxidizing nature for the hydrothermal fluids that altered the original shales. Alteration took place before or during greenschist facies metamorphism, in view of the composition of the veins and the preferred lepidoblastic orientation of the chlorites. Further investigations will be targeted to reveal if this type of hydrothermal activity has implications for the gold mineralization.

The Bemau Ultramafic Complex and the Borgia Hill Chromite Complex: Two contrasting ultramafic complexes in the Paleoproterozoic basement of Suriname

Renoesha Naipal

Department of Geosciences,
Anton de Kom University of
Suriname; also at Faculty
of Geosciences, Utrecht
University

Leysweg 86, Paramaribo,
Suriname

renoesha.naipal@uvs.edu

Salomon Kroonenberg

Department of Geosciences,
Anton de Kom University of
Suriname; also at Delft University
of Technology

Leysweg 86, Paramaribo,
Suriname

salomonkroonenberg@gmail.com

Paul R. D. Mason

Faculty of Geosciences, Utrecht
University

Vening Meinesz
building A,
Princetonlaan 8a,
3584 CB Utrecht,
Netherlands

p.mason@uu.nl

Leo M. Kriegsman

Faculty of Geosciences,
Utrecht University; also at
Department of Research &
Education, Naturalis
Biodiversity Center

Darwinweg 2, 2333 CR
Leiden

leo.kriegsman@naturalis.nl

SUMMARY

The Bemau Ultramafic Complex (BUC) along the Saramacca River forms part of the Paleoproterozoic Marowijne Greenstone Belt of northeastern Suriname and is closely associated with the Paramaka Formation metabasalts which form the base of the volcanosedimentary sequence of the greenstone belt. The Borgia Hill Chromite Complex (BHCC), discovered in 1963 by Bisschops (1966), crops out in an isolated greenstone enclave in granitoid terrain in central Suriname. Although both complexes consist of plutonic cumulates and associated altered ultramafic schists, we show here that their origin differs on the basis of their rock associations, mineral assemblages, alteration texture, and geochemistry.

The BUC cumulates consist of partly serpentinized dunites, wehrlites, clinopyroxenites, websterites and gabbros (Veenstra, 1983; Naipal et al., 2019; Teuling, 2019). The associated ultramafic schists, mainly talc-tremolite-chlorite-carbonate schists, show textures indicative of a volcanic origin. The main spinel-group mineral is magnetite, mostly of secondary origin. The ultramafic schists associated with the BHCC cumulate chromite bodies are talc-tremolite schists, chlorite schists, tremolite-rich rocks, and anthophyllite-rich rocks. In contrast to the BUC ultramafic schists, they show relict cumulate textures, suggesting they represent altered plutonic cumulate rocks.

Geochemically the metavolcanic ultramafic schists from BUC show significantly lower SiO₂ (46 wt%) and higher MgO (31 wt%) values than the metaplutonic ones from the BHCC (54 wt% SiO₂; 28 wt% MgO). The trace elements of the BUC ultramafic schists show flat primitive mantle-normalized patterns, whereas those of the BHCC have more enriched and variable values. Geochemical affinity based on Nb/Th vs Zr/Nb ratios (Condie, 2003) suggest an arc-related affinity for the cumulates from both the BUC and BHCC. The Incompatible element diagrams after Condie (2003) indicate that the BUC ultramafic schists were derived from a primitive mantle source and are probably of komatiitic origin.

Key words: ultramafic schist, cumulates, altered, greenstone belt, Guiana Shield, chromite, komatiitic

REFERENCES

- Bisschops, J. H. (1966). *An occurrence of chromite near Emma Range, Suriname*, Geological and Mining Service, Surinam, p. 11–21.
- Condie, K. C. (2003). *Incompatible element ratios in oceanic basalts and komatiites: Tracking deep mantle sources and continental growth rates with time*. *Geochem. Geophys. Geosyst.* 4 (1), 1005.
- Naipal, R., Kroonenberg, S. B., & Mason, P. R. D. (2019). *Ultramafic Rocks of the Paleoproterozoic Greenstone Belt in the Guiana Shield of Suriname, and Their Mineral Potential*. Conference: 11th Inter Guiana Geological Conference, Paramaribo, Suriname: Mededeling Geologisch Mijnbouwkundige Dienst Suriname 29, 143–146.
- Teuling, F. S. R. (2019). *Petrogenesis of the Bemau Ultramafic Complex, Guiana Shield, Suriname*. MSc Thesis, Utrecht University-Department of Geosciences, pp. 143.
- Veenstra, E. (1983). *Petrology and Geochemistry of Sheet Ston Broeke, Sheet 30, Suriname*. In *Mededelingen van de G.M.D. Suriname* 26.

Stratigraphy and Structure of the Makapa Project, Guyana

Kumar Persaud

Barrick Guyana Incorporated

Summary

The Makapa-Kuribrong Shear Zone (MKSZ) is interpreted as a regional scale lithospheric structure of the Guiana Shield. This NW-SE trending structure is proximal to several gold deposits within Guyana-- the largest being Omai (3.5 Moz). The Makapa project area is underlain by a ~60km segment of the MKSZ north of the Kuribrong river and ~35km west of the Omai deposit. The project area is also located ~15km southwest of the Karouni mine, where the geologic framework is described in detail by (Tedeschi (2018)). The geologic framework established from new surface mapping and drilling indicates that the district is underlain by mafic to intermediate volcanics, volcanoclastics, interbedded sandstone & siltstone sequences altogether punctuated by a series of pre-/syn- to post deformation felsic to intermediate plutons and plugs (Fig 1). Supracrustals are penetratively foliated with multiple higher strain zones possibly related to the MKSZ. Megascopic folding with an interpreted wavelength of 2- 6km (Fig 5, 6 and 7) prevails in the vicinity of the MKSZ. Rheologically contrasting lithotypes are better hosts to gold-bearing hydrothermal fluids nearby the MKSZ.

Lithostratigraphy

Lithotypes of the Makapa project area comprise three broad components: Volcanic, Metasedimentary, and Intrusive. Older rocks would be fine grained mafic volcanic rocks with up to 30-40% ferromagnesian phenocrysts (olivine & pyroxene) and up to 1-3% magnetite. Modal composition ranges from fine-grained, aphanitic, rich in ferromagnesian to weakly felspathic (up to 15% plagioclase and <10% silica). Fig 2.

Volcanism evolved to more intermediate volcanic rocks (andesite) which generally have a fine-grained ground mass with ~20% quartz phenocrysts, along with lesser amounts of magnetite (~1%). Several facies have been recognized from fine grained, aphanitic, dark to trachy andesite with larger porphyritic plagioclase. (Fig 2). This unit is intercalated with volcanoclastic rocks containing euhedral to sub-rounded clasts of mafic to intermediate volcanic composition that range from millimetric scale to >5cm in diameter. These clasts are floating in a siliceous crystalline matrix and their composition indicates that this unit is of relative age as the mafic/intermediate package with chlorite phenocrysts. Fig 2. Sediments define a thick package of schistose-- 2-6km 'swaths' of interbedded sandstone and siltstone. Sandstones are more abundant to the NW where beds are up to 3m thick. Fig 3. This sedimentary unit is bounded by a high strain zone (interpreted as the MKSZ) and grades from thicker more siliceous sandstone beds to finer grained, well bedded siltstone with occasional detrital magnetite observed with sericite alteration. In addition to this extensive sedimentary package, discrete sequences of well bedded, intercalated siltstone and mudstone, included thin carbonaceous siltstones, have been observed. Fig 3.

A number of large felsic to intermediate plutons (from 5km in width to 25 km in length) intrude the supracrustal sequence. Larger bodies include the NW-trending Karouni Granite (2097 Ma) (Tedeschi et al. 2018), the round shaped Apanachi Granite (1955 Ma) and the Kuribrong Intrusive Body (KIB; pending U-Pb analysis). Smaller intrusive bodies also seem to be stitching the MKSZ. The larger pre-syn deformation intrusives have been defined in detail at the Karouni camp and are suite of strongly foliated quartz-monzonite plutons, weakly foliated to unfoliated granodiorite and granite. These are coarsely crystalline with 15-30% ferromagnesian, 20-25% plagioclase and 10-20% quartz. (Tedeschi et al. 2018) Strain in these intrusives manifests as alignment of ferromagnesian minerals and "cloudy" felspars. Fig 4.

The youngest rocks of the region consist of swarms of dolerite dikes that may be part of the Avanavero LIP. These younger dikes cut across the stratigraphy and trend dominantly NE. (Bardoux et al. 2017; see Fig 1).

Makapa Stratigraphic Column

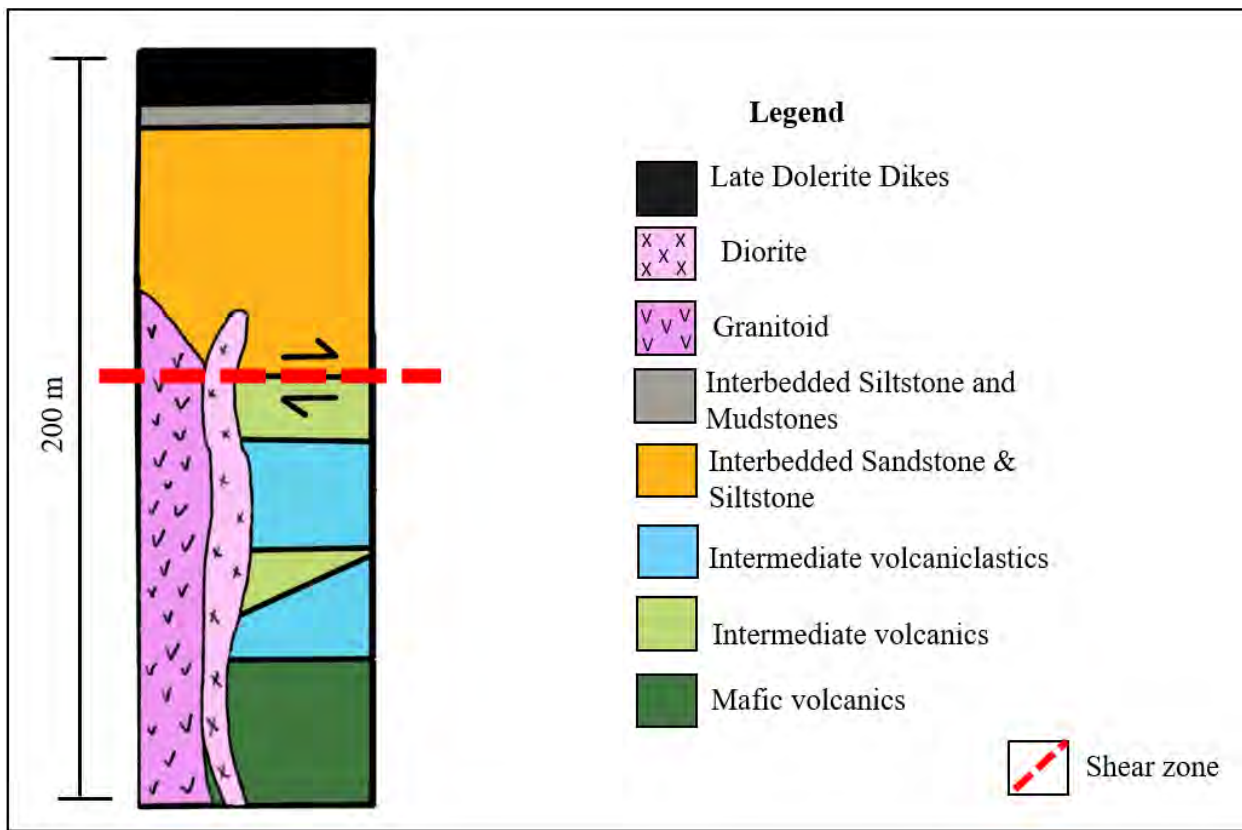


Fig 1. Stratigraphic column of the Makapa project area.

Lithologies across the Makapa Project





Fig 2.

Volcanic Types. A) Mafic volcanic—fresh, finely crystalline with weak foliation. B) Mafic volcanic—sap rock, red, with hematite stains. C) Intermediate volcanics (andesite) grey, finely crystalline and weakly felspathic (10%). D) Andesite—green, with chlorite phenocrysts. E) Intermediate volcaniclastics with clasts (2-5cm) of mafic/intermediate volcanics. F) Intermediate volcaniclastics with weakly strained smaller clasts (~1cm).



Fig 3.

Metasedimentary types. A) Tan interbedded sandstone with silica grains and feldspars in matrix. B) Thinly bedded siltstone with carbonaceous beds (mm scale). C) Red sandstone, fine-grained and weakly foliated. D) Grey siltstone interbedded with cm scale sandstone

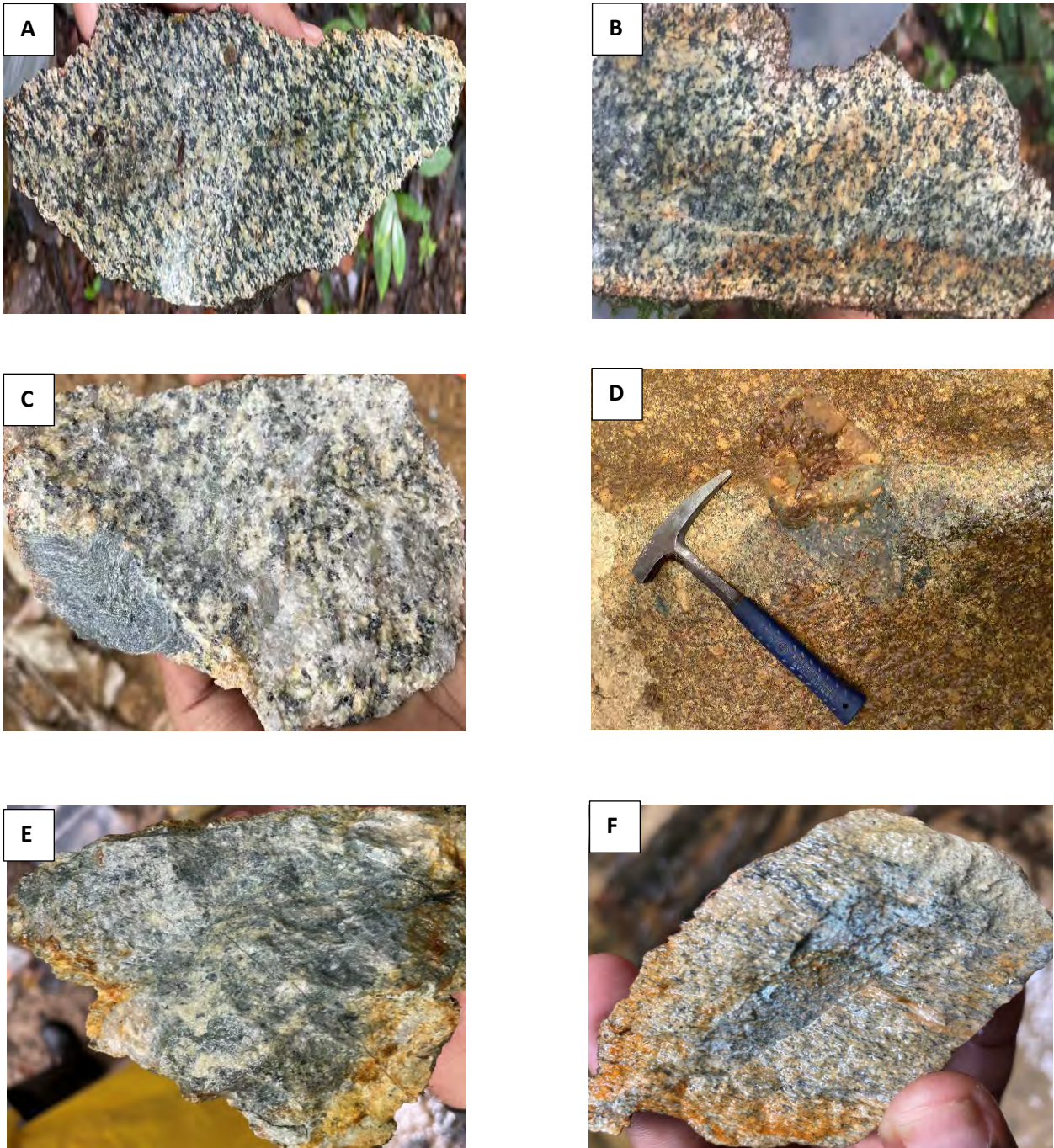


Fig 4. Intrusive Types. A) Karouni granite (2097Ma) coarsely crystalline and weakly strained with ferromagnesian aligned and 'cloudy' feldspar. B) Kuribrong intrusive body—KIB (to be dated) Coarsely crystalline, weakly strained with increased ferromagnesian (~30%). C & D) Apanachi granite (1955 Ma)—coarsely crystalline and unstrained. E & F) Diorite (small intrusive) moderately strained with ~15% ferromagnesian and 20% plagioclase.

Geological Maps and Cross Sections

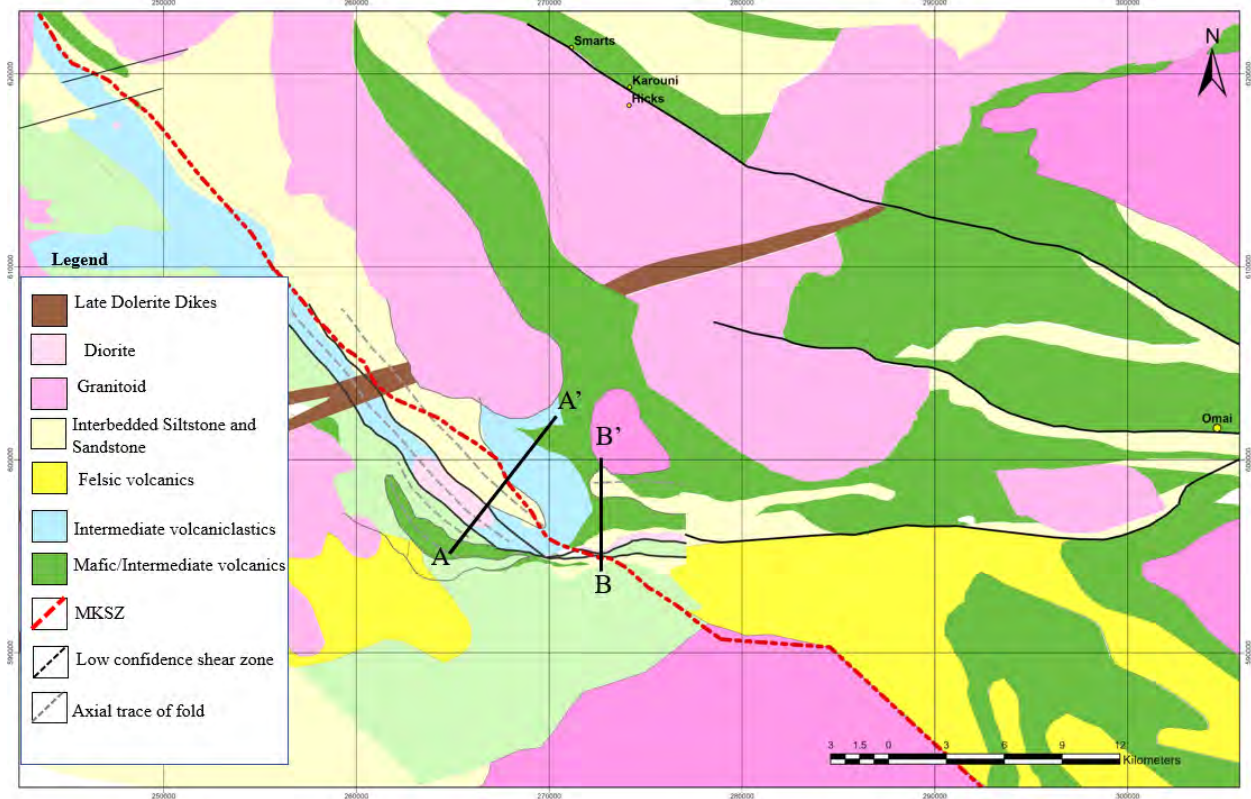


Fig 5. Geologic map of the Makapa project showing location of section lines.

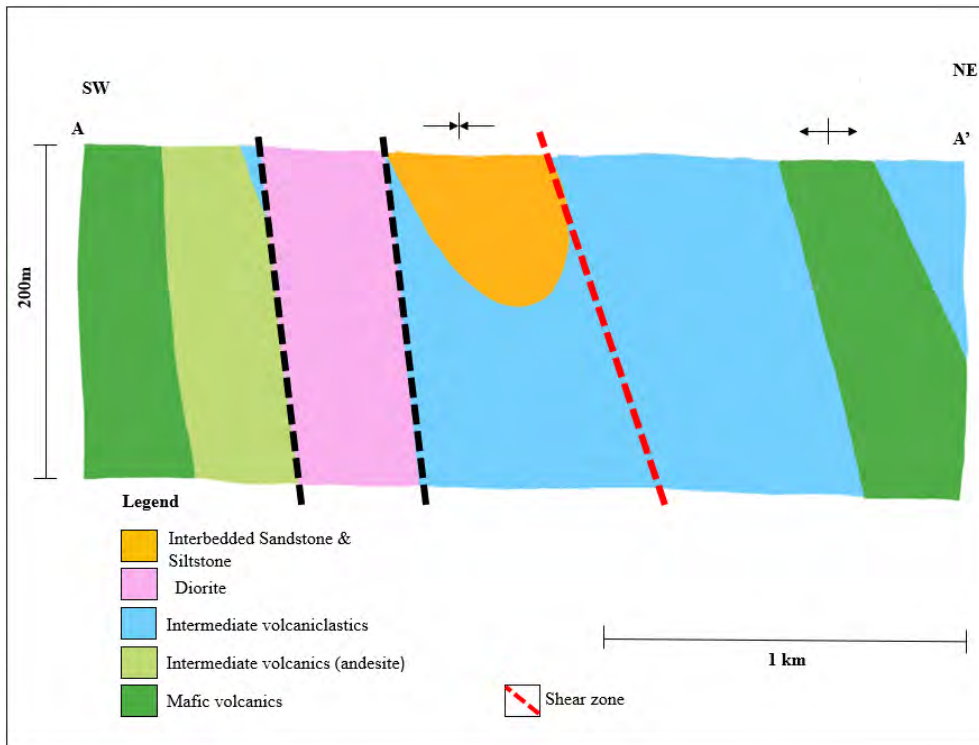


Fig 6. Cross section of the Makapa project area, looking northwest.

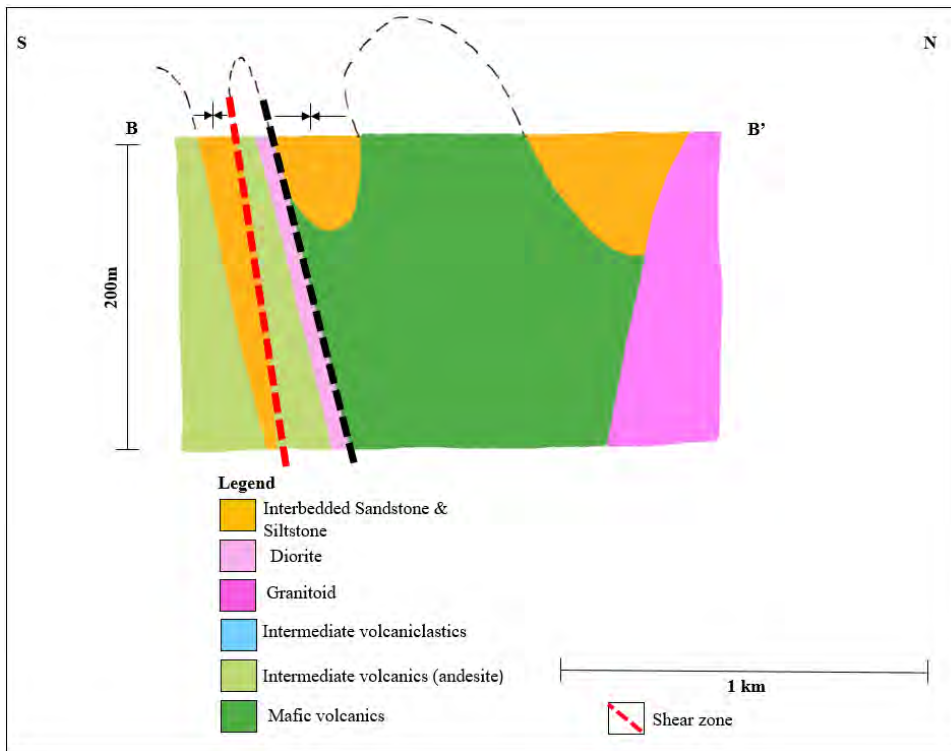


Fig 7. Cross section of the Makapa project area looking west.

Tectono-metamorphic framework of the Rosebel and Armina unit, French Guiana.

Alexis Plunder*¹, Geoffrey Aergeerts^{2,3}, Harmony Suire¹, Abdeltif Lahfid¹, Arnauld Heuret⁴, Alexandre Casanova⁵

¹BRGM, F-45060 Orléans, France, * a.plunder@brgm.fr

²BRGM, F-35700 Rennes, France

³BRGM, F-97300 Cayenne, France

⁴Université de Guyane, Géosciences Montpellier, UMR5243, Cayenne, France

⁵Université de Guyane, 97300, Cayenne, France

SUMMARY

In French Guiana, gold mineralisations are well known. However, the geological history of the gold-bearing unit remains little studied. We here present the first tectonometamorphic study including state of the art pressure temperature condition determination of the Armina and gold-bearing Rosebel unit of French Guiana. Our study points to two deformation phases at least that can be linked to the main (D2a) and late (D2b) Transamazonian events. Our petrological study points to the fact that the Rosebel unit suffered metamorphic conditions at the greenschist to amphibolite facies transition favourable for gold deposit formation whereas the Armina unit clearly suffered regional amphibolite facies conditions.

Key words: petrological study, Guiana shield, Greenstone belt, mineral exploration.

INTRODUCTION

Gold mineralisation is well known in French Guiana and occurs mostly in the two greenstone-belts that crop out in the northern and southern part of the French Guiana. Among these belts, the north one is mainly composed of meta-volcano-sedimentary rocks (Armina unit; metapelite and quartzite) and meta-detrital rocks (Rosebel-Bonidoro unit, metaconglomerate) (e.g. Kroonenberg et al., 2016; Naipal and Kroonenberg, 2016). Two main deformation events (D1 and D2) are usually described. The D1 is poorly documented and was not described in the Rosebel-Bonidoro unit (Egal et al., 1995, 1994, 1991), whereas in the Armina Formation, D1 was characterised by tiny oriented sericite mineralisation (Egal et al., 1995, 1994, 1991). The D2 event was described in both the Armina and Rosebel-Bonidoro units. Two main deformation stages are known. The first one (D2a-b) is a NE-SW sinistral transtensional sliding followed by a sinistral stretching (Daoust et al., 2011; Delor et al., 2003; Egal et al., 1991, 1994, 1995). The second one (D2c?) was identified in the Rosebel gold deposit district (Surinam), where a NE-SW to N-S dextral transpression was described (Daoust et al., 2011). This latter is characterised by tension and shear veins that are associated with gold mineralization which is assumed to be coeval to a late transamazonian event (2.023-1.955 Ga) and to the late calc-alkaline volcanism and plutonism of the south Guiana Shield (Daoust et al., 2011).

In French Guiana, gold mineralisation was also described in both the Rosebel-Bonidoro and Armina units (Nagel 1996 and references therein). Nevertheless, neither petrological nor metamorphic studies were conducted on these units since the work of Vanderhaeghe et al. (1998) and Delor et al. (2003). A complete study of the structure (Armina and Rosebel units) of the French Maroni bank was provided by Egal et al. (1991). Blast of biotite related to a static thermal

metamorphism was described in the Armina unit, but garnet-amphibole-tourmaline-epidote assemblage is not well characterised in terms of pressure-temperature (PT) condition.

In a recent drilling water program, garnet-staurolite bearing micaschist was identified in the Armina formation by the French Guyana geological survey. Garnet and staurolite appear as porphyroclast and suggest an amphibolite facies metamorphism. Furthermore, Cassard et al. (2008) suggested that the Armina unit gold deposit has been under evaluated.

The drilling program conducted by the BRGM in the GU04K district (Rosebel unit; Espérance (drills ESP1-2-3)) of the French Guiana mining inventory has shown that gold-bearing quartz veins are parallel to the main foliation suggesting that these structures are syn-metamorphic structures. Nevertheless, related metamorphism and gold mineralisation are assumed to be coeval to intrusion of granitoid (Egal et al., 1991; Plat and Lamouille, 1982). In the Cayenne area, the Rosebel-Bonidoro unit recorded an amphibolite facies metamorphism during the D2 event, estimated P-T provided by Vanderhaeghe et al. (1998) are around 4-7 kbar and 575-645°C. Important gold deposits were also described in this area (e.g. Kaw montain ; Nagel 1996 and references therein).

RESEARCH APPROACH

In this context, the objectives of the project are to provide new petrological and thermobarometric constrains on the PT condition path of both the Rosebel-Bonidoro unit and the Armina unit. It will contribute to provide a better geological understanding for gold mineralisation exploration and for gold unit mapping.

We studied a geological transect from Apatou to Grand Santi, along the Maroni riverbank as well as cores from the Sparouine an Esperance drills. We collected fifty samples in the field (Maroni transect and cores) amongst which we sent 20 for geochemical analysis (major and trace elements). We considered the tectonic setting diagram of Pearce et al. (1984) as a first order proxy to study the source of our samples. We conducted a detailed petrological study of 50 thin section under the microscope. Amongst these samples, we chose 13 for detailed petrological and analytical work, including Ti in biotite thermometry (Henry et al., 2005). We also selected a set of 4 samples for maximum temperature determination using the Raman spectroscopy on carbonaceous material (Beysac et al., 2002) and 15 others for detailed microtectonics. Finally, we selected 4 sample to construct PT pseudosection using Perple_X and the relevant thermodynamic database (Connolly, 2009, 2005; Holland and Powell, 2011).

BUILDING UP THE TECTONOMETAMORPHIC FRAMEWORK ALONG THE MARONI TRANSECT

Thin section observation confirms the sedimentary nature of the Rosebel Bonidoro and Armina unit samples and allow to decipher their geological history:

- In the Rosebel Bonidoro unit, samples consist of detrital rocks in which we observe mainly a mild foliation that develops parallel to the bedding. In these, metamorphic minerals (e.g. biotite, garnet, epidote) are generally detrital. Some samples exhibit a more important development of the foliation and experienced grain size reduction. They were typical identified as possible shear zone in the field. Metamorphic minerals consist of biotite, both in the main fabric or postdating it, garnet detrital or metamorphic and epidote that is both detrital and metamorphic. One sample shows a chloritoid, chlorite quartz, muscovite, ilmenite assemblage were the rosette shaped chloritoid show a static growth. Our microtectonic study on the most deformed samples give both sinistral and dextral sense of shear. The deformation fabrics consist of quartz recrystallization by sub grain rotation, undulose extinction of quartz, sigma clast of quartz, mica fish structures and shear band cleavage fabrics. The majority of samples show sinistral sense of shear. Only a few ones

yielded dextral sense of shear that were not documented yet in this region but known in the Rosebel unit (e.g. Daoust et al., 2011). In a sample, the dextral sense of shear postdate the sinistral movements.

All petrological method we applied (RSCM, Ti in biotite thermometry and pseudosection modelling) point to temperature of metamorphism for the Rosebel unit sample of $550 \pm 50^\circ\text{C}$. The pressure is constrained on two samples between 0.3 to 0.5 GPa using pseudosection modelling.

Major elements show that our rocks are peraluminous, intermediate to acidic, with a chemistry of a diorite to granite. Using the Nb/Y and the Ta/Yb diagram of Pearce et al. (1984) our samples plot in the volcanic arc orogeny field.

- In the Armina unit, the garnet staurolite micaschist of the Sparouine drill shows a well-developed lepidoblastic fabric. The assemblage is made of garnet, staurolite, biotite, muscovite, quartz, feldspar, tourmaline and ilmenite. Both the staurolite and garnet appear at equilibrium. We could not study the deformation in this series of samples as they were taken in non-oriented cores. Altogether, the Ti in biotite thermometry, Raman thermometry and pseudosection modelling point to a temperature of climax metamorphic condition at $600 \pm 50^\circ\text{C}$ and a pressure of 0.48 ± 0.1 GPa. The geochemical affinity is similar to that of the Rosebel samples (volcanic arc orogeny, granitic chemistry and peraluminous).

IMPLICATIONS FOR MINERAL EXPLORATION

Our study shows clear differences in PT conditions between selected samples and studied area. Specifically, there is a great difference between garnet-staurolite bearing micaschists of Sparouine (Armina formation) and quartzites of Esperance, which is well known as gold-rich part of the Rosebel-Bonidoro formation. In Armina formation, Cassard et al. (2006), based on a gold predictivity mapping, suggest that the Armina Formation was underestimated in terms of gold potential. Our preliminary PT data does not support such a conclusion. Indeed, orogenic gold mineralisation are commonly found in greenschist to amphibolite facies units (Phillips and Powell, 2010). Thus, gold investigation in this unit must be taken with caution in the Armina formation and staurolite-garnet micaschist does not seem to be a good target. However, the Rosebel formation stands at this metamorphic transition. Furthermore, ductile deformation in Esperance sample (i.e., protomylonitic to mylonitic related to regional shearzone) was not identified in the other place of the Rosebel-Bonidoro unit meaning probably that gold deposit need both greenschist PT condition and regional ductile deformation. Shear zone are not well identified in French Guiana or Surinam. It could be interesting to focus exploration on identifying those shear zones.

CONCLUSIONS

We provide the first quantitative PT condition for both the Rosebel and the Armina unit. In the Armina unit, the staurolite-garnet bearing micaschist recorded peak PT condition of 0.48 ± 0.1 GPa and $600 \pm 50^\circ\text{C}$. This combined with the occurrences of other staurolite-bearing micaschist in French Guiana and in Suriname point towards a metamorphism a regional origin for this unit. In the Rosebel unit, the calculated PT condition show climax condition on 0.4 ± 0.1 GPa and $500 \pm 50^\circ\text{C}$. We point that all independent petrological methods are in very good agreement for both the Rosebel and Armina unit. Further investigation could strengthen this point, for example with the comparison of the "upper sedimentary units" in Mt Tortue area of Western French Guiana where petrological studies point to similar but not yet quantitative PT conditions (Vanderaeghe et al., 1998). In a similar way, this points the need to better constrain the staurolite bearing Armina unit that extend farther west to Surinam (e.g. Kroonenberg et al., 2016).

ACKNOWLEDGMENTS

This work was supported through the South America Exploration Initiative Stage 2 (SAXI2). We acknowledge AMIRA Global and industry sponsors for their support of the SAXI2 project (P1061B).

REFERENCES

- Beysac, O., Goffé, B., Chopin, C., Rouzaud, J.N., 2002. Raman spectra of carbonaceous material in metasediments: a new geothermometer. *J. Metamorph. Geol.* 20, 859–871. <https://doi.org/10.1046/j.1525-1314.2002.00408.x>
- Cassard, D., Billa, M., Lambert, A., Picot, J.C., Husson, Y., Lasserre, J.L., Delor, C., 2008. Gold predictivity mapping in French Guiana using an expert-guided data-driven approach based on a regional-scale GIS. *Ore Geol. Rev.* 34, 471–500. <https://doi.org/10.1016/j.oregeorev.2008.06.001>
- Connolly, J.A.D., 2009. The geodynamic equation of state: What and how. *Geochemistry, Geophys. Geosystems* 10, Q10014, doi:10.1029/2009GC002540. <https://doi.org/10.1029/2009GC002540>
- Connolly, J.A.D., 2005. Computation of phase equilibria by linear programming: A tool for geodynamic modeling and its application to subduction zone decarbonation. *Earth Planet. Sci. Lett.* 236, 524–541. <https://doi.org/10.1016/j.epsl.2005.04.033>
- Daoust, C., Voicu, G., Brisson, H., Gauthier, M., 2011. Geological setting of the Paleoproterozoic Rosebel gold district, Guiana Shield, Suriname. *J. South Am. Earth Sci.* 32, 222–245. <https://doi.org/10.1016/j.jsames.2011.07.001>
- Delor, C., Lahondère, D., Egal, E., Lafon, J.-M., Cocherie, A., Guerrot, C., Rossi, P., Truffert, C., Théveniaut, H., Phillips, D., Gama de Avelar, V., 2003. Transamazonian crustal growth and reworking as revealed geological map of French Guiana (2 nd edition). *Geol. Fr. Surround. areas.*
- Egal, E., Mercier, D., Itard, Y., Mounié, F., 1991. Le protérozoïque inférieur de Guyane : révision lithostructurale le long du fleuve Maroni. *Rpport BRGM R33180.*
- Egal, E., Milesi, J., Ledru, P., Cautru, J., Freyssinet, P., Thiéblemont, D., Vernhet, Y., Cocherie, A., Hottin, A., Tegye, M., Vanderhaeghe, O., 1994. Ressources minérales et évolution lithostructurale de la Guyane - Carte thématique minière à 1/100 000. Feuille de Cayenne. *Rapport BRGM R 38019, 59p., 11Fig., 3 annexes, 1 carte.*
- Egal, E., Milesi, J., Vanderhaeghe, O., Ledru, P., Cocherie, A., Thiéblemont, D., Cautru, J., Vernhet, Y., Hottin, A., Tegye, M., Martel-Jantin, B., 1995. Ressources minérales et évolution lithostructurale de la Guyane - Carte thématique minière à 1/100 000. Feuille de Régina. *Rapport BRGM R 38458, 66p., 13Fig., 3 annexes.*
- Henry, D.J., Guidotti, C. V., Thomson, J.A., 2005. The Ti-saturation surface for low-to-medium pressure metapelitic biotites: Implications for geothermometry and Ti-substitution mechanisms. *Am. Mineral.* 90, 316–328. <https://doi.org/10.2138/am.2005.1498>
- Holland, T.J.B., Powell, R., 2011. An improved and extended internally consistent thermodynamic dataset for phases of petrological interest, involving a new equation of state for solids. *J. Metamorph. Geol.* 29, 333–383. <https://doi.org/10.1111/j.1525-1314.2010.00923.x>
- Kroonenberg, S.B., De Roeve, E.W.F., Fraga, L.M., Reis, N.J., Faraco, T., Lafon, J.M., Cordani, U., Wong, T.E., 2016. Paleoproterozoic evolution of the Guiana Shield in Suriname: A revised model. *Geol. en Mijnbouw/Netherlands J. Geosci.* 95, 491–522. <https://doi.org/10.1017/njg.2016.10>
- Nagel, J.-L., 1996. Inventaire minier de la Guyane : bilans des travaux et résultats. *Rapport BRGM/R-38633, 112 p., 15 fig., 8 tabl., 1 ann., 6pl.*
- Naipal, R., Kroonenberg, S.B., 2016. Provenance signals in metaturbidites of the Paleoproterozoic greenstone belt of the Guiana Shield in Suriname. *Geol. en Mijnbouw/Netherlands J. Geosci.* 95, 467–489. <https://doi.org/10.1017/njg.2016.9>
- Pearce, J. a., Lippard, S.J., Roberts, S., 1984. Characteristics and tectonic significance of supra-subduction zone ophiolites. *Geol. Soc. London, Spec. Publ.* 16, 77–94. <https://doi.org/10.1144/GSL.SP.1984.016.01.06>
- Phillips, G.N., Powell, R., 2010. Formation of gold deposits: a metamorphic devolatilization model. *J. Metamorph. Geol.* 28, 689–718. <https://doi.org/10.1111/j.1525-1314.2010.00887.x>
- Plat, R., Lamouille, B., 1982. Inventaire du département de la Guyane, recherche des minéralisations aurifères : Prospect d'espérance (GU04K), résultats de propection de 1978 à 1982. 33p., 9Fig., 4 tabl., 6 ann.

Vanderhaeghe, O., Ledru, P., Thie, D., Egal, E., Cocherie, A., Tegye, M., Milési, J., 1998. Contrasting mechanism of crustal growth Geodynamic evolution of the Paleoproterozoic granite – greenstone belts of French Guiana. *Precambrian Res.* 92, 165–193.

Nature of the relationship between the Marowijne greenstone belt and the Gran Rio granite of the Rhyacian Transamazonian orogenic belt, Suriname: Significance of the Sara's Lust migmatite

Fydji Sastrohardjo

Anton de Kom University of Suriname
Leysweg 87
Paramaribo, Suriname
fydji.sastrohardjo@uvs.edu

Olivier Vanderhaeghe

GET, Université Toulouse III, CNRS,
IRD, CNES
Avenue Édouard Belin 31400
Toulouse, France
olivier.vanderhaeghe@get.omp.eu

Leo Kriegsman

Naturalis Biodiversity Center ,
Leiden, Netherlands
also at: Utrecht University,
Faculty of Geosciences
leo.kriegsman@naturalis.nl

Aurélien Eglinger

GeoRessources Université de Lorraine
Nancy, France
aurelien.eglinger@univ-lorraine.fr

Salomon Kroonenberg

Anton de Kom University of Suriname
Leysweg 86
Paramaribo, Suriname
salomonkroonenberg@gmail.com

Marc Bardoux

Barrick
Ontario, Canada
mbardoux@barrick.com

SUMMARY

Precambrian greenstone belts and granitoid-gneiss complexes provide a record of the formation and evolution of the early Terrestrial crust and related ore deposits. Models proposed include (i) deposition-emplacment of greenstone supracrustals on top of a pre-existing granitic basement, (ii) magmatic differentiation of mantle mafic magmas followed by TTG magmatism, (iii) tectonic accretion of multiple terranes, or (iv) a metamorphic gradient superimposed onto supracrustals reaching partial in-situ melting and creating granitoids.

Work conducted in the Sara's Lust quarry, along the Suriname River and along the Tapanahony River in the Rhyacian Marowijne greenstone belt (MGB) and the Gran Rio granite (also called "older granite") in east central Suriname indicates that (i) the MGB is intruded by granodiorite-tonalite plutons that are petrologically distinct to the Gran Rio granites, and (ii) the contact between de Marowijne supracrustals and the Gran Rio granitoid-gneiss is a domain of migmatites developed at the expense of amphibolites and metapelites-metagreywackes. These migmatites display structures that are similar to those of the regional strain framework which indicates that such deformation was synchronous to melt segregation and pluton emplacement suggesting that the contact is likely a metamorphic gradient from greenschist facies to amphibolite facies reaching partial melting. This proposition does not preclude the possibility of distinct protoliths for the greenstones and granitoid-gneiss. To test the different working hypotheses, we plan to (i) quantify the PTt conditions recorded along this gradient, (ii) constrain the age of metamorphism with U-Pb geochronology on zircon and (iii) test the potential link between the greenstones and the granite using whole rock geochemistry as well as U-Pb and Lu-Hf isotopic tracing on zircon. Deciphering the nature of this link is pivotal to reconstruct the thermal-mechanical evolution of the Transamazonian belt and will provide a guide for metallogenic processes in terms of fluid- and metal sources as well as timing and structural control of ore deposition.

Key words: Rhyacian, Transamazonian orogenic belt, granite-greenstone belts, migmatites, Marowijne Greenstone Belt, older granites, partial melting

INTRODUCTION

Greenstone belts and granitoid-gneiss complexes are the key components of the Archean and Rhyacian (Condie, 1984; Corfu, 1993; de Wit et al., 2011; Hickman & van Kranendonk, 2012; Anhaeusser, 2014; Jessell & Liégeois, 2015). Despite numerous studies of these terranes (Wyman et al., 1999; Masurel et al., 2022) the geodynamic context of the formation of these crustal segments is still debated. Authors debate between mantle plumes or plate tectonic regimes (Abouchami et al., 1990; Hill et al., 1992; Tomlinson & Condie, 2001; van Kranendonk et al., 2004; Baratoux et al., 2011). Part of the

solution relies on the interpretation of the relationship between greenstone supracrustals and granitoid-gneiss complexes and on the significance of migmatitic gneisses, also designated as TTG gneisses, which form a significant part of the granitoid-gneiss complexes.

This study benefits from one of the rare nearly continuous exposures from Greenstone to migmatites to TTGs on the planet. It looks at two edges of the Marowijne greenstone belt. In the north it looks at the Sara's Lust Gneiss (migmatitic complex), in the south the Gran Rio granitoid-gneiss complex (Kroonenberg et al., 2016). It examines several scenarios including (1) the granitoid-gneiss complex may be a basement to the MGB, (2) granitoid-gneiss complex and greenstones may be tectonically accreted terranes, juxtaposed onto the greenstones, (3) the granitoid-gneiss complex may be deformed plutonic rocks within the supracrustal rocks or, (4) the granitoid-gneiss complex and migmatites are partially molten equivalent of the volcano-sedimentary series.

GEOLOGICAL CONTEXT

The geology of the Northern Guiana Shield where this study takes place is made almost exclusively of Rhyacian granite-greenstone belts (Choubert, 1974; Gibbs & Barron, 1993). The structural and metamorphic record of these rocks has been attributed to the Transamazonian orogeny resulting in the assembly of Amazonia with Gondwana (Cohen & Gibbs, 1989; Teixeira et al., 1989; Ledru et al., 1994). This succession of magmatic and tectonic accretion during the Transamazonian orogeny has been attributed to subduction related processes (Gruau et al., 1985; Vanderhaeghe et al., 1998; Abouchami et al., 1990; Voicu et al., 2001; Delor et al., 2003; Daoust et al., 2011) and an oceanic plateau setting related to mantle plume activity (Velásquez et al., 2011; Beek, 2019).

The Rhyacian rocks of northern Suriname, consists mainly of MGB that defines a regional-scale synclinorium, intruded by the Kabel TTG plutonic rocks and Patamacca two-mica granites, flanked by the Sara's Lust migmatite gneiss to the north and southwest and by the Gran Rio granite to the south (Figure 1).

The greenstone sequences comprise from older to younger: the volcanic and volcano-sedimentary rocks of the Paramaka Formation and flysch-type sedimentary rocks of the Armina Formation that are altogether unconformably overlain by shallow marine sedimentary rocks ranging from basal conglomerate to arenite of the Rosebel Formation (Watson et al., 2008; Daoust et al., 2011). All rock types are metamorphosed to greenschist facies and intruded by multiple plutonic bodies (Kroonenberg et al., 2016; Ramlal, 2018; Kromopawiro, 2019).

The Kabel TTGs intrude the greenstone belt and surround the Paramaka metavolcanics, resulting in an amphibolite facies contact metamorphism. Tonalites occur mostly along the contact with the greenstones, while trondhjemites and granodiorites make up the central parts of the plutons (Veenstra, 1983; Delor et al., 2003). At the contact with the greenstones the tonalite transitions into banded migmatitic gneisses and amphibolites (Kroonenberg et al., 2016). Younger multi-stage Patamacca two mica granites are also intruding the greenstone belt (Kromopawiro, 2019)

The Sara's Lust Gneiss is a high-grade metamorphic complex characterized by migmatitic gneisses and amphibolites (de Munck, 1953; Barink, 1975; Bosma et al., 1983; Ho Len Fat, 1975; Kroonenberg et al., 2016). The migmatitic gneisses include hornblende–biotite gneisses, biotite–plagioclase gneisses, garnet–biotite gneisses and quartzofeldspathic gneisses, with minor amphibolites, locally with garnet or clinopyroxene, and furthermore pelitic sillimanite–biotite–muscovite gneisses and calcsilicate rocks mostly in the northern part (Kroonenberg et al., 2016). In the southwestern part andalusite-cordierite sillimanite schists are also found (van Eijk, 1961). Metamorphism is mainly in the higher amphibolite facies in some places reaching the granulite facies as evidenced by the occurrence of hypersthene (Ho Len Fat, 1975).

The Gran Rio granite (also referred to as the older granites) is a granitoid complex consisting of hornblende tonalite and granodiorites. Amphibolite lenses and enclaves may be present, but their occurrence decreases towards the centre of the granitoid complex, transitioning into a more granitic composition distal to the contact with the Sara's

Lust Gneiss and the greenstone belt (Ijzerman, 1931; de Munck, 1953; Ho Len Fat, 1975). Aplite dikes intrude the granitoid complex along fault planes (de Munck, 1953)

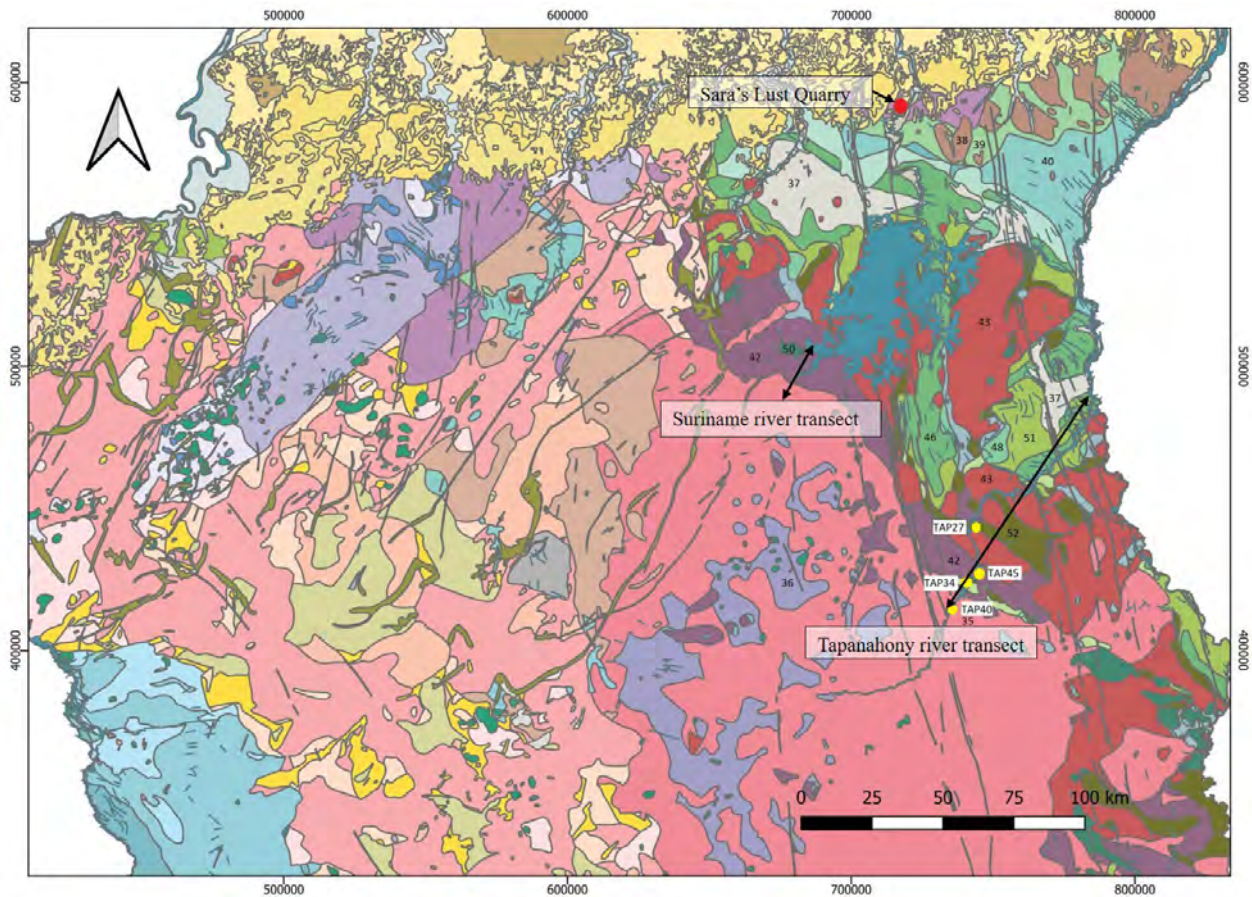


Figure 11: Geological map of eastern Suriname modified after (Kroonenberg et al., 2016; Geological and Mining Service of Suriname, 2018). The location of the Sara's Lust Gneiss (purple, 41, 42) is indicated by a red spot, to the North of the Marowijne belt. The Suriname River transect is indicated in black line in the centre exposing a section across the Sara's Lust Gneiss (42) and the Gran Rio granite (light pink, 35). The Tapanahony transect, indicated by a black line, exposes a unique section across the greenstones (green colours), Kabel biotite-tonalite (burgundy, 43), Sara's Lust Gneiss (41, 42), and the Gran Rio granite (light pink, 35).

NEW FIELD OBSERVATIONS

The Tapanahony river transect exposes a unique and nearly complete 80 km long section through the volcano-sedimentary greenstones, the Sara's Lust Gneiss and the Gran Rio older granites (Figure 1). Here, the following lithological sequences were observed:

- Fine grained metasediments of the MGB, comprised of metapelites and metasandstones with garnet and detrital magnetite, attributed to the Armina and Rosebel Formations. These rocks display a steep-dipping east-west striking foliation with locally transposed mm-sized veins (Figure 2A).
- Metatexite migmatite of the Sara's Lust Gneiss derived from amphibolite and metagreywacke-metapelite with a syn(pre?)migmatitic foliation marked by continuous network of concordant and discordant leucosome veins. The syn(pre?)migmatitic foliation is further folded with axial planar leucosome veins (Figure 2B).
- Syntectonic NS oriented granodiorite-tonalite plutons showing relatively sharp contacts with the supracrustal rocks and amphibolites and forming a network of dikes preferentially localized in axial planes of folds and partially transposed in the main foliation of their host rocks (Figure 2C & 2D)

- Diatexite migmatite of granitoid composition with numerous enclaves and schlieren of amphibolite and metagreywackes. Quartz, biotite, plagioclase, k-feldspar depict a heterogeneous texture (Figure 2E)
- Granodiorite with euhedric plagioclase and quartz, strongly magnetic showing low strain preferred orientation fabric (L-tectonite) pronounced by biotite.

To the north of the MGB, in the Sara's Lust quarry the migmatitic Sara's Lust gneiss with intercalated metasedimentary rocks from the greenstone belt can be observed. The different lithologies consist of:

- metagreywackes and metapelite from the Marowijne belt showing cm-scale bed thicknesses, bedding parallel to the main foliation, strike 30 dipping 50 to the east. These are intruded by granitic veins with a coarse grained to aplitic texture.
- Metatexite migmatitic derived from metagreywackes with calc-silicate and metapelite lenses. It is characterized by the presence of garnet and leucosomes of granitic composition crosscutting or parallel to the foliation, and are locally folded and boudinaged. Net-structured leucosomes consisting of quartz, plagioclase, biotite, garnet and pyrite are present along with diffuse mesosomes characterized by predominantly biotite, quartz, plagioclase, pyrite and garnet. Garnet is more abundant in mesosomes. Leucosomes display evidences of sulfidization.
- Metatexite migmatite derived from amphibolite is characterized by cm-scale pockets of plagioclase-rich leucosomes pervasively distributed and are surrounded by (peritectic) hornblende porphyroblasts.
- Diatexitic biotite gneiss with isoclinally folded leucocratic veins bordered by biotite.

Along the Suriname River transect the transition from the TTG Kabel Tonalite to the Sara's Lust gneiss and Gran Rio older granites is observed. From north to south the following lithologies can be distinguished:

- Granodiorite and tonalite of the TTG Kabel Tonalite characterized by quartz, plagioclase, hornblende, biotite. Locally contact zones were observed with amphibolite schlieren of approximately 2-3m.
- Migmatitic amphibolite, often showing leucosomes containing hornblende interlayered with dark melanosome characterized by amphibole and crosscut by aplite dikes.
- Metatexite biotite gneiss with fine grained K-feldspar, locally showing preserved primary sedimentary bedding. The bedding structures are pronounced by magnetite occurrences and are observed parallel to the foliation. Locally these are intersected by aplite dikes.
- Diatexite migmatite belonging to the Gran Rio granites showing a decrease in amphibolite enclave occurrences further upstream.
- Late leucocratic pegmatite veins with coarse ~3cm plagioclase, magnetite, biotite, muscovite and pyrite which intrude the amphibolite and migmatite biotite gneiss.

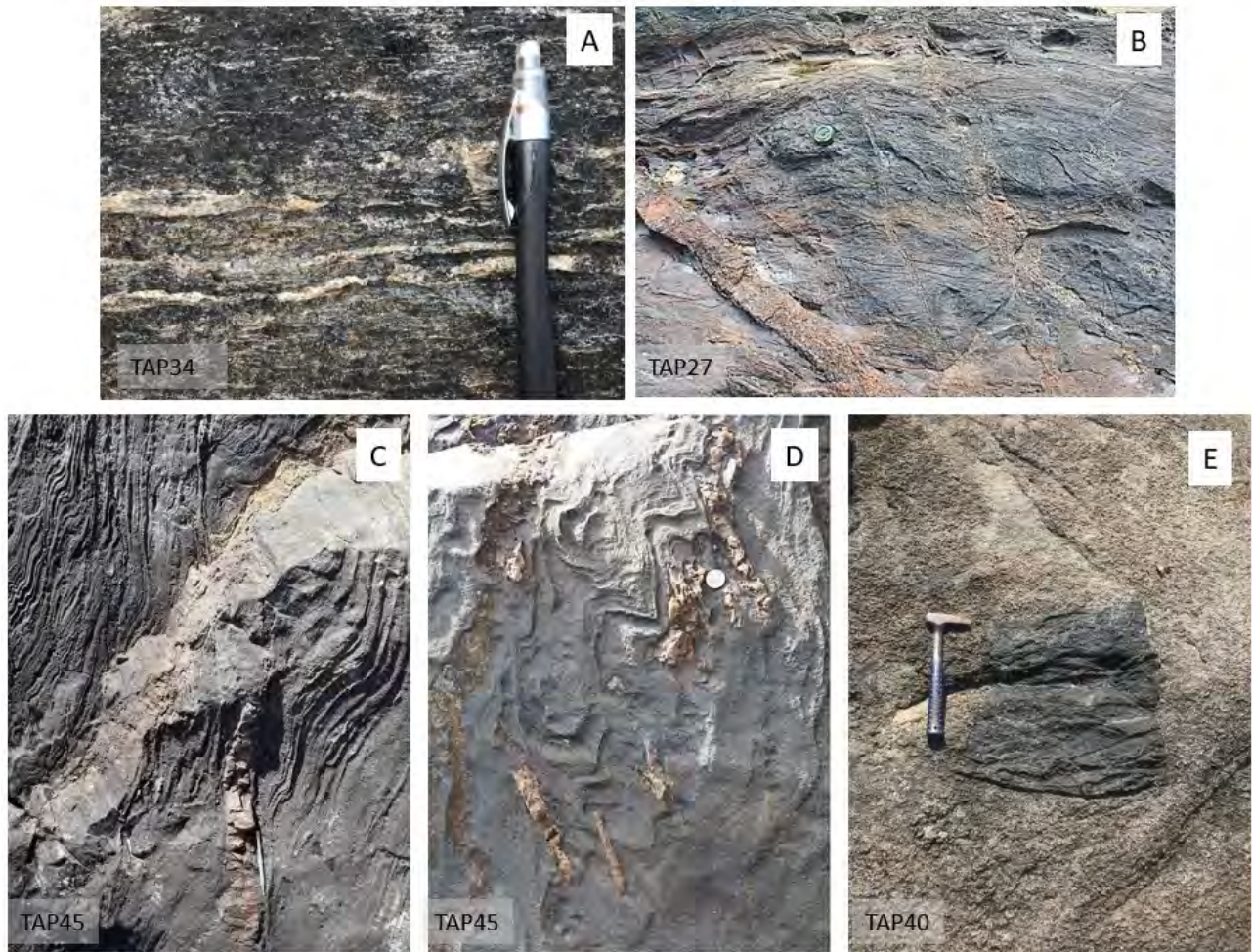


Figure 2: Lithological units exposed along the Tapanahony River transect showing (A) metasediments with transposed and dismembered veins, (B) Metatexite migmatite derived from amphibolite and metagreywacke-metapelite with a network of concordant and discordant leucosome veins, (C&D) granodiorite-tonalite in sharp contact with the supracrustal rocks and amphibolites, forming a network of dikes preferentially localized in axial planes of folds and partially transposed in the foliation of their host rocks diatexite migmatite with remnants of metatexite as well as remnant foliation (E) diatexite migmatite of granitic composition containing mafic enclave or restite of amphibolite and showing remnant foliation. Location of photos indicated in Figure 1 according to field name.

CONCLUSIONS

Field observations indicate that the transition from the metasedimentary-metavolcanic rocks of the MGB to the Sara's Lust Gneiss (migmatitic complex) and subsequently diatexite (Gran Rio biotite granite) is gradual and may represent progressive metamorphic gradients (and structural depths). The leucosome bodies that are forming a texturally continuous network of concordant to discordant veins to the older syn (pre) migmatitic foliation indicates that further deformation occurred in the presence of melt and developed melt segregation. The enclaves and schlieren structure of the Gran Rio granite, is consistent with its migmatitic character and contrasts with the magmatic character of the Kabel granodiorite-tonalite plutons that intruded at higher structural level within the MGB. These observations support the idea that partial melting post-dated the creation of greenstone sequences and occurred during progressive stages of the Transamazonian orogeny. In order to further test whether the metasedimentary-metavolcanic rocks of the Marowijne belt might, or not, represent the protolith of the Sara's Lust migmatites and of the Gran Rio granite as well as the source of the Kabel granodiorite-tonalite plutons, we plan to (i) determine the PTt conditions of metamorphism along the Tapanahony transect and on rocks of the Sara's Lust quarry by thermobarometric modelling, and (ii) constrain the whole rock geochemical and isotopic zircon U-Pb and Lu-Hf signatures of these different lithological units. These

results should provide a craton-scale framework for its thermal-mechanical evolution during the Transamazonian orogeny and thus a guide for metallogenic models.

REFERENCES

- Abouchami, W., Boher, M., Michard, A., & Albarede, F. (1990). A major 2.1 Ga event of mafic magmatism in West Africa: an early stage of crustal accretion. *Journal of Geophysical Research*, 95(B11). <https://doi.org/10.1029/jb095ib11p17605>
- Anhaeusser, C. R. (2014). Archaean greenstone belts and associated granitic rocks - A review. *Journal of African Earth Sciences*, 100(December), 684–732. <https://doi.org/10.1016/j.jafrearsci.2014.07.019>
- Baratoux, L., Metelka, V., Naba, S., Jessell, M. W., Grégoire, M., & Ganne, J. (2011). Juvenile Paleoproterozoic crust evolution during the Eburnean orogeny (~2.2-2.0Ga), western Burkina Faso. *Precambrian Research*, 191(1–2), 18–45. <https://doi.org/10.1016/j.precamres.2011.08.010>
- Barink, H. W. (1975). Geology of the Gonini River area, SE Suriname. *Mededelingen Geologisch Mijnbouwkundige Dienst* 23, 155–164.
- Beek, S. K. (2019). *Basalt-hosted gold in the Paleoproterozoic Marowijne greenstone belt (Suriname): Insights into geological setting and alteration style of the Saramacca deposit*. Anton de Kom University of Suriname.
- Bosma, W., Kroonenberg, S. B., Maas, K., & de Roever, E. W. F. (1983). Igneous and metamorphic complexes of the Guiana Shield in Suriname. *Geologie En Mijnbouw*, 62(2), 241–254.
- Choubert, B. (1974). Le précambrien des Guyanes (Vol. 81). *Éditions BRGM*.
- Cohen, H. A., & Gibbs, A. K. (1989). Is the Equatorial Atlantic Discordant? In *Precambrian Research* (Vol. 42).
- Condie, K. C. (1984). *Archean Greenstone Belts. Developments in Precambrian Gology* (Vol. 3). Elsevier Scientific Publishing Company.
- Corfu, F. (1993). The Evolution of the Southern Abitibi Greenstone Belt in Light of Precise U-Pb Geochronology. *Economic Geology*, 88, 1323–1340.
- Daoust, C., Voicu, G., Brisson, H., & Gauthier, M. (2011). Geological setting of the Paleoproterozoic Rosebel gold district, Guiana Shield, Suriname. *Journal of South American Earth Sciences*, 32(3), 222–245. <https://doi.org/10.1016/j.jsames.2011.07.001>
- de Munck, V. C. (1953). Voorlopige geologische resultaten van de Medisch-Wetenschappelijke Expeditie naar de Zuidgrens van Suriname in 1952. *Geol. En Mijnb.* 15, 152–162.
- de Wit, M. J., Furnes, H., & Robins, B. (2011). Geology and tectonostratigraphy of the Onverwacht Suite, Barberton Greenstone Belt, South Africa. *Precambrian Research*, 186(1–4), 1–27. <https://doi.org/10.1016/j.precamres.2010.12.007>
- Delor, C., Lahondere, D., Egal, E., Lafon, J., Cocherie, A., Guerrot, C., Rossi, P., Truffert, C., Theveniaut, H., & Phillips, D. (2003). Transamazonian crustal growth and reworking as revealed by the 1:500,000-scale geological map of French Guiana (2. *Géologie de La France*, 2, 5–57.
- Gibbs, A. K., & Barron, C. N. (1993). Geology of the Guiana Shield. *Oxford Monographs on Geology and Geophysics*, 22, 246.
- Geological and Mining Service of Suriname. (2018). *Geological Map of Suriname 1:500,000*. Geologisch Mijnbouwkundige Dienst van Suriname.
- Gruau, G., Martin, H., Leveque, B., & Capdevila, R. (1985). Rb-Sr and Sm-Nd geochronology of lower Proterozoic granite-greenstone terrains in French Guiana, South America. *Precambrian Research*, 30, 63–80.
- Hickman, A. H., & van Kranendonk, M. J. (2012). Early Earth evolution: Evidence from the 3.5-1.8 Ga geological history of the Pilbara region of Western Australia. *Episodes*, 35(1), 283–297. <https://doi.org/10.18814/EPIIUGS/2012/V35I1/028>
- Hill, R. I., Chappell, B. W., & Campbell, I. H. (1992). Late Archaean granites of the southeastern Yilgarn Block, Western Australia: Age, geochemistry, and origin. *Transactions of the Royal Society of Edinburgh: Earth Sciences*, 83(1–2), 211–226. <https://doi.org/10.1017/S0263593300007902>
- Ho Len Fat, A. G. (1975). Geology of the Pikien Rio–Beneden Tapanahony area (E. Suriname). *Mededelingen Geologisch Mijnbouwkundige Dienst Suriname* 23, 165–175.

- Ijzerman, R. (1931). *Outline of the geology and petrology of Surinam, (Dutch Guyana)*. 223–236.
- Jessell, M. W., & Liégeois, J. P. (2015). 100 years of research on the West African Craton. In *Journal of African Earth Sciences* (Vol. 112, pp. 377–381). Elsevier Ltd. <https://doi.org/10.1016/j.jafrearsci.2015.10.008>
- Kromopawiro, S. C. (2019). *2.12 – 2.07 Ga Late- to post-collisional peraluminous granitoid magmatism in the Marowijne Greenstone Belt of Suriname*. Anton de Kom University of Suriname.
- Kroonenberg, S. B., de Roever, E. W. F., Fraga, L. M., Reis, N. J., Faraco, T., Lafon, J. M., Cordani, U., & Wong, T. E. (2016). Paleoproterozoic evolution of the Guiana Shield in Suriname: A revised model. *Geologie En Mijnbouw/Netherlands Journal of Geosciences*, 95(4), 491–522. <https://doi.org/10.1017/njg.2016.10>
- Ledru, P., V6ra, J., Mil6si, J. P., & Tegye, M. (1994). Pretumbriun Resenrth Markers of the last stages of the Palaeoproterozoic collision: evidence for a 2 Ga continent involving circum-South Atlantic provinces. In *Precambrian Research* (Vol. 69).
- Ramlal, S. (2018). *An investigation of the Brincks intrusion and its relationship to surrounding gold deposits, Brokopondo, Suriname, South Americ*s. Anton de Kom Universiteit van Surinamr.
- Teixeira, W., Tassinari, C. C. G., Cordani, U. G., & Kawashita, K. (1989). A review of the geochronology of the Amazonian Craton: Tectonic implications. *Precambrian Research*, 42(3–4), 213–227. [https://doi.org/10.1016/0301-9268\(89\)90012-0](https://doi.org/10.1016/0301-9268(89)90012-0)
- Tomlinson, K. Y., & Condie, K. C. (2001). Archean mantle plumes: Evidence from greenstone belt geochemistry. *Special Paper of the Geological Society of America*, 352, 341–357. <https://doi.org/10.1130/0-8137-2352-3.341>
- van Eijk, H. T. L. (1961). Preliminary geological sketch-map, sheet De Goejegebergte-H9 (69), scale 1:200,000. *Geologisch Mijnbouwkundige Dienst Suriname. Jaarboek 1956-1958*, 26–29.
- van Kranendonk, M. J., Collins, W. J., Hickman, A., & Pawley, M. J. (2004). Critical tests of vertical vs. horizontal tectonic models for the Archaean East Pilbara Granite-Greenstone Terrane, Pilbara Craton, Western Australia. *Precambrian Research*, 131(3–4), 173–211. <https://doi.org/10.1016/j.precamres.2003.12.015>
- Vanderhaeghe, O., Ledru, P., Thiéblemont, D., Egal, E., Cocherie, A., Tegye, M., & Milési, J. P. (1998). Contrasting mechanism of crustal growth. Geodynamic evolution of the Paleoproterozoic granite-greenstone belts of French Guiana. *Precambrian Research*, 92(2), 165–193. [https://doi.org/10.1016/S0301-9268\(98\)00074-6](https://doi.org/10.1016/S0301-9268(98)00074-6)
- Veenstra, E. (1983). Petrology and geochemistry of sheet Stonbroekoe, sheet 30, Suriname. . *Mededelingen Geologisch Mijnbouwkundige Dienst Suriname*, 26, 1–138.
- Velásquez, G., Béziat, D., Salvi, S., Tosiani, T., & Debat, P. (2011). First occurrence of Paleoproterozoic oceanic plateau in the Guiana Shield: The gold-bearing El Callao Formation, Venezuela. *Precambrian Research*, 186(1–4), 181–192. <https://doi.org/10.1016/j.precamres.2011.01.016>
- Voicu, G., Bardoux, M., & Stevenson, R. (2001). Lithostratigraphy, geochronology and gold metallogeny in the northern Guiana Shield, South America: a review. In *Ore Geology Reviews* (Vol. 18). www.elsevier.com/locate/oregeorev
- Watson, T., Lapoint, D., Stewart, K., & Coleman, D. (2008). *Volcanism and Sediment Deposition in a Synkinematic Paleoproterozoic Basin: Rosebel Gold Mine, Northeastern Suriname*. University of North Carolina at Chapel Hill.

The Geological Setting and Hydrothermal Alteration at the Tucano Gold Deposit, Guiana Shield, Brazil

Gabriel A. R. Soares

Geology Graduate Program,
CPMTC, Institute of Geosciences,
UFMG, 6627 Pres. Antonio Carlos Avenue
Belo Horizonte, MG, 31270-901
gabriel7soares@gmail.com

Rosaline C. Figueiredo e Silva

Geology Graduate Program,
CPMTC, Institute of Geosciences,
UFMG, 6627 Pres. Antonio Carlos Avenue
Belo Horizonte, MG, 31270-901
rosalinecris@yahoo.com.br

Steffen G. Hagemann

Centre for Exploration Targeting,
School of Earth Sciences,
UWA, 35 Stirling Highway
Crawley WA6009
steffen.hagemann@uwa.edu.au

Lydia M. Lobato

Geology Graduate Program,
CPMTC, Institute of Geosciences,
UFMG, 6627 Pres. Antonio Carlos Avenue
Belo Horizonte, MG, 31270-901
llobato.ufmg@gmail.com

Rogério A. Lucena

Great Panther Mining Limited,
Km 15, Tapereba Road
Pedra Branca do Amapari, AP, 68945-000
rogerio.alves@greatpanther.com.br

SUMMARY

Preliminary results from geological mapping, petrographic studies and whole-rock and mineral chemistry data indicate that the Tucano gold deposit is a shear-zone hosted, hypozonal orogenic gold system equilibrated under amphibolite facies conditions. Its silicate hydrothermal assemblage comprising clinopyroxene, amphiboles, garnet and lesser biotite places Tucano in a rare class of high-temperature gold deposits. Some unique features that set Tucano apart from its high-temperature analogues are the abundance of magnetite and lack of plagioclase in the hydrothermal assemblage. Gold mineralization is associated with sulfidation, although sulfide content cannot be used as a proxy for contained gold. Pyrrhotite is the main ore mineral, whereas other sulfides, such as arsenopyrite, chalcopyrite and pyrite, are much less abundant. Free gold is not commonly observed and, where found, it is usually associated with both sulfide and silicate minerals.

Key words: Tucano gold deposit, orogenic, high-temperature, magnetite, pyrrhotite.

INTRODUCTION

Gold-only hydrothermal deposits in metamorphic belts share several common features and are thus collectively referred to as orogenic gold deposits (Groves et al., 1998). They define a coherent group with regards to tectonic setting, geology of host terrains, structural controls, alteration mineralogy, nature of ore fluids and timing of gold mineralization, with the vast majority equilibrated under greenschist facies conditions (Gebre-Mariam et al., 1995; Groves et al., 1998; Eilu et al., 1999; Goldfarb et al., 2001, 2005; Goldfarb and Groves, 2015; Groves et al., 2020). Nonetheless, a restricted number of these deposits are interpreted to have formed in the deeper parts of hypozonal systems, where temperatures may be high enough to stabilize skarn calc-silicate assemblages, whether associated or not with plutonism (Meinert et al., 2005). The Tucano deposit in northern Brazil belongs to this small class of uncommon high-temperature gold systems. Located in the southeastern Guiana Shield, the Tucano gold deposit is located in one the NW-SE-trending Rhyacian greenstone belts (Ricci et al., 2001; McReath and Faraco, 2006), hosted in a N-S subvertical brittle-ductile shear zone (Cavalcante, 2009). The local geology encompasses metasedimentary units, both chemical (iron formations and carbonate rocks) and siliclastic (schists and quartzites), and minor mafic metavolcanic rocks, as well as leucogranite stocks and dikes, with all previous units crosscut by diabase dikes (Melo, 2001; Horikava, 2008; Scarpelli and Horikava, 2017). Gold mineralization is mostly restricted to iron formations and carbonate rocks along the extent of the shear zone.

MATERIALS AND METHODS

Given the limited knowledge of the geological setting and controls on gold mineralization at the Tucano deposit, due to the lack of a more robust body of previous scientific work, the current research aims to present the first detailed, in-depth investigation of this high-temperature gold deposit. The Tucano gold deposit encompasses a series of open pits aligned

along the shear zone extent and are clustered into three groups, i.e., the northernmost Urucum pits, the central TAP C pits and the southernmost TAP AB pits. This work is focused on one of the central pits (TAP C1). Field reconnaissance and systematic drill core sampling, supported by selected surface samples, provided the basis for this work. Analytical work comprises petrographic studies using transmitted and reflected light microscopy, whole-rock geochemical analyses of selected samples (least-altered and hydrothermally altered) and SEM-EDS and EPMA analyses aiming at quantifying the chemical composition of selected silicate, carbonate, oxide and sulfide phases.

LITHOSTRATIGRAPHY AND GEOLOGICAL SETTING

The Tucano gold deposit is located in the supracrustal units of the Vila Nova Greenstone Belt. The basement rocks that underlay this metavolcanosedimentary sequence are neither exposed in the mine area nor intersected in drill cores. The stratigraphically lower unit, only seen in drillcores, is represented by a mafic metavolcanic rock featuring hornblende, plagioclase (mostly altered to epidote), tourmaline, and lesser amounts of muscovite, chlorite, quartz, titanite and ilmenite. This unit is overlain by a chemical package, being divided in a lower banded iron formation (BIF) and upper carbonate units. Least hydrothermally altered rocks indicate the dominance of amphibole-quartz-magnetite-dominated iron formations, although carbonate-magnetite-dominated types are also common. Amphiboles are the most abundant hydrothermal minerals in this deposit and the overall lack of unaltered rocks makes it difficult to ascribe amphiboles to the metamorphic assemblage in BIF as well, although is highly likely given metamorphic conditions. A few kilometers southeast from the Tucano mine, iron formations display hematite as the main iron oxide mineral. Carbonate units overlay the iron formations and are distinguished by olivine as the most abundant and widely distributed silicate mineral, with minor phlogopite ± tremolite ± spinel ± clinohumite. Where olivine occurs in significant amounts, the dominant carbonate mineral is calcite, whereas dolomite prevails in olivine-poor intervals.

Lithochemical analyses indicate the composition of a siliceous dolostone for this carbonate rock. EPMA results for carbonate minerals indicate up to 2.5 wt% MnO and tefroite contents ranging from 1.0 to 3.5 % in olivine. As a result, weathered profiles developed over these rocks often show strong fizzing to H₂O₂. Calc-silicate intervals are rather scarce as part of the metasedimentary sequence. The carbonate units are overlain by a siliciclastic package encompassing biotite schists, muscovite-quartz schists and quartzites. The supracrustal sequence is cut by numerous small intrusive bodies, where the dominant composition is a garnet-bearing, two-mica leucogranite. Much later N-S to NNW-SSE diabase dikes crosscut all above-mentioned units (Figure 1).

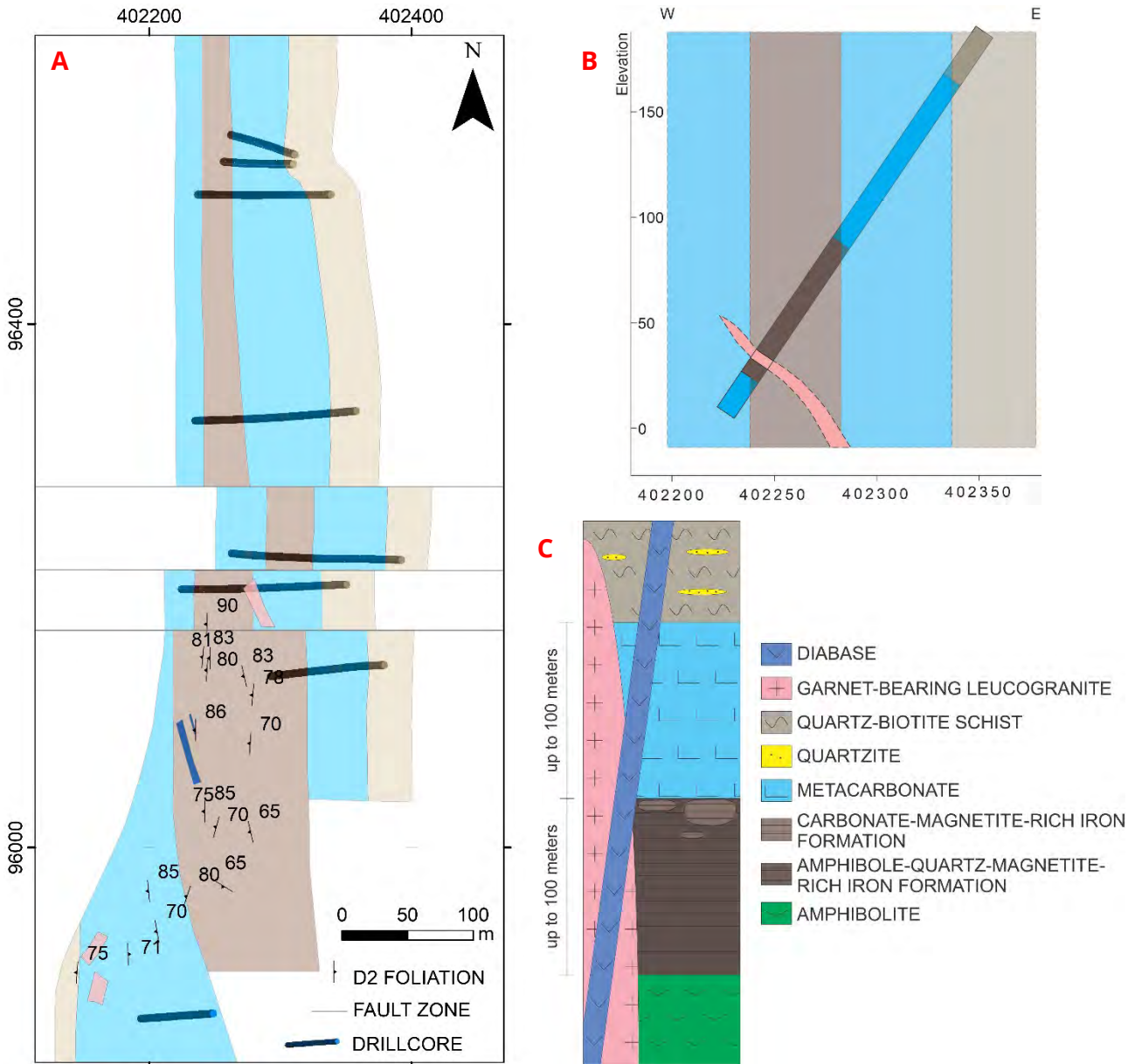


Figure 1: A) Geological map of the TAP C open pit integrated from combined drillcore and surface data. B) Schematic E-W geological cross section of the central part of the pit. Granites typically occur as small, irregular bodies and are thus difficult to model. C) Proposed stratigraphic sequence for the Tucano gold deposit area. Mafic metavolcanic rocks are not intersected at the studied open pit, but are recorded elsewhere in the Tucano gold deposit.

Regional metamorphism reached amphibolite facies conditions. First temperature estimates based on the garnet-biotite (Holdaway, 2000) and calcite-dolomite (Anovitz and Essene, 1987) geothermometry yielded values of 574°C and 546°C for peak thermal metamorphic conditions, respectively. Further geothermometry will be conducted to better constrain the temperature uncertainty. Lower temperatures (480-490°C) for some matrix calcite may record retrograde metamorphism, re-equilibration, and possibly indicate the closure temperature of Mg diffusion and unmixing during cooling (Mizuochi et al., 2010). The structural setting is defined by the regional NW-SE foliation (D1), which in the deposit is crosscut by a sub-vertical N-S shear foliation (D2) associated with an approximately 7 km-long dextral shear zone. Late D3 structures are manifested as medium- to high-angle E-W fault zones.

HYDROTHERMAL ALTERATION AND GOLD MINERALIZATION

Hydrothermal alteration at the Tucano gold deposit features high-temperature assemblages comprising clinopyroxene-amphiboles-garnet-biotite-quartz-carbonate-magnetite-sulfides. Gold mineralization is associated with sulfidation and characterized by a replacement-style alteration and a general lack of veins. The sulfide assemblage is dominated by pyrrhotite with lesser amounts of chalcopyrite, pyrite and arsenopyrite. The first stage of alteration is represented by quartz-clinopyroxene \pm garnet and typically lacks sulfides and gold enrichment, being morphologically manifested as either irregular masses or veins sub-parallel to the D2 foliation. Clinopyroxene belongs to the diopside-hedenbergite series with X^{Fe} (molar Fe/Fe+Mg) ranging from 0.18 to 0.55. m Amphiboles characterize the main alteration stage and whenever in contact with the earlier hydrothermal clinopyroxene, disequilibrium textures are seen. Amphiboles vary greatly in composition, encompassing members of the cummingtonite-grunerite and tremolite-Fe-actinolite series, plus hornblende (both magnesian- and iron-rich) and rare edenite. Broadly speaking, the relationship between these various amphiboles indicate that they are in equilibrium, with rocks usually displaying intergrowth textures between a Ca-poor and a Ca-rich variety. Despite that, more Fe-rich specimens tend to occur in Fe-rich rocks (especially magnetite-rich rocks). Amphiboles are usually in equilibrium with carbonate (mainly calcite), minor biotite (only locally abundant) and garnet. Titanite, and especially apatite, are important accessory phases coeval with amphibole formation, which is also accompanied by magnetite and/or sulfides. The iron oxide can be astonishingly abundant in certain locations where it may reach up to 50% modal proportion.

Petrographic studies suggest at least two generations of hydrothermal magnetite: the first is fine-grained and the second medium-grained, although both are thought to be part of this single broad stage of amphibole development. The second hydrothermal magnetite seems to be roughly contemporaneous to the main sulfidation and gold event, although crosscutting relationships between this magnetite and pyrrhotite indicate sulfide precipitation outlasts magnetite. Free gold is associated with both sulfide and silicate minerals. In the former case, gold may be found partially or totally encapsulated by pyrrhotite and arsenopyrite, whereas in the second it is recorded as fracture filling in garnet and may also precipitate along amphibole grain boundaries. Pyrite is relatively scarce in the study area, although greater abundances are reported in other pits in the same mine. This mineral is typically described as euhedral or as lamellae overgrowths in pyrrhotite, apparently postdating the main gold event. Conversely, gold-bearing arsenopyrite may exhibit a habit resembling pyrite, which may indicate phase transition from pyrite to arsenopyrite, thus suggesting an early pyrite generation. Though of limited occurrence, mm-thick pyrrhotite-bearing quartz-carbonate veins and veinlets are identified and record two main orientations: NW-SE and E-W, the latter being part of the D3 structures.

Retrograde alteration is scattered and mainly represented by chlorite, serpentine and epidote, and subordinately fine-grained actinolite. Locally, quartz and carbonate (mostly calcite) are also observed in this lower temperature stage. Chlorite occurs as individual lamellae or aggregates and most commonly replaces biotite and, to a lesser extent, amphibole. Serpentine usually develops pseudomorphs after olivine, yet it is also described in veins and veinlets. For instance, E-W veins usually feature this phase as one of its main constituents. Fine-grained epidote replaces commonly clinopyroxene. Fine- to medium-grained magnetite, intergrown with ilmenite, may have been formed at this stage.

Thin garnet-clinopyroxene-amphibole rims around small granitic intrusions are a common hydrothermal feature, although its genetic and time relationship to the gold-related hydrothermal event remains unclear.

CONCLUSIONS

The Tucano gold deposit is one of a few unique examples of a shear zone-hosted, hypozonal gold system. High-temperature hydrothermal assemblages are relatively unusual for orogenic gold systems, not only in Brazil but worldwide. Some potential analogues are the Marvel Loch (Mueller et al., 1991) and Nevoria (Mueller et al., 1997) deposits in the Southern Cross Greenstone Belt (Yilgarn Craton, Australia) as well as the Fäboliden deposit in the Svecofennian Orogen, in Sweden (Bark and Weihed, 2012). Due to comparable mineral assemblages and crustal level, some of these deposits are alternatively placed in the Au-skarn class. Despite sharing similarities with the aforementioned examples, the Tucano deposit distinguishes itself from other high-temperature orogenic systems by the large amount of hydrothermal magnetite and the overall lack of plagioclase in the alteration assemblage.

This is an ongoing work, and we expect to be able to unravel some of the questions that remain open on the geological evolution of this deposit over the next steps of the research. Future work will be focused on better constraining the paragenetic sequence, documenting different stages of the hydrothermal alteration via trace element geochemistry of

magnetite and pyrrhotite, and on the attempt to date the gold-related hydrothermal event and the garnet-bearing leucogranite.

ACKNOWLEDGMENTS

This work has been supported through the South American Exploration Initiative (SAXI). We acknowledge AMIRA Global and industry sponsors, as well as Great Panther Mining for their support of the current project, in particular their exploration staff who wholeheartedly assisted us during field activities and kindly provided us with crucial data indispensable for the success of this project.

REFERENCES

- Anovitz, L.M., and Essene, E.J., 1987, Phase Equilibria in the System $\text{CaCO}_3\text{-MgCO}_3\text{-FeCO}_3$: *Journal of Petrology*, v. 28, p. 389-415.
- Bark, G., Weihed, P., 2012, Geodynamic settings for Paleoproterozoic gold mineralization in the Svecofennian domain: a tectonic model for the Fäboliden orogenic gold deposit, northern Sweden: *Ore Geology Reviews*, v. 48, p. 403-412.
- Cavalcante, G.C.G, 2009, Tectonic geometry, kinematics and modelling of the Vila Nova Group rocks in the Pedra Branca do Amapari region in AP: M.Sc. thesis, Belém, Brazil, Federal University of Pará, 168 p.
- Eilu, P.K., Mathison, C.I., Groves, D.I., and Allardyce, W.J., 1999, Atlas of alteration assemblages, styles and zoning in orogenic lode-gold deposits in a variety of host rock and metamorphic settings: Perth, The University of Western Australia Publication, 30, 50 p.
- Gebre-Mariam, M., Hagemann, S.G., and Groves, D.I., 1995, A classification scheme for epigenetic Archaean lode-gold deposits: *Mineralium Deposita*, v. 30, p. 408–410.
- Goldfarb, R.J., and Groves, D.I., 2015, Orogenic gold: Common vs evolving fluid and metal sources through time.: *Lithos*, v. 223, p. 2–26.
- Goldfarb, R.J., Groves, D.I., and Gardoll, S., 2001, Orogenic gold and geologic time: A global synthesis: *Ore Geology Reviews*, v. 18, p. 1–75.
- Goldfarb, R.J., Baker, T., Dubé, B., Groves, D.I., Hart, C.J.R., and Gosselin, P., 2005, Distribution, character, and genesis of gold deposits in metamorphic terranes: *Economic Geology 100th Anniversary*, p. 407–450.
- Groves, D.I., Goldfarb, R.J., Gebre-Mariam, M., Hagemann, S.G., and Robert, F., 1998, Orogenic gold deposits: A proposed classification in the context of their crustal distribution and relationship to other gold deposit types: *Ore Geology Reviews*, v. 13, p. 7–27
- Groves, D.I., Santosh, M., and Zhang, L., 2020, A scale-integrated exploration model for orogenic gold deposits based on a mineral system approach: *Geoscience Frontiers*, v. 11, p. 719-738.
- Holdaway, M.J., 2000, Application of new experimental and garnet Margules data to the garnet-biotite geothermometer: *American Mineralogist*, v. 85 (7), p. 881-892.
- Horikava, E.H., 2008, Geoquímica de Solo e Geologia da Região do Depósito de Ouro do Amapari – AP: M.Sc thesis, Belo Horizonte, Brazil, Federal University of Minas Gerais, 2 vol.
- McReath, I., and Faraco, M.T.L., 2006, Paleoproterozoic Granite-Greenstone Belts in Northern Brazil and the Former Guyana Shield – West African Craton Province: *Geologia USP Série Científica*, v. 5 (2), p. 49-63.
- Meinert, L.D., Dipple, G.M., and Nicolescu, S., 2005, World Skarn Deposits, in Hedenquist, J.W., Thompson, J.F.H., Goldfarb, R.J., and Richards, J.P., eds., *Economic Geology 100th Anniversary Volume*: Littleton, Society of Economic Geologists, p. 299-336.
- Melo, L.V., 2001, Estudo do campo Urucum do depósito Amapari, Amapá, com base em dados petrográficos, de química mineral e microtermométricos: M.Sc. thesis, Belém, Brazil, Federal University of Pará, 112 p. (in Portuguese with English abs.).
- Mizuochi, H., Satish-Kumar, M., Motoyoshi, Y., and Michibayashi, K., 2010, Exsolution of dolomite and application of calcite-dolomite solvus geothermometry in high-grade marbles: An example from Skallevikshalsen, East Antarctica: *Journal of Metamorphic Geology*, v. 28, p. 509-526.

- Mueller, A.G., 1991, The Savage Lode magnesian skarn in the Marvel Loch gold-silver mine, Southern Cross greenstone belt, Western Australia. Part 1: Structural setting, petrography, and geochemistry: *Canadian Journal of Earth Sciences*, v. 28, p. 659–685.
- Mueller, A.G., 1997, The Nevoria gold skarn deposit in Archean iron formation, Southern Cross greenstone belt, Western Australia: Tectonic setting, petrography, and classification: *Economic Geology*, v. 92, p. 181–209.
- Ricci, P.S.F., Carvalho, J.M.A., Rosa-Costa, L.T., Klein, E.L., Vasquez, M.L., Vale, A.G., Macambira, E.M.B., and Araújo, O.J.B., 2001, *Geologia e recursos minerais do Projeto RENCA - Fase I: Brazilian Geological Survey*, Belém, Brazil, 69 p. (in Portuguese).
- Scarpelli, W., and Horikava, E.H., 2017, Gold, iron and manganese in central Amapá, Brazil: *Brazilian Journal of Geology*, v. 47 (4), p. 703-721.

Preliminary Lithostratigraphy of the Rhyacian Greenstone Belts of Northern Guyana and Suriname

Michael Tedeschi*

*Harquail School of Earth Sciences,
Laurentian University, 935 Ramsey
Lake Road, Sudbury, ON, Canada*
mtedesch@laurentian.ca

Stéphane Perrouty

*Harquail School of Earth Sciences,
Laurentian University, 935 Ramsey
Lake Road, Sudbury, ON, Canada*
sperrouty@laurentian.ca

La Donna Fredericks

*Guyana Geology and Mines
Commission, Upper Brickdam,
Georgetown, Guyana*
ladonna_fredericks@yahoo.com

Marc Bardoux

*Barrick Gold Corporation
161 Bay Street
Toronto, ON, Canada*
mbardoux@barrick.com

SUMMARY

A four-part preliminary stratigraphic sequence for the Rhyacian greenstone belts has been observed in both Guyana and Suriname. Similar sequences of mafic and intermediate-felsic volcanic rocks and correlations between large siliciclastic basins suggests a similar mode of formation across the Trans-Amazonian Province. More precise timing relationships between these components will be tested with new geochronological studies of volcanic and sedimentary rocks collected in the various transects. Units such as the Muruwa Formation and Orocaima Group do not belong to the greenstone belt sequence and were likely deposited after a considerable period of uplift and erosion following the Trans-Amazonian Orogeny. The lithostratigraphic boundaries revealed by this study such as those between siliciclastic basins and the mafic volcanic / calc-alkaline sequences may be indicative of the early crustal structure and thus may provide an important guide to future exploration efforts.

Key words: Greenstone Belt, Lithostratigraphy, Guiana Shield, Trans-Amazonian Orogeny, Mineral Exploration.

INTRODUCTION

The Guiana Shield of South America is one of the last true frontiers for gold exploration. Over the last 50 years several world-class gold deposits have been discovered in Rhyacian-age greenstone belts (2.2-2.1 Ga), including the 18 Moz Rosebel Mine and the 24 Moz El Callao district, indicating the high exploration potential of the region. However, overall Au resources, production and exploration spending are minor compared to the analogous Baoule-Mossi Domain of the West Africa Craton. This disparity is likely due to factors including difficult terrain, challenging access, and geopolitics; however, a lack of a modern lithostratigraphic and structural framework across this vast region also hampers exploration efforts. Although geological investigations in Guyana and Suriname have been undertaken for over two centuries, the region has largely been ignored by the geoscience community since the 1970s, missing several generations' worth of modern ideas, methods, and analytical advances. Furthermore, a great deal of this historical work, much of which is of high quality, has sat unpublished in scattered libraries around the world (or lost) and thus has been largely inaccessible. This stagnation has left the understanding of greenstone belt lithostratigraphy in Guyana and Suriname bound by antiquated geological interpretations and divided by varied and complex local naming conventions. Furthermore, the structural evolution of the region has been oversimplified and the timing and kinematics of the major zones of deformation, the key regional controls of mineral deposits have only been studied at the local scale.

To address these shortcomings, this study seeks to unravel the regional lithostratigraphy through detailed geological mapping of key transects across greenstone belts in both Guyana and Suriname and the reinterpretation of historical datasets. Petrography, whole rock geochemistry and the first comprehensive geochronology study will provide further constraints on the composition and timing of these rocks. This will allow for new interpretations of the paleo-tectonic environment of greenstone deposition, their early architecture and insight into the tectonic processes which have deformed them and created pathways for mineralizing fluids.

BACKGROUND

Rhyacian rocks of the Trans-Amazon Province are found on the NE margin of the Guiana Shield. Further south, rocks decrease in age and are interpreted to represent multiple accretionary and anorogenic magmatic events (Gibbs and Barron, 1993). NW-SE trending granitoid-greenstone belts of Rhyacian age are bounded by a lesser component of Mesoarchean rocks in the NW (Imataca Complex) and Neoproterozoic rocks in SE (Amapá Block). Rhyacian greenstone belts are known by a variety of names including the Barama-Mazaruni Supergroup in Guyana, Pastora Group in Venezuela, Marowijne Supergroup in Suriname, Paramaca Supergroup in French Guiana, and Vila Nova Group in Brazil, and all have been considered to be tectono-stratigraphically equivalent (Gibbs, 1980; Gibbs and Barron, 1993; Delor et al., 2003b). Each belt comprises metamorphosed sequences of mafic to felsic volcanic and volcanoclastic rocks overlain by clastic sedimentary basins with an estimated thickness of 8-10 km (Gibbs, 1980). In Suriname and French Guiana, greenstones are overlain by late alluvial/fluviol basins of the Rosebel Formation in

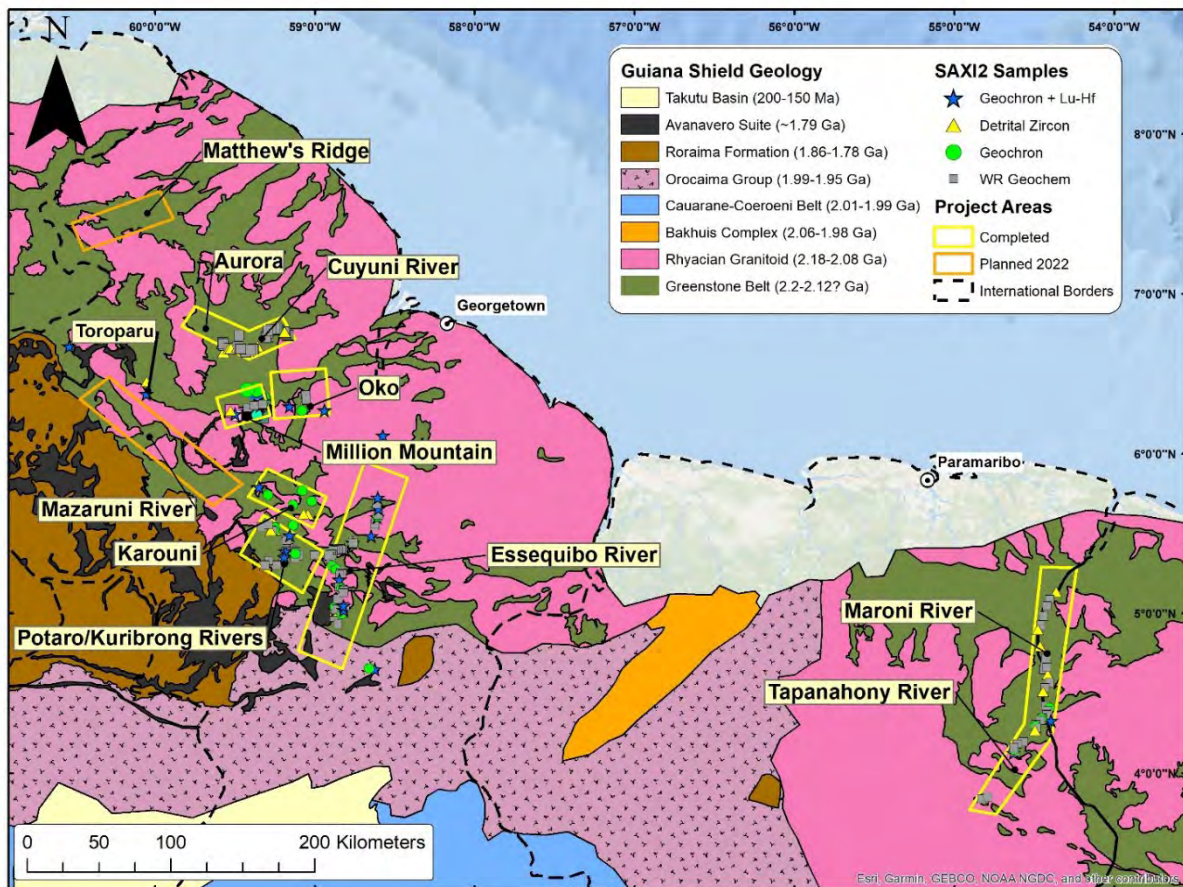


Figure 12 Regional Geological Map of northern Guyana and Suriname (compiled from the national geological maps of Guyana and Suriname) showing field areas and sample locations

Suriname or the Upper Sedimentary Unit in French Guiana (De Vletter, 1984; Vanderhaeghe et al., 1998; Delor et al., 2003b). Other clastic sequences of the Muruwa Formation in Guyana and the Ston Formation in Suriname have an unknown age but are stratigraphically younger than the Greenstones. Voluminous felsic volcanic rocks of the Orocaima Group overlie the Muruwa/Ston Formation and have been dated to 1.99 Ga (Fraga et al., 2017) and they are in turn overlain unconformably by thick sandstones and conglomerates of the Roraima Group (Figure 1).

The greenstone belts are divided by voluminous granitoid masses grouped in two main pulses: a first pulse coeval with greenstone belt oceanic magmatism (2.16-2.14 Ga), and a second pulse with collision magmatism (2.11-2.09 Ga; Delor et al., 2003a; Tedeschi et al., 2020). Rhyacian supracrustal sequences and coeval granitoids were deformed in a 100Ma

long deformation cycle referred to as the Trans-Amazonian orogeny, interpreted to be caused by the collision with the Archean Kenema-Man Craton of West Africa (Delor et al., 2003b). However, it is not clear that Kenema-Man Craton was responsible for such deformation in the Guiana Shield (Voicu et al., 2001; Ernst and Bardoux, 2017)

RESEARCH APPROACH

Maps, cross-sections, stratigraphic columns, and structural analyses were produced from six traverses on the major rivers of Guyana and Suriname. Traverses were completed along the Essequibo, Potaro, Kuribrong, Mazaruni, Maroni and Tapanahony rivers. Additional mapping was conducted in an around exploration sites and mines including Karouni, Oko, Million Mountain, Toroparu, Aurora, and Matthew's Ridge. Additional samples and data were donated by industry partners. Samples were analyzed for petrography, whole rock geochemistry and geochronology, both felsic volcanic rocks and detrital zircon studies of metasedimentary rocks. Best efforts are made to obtain fresh, unaltered rock but in cases where these are not available, samples of clean, in-situ saprolite were used instead. These results are then integrated with historical mapping data and regional geophysical datasets to build a new 1:1,000,000 scale geological map for the region.

PRELIMINARY RESULTS

The initial results of our mapping in Guyana and Suriname show that greenstone belt stratigraphy can be divided into four general units:

- 1) A dominantly mafic volcanic sequence including massive to pillowed tholeiitic basalts (Voicu, 1999), volcanoclastic rocks and lesser laminated siltstones, carbonaceous shales, and chert. Ultramafic intrusive rocks are rare but have been noted in the vicinity of the Karouni Mine. Sedimentary units within this unit are notable for their overall lack of quartz and dominance of detrital feldspar and phyllosilicate minerals. Localities for this unit include Karouni, Omai, Oko and Toroparu. Geochronological constraints provided by a cross-cutting intermediate porphyry dike at Karouni suggest this unit is older than $2147 \pm$ Ma (Tedeschi et al., 2020).
- 2) Intermediate to felsic calc-alkaline volcanic rocks has been observed in a continuous belt exposed on the Essequibo, Potaro and Kuribrong rivers in Guyana. This consists of flows of porphyritic andesite, dacite, rhyolite, felsic tuffs, volcanoclastic breccias and lesser laminated sedimentary rocks. Possible equivalents have been observed in the vicinity of Million Mountain, at Toroparu, and on the Tapanahony river in Suriname. Rhyolite and andesite samples will be utilized for geochronology to establish the age of this unit.
- 3) A sequence of siliciclastic sediments in large basins. In the approximately 60 km wide Armina Basin, exposed in the Maroni River, these rocks consist of fine to medium grained turbiditic sandstone and shale, metamorphosed from mid greenschist to lower amphibolite facies. The 30 km wide Cuyuni Basin in Guyana consists of lower greenschist facies basal conglomerates overlain by coarse to fine sandstone, lesser siltstone and minor intercalated intermediate to felsic volcanic rocks, exposed on the Cuyuni River and further south in the Million Mountain and Aremu regions. At the Million Mountain Au prospect, this unit is found in thrust contact with the underlying andesites. Detrital zircon samples from this unit will be used to establish its maximum depositional age and interbedded felsic volcanic rocks should provide an absolute age of deposition.
- 4) A sequence of alluvial/fluviol sedimentary rocks known in Suriname as the Rosebel Formation. Although it is best represented at its type locality at the Rosebel Mine, an unconnected but similar basin outcrops in the Maroni river where it is approximately 20 km across. It consists of moderately dipping, thickly bedded conglomerate and sandstone with the trough cross-bedding and magnetite grains typical of the Rosebel Formation. Similar basins is have yet to be identified in Guyana. At Rosebel, a detrital zircon study by Daoust, (2016), suggests a maximum depositional age of ~ 2110 Ma.

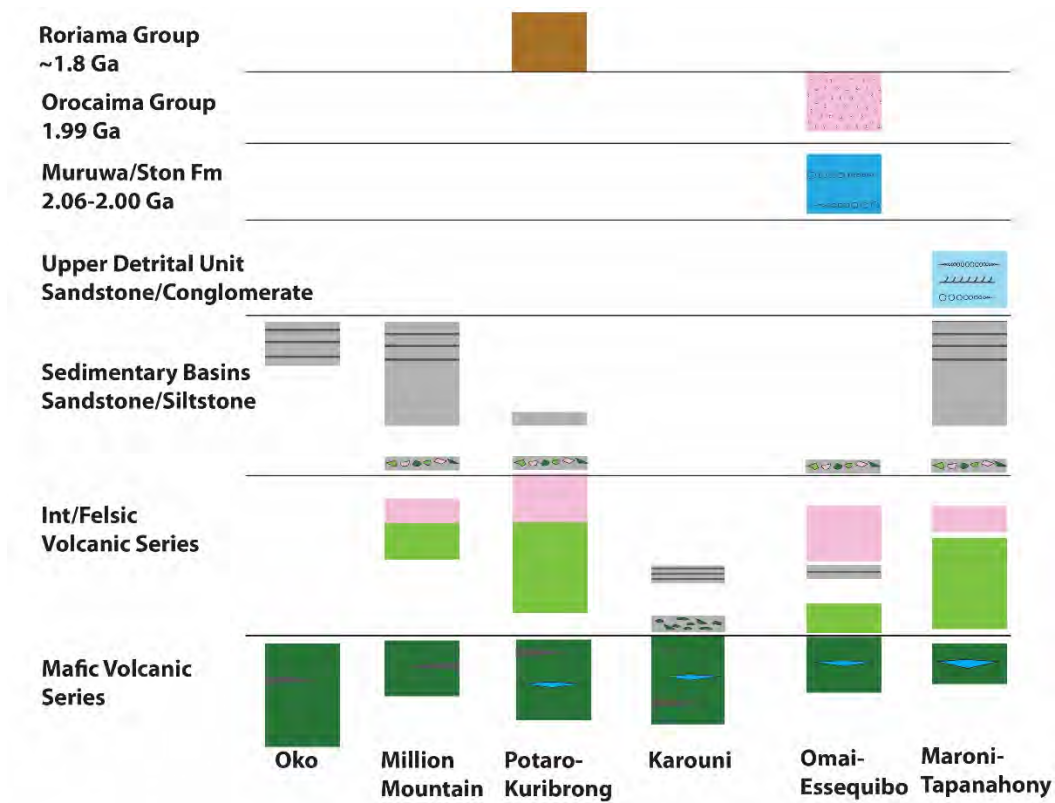


Figure 13 Preliminary stratigraphic correlations

Additional stratigraphic units such as the sandstone/conglomerate of the Muruwa and Roraima Formations and the felsic volcanics of Orocaima Group (known in Guyana as the Iwokrama Formation) are stratigraphically above the greenstone belts and show clear unconformable relationships and a lack of Rhyacian deformation. On the Essequibo River, the contact between steeply dipping, amphibolite facies metasedimentary rocks and the flat lying, unmetamorphosed Muruwa Formation is represented by an angular unconformity. The Muruwa Formation is in turn overlain by and may be intercalated with the felsic volcanic rocks of the Orocaima Group. A similar unconformable relationship was noted on the Potaro River between steeply dipping Rhyacian metasedimentary rocks and flat laying sandstone of the Roraima Formation.

CONCLUSION

A four-part preliminary stratigraphic sequence for the greenstone belts has been observed in both Guyana and Suriname. Similar sequences of mafic and intermediate-felsic volcanic rocks and correlations between large siliciclastic basins suggests a similar mode of formation across the Trans-Amazonian Province. More precise timing relationships between these components will be tested with new geochronological studies of volcanic and sedimentary rocks collected in the various transects. Units such as the Muruwa Formation and Orocaima Group do not belong to the greenstone belt sequence and were likely deposited after a considerable period of uplift and erosion following the Trans-Amazonian Orogeny. The lithostratigraphic boundaries revealed by this study such as those between siliciclastic basins and the mafic volcanic / calc-alkaline sequences may be indicative of the early crustal structure and thus may provide an important guide to future exploration efforts.

REFERENCES

- Bardoux, M and Ernst, R., 2017. From LIPs To Gold In Rhyacian Metawackes. Society for Geology Applied to Mineral Deposits 14th Biennial Meeting, August 20-23rd, 2017, Extended Abstracts, p. 229-232.
- Daoust, C., 2016. Caractérisation stratigraphique, structurale et géochimique du district minéralisé de Rosebel (Suriname) dans le Cadre de l'évolution géodynamique de Bouclier Guyanais. PhD Thesis. Université du Québec à Montréal, Montréal, pp. 330. Gibbs, 1980
- Delor, C., Lahondère, D., Egal Cocherie, E., Lafon, A., Guerrot, C., Rossi, P., Truffet, C., Theveniaut, H., Phillips, P., Avelar, V.G., 2003a. Transamazonian crustal growth and reworking as revealed by the 1: 500000 scale geological map of French Guiana. *Géol. France* 2-3-4, 5–57.
- Delor, C., de Roever, E.W.F., Lafon, J.-M., Lahondère, D., Rossi, P., Cocherie, A., Guerrot, C., Potrel, A., 2003b. The Bakhuis ultra-high-temperature granulite belt (Suriname): II. Implications for the late Transamazonian crustal stretching in a revised Guiana Shield framework. *Geol. France* 2-3-4, 207–230.
- Gibbs, A.K., 1980. Geology of the Barama-Mazaruni Supergroup of Guyana: Unpublished Ph.D. Thesis. Harvard University, Cambridge, MA, pp. 385.
- Gibbs, A.K., Barron, C.N., 1993. Geology of the Guiana Shield. Oxford University Press, Oxford, pp. 246.
- Tedeschi, M.T., Hagemann, S.G., Kemp, A.I.S., Kirkland, C.L. and Ireland, T.R., 2020. Geochronological constraints on the timing of magmatism, deformation and mineralization at the Karouni orogenic gold deposit: Guyana, South America. *Precambrian Research*, 337, p.105329.
- Voicu, G., Bardoux, M., Stevenson, R., 2001. Lithostratigraphy, geochronology and gold metallogeny in the northern Guiana Shield South America: a review. *Ore Geol. Rev.* 18, 211–236.
- Voicu, G., Bardoux, M., Jébrak, M., Crépeau, R., 1999. Structural, Mineralogical, and Geochemical Studies of the Paleoproterozoic Omai Gold Deposit, Guyana. *Econ. Geol.* 94, 1277–1304.

Rhyacian crustal evolution of the Guyana Shield revealed through U-Pb and Lu-Hf analyses

Nicolas Thébaud*

*School of Earth Sciences, CET,
UWA, 35 Stirling Highway
Crawley WA6009
nicolas.thebaud@uwa.edu.au*

Michael Tedeschi

*Harquail School of Earth Sciences,
Laurentian University,
935 Ramsay Lake Rd.
Sudbury, ON, Canada
mteschi@laurentian.ca*

SUMMARY

Continental lithosphere growth and evolution is intimately associated to the metallogenic process that led to metal accumulation in the Earth crust. This study presents in-situ U-Pb and Lu-Hf isotope analyses carried out on single zircon grains separated from plutonic complexes from Guyana and Surinam with the objective to shed light on the process leading to the formation of the Guyana Shield. We analysed ten samples and show that crustal growth during the Rhyacian at ca. 2300 to 2100 Ma was predominately the result of juvenile crust formation associated with island arc composition evolving into continental arc and later to a continent-to-continent collision setting over ~200Ma. Such crustal growth appears to have formed in proximity to pre-existing Archean crust pointing towards a complex crustal architecture which is likely to have influenced the formation of mineral systems (e.g. Au) in the region. This record echoes greatly with that recorded in the anciently neighbouring West African Craton which shared a common Paleoproterozoic history. Our preliminary yet sparse dataset warrants further investigation so that the lithospheric architecture of the Guyana Shield may be further constrained. Such dataset may reveal critical to further unravel the metallogenic evolution and spatial distribution of major ore systems in the region.

Key words: Guyana Shield, Rhyacian crustal evolution, U-Pb geochronology and Lu-Hf isotopic geochemistry, Metallogenic evolution

INTRODUCTION

A large number of studies have demonstrated that the combination of in-situ U-Pb and Lu-Hf isotope analyses carried out on single zircon grains provides a powerful tool to further understand crustal formation and reworking processes through time (e.g. Eglinger et al., 2017). When combined with lithogeochemical data, such analysis may help to fingerprint the different magma sources at play through the crust formation processes and therefore help for the definition of the geodynamic models at play in the Precambrian. In parallel, it is notable that mineral deposits are a local manifestation of a range of earth processes that take place at different temporal and spatial scales (e.g., Bierlein et al., 2006; McCuaig et al., 2010). At the lithospheric scale geodynamic processes and associated lithospheric structures are commonly proposed to apply a strong control on metal endowment of mineralised provinces (Begg et al. 2014). Increasing high-resolution geochronological constraints on ore deposits further suggest that deposits form during a very narrow time interval over a prolonged geodynamic evolution; suggesting a transient regional scale geodynamic setting (i.e. tectonic plate reorganisation, geodynamic transition from long compression period to a period of transcurrent tectonic (Goldfarb et al., 2005). Within such transient geodynamic process, inferred basement architecture is proposed to apply a first order control on mineralised camp localisation. Often cryptic in the rock record, such architecture may be imaged through mapping of geochemical and isotopic geochemistry domains (Mole et al., 2014). In this paper, we present the initial results of in-situ U-Pb and Lu-Hf isotope acquired on plutonic samples from Guyana and Surinam in order to evaluate the crustal evolution of the Guyana Shield from the Archean to the Proterozoic.

RESEARCH APPROACH

Ten samples of plutonic rocks were collected in the field (Guyana) as well as sourced from existing sample collections (Surinam). Zircon grains were separated from 1-5 kg rock samples powdered with a jaw crusher and a roller mill and concentrated using heavy liquids (bromoform: density = 2.84 g/cm³; diiodomethane: density = 3.31 g/cm³) and a Frantz isodynamic magnetic separator. Individual grains were handpicked, mounted in epoxy blocks, and polished to expose their cores at the University of Western Australia. Prior to in-situ isotope analyses the internal texture of each grain was characterized by means of cathodoluminescence (CL) and back scattered electron (BSE) imaging performed with a Tescan Vega-3 scanned electron microscope at the Centre for Microscopy, Characterisation and Analysis of the University of Western Australia in Perth.

U-Pb analysis was carried out utilizing secondary ion mass spectrometry (SHRIMP-RG) at the Research School of Earth Science at the Australian National University, Canberra. U-Pb reference zircons used were CUYZ (207Pb/206Pb age of 569.49 Ma; A. Kennedy, Personal Communication, 2017) and OGC-1 (207Pb/206Pb age of 3465.4 ± 0.6 Ma; Stern et al., 2009); SL13 was used for U concentration calibration. Setup and operating parameters are outlined in Ireland and Williams, 2003 and Ireland et al., 2008. Raw U-Pb-Th data was reduced with the program SQUID (Ludwig, 2003) and processed using IsoPlot (Ludwig, 2009). The common Pb correction followed the 204Pb method using the terrestrial Pb model of Stacey and Kramers (1975).

Once dated, the samples were analysed for hafnium composition on selected zircon pits previously analysed with the SHRIMP-RG. In situ measurements of Lu–Hf isotopes were carried out using a GeoLas ArF gas (193 nm) laser ablation system coupled to a Thermo Finnigan Neptune Multicollector ICPMS at the University of Western Australia. The instrumental set-up has been described by Kemp et al. (2009) and Naraa et al. (2012). Data were obtained with a laser fluence of 5–6 J/cm², ablation rate of 4 Hz and a laser pulse repetition rate over a 60 second ablation period. Beam diameter was 31, 42 or 58 μm, depending on the size of the targeted zircon growth phase. Care was taken to ensure that the analytical site was within the same CL-defined growth domain from where the age data were obtained.

All zircon Hf isotope data (samples and reference zircons Temora-2 and, FC-1) are normalized to the solution ¹⁷⁶Hf/¹⁷⁷Hf value of Mud Tank zircon (0.282507 ± 6, Woodhead and Hergt (2005), reported relative to JMC 475 ¹⁷⁶Hf/¹⁷⁷Hf = 0.282160) using the laser ablation data generated from this zircon in each analytical session. Analytical uncertainties combine the in-run error with the reproducibility of Mud Tank zircon analyses from the same session, added in quadrature. Hf isotope data for reference zircons Temora-2, FC-1. Data are quoted at 2 standard deviations. Analytical uncertainties combine the in-run error with the reproducibility of Mud Tank zircon analyses from the same session, added in quadrature.

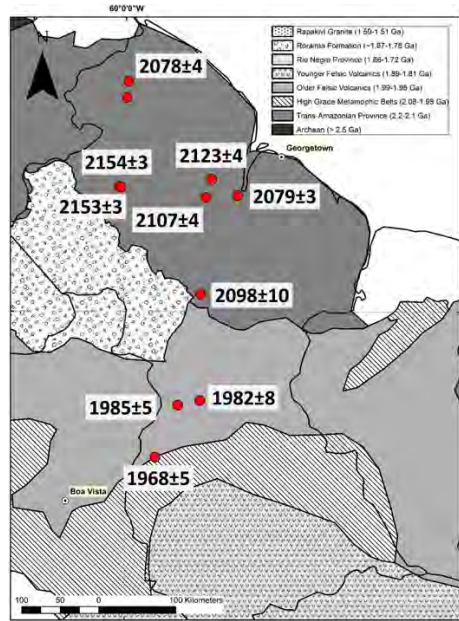


Figure 14: Geological map of Guyana showing the localisation of the samples analysed. The ages provided were calculated from zircon SHRIMP-RG analyses (weighted mean $^{207}\text{Pb}/^{206}\text{Pb}$).

RESULTS

The samples analysed returned a range of igneous crystallization ages from 2154 to 1982 Ma with concordant $^{207}\text{Pb}/^{206}\text{Pb}$ weighted means (Figure 1). The samples display inherited grains with ages spanning from the Neoproterozoic to the Paleoproterozoic. Specifically, most samples returned Trans-Amazanian zircons up to ~2200 Ma. Samples from the Iwokrama rocks returned inheritance between 2000 and 2029 Ma whereas biotite-garnet gneiss from the Kanuku Complex returned inherited grains between 1985 and 2057 Ma and one Archean aged inherited grain (2635 ± 30 Ma). Metamorphic rims analysed from Kanuku Complex zircons were dated at 1968 ± 5 Ma. Lu-Hf data acquired during SAXI 1 in Surinam and Guyana show mainly superchondritic ϵHf values comprised between -6.15 and +4.89 pointing toward juvenile crust extraction from a depleted mantle (TDMc= 2.2 to 2.4 Ga) source with little contribution from Archean crustal material.

DISCUSSION

The older ages obtained in this study fit well into the D1, D2a, D2b of the Trans-Amazanian Orogeny (Delor et al., 2003) whereas the youngest ages obtained appear to belong to the Oroaima/Surumu Volcanic Event (D2c) (Figure 2).

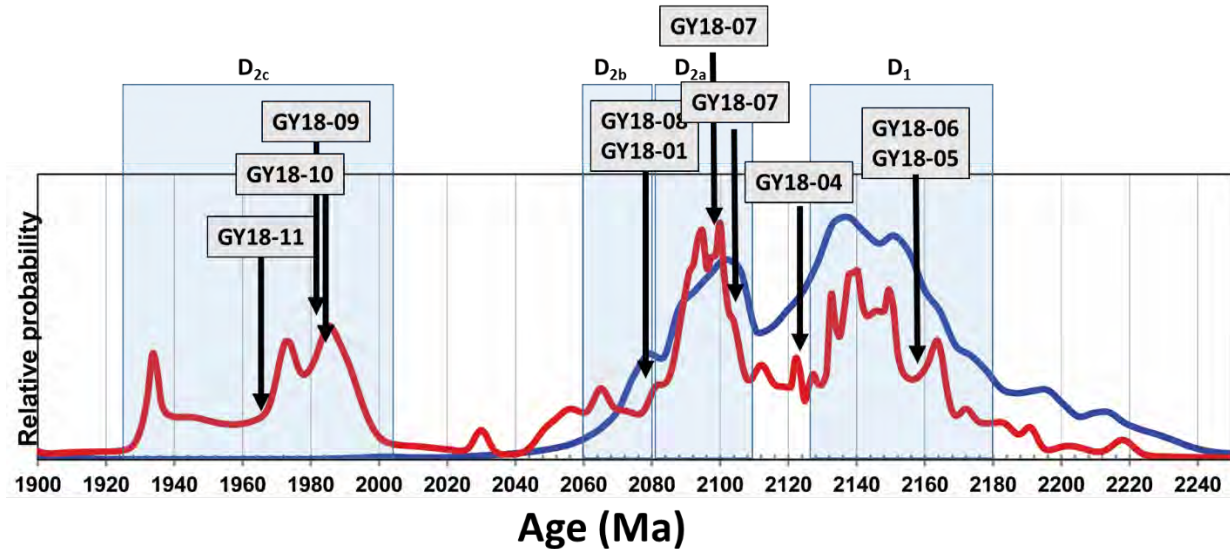


Figure 2: Probability diagram of a compilation of U-Pb zircon geochronology from the Guiana Shield (Tedeschi et al., 2020) with the interpreted orogenic stages (Delor et al., 2003) and results of this study.

Lu-Hf analyses produce a range of values controlled primarily by mixing between the original melt source and crustal (unradiogenic) material. This may occur via a number of processes, but recycling of the crust, juvenile or evolved, to a more reworked composition and the addition of juvenile material to a reworked source (or vice-versa) are causes commonly proposed to explain $^{176}\text{Hf}/^{177}\text{Hf}$ data arrays. The range of values produced for a suite of analyses is controlled by the difference in crustal residence age (TDMc) between the original melt and the contaminant. If the initial melt is contaminated by very old material, then the range may be large, representing in part the initial melt (more +ve ϵHf values if juvenile) and the older crust (-ve ϵHf values) (Mole et al., 2012). In both cases the 'whole-rock' representative Lu-Hf isotopic composition of the final fluid/magma and subsequently the crystallised rock, is the combination and mixture of both these sources.

Lu-Hf data acquired on Paleoproterozoic zircons from the Guyana Shield exhibit ϵHf values between -6.15 and +4.89 pointing toward juvenile crust extraction from a depleted mantle (TDMc= 2.2 to 2.4 Ga) source with little contribution from Archean crustal material (Figure 3). Interestingly, the samples analysed in this study show a downwards trend of ϵHf values with age, suggesting that the younger magmatic events dated at ca. 1980 Ma and even ca. 2080 Ma progressively reworked early juvenile crustal input dated at ca. 2160 Ma. Such trend is characteristic of progressive crustal thickening associated with a convergent tectonic context. One sample GY18-01 from Northern Guyana exhibits ϵHf values comprised between -5.95 and -6.15 suggesting the reworking of Archean crust with modelled age extraction dated at (TDMc) 3.09 to 3.14 Ga. This sample highlights the fact that although dominantly juvenile, the Guyana Shield crust evolution derived from the progressive and complex agglomeration of crustal blocks, some of which of Archean origin. Specifically, the limited data available to date suggest the juvenile input of Paleoproterozoic crust between the Amapa region to the South and the Imataca complex to the North. The localised presence of reworked Archean crust in Northern Guyana suggests that such juvenile crustal growth developed in proximity to pre-existing crust, pointing towards a complex crustal architecture.

Previous isotopic studies conducted in the West African Craton (Parra-Avila et al., (2015)) which represent the eastern extension of the Guyana Shield highlighted similar trend suggesting that the crustal growth during the Rycian at ca. 2300 to 2100 Ma was predominately the result of juvenile crust formation associated with island arc composition evolving into continental arc and later to a continent-to-continent collision setting. The results presented here show a similar trend.

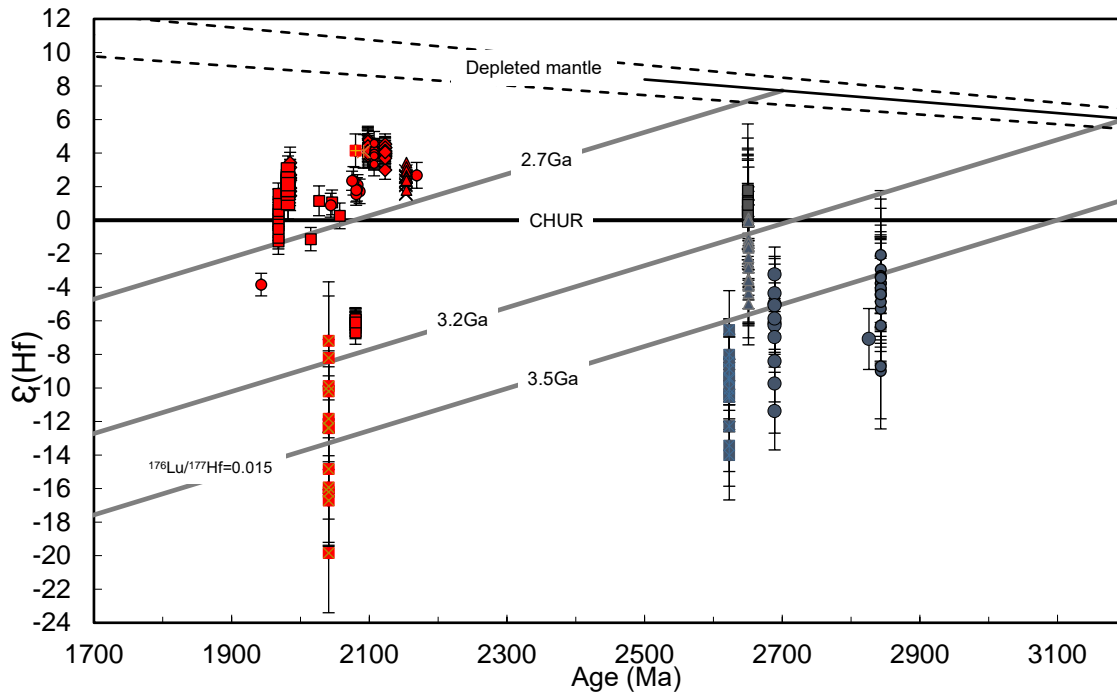


Figure 3: $\epsilon(\text{Hf})$ vs age plot for new (red) and published (grey) data. Published data were sourced from Neto and Lafon, 2019.

CONCLUSIONS

Our initial study of the crustal evolution of the Guyana shield suggest that the Paleoproterozoic continental lithosphere developed through a major episode of juvenile mantle extraction at ca. 2160 Ma in the vicinity of pre-existing Archean crustal blocks (Amapá and Imataca complexes). Ongoing plutonism that spans nearly ~200 Ma lead to further progressive reworking of the juvenile Paleoproterozoic crust in a convergent tectonic setting. Such evolution mimics that recorded in the West African Craton which preserves Rhyacian granite-greenstone belts of similar age.

Ore-forming processes involve the concomitant development of several critical elements including a favourable lithosphere architecture (e.g. McCuaig et al., 2014). As proposed by Bierlein et al. (2006), it is suggested that the thickness of subcontinental lithospheric mantle at the time of ore deposit formation (e.g. Au and Ni) controls the potential for giant mineral systems: the thinner the SCLM, the greater the potential for high heat flux and metal transfers across the continental lithosphere. Accordingly, region of increased juvenile magmatic input ($\epsilon\text{Hf} > 0$) have been proposed to represent regions of increased prospectivity for nickel and gold mineralisation (Mole et al., 2014). Accordingly, the data presented here show that Paleoproterozoic terranes from Guyana and adjacent Surinam are indeed associated with the occurrence of juvenile crustal during the Paleoproterozoic and are accordingly prospective for metal accumulation. Further analyses are currently underway to further document the crustal evolution of the Guyana Shield and unravel its metallogenic record.

ACKNOWLEDGMENTS

This work was supported through the South American Exploration Initiative (SAXI). We acknowledge AMIRA Global and industry sponsors. We acknowledge the assistance of the Guyana Geology and Mines Commission and especially La Donna Fredericks for facilitating field work in Guyana and Leo Kringsman and Salomon Kroonenberg for supplying samples from Surinam.

REFERENCES

- Begg, G.C., Griffin, W.L., Natapov, L.M., O'Reilly, S.Y., Grand, S., O'Neill, C.J., Hronsky, J.M.A., Poudjom Djomani, Y., Deen, T., and Bowden, P. 2009, The lithospheric architecture of Africa: Seismic tomography, mantle petrology and tectonic evolution: *Geosphere*, v. 5, p. 23–50
- Bierlein, F.P., Groves, D.I., Goldfarb, R.J., and Dubé, B., 2006. Lithospheric controls on the formation of provinces hosting giant orogenic gold deposits. *Mineralium Deposita* 40, 874-886.
- Delor, C., de Roever, E.W.F., Lafon, J.-M., Lahondère, D., Rossi, P., Cocherie, A., Guerrot, C., Potrel, A., 2003b. The Bakhuis ultra-high-temperature granulite belt (Suriname): II. Implications for the late Transamazonian crustal stretching in a revised Guiana Shield framework. *Geol. France* 2-3-4, 207–230.
- Eglinger A., Thébaud N., Zeh A., Davis J., Miller J., Parra-Avila L.A., Loucks R., McCuaig C., Belousova E. (2017) New insights into the crustal growth of the Paleoproterozoic margin of the Archean Kéména-Man domain, West African craton (Guinea): Implications for gold mineral system, *Precambrian Research* 292, 258-289
- Goldfarb, R.J., Baker, T., Dubé, D., Groves, D.I., Hart, C.J.R., and Gosselin, P., 2005, distribution, character, and genesis of gold deposits in metamorphic terranes: *Economic Geology 100th Anniversary Volume*, p. 407–450.
- Ludwig, K.R., 2009. SQUID 2: a user's manual: Berkeley Geochronology Center Special. Publication 2, 100.
- Ludwig, K.R., 2003. User's manual for a geochronological toolkit for Microsoft Excel (Isoplot/Ex version 3.0). *Berkeley Geochronol. Cent. Spec. Publ.* 4, 1–71.
- McCuaig, T.C., Hronsky, J.M.A., 2014. The mineral system concept: the key to exploration targeting. *Econ. Geol. Spec. Publ.* 18,153–175.
- Mole DR, Fiorentini ML, Thebaud N, Cassidy KF, McCuaig TC, Kirkland CL, Romano SS, Doublier MP, Belousova EA, Barnes SJ, Miller J (2014) Archean komatiite volcanism controlled by the evolution of early continents, *Proceedings of the National Academy of Sciences* 111 (28), 10083-10088
- Næraa, T., Scherstén, A., Rosing, M.T., Kemp, A.I.S., Hoffmann, J.E., Kokfelt, T.F., Whitehouse, M.J., 2012. Hafnium isotope evidence for a transition in the dynamics of continental growth 3.2 Gyr ago. *Nature* 485, 627–630. <https://doi.org/10.1038/nature11140>
- Parra-Avila, L.A., 2015. 4D Evolution of the Paleoproterozoic Baoul.-Mossi domain of the West African Craton. Unpublished Ph.D. Thesis, The University of Western Australia.
- Scherer, E., Münker, C., Mezger, K., 2001. Calibration of the lutetium-hafnium clock. *Science* 293, 683–687
- Segal, I., Halicz, L., Platzner, I.T., 2003. Accurate isotope ratio measurements of ytterbium by multiple collection inductively coupled plasma mass spectrometry applying erbium and hafnium in an improved double external normalization procedure. *J. Anal. At. Spectrom.* 18, 1217–1223. <https://doi.org/10.1039/B307016F>
- Tedeschi, M.T., Hagemann, S.G., Kemp, A.I.S., Kirkland, C.L. and Ireland, T.R., 2020. Geochronological constrains on the timing of magmatism, deformation and mineralization at the Karouni orogenic gold deposit: Guyana, South America. *Precambrian Research*, 337, p.105329.
- Stacey, J.S. and Kramers, J.D. (1975) Approximation of Terrestrial Lead Isotope Evolution by a Two-Stage Model. *Earth and Planetary Science Letters*, 26, 207-221.
- Vervoort, J.D., Patchett, P.J., Söderlund, U., Baker, M., 2004. Isotopic composition of Yb and the determination of Lu concentrations and Lu/Hf ratios by isotope dilution using MC-ICPMS. *Geochem. Geophys. Geosystems* 5. <https://doi.org/10.1029/2004GC000721>
- Woodhead, J., Hergt, J., Shelley, M., Eggins, S., Kemp, R., 2004. Zircon Hf-isotope analysis with an excimer laser, depth profiling, ablation of complex geometries, and concomitant age estimation. *Chem. Geol.* 209, 121–135.
- Woodhead, J.D., Hergt, J.M., 2005. A preliminary appraisal of seven natural zircon reference materials for in situ Hf isotope determination. *Geostand. Geoanalytical Res.* 29, 183–195.

Paleocene groundwater salinity mapping in coastal aquifers using geophysical well logs: A Suriname case study

Oclaya Verwey¹, Vanessa Sabajo¹, Jacobus Groen², Theo wong¹

¹Anton De Kom University of Suriname, Leysweg, Paramaribo, Suriname

²Groen Water Solutions, Leiden, Netherlands

SUMMARY

Geophysical well logs from oil exploration wells were analyzed in order to map groundwater salinity patterns from aquifers of different formations in the coastal plain of Suriname, which is part of the Guiana Basin. The well logs have been interpreted based on the Archie equation method using borehole resistivity, porosity and temperature to derive the chloride concentrations. Results from these analyses shows varying groundwater salinities from West to East of the country, whereas bodies of fresh groundwater were confirmed at several depths in the Zanderij, Coesewijne, Saramacca and Nickerie formation. The later revealed that there's a large body of fresh groundwater present in the Saramacca formation from Paleocene age. Comparison of calculated chlorite contents with well sample data shows that the calculated chloride contents appears to be higher than the actual chloride contents assuming an overestimation of the chloride contents by the used model. This may lead to possible larger contents of fresh groundwater.

Key words: groundwater exploration, groundwater salinity, coastal aquifers, hydrogeology.

INTRODUCTION

The coastal area of Suriname is part of the Guiana Basin, which consists of clastic Mesozoic and Cenozoic sediments. Groundwater research in the Suriname Guiana Basin is mainly focused on the most important and exploitable coastal aquifers in the Tertiary formations, which are forming the source for potable water supply to the population (HACAS, 2016). These groundwater bearing formations, consisting of the Burnside (A-sand) formation and the relatively shallower Coesewijne- and Zanderij formations are not homogeneous. The sand and clay strata in these formations are forming complex alternations with varying thicknesses (Hanou, 1981, Wong, 1989). Previous studies confirmed that groundwater in the coastal part of these formations is stagnant, quite old, 3000 to 35000 years BP (paleogroundwater) and is not recharged (UNDP/WHO, 1973; Verleur, 1991; Post, 1996; Groen, 2002). Several studies attempted to derive a groundwater salinity pattern for the coastal sediments of the deeper Saramacca formation (UNDP/WHO, 1973; Frederic. R. Harris, IWACO & SUNECON, 1991e; Groen et al, 2000a; Groen, 2002). The salinity pattern by Groen (2002) shows a gradually increase of the groundwater salinity near the coastline from fresh meteoric to saline marine groundwater, with chloride contents of <1000mg/l for the fossil groundwater.

RESEARCH APPROACH

A total of 54 available exploration oil well logs from Staatsolie, Suriname's state oil company have been used within this study. From these available logs a number of eight (8) North-South and one (1) East-West cross sections were made across the coastal plain using Petrel software. These boreholes have been drilled to great depths of >1000ft into the Nickerie formation descending from the "late Cretaceous" age. Gamma ray, resistivity and density data were retrieved from the well logs. Gamma ray logs are used to distinct clean sand strata based on the 80 gAPI criteria (Sabajo, 2016). The resistivity logs are used to retrieve the formation resistivity using the Archie's equation for clean sand strata ,based on earlier applied methodology by Groen et al (2000), while porosity was calculated based on the density logs (HACAS, 2016). The calculated porosity was used to determine a formation factor which linearly relates the formation resistivity to water resistivity (Groen et al, 2000a). An average geothermal gradient from UNDP/WHO (1973) was used to determine the formation temperature, which was then corrected to reference temperature. After correction the calculated water resistivity was converted to chloride concentrations in water making use of previous determined empirical relationship by Groen et al (2000a) and Groen (2000) (Hacas, 2016).

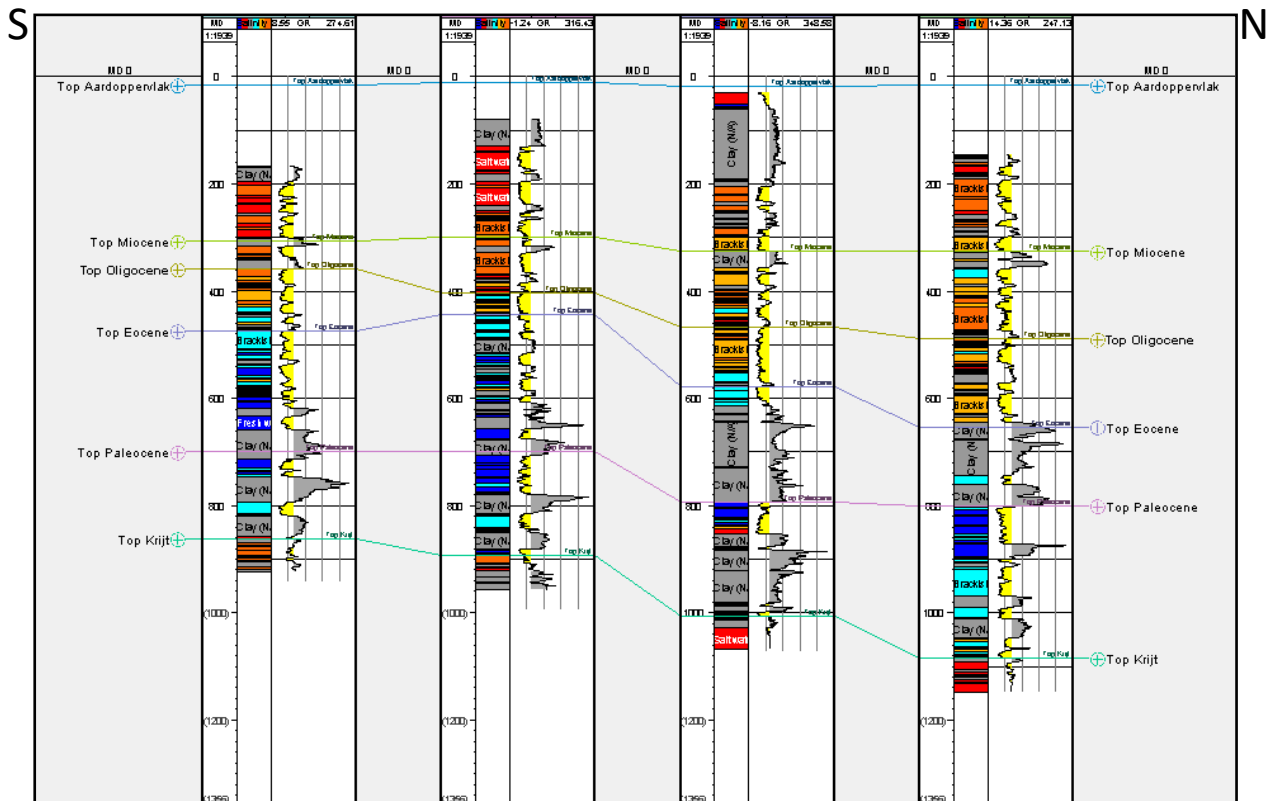


Figure 15: South – North cross section of geophysical well logs showing the gamma ray (GR) with interpreted sand (yellow) and clay (grey) layers. The column on the left shows the calculated groundwater salinity in several classes (Sabajo, V., 2016)

RESULTS AND DISCUSSIONS

In order to distinguish between fresh and saline groundwater, the calculated salinities are divided into several classes of chlorine concentration; 0-250 mg/L, 250-500 mg/L, 500-1000 mg/L, 1000-2000 mg/L and >2000 mg/L. In these classes fresh groundwater is represented by a chloride concentration smaller than 250mg/L and Salt/ Saline groundwater represented by a chloride concentration higher than 2000 mg/L. Groundwater containing chloride concentrations in between are classified as brackish. These salinity classes are depicted in columns over the depth of the borehole logs of the several cross-sections, correlating with their interpreted sand sections of the respective formations. In order to verify the calculated chloride concentrations, a comparison was made of the calculated chloride concentrations based on the well logs with available water samples taken from drinking water production wells of the same formation. This comparison indicates that there's no match between the chloride content, whereas the calculated chloride values based on the well logs appears to be higher than the laboratory analyzed water samples of the water production wells(HACAS, 2016).

CONCLUSIONS

Based on the results it can be concluded that the groundwater salinity from the Saramacca formations varies from brackish at the central part of the country in Paramaribo to fresh groundwater in the western part, where thick layers of 20 to 60 meters of groundwater are found near Wanica and Saramacca district. Cross sections in the farthest West of the country in the district Nickerie are also indicating bodies of fresh groundwater up to 750 meter depths into the Cretaceous Nickerie Formation, which confirms the presence of fresh groundwater bodies in the deeper parts of the Saramacca formation as suggested in earlier studies by UNDP/WHO (1973). Based on the uncertainties of the calculated chloride concentrations which appear to be higher, it may be concluded that the amount of available fresh water will be higher. This will be included in further scientific research to be carried out.

ACKNOWLEDGMENTS

This work was supported through a grant from the International Development Bank (IDB) to the Suriname Water Company, through the government of Suriname, to conduct a Hydrogeological Assessment of the Coastal Aquifers of Suriname (HACAS, 2016).

REFERENCES

- Frederic R. Harris, IWACO & SUNECON, Jan 1991^e, Water supply systems for Paramaribo and its metropolitan area, IADB, Special report 10 water resources.
- Groen, J., 2002. The effects of transgression and regression on coastal and offshore groundwater. A case study of Suriname and generetic studies into groundwaterflow systems, salinity patterns and paleo groundwater. Vrije Universiteit Amsterdam.
- Groen, J., 2002. The effects of transgressions and regressions on coastal and offshore groundwater. PhD Thesis Vrije Universiteit Amsterdam.
- Groen, J., Velstra, J. and meesters, A.G.C.A., 2000a. Salinization processes in paleowaters in coastal sediments of Suriname : evidence from $\delta^{37}\text{Cl}$ analysis and diffusion modelig. Journal of Hydrology 234, 1-20.
- HACAS, 2016, Hydrogeological Assessment of the Coastal Aquifers in Suriname, Final Report-Volume II Hydrogeological Assessment.
- Hanou, M. J., 1981. Geologic and petroleum analysis of the Suriname coastal region. Staatsolie Maatschappij Suriname N.V, Paramaribo, Suriname.
- Post, V. E. A., 1996. Modelling of the paleohydrological situation in the coastal plain of Surinam. MSc. Thesis, Vrije Universiteit Amsterdam.
- Sabajo, V., 2016. Mapping of Groundwater Salinities in the aquifers of the coastal plain of Suriname. MSc. Thesis, Anton de Kom Universiteit van Suriname.
- UNDP/WHO, 1973. Public water supplies and sewerage project, Volume III: Water Resources (Hydrogeological and Hydrological Studies). United Nations Development programme and World Health Organization.
- Verluer, H., 1991. Hydrogeological survey of the coastal plain of Surinam. MSc. Thesis, Vrije Universiteit Amsterdam.
- Wong, Th. E., 1989. Outline of the stratigraphy of the coastal plain of Suriname. Mededeling Natuurwetenschappelijke Studiekring voor Suriname en de Nederlandse Antillen No.123.

Petrography of the metamorphic rocks in the Kabofe and Jaikreek area, Marowijne Greenstone Belt, Suriname

Santoucha Woodyly

Anton de Kom University of Suriname

Paramaribo, Leysweg 86

sanwood99@hotmail.com

SUMMARY

The characteristics of the rocks in the research area are compared to the Sara's Lust gneisses located in the north and the Coeroeni gneisses from the southwest of Suriname. The results show that the majority of the Kabofe and Jaikreek gneisses match the Sara's Lust gneisses mentioned in the paper of Kroonenberg, et al. (2016), based on the mineral composition, protolith and the metamorphic facies and grade. The gneisses are in the amphibolite facies and have a supracrustal origin. The only difference was the absence of orthopyroxene, which would indicate the granulite facies was reached. The existence of migmatitic gneisses simplifies the understanding of granite and granitic rocks. The migmatites are later intruded with pegmatite dykes or sills. And the gneisses are intruded by dolerites.

Keywords: Sara's Lust gneiss, metamorphic facies, migmatite

INTRODUCTION

The Marowijne Greenstone Belt of northeastern Suriname is bounded on both its northern and southern flanks by a narrow belt of high-grade metamorphic rocks, together labeled as Sara's Lust Gneiss. This study aims to investigate whether the southern flank is similar to the northern one, and whether there is a relation with similar high-grade rocks in southwestern Suriname, the Coeroeni Gneiss Belt. The study areas are along the southwestern flank of the Marowijne greenstone belt, bordered by a zone of high-grade metamorphic rocks. According to Kroonenberg, et al. (2016) the southwestern flank predominantly consists of garnet-biotite gneisses, andalusite-cordierite sillimanite schists and ortho- and clinopyroxene gneisses in which the presence of orthopyroxene, if metamorphic, would evidence that metamorphic conditions were up to granulite facies. It is, however, unknown whether orthopyroxene is present as a magmatic or a metamorphic mineral. Nonetheless, according to Goumans (2019) the Sara's Lust Gneisses in the northern flank mainly consist of amphibolite facies metamorphic rocks.

RESEARCH APPROACH

This research will help understand and define, whether the rocks observed in the study areas, match the characteristics of the Sara's Lust rocks. This will make it easier to create a more detailed geological map in that area. Further to that, the identification of minerals will help determine the metamorphic facies needed for future P-T-t studies. The geochemical analyses are not part of this research.

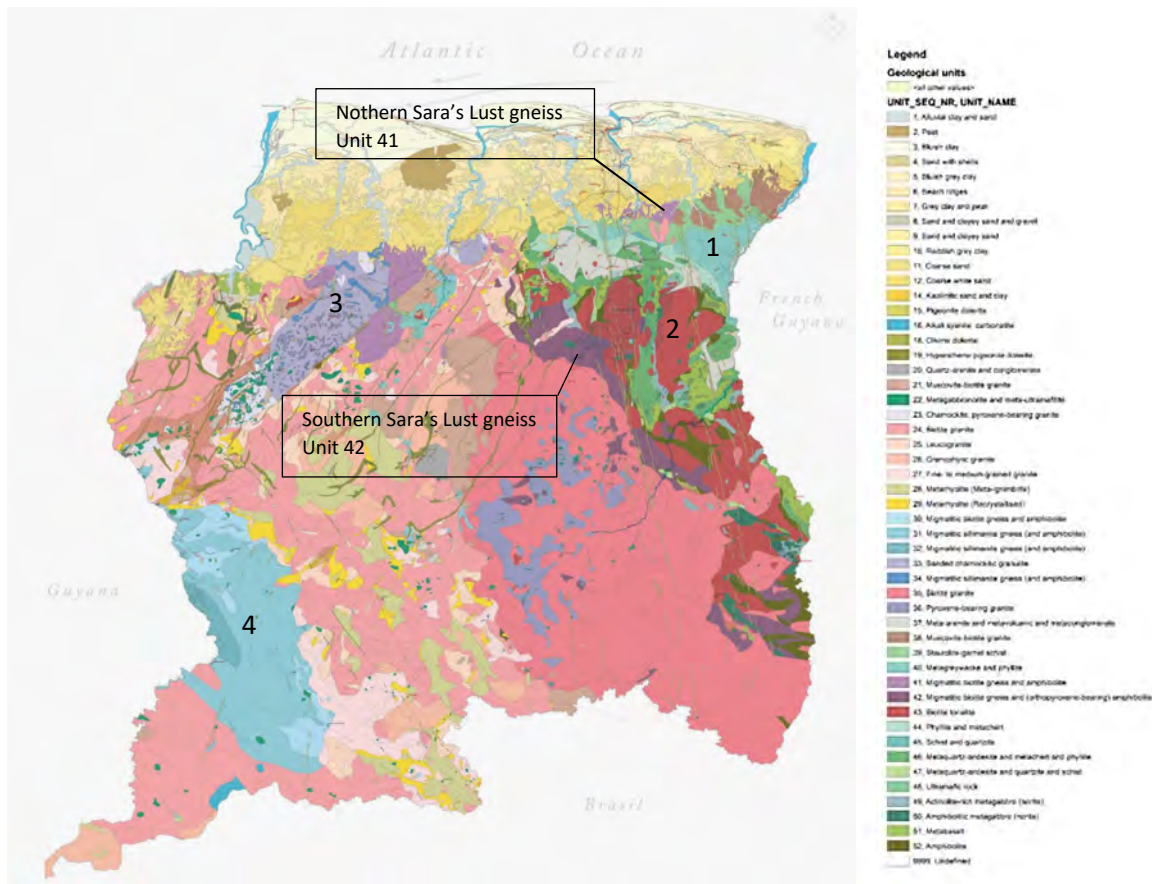


Figure 16- Geological map of Suriname, produced by TNO (2018). Sara's Lust Gneisses in purple, the Marowijne Greenstone Belt includes the Paramaka Formation in several shades of green and the Armina Formation in turquoise (1), the Kabel Tonalite in dark red (2), the Bakhuis Granulite Belt in violet (3), the Cauarane-Coeroeni Gneiss Belt in blue (4).

RESULTS

For each thin section, petrographic observations were obtained regarding the mineral composition and textures. As a result, five different rock types; amphibolite, gneiss, dolerite, felsic igneous rock, and pegmatite were classified. Gneisses come in five different varieties: sillimanite gneiss, biotite gneiss, garnet-muscovite-biotite gneiss, garnet-biotite gneiss, and hornblende-biotite gneiss. Amphibolite has a mafic supracrustal protolith. Sillimanite gneiss, garnet-muscovite-biotite gneiss, and garnet-biotite gneiss have a pelitic supracrustal protolith. Hornblende-biotite gneiss and biotite gneiss have a quartzofeldspathic supracrustal protolith.

COMPARISON WITH SARA'S LUST GNEISSES AND COEROENI GNEISSES

In the paper of Kroonenberg et al (2016), the rocks in the northern segment are predominantly migmatitic hornblende-biotite gneisses, biotite-plagioclase gneisses, garnet-biotite gneisses and quartzofeldspathic gneisses, with minor amphibolites, locally with garnet or clinopyroxene, and furthermore pelitic sillimanite-biotite-muscovite gneisses and calcisilicate rocks, clearly of supracrustal origin. And in the southwestern flank, the Sara's Lust Gneisses predominantly consist of garnet-biotite gneisses, andalusite-cordierite sillimanite schists and ortho- and clinopyroxene gneisses. Comparing it with the results of this research, the rocks are almost the same. Only orthopyroxene and cordierite are not found in these thin sections. This means the granulite facies is not reached in these areas. The migmatitic rocks are hornblende-biotite gneiss and biotite gneiss. The amphibolite rocks correspond with the LB107B amphibolite thin section in Goumans (2019) from the northern segment.

The Sara's Lust gneisses were once considered part of the Coeroeni gneiss Belt. But after research, it seems that the Sara's Lust gneisses were 100 Ma older than the Coeroeni gneisses (Kroonenberg, et al., 2016). If we look at the rock

types, they are almost the same as Sara's Lust. The rocks of this research also correspond to the Coeroeni gneisses, except for the fact that the cordierite mineral was not present. Based on mineralogical analyses, it is difficult to separate the Coeroeni from the Sara's Lust gneisses, because they are the same rock types, only the age does not match. Looking at the geological map of Suriname (2018), the gneiss sample locations are in the southern segment of the Sara's Lust gneisses, so they will be considered as Sara's Lust gneisses. To confirm this, further study is needed.

CONCLUSION

The metamorphic rocks of the Kabofe and Jaikreek area are characterized by their supracrustal origin, and the amphibolite metamorphic facies. The gneisses of the study area correspond to the Sara's Lust gneisses, based on the mineral composition and the metamorphic facies. The metamorphic grade of the rocks in Kabofe and Jaikreek are intermediate to more high-grade, because most of the rocks indicate temperature greater than 400° C. There are no minerals observed that indicate the granulite facies was reached.

The conclusion was made that these rocks could have undergone regional metamorphism according to the metamorphic facies diagram and parts of the supracrustal rocks also underwent metasomatism, which invaded the protolith. The presence of migmatitic gneisses, makes it easier to understand granite and granitic rocks observed. The granite magma maybe from diatexite migmatites derived from supracrustal rocks of pelitic composition. Biotite remained stable and serves as a tracer for the solid fraction during melt segregation. The migmatites are later intruded with pegmatite dykes or sills. Dolerites are later intruded into the gneisses. The grain size is coarse, meaning it has had enough time to cool and it is not affected by metamorphism.

ACKNOWLEDGEMENTS

My grateful appreciation goes to Professor Salomon Kroonenberg and Fydji Libby-Sastrohardjo, MSc, for mentoring me through this research of petrographical analysis.

REFERENCES

- Goumans, J. (2019). Petrogenesis and peak metamorphic conditions of Sara's Lust gneisses, Suriname.
- Kroonenberg, S., De Roever, E., Fraga, L., Reis, N., Faraco, T., & Lafon, J. (2016). Paleoproterozoic evolution of the Guiana Shield in Suriname: A revised model. *Netherlands Journal of Geosciences*, 491-522.

